Kinetics and Modelling of Enzymatic Process for *R*-phenylacetylcarbinol (PAC) Production

Noppol Leksawasdi

**A thesis submitted in fulfilment
of the requirements for the Degree of
Doctor of Philosophy**

**School of Biotechnology and Biomolecular Sciences
University of New South Wales
Sydney, Australia**

August, 2004

Declaration

I hereby declare that this submission is my own work and to the best of my knowledge it contains no material previously published or written by another person, nor material which to a substantial extent has been accepted for the award of any degree or diploma at UNSW or any other educational institution, except where due acknowledgement is made in this thesis. Any contribution made to the research by others, with whom I have worked at UNSW or elsewhere, is explicitly acknowledged in the thesis.

I also declare that the intellectual content of this thesis is the product of my own work, except to the extent that assistance from others in the project's design and conception or in style, presentation and linguistic expression is acknowledged.

_____

Noppol Leksawasdi

For The Royal Thai Government

Acknowledgements

I wish to express my greatest gratitude and thanks to my supervisor, Professor Peter L. Rogers and my co-supervisor, Dr. Bettina Rosche for their excellent guidance, invaluable advice, support and encouragement throughout the course of this study and preparation of this thesis.

I am very grateful to the Royal Thai Government (RTG) for the award of this scholarship and for providing me with the opportunity to undertake this study. I will always be grateful for the reassurance of continual financial support throughout my study from the RTG when our country faced an economic crisis during 1997-1998.

I would like to thank the sponsors of the project, BASF Ludwigschafen, for their financial support for equipment and materials.

My sincere thanks are also due to Dr. Russell Cail, Malcolm Noble, Martin Zarka, Wolfgang Nittel and Dr. Christopher Marquis for their technical assistance and thoughtful suggestions.

A very special thank you to Alan, Vanessa, Allen, Gernalia, Cindy, Richard, Charles, Nick, Eny, Jae, Apple, Jeab, Mallika, Ronachai, Olarn, Astutiati, Caleb and Fiona for their help and suggestions. I wish to extend my thanks also to the students and staffs of the School of Biotechnology and Biomolecular Sciences (BABS) for their valued friendship.

My heartfelt appreciation goes to my parents and my brothers for their understanding, encouragement and endurance during the years. I am also grateful to the kindness and generosity of my landlord and landlady, Arthur and Marge Keeble as well as my former landlady, Wendy Ryan. Last but not least, I wish to thank Onn for her kindness, friendship, support, wonderful meals and innumerable help.

Abstract

R-phenylacetylcarbinol (PAC) is used as a precursor for production of ephedrine and pseudoephedrine, which are anti-asthmatics and nasal decongestants. PAC is produced from benzaldehyde and pyruvate mediated by pyruvate decarboxylase (PDC).

A strain of *Rhizopus javanicus* was evaluated for its production of PDC. The morphology of *R. javanicus* was influenced by the degree of aeration/agitation. A relatively high specific PDC activity (328 U decarboxylase g^{-1} mycelium) was achieved when aeration/agitation were reduced significantly in the latter stages of cultivation.

The stability of partially purified PDC and crude extract from *R. javanicus* were evaluated by examining the enzyme deactivation kinetic in various conditions. *R. javanicus* PDC was less stable than *Candida utilis* PDC currently used in our group.

A kinetic model for the deactivation of partially purified PDC extracted from *C. utilis* by benzaldehyde (0–200 mM) in 2.5 M MOPS buffer has been developed. An initial lag period prior to deactivation was found to occur, with first order dependencies of PDC deactivation on exposure time and on benzaldehyde concentration.

A mathematical model for the enzymatic biotransformation of PAC and its associated by-products has been developed using a schematic method devised by King and Altman (1956) for deriving the rate equations. The rate equations for substrates, product and by-products have been derived from the patterns for yeast PDC and combined with a deactivation model for PDC from *C. utilis*.

Initial rate and biotransformation studies were applied to refine and validate a mathematical model for PAC production. The rate of PAC formation was directly proportional to the enzyme activity level up to 5.0 U carboligase ml^{-1}. Michaelis-Menten kinetics were determined for the effect of pyruvate concentration on the

Abstract

reaction rate. The effect of benzaldehyde on the rate of PAC production followed the sigmoidal shape of the Monod-Wyman-Changeux (MWC) model. The biotransformation model, which also included a term for PDC inactivation by benzaldehyde, was used to determine the overall rate constants for the formation of PAC, acetaldehyde and acetoin.

Implementation of digital pH control for PAC production in a well-stirred organic-aqueous two-phase biotransformation system with 20 mM MOPS and 2.5 M dipropylene glycol (DPG) in aqueous phase resulted in similar level of PAC production [1.01 M (151 g l^{-1}) in an organic phase and 115 mM (17.2 g l^{-1}) in an aqueous phase after 47 h] to the system with a more expensive 2.5 M MOPS buffer.

Publications

Published papers

(1)   PAC production

Rosche, B., **Leksawasdi, N.**, Sandford, V., Breuer, M., Hauer, B. and Rogers, P.L. (2002). Enzymatic (*R*)-phenylacetylcarbinol production in benzaldehyde emulsions, Applied Microbiology and Biotechnology 60: 94-100.

Leksawasdi, N., Breuer, M., Hauer, B., Rosche, B. and Rogers, P.L. (2003). Kinetics of pyruvate decarboxylase deactivation by benzaldehyde, Biocatalysis and Biotransformation 21: 315-320.

Leksawasdi, N., Chow, Y.Y.S., Breuer, M., Hauer, M., Rosche, B. and Rogers, P.L. (2004). Kinetic studies and model validation of enzymatic (*R*)-phenylacetylcarbinol batch biotransformation process, Journal of Biotechnology, 111: 179-189.

(2)   Others

Leksawasdi, N., Joachimsthal, E.L. and Rogers, P.L. (2001). Mathematical modelling of ethanol production from glucose/xylose mixtures by recombinant *Zymomonas mobilis*, Biotechnology Letters 23: 1087–1093.

Boonmee, M., **Leksawasdi, N.**, Bridge, W. and Rogers, P.L. (2003). Batch and continuous culture of *Lactococcus lactis* NZ133: experimental data and model development, Biochemical Engineering Journal 14: 127-135.

Pulsawat, W., **Leksawasdi, N.**, Rogers, P.L. and Foster, L.J.R. (2003). Anion effects on biosorption of Mn(II) by extracellular polymeric substance (EPS) from *Rhizobium etli*, Biotechnology Letters 25: 1267-1270.

Papers in preparation

(1)   PAC production

Leksawasdi, N., Breuer, M., Hauer, B., Rosche, B. and Rogers, P.L. (2004). Production of pyruvate decarboxylase from *Rhizopus javanicus* and its deactivation kinetics, Manuscript Submitted (Enzyme and Microbial Technology).

Leksawasdi, N., Breuer, M., Hauer, B., Rosche, B. and Rogers, P.L. (2004). Mathematical model for kinetics of enzymatic conversion of benzaldehyde and pyruvate to (*R*)-phenylacetylcarbinol, Manuscript Submitted (Biochemical Engineering Journal).

Leksawasdi, N., Breuer, M., Hauer, B., Rosche, B. and Rogers, P.L. (2004). Cost effective development of two-phase biotransformation for (*R*)-phenylacetylcarbinol production, Manuscript in preparation.

Sandford, V., **Leksawasdi, N.**, Breuer, M., Hauer, B., Rosche B. and Rogers, P.L. (2004). Factors affecting product formation and enzyme stability in the production of (*R)*-phenylacetylcarbinol by *Candida utilis* pyruvate decarboxylase, Manuscript in preparation.

(2)   Others

Boonmee, M., **Leksawasdi, N.**, Bridge, W. and Rogers, P.L. (2004). Evaluation of electrodialysis for lactate removal and pH control in the production of the dairy starter culture *Lactococcus lactis* NZ133, Manuscript Submitted (Journal of Membrane Science).

Boonmee, M., **Leksawasdi, N.**, Bridge, W. and Rogers, P.L. (2004). Use of anion exchange resin for lactate removal and pH control in the production of the dairy starter culture *Lactococcus lactis* NZ133, Manuscript in preparation.

Conference Proceedings

Borompichaichartkul, C., Moran, G., Srzednicki, G., Driscoll, R., **Leksawasdi, N.** and Ball, G. (2001). Studies of physical state of water in frozen china maize (Huangmo 417) using NMR technique-deuterium relaxation and DSC, Quality management and market access: Proceedings of the 20th ASEAN/2nd APEC, seminar on postharvest technology. Lotus Hotel Pang Suan Kaew, Chiang Mai, Thailand, 11–14 September, pp. 215-220, ISBN 974 436 249 9.

Poster and oral presentations

(1)   PAC production

Leksawasdi, N., Rosche, B. and Rogers, P.L. (2002). Mathematical model development of *R*-PAC biotransformation in benzaldehyde emulsions, School of Biotechnology and Biomolecular Sciences First Annual Symposium, Sydney, Australia, 8 November 2002, oral presentation III-2, ISBN 0 7334 1581 4.

Leksawasdi, N., Breuer, M, Hauer, B., Rosche, B. and Rogers, P.L. (2003). Model development of pyruvate decarboxylase deactivation kinetics by benzaldehyde, School of Biotechnology and Biomolecular Sciences Second Annual Symposium, Sydney, Australia, 7 November 2003, poster presentation P-22, ISBN 0 7334 1581 4.

Leksawasdi, N., Breuer, M., Hauer, B., Rogers, P.L. and Rosche, B. (2003). Prediction of *R*-PAC batch biotransformation with mathematical model, Fermentation and Bioprocessing Conference: Ideas into products. The Garvan Institute for Medical

Research, Sydney, Australia, 14-15 April, oral presentation Session 3.4, p. 34, ISBN 0 7334 2023 0.

Leksawasdi, N., Breuer, M., Hauer, B., Rosche, B. and Rogers, P.L. (2003). Theoretical and experimental studies in developing rate equations for the enzymatic production of *R*-phenylacetylcarbinol and by-products, BioThailand 2003: Technology for Life. Pattaya Exhibition and Convention Hall, Pattaya, Thailand, 17-20 July, poster presentation P-ENZ-13, p.210, ISBN not available.

Rosche, B., Sandford, V., **Leksawasdi, N.**, Chen, A., Satianegara, G., Gunawan, C., Breuer, M., Hauer, B. and Rogers, P.L. (2003). Bioprocess development for ephedrine production, 6th International Symposium on Biocatalysis and Biotransformations. BIOTRANS 2003, Palacky University, Olomouc, Czech Republic, 28 June–3 July, poster presentation P244, ISSN 0009-2770.

Leksawasdi, N., Breuer, M., Hauer, B., Rosche, B. and Rogers, P.L. (2004). Strategy of enhancing *Rhizopus javanicus* pyruvate decarboxylase production and investigation of its deactivation kinetics, Fermentation and Bioprocessing Conference. UQ Centre University of Queensland, Brisbane, Australia, 5-6 July, poster presentation number 18, p. 52, ISBN 0 646 43707 0.

(2)   Others

Leksawasdi, N., Joachimsthal, E.L. and Rogers, P.L. (2001). Model development for ethanol production by recombinant *Zymomonas mobilis* ZM4 (pZB5), 23rd Symposium on Biotechnology for Fuels and Chemicals, Colorado, United States, 6–9 May 2001, poster 2-87, NREL/CP-580-30100.

Leksawasdi, N., Cheung, C.K., Noble, M. and Doran, P.M. (2003). Application of Microsoft$^{®}$ EXCEL and Visual Basic in the design and control of a dynamic bioreactor air feeding system, Fermentation and Bioprocessing Conference: Ideas into products.

Publications

The Garvan Institute for Medical Research, Sydney, Australia, 14-15 April, poster presentation, p.54, ISBN 0 7334 2023 0.

Pulsawat, W., **Leksawasdi, N.**, Rogers, P.L. and Foster, L.J.R. (2003). Anions effects on biosorption of manganese by EPS from *Rhizobium etli* M4, BioThailand 2003: Technology for Life. Pattaya Exhibition and Convention Hall, Pattaya, Thailand, 17-20 July, poster presentation P-ENV-10, p.307, ISBN not available.

Table of Contents

Table of Contents

Table of Contents

Table of Contents

List of Tables

List of Tables

List of Figures

List of Figures

Objectives of the current study

Research on the biotransformation of pyruvate and benzaldehyde by pyruvate decarboxylase (PDC) to produce *R*-phenylacetylcarbinol (PAC) has been conducted by our group for more than 15 years. This process has shown significant improvements when compared to the traditional yeast-based fermentation process. The screening studies by Rosche et al. (2001) suggested that *Rhizopus javanicus* can be used as an alternative PDC source to the previously employed *Candida utilis*. This study extends the earlier research further by examining various cultivation conditions for optimum production of PDC and compares the stability of PDC from both sources to select the best candidate for subsequent development of a comprehensive mathematical model describing the enzymatic biotransformation. Several modifications of a model developed previously by Chow (1998) are necessary because of improved biotransformation conditions, which employed 2-2.5 M MOPS (Rosche et al. 2001, 2002a,b, 2003a) instead of 40 mM phosphate buffer. The model forms the basis for the design of optimal feeding of pyruvate and/or benzaldehyde and the future development of a model describing the organic-aqueous two-phase biotransformation process. The study presented here also includes detailed kinetic evaluations of the two-phase emulsion system with implementation of pH control, which is a continuation of the two-phase research originally conducted by Sandford (2002) and is the subject of a recent patent application by our group (Hauer et al. 2003).

The specific objectives of this investigation are:

(1)   to construct a theoretical model for the PAC biotransformation process using the schematic method of deriving rate laws for complex enzyme-catalysed reactions developed by King and Altman (1956),

(2) to investigate the growth of a strain of the filamentous fungi *R. javanicus* in various fermentation conditions and identify several key factors influencing the production of PDC for PAC formation,

(3) to assess the stability of *R. javanicus* PDC in a range of conditions with detailed deactivation kinetics and compare this to *C. utilis* PDC in order to determine the most suitable source of PDC for the biotransformation process,

(4) to obtain an equation describing the deactivation of the selected PDC in the improved buffering conditions (2.5 M MOPS, pH 7.0, 6°C) reported previously by our group. This equation will be used as one of a series of differential equations for the overall modelling and simulation of PAC batch biotransformation profiles,

(5) to modify the theoretical model obtained in part (1) by performing initial rate experiments on a range of substrate concentrations and enzyme activities. Independent batch biotransformations will then be used for the estimation of PAC and by-products rate constants, refinement of parameter constants estimated from the initial rate studies as well as for model validation,

(6) to further evaluate the laboratory scale two-phase emulsion bioreactor using high precision digital pH control to mitigate any enzyme deactivation effects from rising pH and avoid the use of a highly buffered aqueous phase.

Chapter 1

Literature Review

1.1   INTRODUCTION

The following literature review concentrates on the current trends and new developments in biotransformation processes as well as the characteristics of a biotransformation processes for *R*-phenylacetylcarbinol (PAC), including a comparison of various enzymatic PAC biotransformation processes using pyruvate decarboxylase (PDC) from different sources.

1.2   CURRENT TRENDS IN BIOTRANSFORMATION PROCESSES

According to Leon et al. (1998), biotransformations or biocatalyst-mediated transformations of chemical compounds were known from the time when the science of microbiology was being established by Louis Pasteur (b 1822-d 1895). Biocatalysts have thus long been considered as very important in leading to the manufacture of various intermediates in the agrochemical, fine-chemical, pharmaceutical and food industries (May 1992, May 1997, Turner 2003). One of the oldest examples for an industrial biocatalyst application is the production of acetic acid from ethanol (since 1815) using an immobilized *Acetobacter* strain attached to beech wood shavings (Wandrey et al. 2000). Cherry and Fidantsef (2003) estimated that industrial biocatalysts have application in three sectors; namely, technical and personal care industries (65%), food and baking industries (25%) and animal feed industries (10%). There are many attributes for a reaction which is mediated by a biocatalyst including high regio- and stereo-specificities (Ward and Singh 2000), ability to accept a wide array of complex molecules as substrates, fewer by-products (Schmid et al. 2001), higher reaction rates and milder reaction conditions of temperature and pH, resulting in a lower environmental impact when compared to the chemical route (Schmid et al. 2002, Cherry and Fidantsef 2003). The common problems often associated with chemical processes such as isomerization, racemization and epimerization are also minimized (Patel 2001). Schulze and Wubbolts (1999) suggested that biocatalysts will play an important role in the 21st century in the enhanced and cost effective production of enantiomerically pure chiral intermediates. McCoy (2000) estimated the current

value of the industrial biocatalyst market at $USD 1.5 billion. Of the 25,000 enzymes existing in nature, about 4,000 enzymes have been categorized by the Union of Biochemistry and Molecular Biology (IUBMB). Six major groups of enzymes, based on the type of reaction catalysed, have been classified as: oxido-reductases, transferases, hydrolases, lyases, isomerases and ligases (Hari Krishna 2002).

The characteristics of a particular biotransformation process, which include efficiency of enzyme utilization, yield and productivity as well as product concentration, must be considered to assess its industrial feasibility. Yield determines the efficiency of use of raw materials and reflects the amount of by-product(s) produced while increased productivity is related to decreased capital costs. The difficulties in product purification and recovery can be associated with the level of product concentration and associated by-products. Table 1.1 illustrates some of the recently developed biocatalytic processes and their characteristics (Schmid et al. 2001).

A recent review by Straathof et al. (2002) estimated that the growth of industrial scale biotransformation processes has increased over the past four decades from less than 10 in early 1960s to at least 134 in 2002 (Figure 1.1). The replacement of production of conventional bulk chemicals with biotransformation processes includes the production of phenolic resins using peroxidases and the conversion of acrylonitrile to acrylamide by nitrile hydratase (Schmid et al. 2001). Biotransformation processes might be classified in several ways: for example, by the type of products (Figure 1.2) or by their corresponding industrial sectors (Figure 1.3). According to Stinson (2000), the chiral drug sales within the large pharma sector were estimated to expand at an average of 8% per annum over four years to the net value of $USD 146 billion in 2003.

No specific type of compounds is dominant when the biotransformation processes are grouped according to the type of products (Figure 1.2). In terms of production scale, the major examples are fructose production from glucose using glucose isomerase (1 million tpa) and low-lactose milk manufacture by hydrolysis of lactose using β-galactosidase (up to 0.25 million l day^{-1}) (Liese and Filho 1999). With regard to the industrial sector dominance, however, pharmaceutical applications stand out (Figure

1.3). An important example in this sector is the production of penicillins catalysed by penicillin amidase (Boesten et al. 1996).

Table 1.1: Biocatalytic systems recently employed by various chemical companies (adapted with modification from Schmid et al. 2001).

Company	Product	Substrate	Biocatalyst	Enzyme	Reaction	Scale (tonne y^{-1})
BASF	Enantiopure alcohols	Racemic alcohols	Enzymes	Lipases	Resolution	1000
	R-Amide; S-amine	Racemic amines	Enzymes	Lipases	Resolution	> 100
	R-Mandelic acid	Racemic mandelonitrile	Enzymes	Nitrilases	Hydrolysis	> 1
	L-amino acids	Racemic amino-acid amides	Enzymes	Amidases	Kinetic resolution	> 1 to > 100
	L-Aspartic acid	Fumaric acid	Enzymes	Ammonia lyase	Ammonia addition	1000
DSM	Aspartame	N-protected L-aspartic acid, D/L phenylalanine methyl ester	Enzymes	Thermolysine	Selective coupling	1000
	6-Aminopenicillanic acid	Penicillin G/V	Enzymes	Penicillin acylase	Hydrolysis	1000
	Semisynthetic penicillins	6-Aminopenicillanic acid	Enzymes	Acylases	Selective coupling	> 1 to > 100
Lonza	6-Hydroxynicotinic acid	Niacin	Whole cells	Niacin hydroxylase	Water addition	> 1
	5-Hydroxypyrazine carboxylic acid	2-Cyanopyrazine	Whole cells	Nitrilase/hydroxylase	Water addition	Development product
	6-Hydroxy-S-nicotine	(S)-Nicotine	Whole cells	Hydroxylase	Water addition	Development product
	S-Piperazine-2-carboxylic acid	(R, S)-Piperazine-2-carboxylic acid	Whole cells	Stereospecific amidases	Selective amidase	Development product
	5-Methylpyrazine-2-carboxylic acid	2,5-Dimethylpyrazine	Whole cells	Xylene oxidation	Selective oxidation	> 1
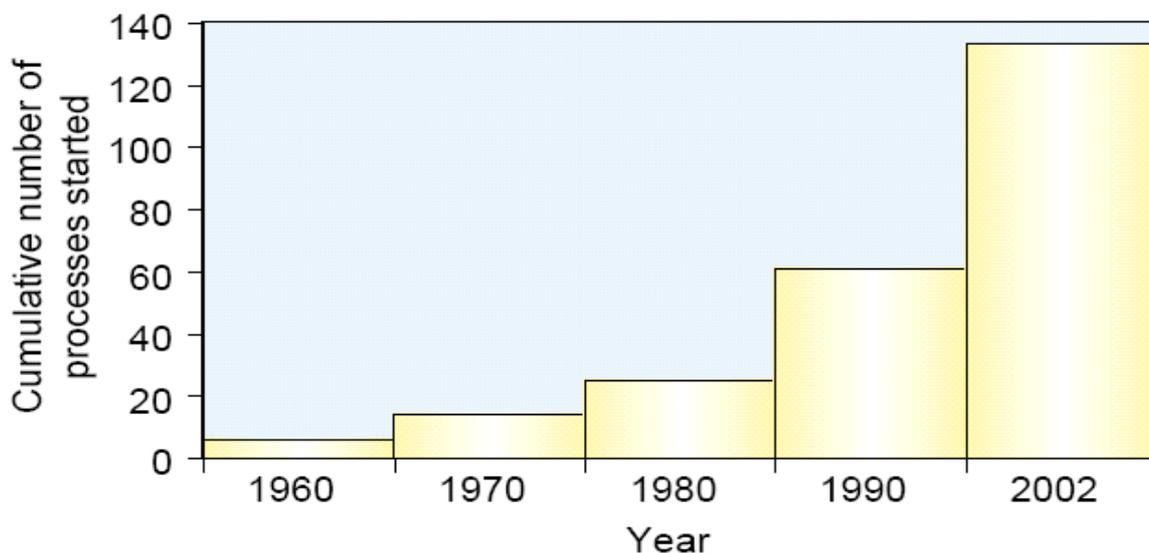
Figure 1.1: Cumulative number of biotransformation processes on an industrial scale (Straathof et al. 2002).
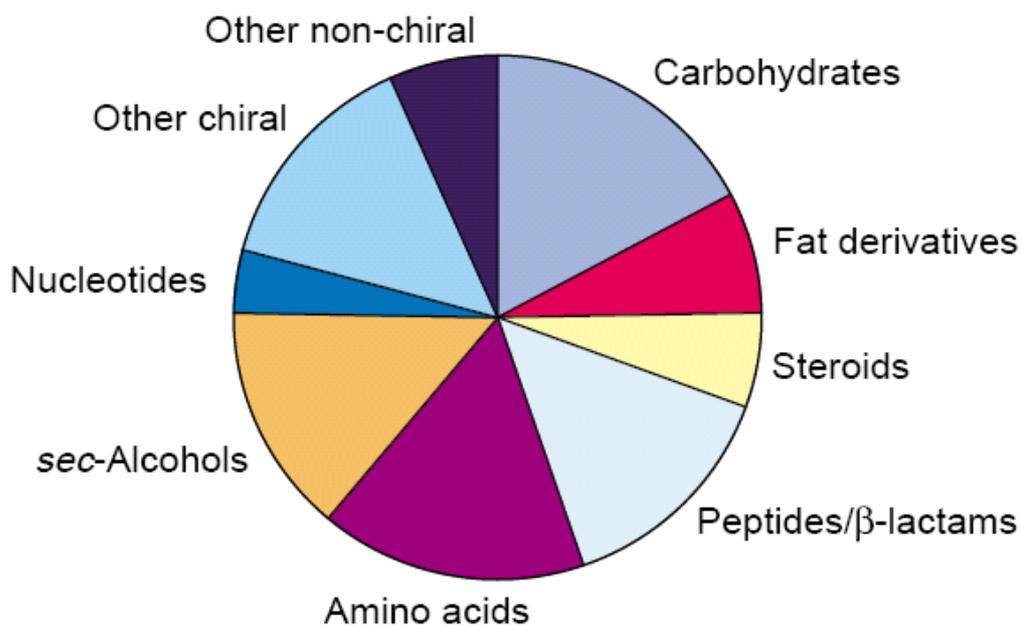
Figure 1.2: The type of compounds produced using biotransformation processes (based on 134 industrial processes) (Straathof et al. 2002).
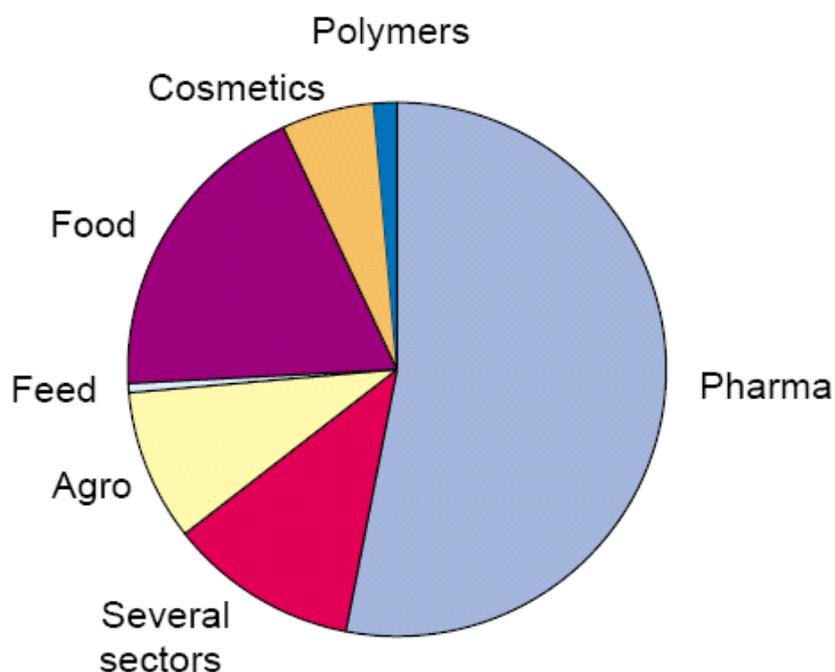
Figure 1.3: Industrial sectors in which the products of industrial biotransformations are used (based on 134 industrial processes) (Straathof et al. 2002).

1.3   EPHEDRINE/PSEUDOEPHEDRINE PRODUCTION BY BIOTRANSFORMATION AND OTHER PROCESSES

1.3.1   Characteristics of ephedrine/pseudoephedrine

R-ephedrine (1-methylamino-ethyl-benzyl alcohol or 2-methylamino-1-phenyl-1-propanol) is a mixed sympathomimetic alkaloid that produces a rise in heart rate, elevates blood pressure, relaxes bronchial smooth muscle and stimulates the central nervous system (Chen and Schmidt 1930, Hu 1969). It is used principally in the temporary treatment of hypotension and bronchial asthma. One of the related alkaloids, *S*-pseudoephedrine, is an important ingredient in cold and influenza medications, in which it acts as a nasal decongestant (Oliver et al. 1999). Pseudoephedrine has a higher diuretic activity but weaker cardiovascular effect than ephedrine (Soni et al. 2004). Other forms of ephedrine optical isomers have similar pharmacologic activities but to a

lesser extent (Chen et al. 1929). Other uses of *R*-ephedrine include the treatment of headaches, aching bones and joints (Leung and Foster 1996). The World Health Organization approved the administration of ephedra (a natural plant source of ephedrine) for nasal decongestion and respiratory tract diseases (WHO 1999). Ephedrine and its related alkaloids exist as four naturally occuring stereoisomers as shown in Figure 1.4 (Sorensen and Spenser 1988).
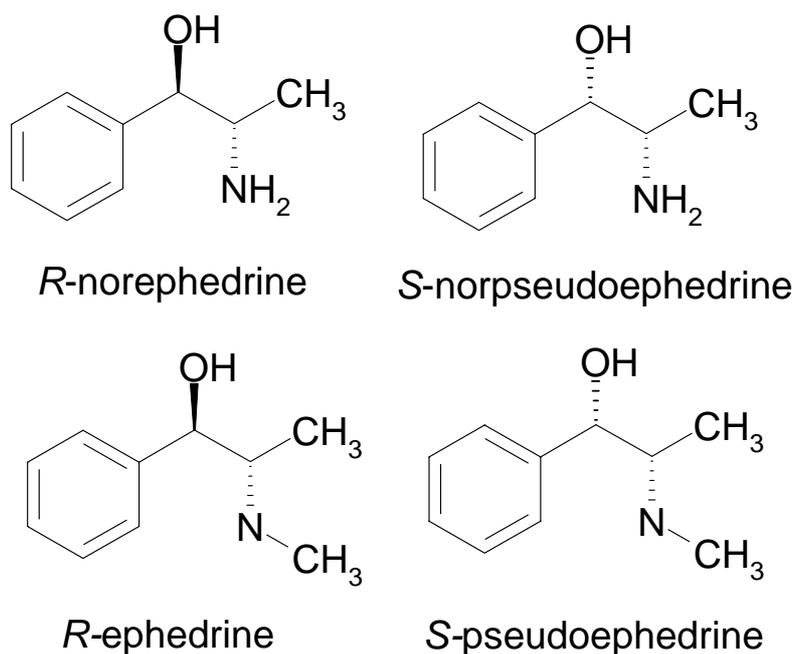
Figure 1.4: The structural formulae of *R*-ephedrine and related alkaloids (adapted with modification from Sorensen and Spenser 1988).

The promotion of *R*-ephedrine as a weight loss aid began in the early 1990s (AHRQ 2003). Astrup et al. (1992a,b, 1995) reported the potential use of *R*-ephedrine alone and *R*-ephedrine in combination of caffeine for the treatment of obesity. The promotion of short-term weight loss was confirmed by Shekelle et al. (2003), however, there were insufficient data to verify the claim of long-term weight loss and enhancement of athletic performance. Kanayama et al. (2001) estimated that up to 2.8 million people consumed ephedrine-containing products for the purpose of enhancing athletic performance during 1999-2001. Knight (2004) reported that various companies have

been marketing ephedra-containing products in the form of dietary tablets and energy drinks. As many as two to three billion doses of these products are estimated to be consumed yearly in the US (Soni et al. 2004). The selling of dietary supplements containing ephedrine related alkaloids has been subjected to regulatory action recently by the Food and Drug Administration (FDA) after it has received more than a thousand complaints of adverse effects over the last few years which included hypertension, myocardial infarction, stroke, arrhythmias, seizures and even death (FDA 2003a,b, Knight 2004, Sola et al. 2004, Soni et al. 2004).

1.3.2   Methods of production

1.3.2.1   *Extraction from plants*

Conventionally, *R*-ephedrine is directly extracted, purified and isolated from numerous plant species of the Genus *Ephedra* (include over 40 species) such as *E. sinica* and *E. equisetina* (Rose 1980, Soni et al. 2004). The plant (Figure 1.5 and 1.6) is also called 'Ma Huang' and has been used for several thousand years in China in folk remedies for removing fever, soothing breath and as a diuretic (Hu 1969). The ancient Indian Aryans and Romans applied it as a stimulant and longevity medicine (Soni et al. 2004). At the present time, *Ephedra* plants are widely distributed and cultivated in China, India, Japan and Southern Siberia (Soni et al. 2004). However, this method of production results in various undesired by-products. It is also laborious, costly and time consuming (Shukla and Kulkarni 2000). Even though the active ingredient, *R*-ephedrine, was first isolated in 1885 from plants (Soni et al. 2004), it was not until 1930 that Chen and Schmidt published data on the cardiovascular effects of this drug and noted its similarities to epinephrine (Hu 1969).

1.3.2.2   *Chemical synthesis*

A chemical process was also used in Germany (Tilston 1988) using mandelic acid to synthesize *R*-ephedrine with subsequent resolving of racemic mixtures (Voets et al.

1973, Netrval and Vojtisek 1982), but the associated cost and toxicological problems prevented further development of this method (Stinson 1993).

Figure 1.5: Photographs of *Ephedra* sp. (Maddison 1995).

1.3.2.3   Combined fermentation and chemical synthesis

The alternative semibiological method of *R*-ephedrine production was established on the industrial scale during the 1930s (Breuer and Hauer 2003). *R*-phenylacetylcarbinol (PAC) is produced micro-biologically from an acyloin-type (chiral α-hydroxyketone) condensation of substrates pyruvate and benzaldehyde on the active site of PDC. It is used as a building block for the production of *R*-ephedrine and its related alkaloids. This reaction is considered as one of the first commercialised biotransformation processes combining microbiological and chemical syntheses (Hildebrandt and Klavehn 1932, 1934) and has been intensively investigated in terms of yield improvement and biocatalyst stability (Sprenger and Pohl 1999).

PAC produced from a biotransformation reaction using various yeasts (Figure 1.7) is later converted to *R*-ephedrine by a chemical reductive amination with methylamine as illustrated in Figure 1.8 (Hildebrandt and Klavehn 1934, Kheradmandy 1990, Seely et al. 1990). The world largest ephedrine production plant has been in operation since

1935 at BASF PharmaChemikalien GmbH and Co. KG Factory Minden, Germany (BASF 2004).
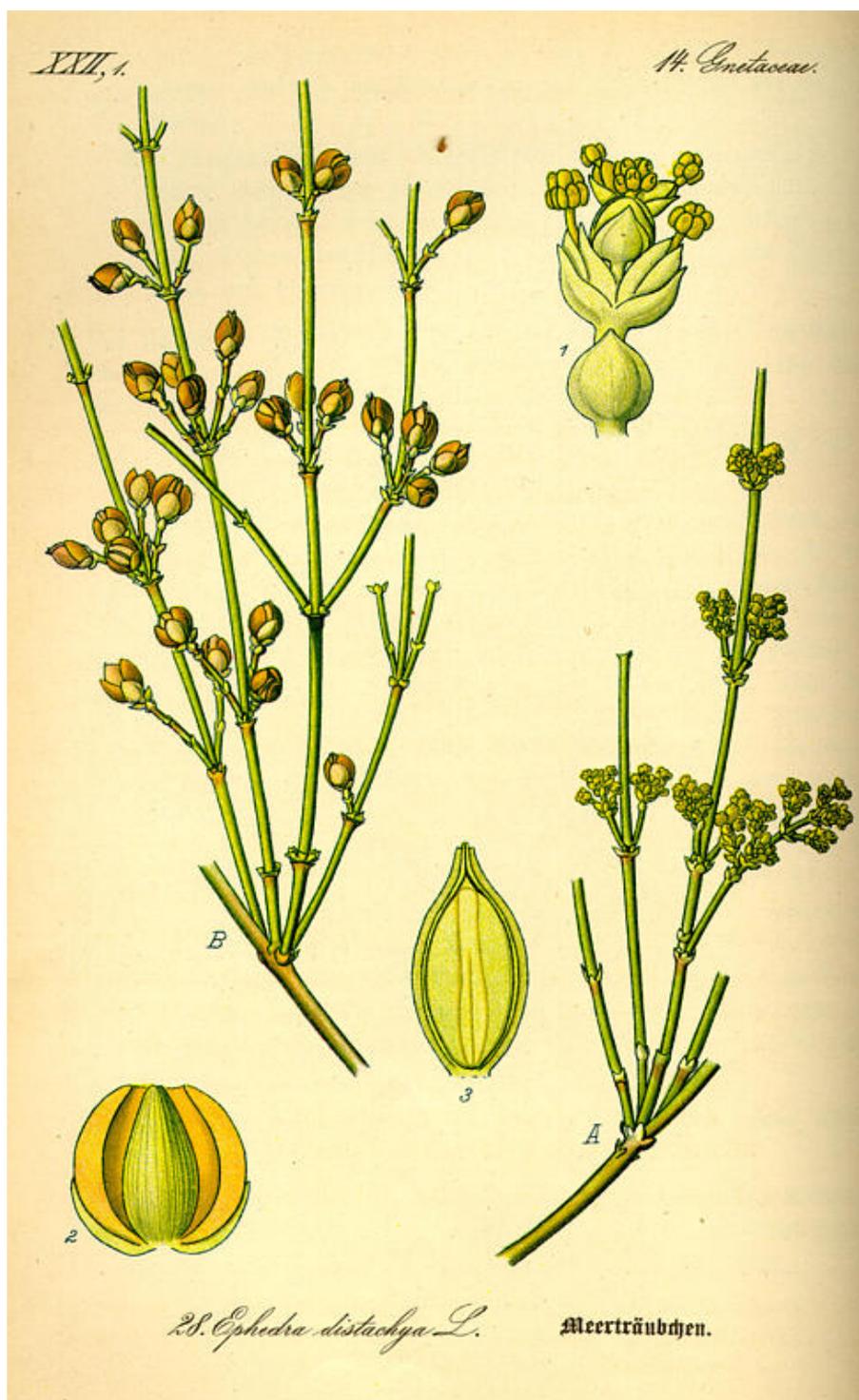
Figure 1.6: Drawing of *E. distachya* (Thome 1885).
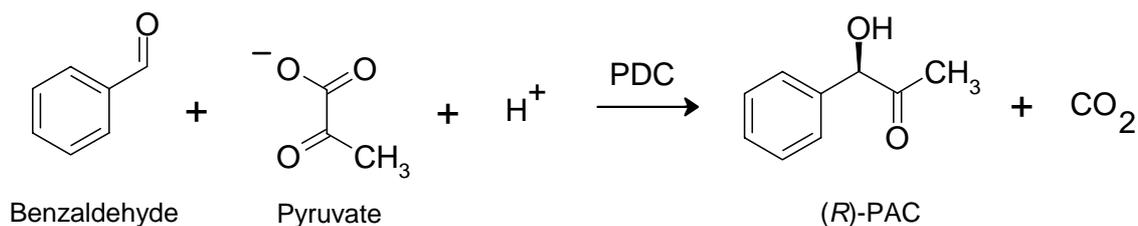
Figure 1.7: Formation of PAC from benzaldehyde and pyruvate catalysed by PDC.
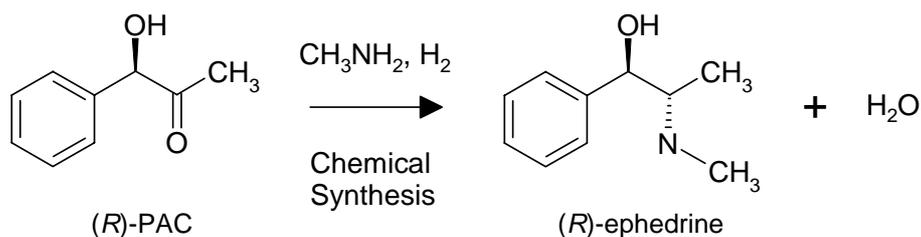
Figure 1.8: Reductive amination of *R*-PAC to produce *R*-ephedrine.

1.4   BIOTRANSFORMATION PROCESSES FOR PAC

1.4.1   Fermentation processes

The production of (1*R*, 2*S*)-ephedrine from benzaldehyde and glucose via PAC with live fermenting yeast is also known as the Knoll procedure (Hildebrandt and Klavehn 1934). The process used commercially can be divided into two stages as follows (Oliver et al. 1999):

(1)   yeast culture is grown in optimal conditions to build up the biomass containing PDC and accumulate sufficient level of pyruvate (fermentative phase),

(2)   benzaldehyde is later added together with sugars to induce production of PAC (biotransformation phase).

An appropriate method of pyruvate feeding may be implemented in the second step if grown yeast cells in resting state are used instead. Because conventional batch fermentation suffers a drawback from the highly toxic benzaldehyde, process research and development has thus been limited to strain improvement and process optimization

(Oliver et al. 1999). An optimum benzaldehyde concentration for a free *Saccharomyces cerevisiae* cell system was estimated to be between 4-16 mM (0.4-1.7 g l^{-1}) (Agarwal et al. 1987, Tripathi et al. 1988). Prolonged cell contact with benzaldehyde has negative impacts on cell permeability, viability and growth (Long and Ward 1989b). It has been reported that the rate of PAC production dropped sharply when a *S. cerevisiae* culture was subjected to 16-20 mM benzaldehyde and completely ceased when the concentration exceeded 20 mM (Agarwal et al. 1987, Long and Ward 1989b). A similar level of benzaldehyde inhibition (9.4-30 mM) was observed with *Candida utilis* (Wang 1993, Dissara 1996). According to Shin and Rogers (1995), three principal factors leading to the cessation of PAC production in a fermentation process include:

(1)   depletion of pyruvate at the end of the biotransformation phase,

(2)   deactivation of PDC caused by prolonged exposure to benzaldehyde and/or end-product inhibition,

(3)   progressive reduction in cell viability due to benzaldehyde as well as accumulated concentrations of benzyl alcohol and PAC.

An inefficient biotransformation with low PAC concentrations and productivities in whole cell batch fermentations has prompted interest by various research groups in the development of a fed-batch process using a variety of benzaldehyde feeding protocols (Becvarova et al. 1963, Vojtisek and Netrval 1982, Culic et al. 1984, Long et al. 1989, Seely et al. 1989a,b). These authors maintained a very low level of benzaldehyde during bioconversion phase to minimize substrate toxicity. Two to four doses of benzaldehyde feeding were used in these cases to generate a maximal PAC level between 40-80 mM (6-12 g l^{-1}).

An optimized multi-stage continuous biotransformation process for *C. utilis* was developed to overcome the cell 'wash-out' problem due to benzaldehyde which occurred in a single stage continuous system (Wijono 1991). A final PAC concentration and productivity of 71 mM and 3.1 mM h^{-1} were attained respectively in a 3-stage process.

Wang (1993) employed a thiamine-free defined medium in the fermentation and early biotransformation phases to limit activity of *C. utilis* PDC so that pyruvic acid could accumulate up to 170-227 mM (15-20 g l^{-1}). Addition of thiamine in later stage reactivated PDC activity with improved control of yeast metabolism and benzaldehyde feeding, a final PAC concentration of 148 mM was achieved with PAC productivity of 3.5 mM h^{-1}.

Cell immobilization has been employed by Seely et al. (1989b) using polyazetidine, and by other authors (Mahmoud et al. 1990b, Shin and Rogers 1995) using calcium alginate beads to create a diffusional barrier between the cells and benzaldehyde. Immobilizing matrices established a concentration gradient between cells and substrates/products resulting in two effects: (1) increased tolerance of cells towards benzaldehyde (up to 70 mM for *C. utilis*), in comparison to 50 mM for free cells (Shin and Rogers 1995) and (2) enhanced the production of PAC, however the by-product concentration, benzyl alcohol, also increased by about 40% compared to that of free *C. utilis* cells at 20$^{°}$C (Shin and Rogers 1995). Further extension of immobilized *S. cerevisiae* to a semi-continuous (up to seven cycles) and fed batch processes by Mahmoud et al. (1990b,c) resulted in maximum PAC concentration of 30 mM and 67 mM respectively. An improvement of PAC production reaching 80 mM was possible by addition of β-cyclodextrins (Mahmoud et al. 1990a). The truncated cone shape structure of the β-cyclodextrin may help protect PDC from the toxic substrate, benzaldehyde, by the mean of molecular encapsulation (Hedges 1998, Szejtli 1998). Shin and Rogers (1995) reported PAC formation in a single stage continuous and fed batch process using immobilized *C. utilis* and achieved a final concentration of PAC in the latter process of 101 mM.

An investigation on the biotransformation of benzaldehyde by live cells of *Rhizopus javanicus* by feeding initially with 10 mM benzaldehyde and subsequently with 20 mM benzaldehyde and 15 mM acetaldehyde every 2 h yielded 19 mM PAC in 8 h which corresponded to PAC productivity of 2.4 mM h^{-1} (Rosche et al. 2001).

The formation of a the by-product, benzyl alcohol (Figure 1.9), from benzaldehyde by alcohol dehydrogenase (ADH) and/or other non-specific oxidoreductases in the biotransformation using live cells (Rogers et al. 1997) limits the maximum PAC molar yield to 25-84% of the theoretical value (Ose and Hironaka 1957, Long and Ward 1989b, Mahmoud et al. 1990a,b,c, Tripathi et al. 1991, Rogers et al. 1997, Iding et al. 1998, Oliver et al. 1999, Rosche et al. 2001).

Benzaldehyde + NADH + H$^+$ $\xrightarrow{\text{ADH}}$ Benzyl alcohol + NAD$^+$
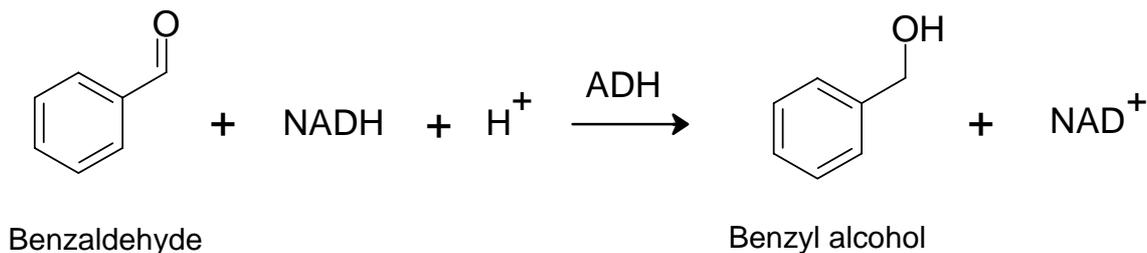
Figure 1.9: Mechanism of benzyl alcohol formation.

Other by-products may include acetoin, 2-hydroxy-1,1-phenylpropanone (Nikolova and Ward 1991), benzoic acid (Smith and Hendlin 1953), benzoin (an analog of PAC), butan-2,3-dione, 1-phenyl-propan-2,3-dione, acetyl benzoyl (Voets et al. 1973, Nikolova and Ward 1991), trans-cinnamaldehyde (Voets et al. 1973) and (1R,2S)-1-phenyl-1,2-propane-diol (Groger et al. 1966). The latter chemical species can occur when PAC is reduced by subsequent ADH activity. The loss of some benzaldehyde by evaporation may also contribute to a lower molar yield of PAC based on benzaldehyde consumed (Oliver et al. 1999).

Hitherto, there has been no successful procedure in eliminating the formation of benzyl alcohol in biotransformation processes using live whole cell cultures. Alternative approaches have been used instead to limit benzyl alcohol formation. Vojtisek and Netrval (1982) reported an improvement of 30% in overall PAC production when sodium pyruvate was externally added to *S. carlsbergensis* cultures. The carbon source replacement in the cultivation medium of glucose by pyruvate (Nikolova and Ward 1991) resulted in an elevated and more reproducible PAC yield. Kostraby et al. (2002) performed whole cell biotransformations with dried *S. cerevisiae* in petroleum spirit, an

organic solvent, at room temperature and at $5°C$ with addition of pyruvic acid. A decrease in benzyl alcohol concentration was observed with an increased conversion of benzaldehyde to PAC when 0.5 % (v/v) ethanol was added to the reaction medium. The amount of benzyl alcohol formed was also found to be inversely proportional to the level of pyruvic acid being employed. Further studies were carried out by substituting pyruvic acid with cheaper lactic acid. Although PAC was produced, its yield was lower with higher amount of benzyl alcohol being generated than for pyruvic acid addition (Laurence et al. 2002). The addition of pyruvate or pyruvic acid as a carbon source instead of glucose bypasses a crucial step in the glycolytic pathway (conversion of glyceraldehyde-3-phosphate to 1,3-bisphoglycerate with glyceraldehyde-3-phosphate dehydrogenase), which is necessary for the replenishment of NADH. Limitation of NADH regeneration, in turn, helps decrease the amount of benzyl alcohol being formed (Long and Ward 1989a,b).

According to Shin and Rogers (1995), benzyl alcohol was preferentially generated instead of PAC when the benzaldehyde was kept below 30 mM for both free and immobilized cells. The biotransformation predominantly produced PAC above 40 mM benzaldehyde. Although higher PAC was observed with immobilized cells compared to free cells, the benzyl alcohol production was also higher than for free cells over the range of benzaldehyde concentrations studied (7.5-38 mM).

1.4.2   Characteristics of PDC involved in biotransformation

1.4.2.1   Introduction

PDC is a thiamine pyrophosphate (TPP), also known as thiamine diphosphate (ThDP), and Mg^{2+} dependent enzyme which catalyses the non-oxidative cleavage (decarboxylation) reaction as well as the acyloin-type condensation (carboligation) reaction of C-C bonds (Iding et al. 1998, Sergienko and Jordan 2002). Furey et al. (1998) stated that PDC is probably one of the simplest of the TPP dependent enzymes. *In vivo*, PDC converts an end-product of the glycolytic pathway, pyruvate, to acetaldehyde, a key intermediate in the ethanol fermentation process. Both

decarboxylase and carboligase activities in fermenting yeast have been reported by Neuberg and coworkers (Neuberg and Karczag 1911, Neuberg and Hirsch 1921, Neuberg and Ohle 1922). However, it was not until almost four decades later that Hanc and Karac (1956) confirmed that the origin of these activities resided in the PDC extracted from the yeast. Since its discovery, PDC has been isolated from various organisms including bacteria, yeasts, fungi and plants (Bringer-Meyer et al. 1986, Pohl 1997, Iding et al. 1998, Konig 1998, Neuser et al. 2000).

1.4.2.2   *Structure of PDC*

PDC extracted from yeast and bacteria consists of four identical subunits with a molecular mass of 240-250 kDa (Furey et al. 1998, Konig 1998). Two of these subunits are tightly, but noncovalently, bound at the interface with TPP (Voets and Voets 1990, Kyte 1995) at pH values below 6.5 (Kern et al. 1997), creating a dimer. Ullrich and Donner (1970) found that pH had an influence on the binding strength of TPP to the binding sites of PDC. Two dimers or 'dimer of dimers' form a loose tetramer (Dyda et al. 1993, Arjunan et al. 1996). Each PDC subunit is a single polypeptide chain of 563 amino acids which is arranged into α, β and γ domains (Furey et al. 1998). Further details of the crystal structure and organization of PDC extracted from yeasts (*S. cerevisiae*, *S. uvarum*), the bacterium (*Zymomonas mobilis*) and germinating seeds of the plant *Pisum sativum* are given by Furey et al. (1998) and Konig (1998). The three-dimensional structure of PDC obtained from *Saccharomyces* sp. was reported by Dyda et al. (1993) and Arjunan et al. (1996). Cys-221 was found to be an essential component in substrate activation of PDC (Zeng et al. 1993, Baburina et al. 1994). Diagrams of a PDC tetramer are shown in Figure 1.10. Structures of Mg^{2+} and TPP binding sites are given in Figure 1.11.
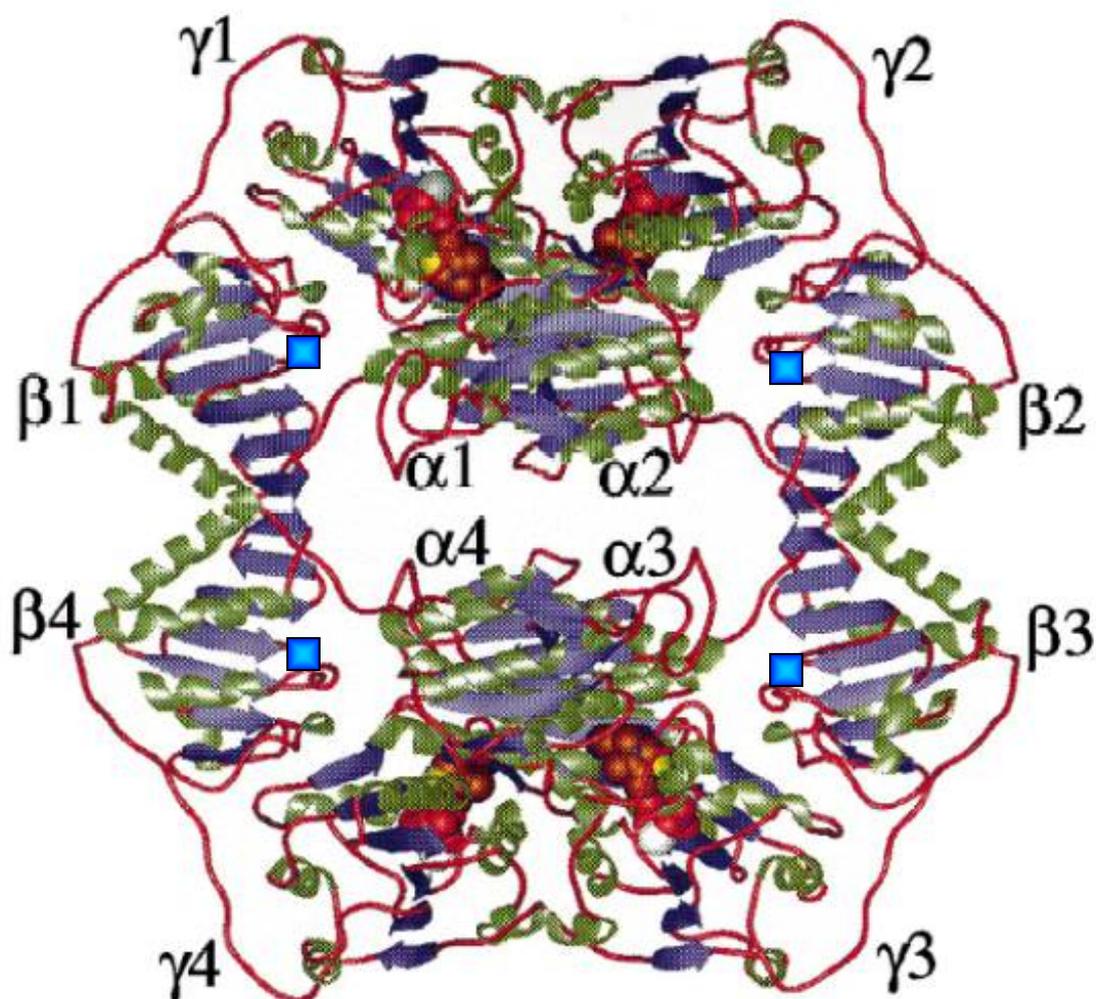
Figure 1.10: A complete ribbon drawing of PDC tetramer. The TPP and Mg^{2+} cofactors are shown as space filling representations. The side chains of Cys-221 which plays an essential role in substrate activation are also shown as blue boxes. (adapted with modification from Furey et al. 1998).
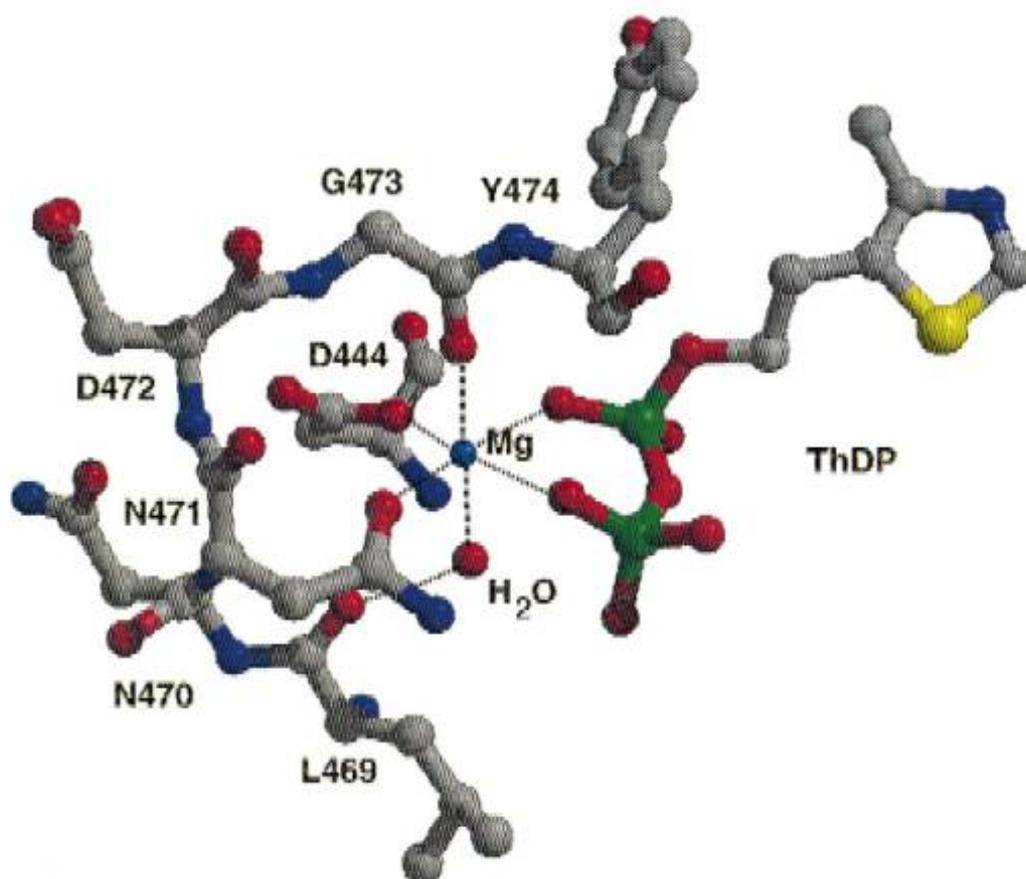
Figure 1.11: Structure of the Mg^{2+} binding site illustrating the octahedral coordination with the protein which also forms strong hydrogen bond with TPP (ThDP). The Figure was made with the program CHAIN (Furey et al. 1998).

1.4.2.3   *Reaction Mechanisms of PDC*

Lohmann and Schuster discovered in 1937 that TPP is the coenzyme of yeast PDC. The requirement of TPP in the decarboxylation reaction of pyruvate was demonstrated by Silverman and Werkman (1941) with *Aerobacter aerogenes*. TPP, once referred to as 'cocarboxylase' (Lohmann and Schuster 1937), is one of the best-known coenzymes (Krampitz 1969, Schellenberger 1998, Jordan 1999). The coenzyme alone can assist the decarboxylation reaction, however, the association of TPP with the apoenzyme at the active site in the PDC holoenzyme accelerates the reaction rate by 10^{12} times (Alvarez et al. 1991). The thiazolium ring of TPP (Figure 1.12) contains a reactive centre (C(2)-H) which can easily lose a proton to form a structure called a ylid (Mathews and van

Holde 1990). The reaction mechanism for pyruvate decarboxylation consists of four steps as follows: (a) nucleophilic attack by the ylid form of TPP on the carbonyl carbon of pyruvate, (b) departure of CO_2 to generate a resonance stabilized carbanion, (c) protonation of the carbanion and (d) release of free acetaldehyde (Voets and Voets 1990). Figure 1.13 described the details of PDC reaction mechanism.
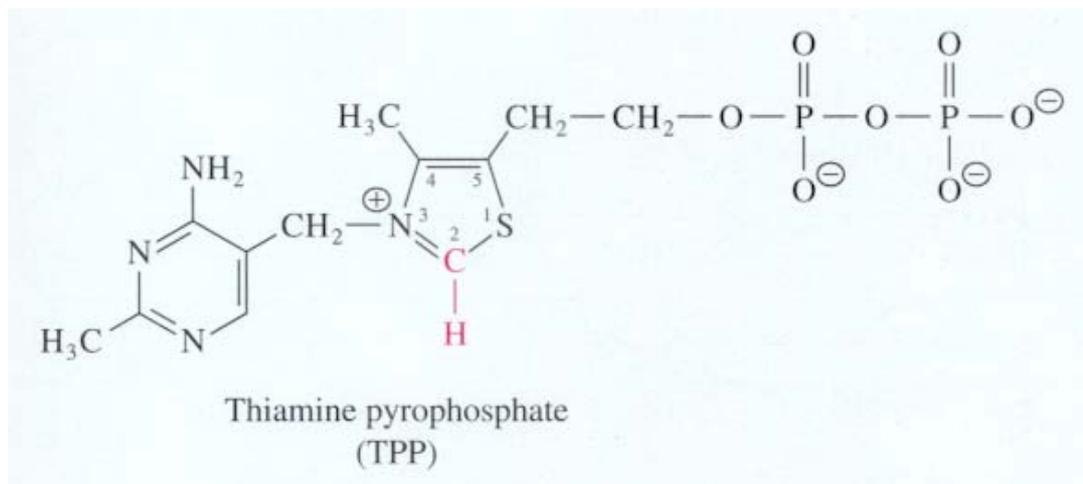
Figure 1.12: The thiazolium ring of TPP contains the reactive centre (red) of the coenzyme (Moran et al. 1994).

1.4.2.4   Role of 'active acetaldehyde'

The descriptive terms such as 'active acetaldehyde' or 'nascent acetaldehyde' were used by early researchers (Breslow 1957, 1958, Breslow and McNelis 1959, Holzer and Beaucamp 1959, Juni 1961) to account for the apparent central role of 2-(1-hydroxyethyl-TPP) in catalytic mechanism of PDC. This 'active acetaldehyde' represents two intermediates of the PDC associated TPP, which has a covalent bond to the C2 residue that originated from pyruvate, i.e.

(1)   hydroxyenamine (stable, low energy state and nonreactive intermediate),

(2)   α-carbanion (negatively charged, high energy state, highly reactive).

R^1 = 4'-amino-2-methyl-5-pyrimidyl

R^2 = β-hydroxyethylpyrophosphate

Figure 1.13: The TPP reaction mechanism on the active site of PDC (adapted from Voets and Voets 1990, Sergienko and Jordan 2002).

These two forms are resonance-stabilized mesomers. In the literature (Malandrinos et al. 2001, Ragsdale 2003), either forms or sometimes only one of the two forms have been referred to as 'active acetaldehyde' or hydroxyethyl-TPP also. The confirmation of hydroxyethyl-TPP was provided by Holzer and Beaucamp (1959) who showed that PDC was able to convert 2-^{14}C-labelled pyruvate to the appropriately labelled 2-([1-^{14}C]-1-hydroxyethyl-TPP).

The further term, 'active aldehyde', representing 2α-carbanion (Alvarez et al. 1991, Sprenger and Pohl 1999, Ragsdale 2003) was used to describe the more active intermediate in the TPP mediated catalytic pathway rather than the 2-(1-hydroxyethyl-TPP) side product. According to Sprenger and Pohl (1999), all TPP-bound enzymes produce 'active aldehyde' intermediates after certain decarboxylation reactions (e.g. PDC decarboxylation) or from a particular donor compound (e.g. xylulose-5-phosphate by transketolase).

1.4.3   Enzyme-based PAC biotransformation

1.4.3.1   Introduction

The application of purified PDC offers the opportunities to overcome the problem of benzyl alcohol formation and to improve molar yields of PAC based on benzaldehyde. While the growth rate of yeasts was greatly affected by benzaldehyde in the range of 10-30 mM, the effect of benzaldehyde toxicity for partially purified PDC from *C. utilis* on the initial rate of PAC formation was only evident at benzaldehyde concentrations higher than 180 mM (Rogers et al. 1997). Because pyruvate must be added to benzaldehyde in this mode of PAC production, there are other possibilities of side reactions leading to the formation of acetaldehyde via decarboxylation and subsequent condensation to acetoin (Figure 1.14). Carbon dioxide is generated also from pyruvate by PDC. The inhibitory effect of acetaldehyde on PAC formation had been reported by several authors (Gruber and Wassenaar 1960, Shin and Rogers 1996b). Recent investigation by Sandford (2002) also indicated a deleterious effect of acetoin on PDC.

1.4.3.2 *PDC from Candida utilis*

Since Shin and Rogers (1996a,b) reported the potential use of partially purified *C. utilis* PDC for the biotransformation of benzaldehyde and pyruvate to PAC, the interest of our group has shifted to characterize, further improve and optimize this enzymatic biotransformation process.

According to Shin and Rogers (1996b), the highest PAC concentration of 191 mM was attained at 7 U ml^{-1} decarboxylase activity, 200 mM benzaldehyde, 2.0 molar ratio of pyruvate to benzaldehyde, 2.0 M ethanol at pH 7.0 and 4°C for partially purified *C. utilis* PDC in 40 mM phosphate buffer. The elevated rates of acetaldehyde formation at higher temperatures (10 and 25°C) were more conducive to a faster rate of pyruvate depletion and possible by-product inhibition by acetaldehyde. As a result of this, the final PAC formation was enhanced at 4°C although the PAC productivity was lower. The maximum PAC concentration and productivity attainable from this system were 191 mM after 8 h and 23.9 mM h^{-1} respectively with molar yield of 95% based on benzaldehyde utilized.
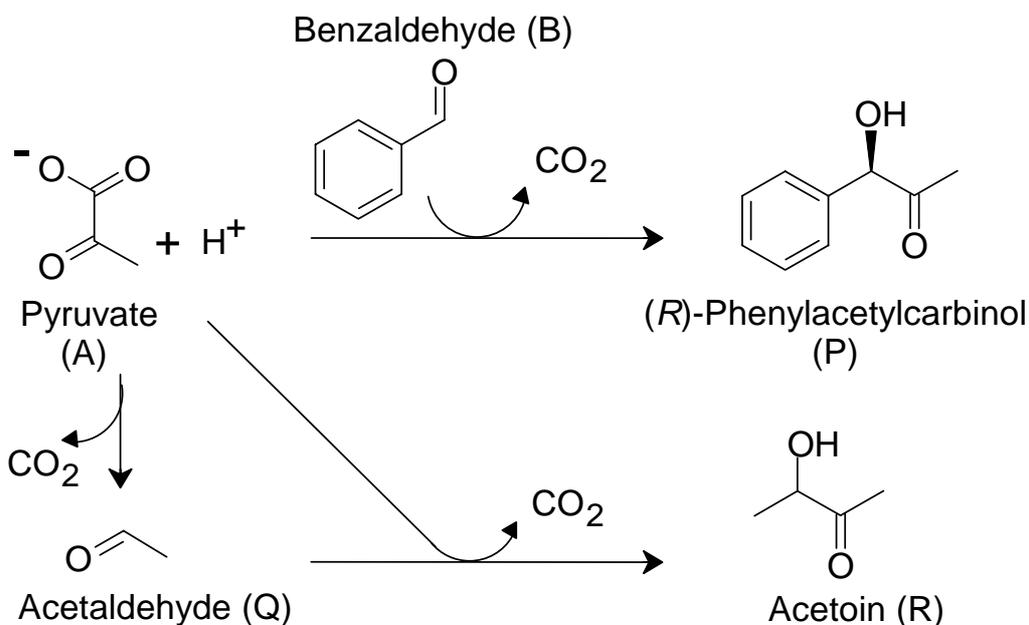
Figure 1.14: Formation of PAC and by-products by yeast PDC.

Furthermore Shin and Rogers (1996a) reported the application of immobilized PDC from *C. utilis* in both batch and continuous processes operated at 4°C. The maximum PAC concentration and productivity obtained from batch process was 181 mM after 16 h and 11.3 mM h^{-1} respectively, based on 300 mM benzaldehyde and 450 mM sodium pyruvate. For a continuous process, an average concentration of PAC formed was 30 mM with productivity of 3.7 mM h^{-1}, based on 50 mM benzaldehyde and 100 mM sodium pyruvate. Even though PDC in the immobilized form had longer half-life (32 days), the increased formation of by-products (acetaldehyde and acetoin) and a slower benzaldehyde uptake decreased PAC molar yield to 60% based on available benzaldehyde.

Chow et al. (1995) published a general decay equation with a time exponent constant of 0.5 to fit *C. utilis* PDC deactivation profiles within a benzaldehyde concentration range of 100-300 mM (11-32 g l^{-1}) in 40 mM phosphate buffer.

1.4.3.3   *PDC from Zymomonas mobilis*

Confirmation of PAC production from benzaldehyde and pyruvate using purified PDC from various sources, including *Z. mobilis, S. carlsbergenis, S. cerevisiae, S. fermentati* and *S. delbrueckii*, was demonstrated by several authors during the late 1980s to early 1990s (Bringer-Meyer and Sahm 1988, Cardillo et al. 1991, Crout et al. 1991, Kren et al. 1993). Bringer-Meyer et al. (1986) isolated and characterized PDC obtained from *Z. mobilis* then established the unsuitability of this enzyme for the biotransformation reaction in later studies (Bringer-Meyer and Sahm 1988). By comparison with yeast PDC (*Saccharomyces* sp., *Candida* sp.), bacterial PDC (*Zymomonas* sp.) had a lower level of benzaldehyde affinity and was subjected to considerable benzaldehyde inhibition (Bringer-Meyer and Sahm 1988, Ward and Singh 2000), even though the pyruvate affinity of the bacterial PDC was similar or higher than that of yeast PDC. PAC formation rate in yeast PDC was higher than *Z. mobilis* by almost 25 times (Bringer-Meyer and Sahm 1988) for the conditions investigated.

However the interest of bacterial PDC in biotransformation continued due to the fact that *Z. mobilis* PDC is considerably more stable than yeast PDC at room temperature with an enzyme half-life in the absence of benzaldehyde of well over 100 h (Bruhn et al. 1995, Iding et al. 1998). It is also able to utilize acetaldehyde as an alternative substrate to pyruvate in the production of PAC (Breuer et al. 2003). Advances in site-directed mutagenesis techniques have facilitated the production of mutant bacterial PDC with 5-6 times greater carboligase activity (Pohl 1997). A continuous process developed by Goetz et al. (2001) and Iwan et al. (2001) with PDC extracted from a potent mutant of *Z. mobilis* was used in a biotransformation process for conversion of acetaldehyde and benzaldehyde to PAC in an enzyme membrane reactor (EMR). A volumetric productivity (space-time yield) of 81 g l^{-1} day^{-1} was reported with final PAC concentration of 22 mM and molar yields of 45% (initial substrates), based on 50 mM reaction mixture of both aldehydes. However the ability of bacterial PDC to produce PAC using only benzaldehyde and acetaldehyde is not shared by yeast PDC. The screening of 105 yeast strains reported by Rosche et al. (2003b) confirmed no detectable carboligase activity with these substrates in any of cell-free yeast extracts.

Allosteric activation behaviour of PDC by substrate pyruvate or substrate analogue pyruvamide has been observed with PDC from all sources, except *Z. mobilis* (Boiteux and Hess 1970, Hubner et al. 1978). The presence of 100 mM inorganic phosphate was reported to have an inhibiting effect on purified PDC obtained from *S. carlsbergensis*, *S. cerevisiae* and *C. utilis* (Boiteux and Hess 1970, Van Dijken and Scheffers 1986, Van Urk et al. 1989).

1.4.3.4   PDC from filamentous fungi

Rosche et al. (2001) examined the PAC production potential of crude extracts obtained from 14 filamentous fungi spanning four classes, namely; Ascomycota (*Aspergillus* sp., *Fusarium* sp., *Neospora* sp.), Zygomycota (*Rhizopus* sp., *Mucor* sp.) and Basidomycota (*Polyporus* sp.). Each of the fungi had been selected for their abilities to produce ethanol (Singh et al. 1992, Skory et al. 1997), a property commonly shared among PDC producers. The crude extracts from *R. javanicus* and *Fusarium* sp. were the most

effective in converting 100 mM benzaldehyde and 150 mM sodium pyruvate to PAC at 23°C in a buffer containing 50 mM MES, pH 7.0, 20 mM MgSO$_4$ and 1 mM TPP. The PAC level obtained from *R. javanicus* crude extract was 78.5 mM after 20 h (3.9 mM h^{-1} of PAC productivity) with 90-93% enantiomeric excess.

Rosche et al. (2002a) confirmed that the proton consuming enzymatic biotransformation leading to the formation of PAC and its by-products (acetaldehyde and acetoin) required a reaction system with high buffering capacity to minimize the effect of enzyme inactivation at pH values above 7.5-8.0. In addition, stabilization of *R. javanicus* PDC could be achieved by application of 2-2.5 M MOPS, 2 M glycerol, 0.75 M sorbitol, 10% (w/v) polyethylene glycol and 1 M KCl. Although Shin and Rogers (1996a) established that an improved initial rate of PAC formation for *C. utilis* PDC could be achieved by the presence of 2 M ethanol with initial substrate concentration of 70 mM benzaldehyde, the same was not observed by Rosche et al. (2002a) with *R. javanicus* PDC at 100 mM benzaldehyde. Up to 337 mM PAC could be attained after 29 h at 6°C using 7.4 U carboligase ml^{-1} of *R. javanicus* PDC in 2.5 M MOPS buffer containing 400 mM benzaldehyde, 600 mM sodium pyruvate, initial pH 6.5, 20 mM MgSO$_4$ and 1 mM TPP. This improvement was independent on the source of PDC as the similar PAC concentrations and productivities were observed in a further investigation using *C. utilis* PDC with 2.5 M MOPS buffer.

The application of high buffer concentration and additives to stabilise PDC had been proposed also by other authors who showed that high concentrations of inorganic phosphate (up to 1.6 M) could stabilise PDC from a wild type and UV mutant of *S. cerevisiae* (Juni and Heym 1968a,b). In 1.0 M phosphate buffer, the half-life of PDC (extracted by 80% saturated (NH$_4$)$_2$SO$_4$) from a UV mutant of *S. cerevisiae* was improved by 3.1 times in comparison with that in 100 mM phosphate. It was suggested by these authors that the high phosphate concentration might have inhibited the proteolytic enzymes from deactivating PDC and prevented dissociation of TPP by a TPP-hydrolysing phosphatase. By contrast, it was found that PAC production was decreased by higher phosphate concentrations (Rosche et al. 2002a) which is consistent with the additional role of phosphate ions in causing reversible inhibition of PDC from

C. utilis (Van Urk et al. 1989), *S. carlsbergensis* (Boiteux and Hess 1970) and *S. cerevisiae* (Van Urk et al. 1989).

A common problem associated with biotransformation of PAC with a high concentration of Mg^{2+} (20 mM) is loss of substrate pyruvate. Rosche et al. (2003a) has improved the pyruvate stability in enzymatic production of PAC by lowering the Mg^{2+} concentration in biotransformation buffer while maintaining the same level of PAC. Using PDC extracted from *R. javanicus*, the molar yield of PAC on pyruvate utilised was improved from 59% to 74% when the Mg^{2+} was decreased from 20 to 0.5 mM. Enhancement from 67% (Shin and Rogers 1996b) to 89% molar yield was also reported for *C. utilis* PDC. In the reaction conditions with excess Mg^{2+}, the carboxyl group of pyruvate might form complexes with Mg^{2+} while the keto group of pyruvate might also be polarized by Mg^{2+}, which in turn results in pyruvate loss (Rosche et al. 2003a).

1.4.3.5 Acetolactate synthase from bacteria

Besides α-keto acid decarboxylases, the potential of other enzymes such as acetolactate synthase (acetohydroxyacid synthase, AHAS), transketolases and dehydrogenases in mediating the formation of C-C bonds was reported by Schorken and Sprenger (1998). Acetolactate synthase (EC 4.1.3.18) from *Escherichia coli* was shown recently by Engel et al. (2003) to be another effective catalyst for production of PAC. These authors showed that a biotransformation performed at $30^{\circ}C$ in a magnetically stirred 100 ml flask containing 50 ml of reaction mixture (40 mM (4.2 g l^{-1}) benzaldehyde, 70 mM (7.7 g l^{-1}) pyruvate and 10% (v/v) dimethyl sulfoxide (DMSO)) resulted in an PAC enantiomeric excess of more than 98% with molar yield of 87% based on theoretical value.

1.4.4   Bioprocess design: two-phase biotransformations

1.4.4.1   Introduction

The development of two-phase biotransformation systems is considered to be one of the four most significant advances (which include also: large-scale enzyme isolation, enzyme and cell immobilization and applications of recombinant DNA technology) in the field of biotransformation that have emerged over 1974-1994 (Lilly 1994). Two-phase biotransformations (also known as biphasic or extractive biotransformations) involve the application of two immiscible liquid phases in which reactants, by-products, product and biocatalyst partition differently (Schmid et al. 2001). According to Leon et al. (1998), the biocatalyst is usually contained in an aqueous phase while an organic solvent is used as the second phase. Alternatively, the terminology of aqueous two-phase system can be applied when the system is created from two polymer solutions or a polymer and a salt solution. Biphasic systems can also exist in the form of reverse micelles: structures of water droplets stabilized by a surfactant in an immiscible organic solvent (Martinek et al. 1986, Ballesteros et al. 1995, Liu et al. 1996, de Carvalho and Cabral 2000, Hari Krishna et al. 2002).

The incorporation of an additional phase (such as organic solvent) can offer several improvements over conventional aqueous monophasic systems which include increased substrate solubility and enhanced enzyme activity and specificity (Schmid et al. 2001). Yield improvements may be achieved by immediate product removal to another phase resulting in a lower level of product inhibition (Schmid et al. 2002). In some cases, the degree of products degradation is also minimized because the partitioning effect reduces the long-term contact between the product and biocatalyst. Overall volumetric productivity and product concentration may be enhanced by several fold with an appropriate *in situ* product recovery technique (Zijlstra et al. 1998, Schmid et al. 2002), which favors biotransformation by shifting the thermodynamic equilibrium and decreasing end-product inhibition (Leon et al. 1998). As a consequence, such processes may be operated continuously by recycling the biocatalyst-containing phase while the

biocatalyst-free product phase is available for further downstream processing (Zijlstra et al. 1998).

The review in this section focuses on the published results from our group for organic-aqueous two-phase biotransformation process with PDC from *C. utilis* and *Z. mobilis*. The principle of this system is shown in Figure 1.15.
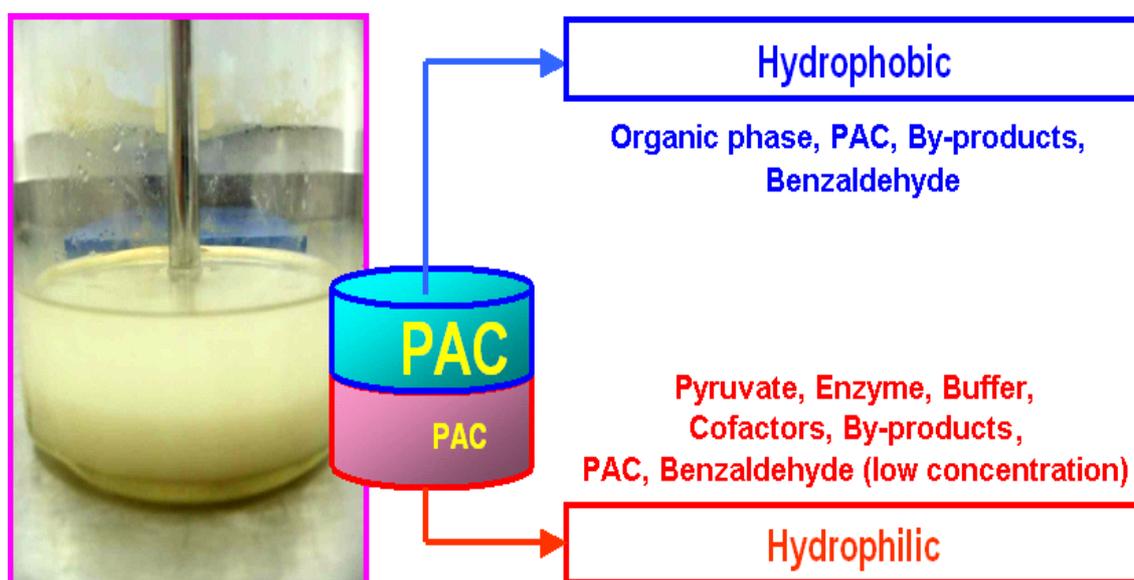
Figure 1.15: Partitioning of chemical species involved in the organic-aqueous two-phase enzymatic biotransformation of PAC (Diagram shows results for octanol-aqueous system).

1.4.4.2   *PDC from C. utilis*

In a preliminary evaluation of solvent suitability, Sandford (2002) investigated the effect of 13 solvents on PDC stability (aqueous phase contained 2 M MOPS, 1 mM TPP, 1 mM MgSO$_4$, pH 7.0, 4°C, PDC with initial carboligase activity of 7 U ml^{-1}, slow stirring and volume ratio of organic to aqueous phase of 1:1) and PDC production (organic phase contained 1.8 M benzaldehyde; aqueous phase contained 1.43 M pyruvate, 2 M MOPS, 1 mM TPP, 1 mM MgSO$_4$, pH 7.0, 4°C, PDC with initial

carboligase activity of 7.3 U ml^{-1} initial carboligase activity, rapid stirring and volume ratio of organic to aqueous phase of 1:1). Figure 1.16 illustrates PDC stability and production of PAC for various solvents in two-phase biotransformation process (Sandford 2002). Although methyl *tert*-butyl ether (MTBE), an octane enhancer commonly used in the gasoline (Elvers et al. 1990), was the only solvent exhibiting a positive effect toward PDC stability after 264 h exposure at 4°C, only 36 mM PAC was measured in the organic phase with an additional 43 mM in the aqueous phase. The highest level of PAC was observed when the organic phase was either octanol [organic phase: 670 mM, aqueous phase: 113 mM] or nonanol [organic phase: 605 mM, aqueous phase: 130 mM]. Both alcohols affected enzyme stability only moderately with 73-80% residual PDC activity after 264 h exposure at 4°C. Octanol was subsequently chosen over nonanol in subsequent studies based on the slightly higher level of PAC production.

Further evaluation in an octanol-aqueous two-phase reactor indicated that the rate of enzyme inactivation and PAC production were greater with rapidly stirred emulsion than with slowly stirred phase separated system. Up to 940 mM PAC in the octanol phase and 127 mM in the aqueous phase containing high concentration of MOPS (2-2.5 M) were attained after 49 h under optimized reactor conditions (Sandford 2002). This level of PAC production was significantly higher than that achieved in an aqueous single-phase benzaldehyde emulsion batch reactor of 333 mM (Rosche et al. 2002a).

1.4.4.3   PDC from Z. mobilis

Rosche et al. (2004a) investigated biotransformation of acetaldehyde and benzaldehyde to PAC in organic-aqueous two-phase system using PDC extracted from a potent mutant of *Z. mobilis* (PDCW392M). A maximum PAC concentration of 111 mM in the organic phase and 11.3 mM in the aqueous phase as well as specific PAC production up to 11 mg U^{-1} were obtained when 1-pentanol, 1-hexanol and isobutanol were used as organic phases.
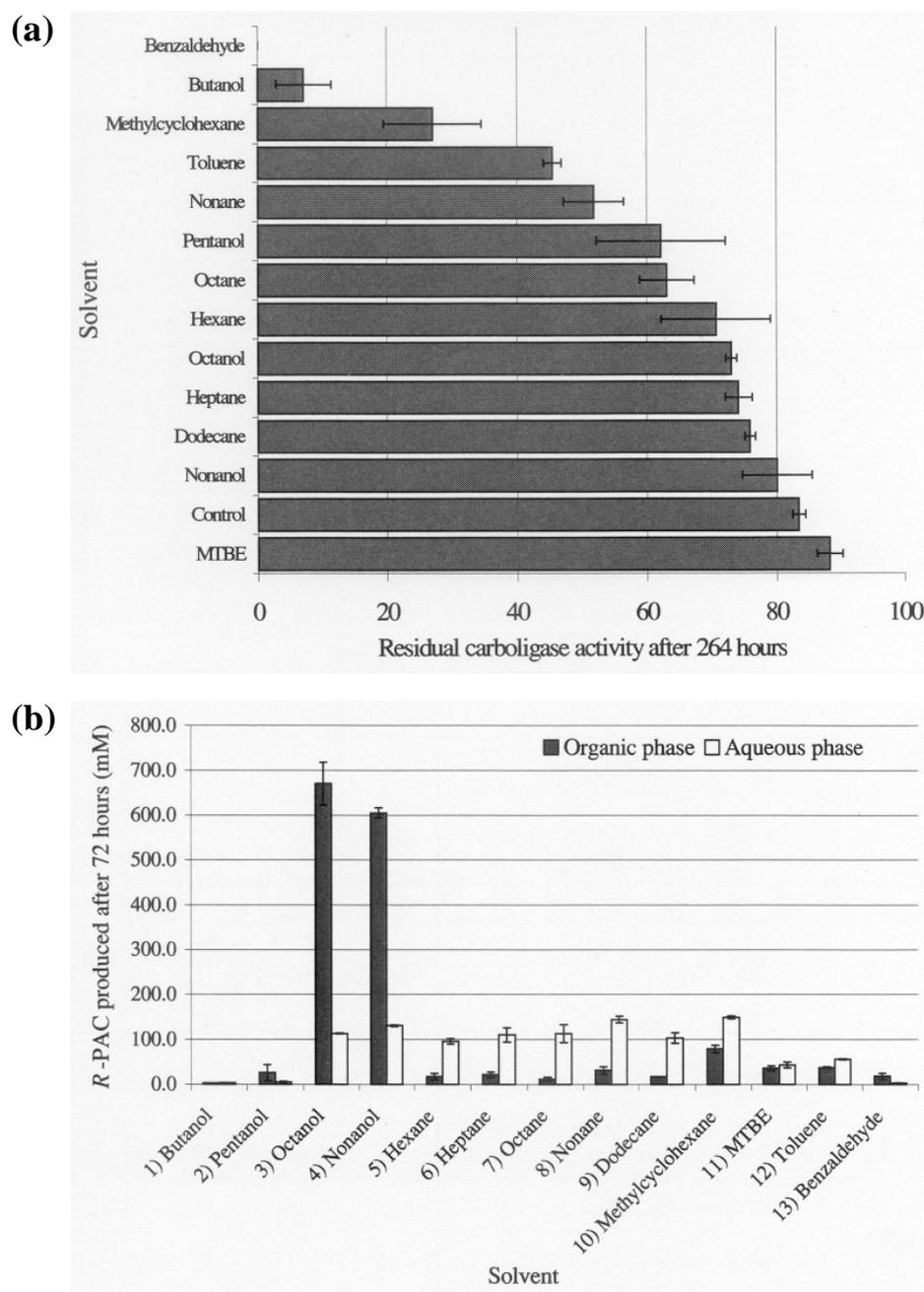
Figure 1.16: Comparison of enzyme stabilities and PAC production in the two-phase system using various organic phase solvents; (a) enzyme stability after 264 h [aqueous phase contained 2 M MOPS, 1 mM TPP and 1 mM $MgSO_4$ at pH 7.0, $4^{\circ}C$, slowly stirred with phase separation maintained and an initial carboligase activity of 7 U ml^{-1}]; (b) production of PAC after 72 h [organic phase contained 1.8 M benzaldehyde; aqueous phase contained 1.43 pyruvate, initial carboligase activity of 7.3 U ml^{-1}, 2 M MOPS, 1 mM TPP and 1 mM $MgSO_4$ at pH 7.0, $4^{\circ}C$, rapidly stirred]. The error bars represent the highest and lowest values (Sandford 2002).

1.4.5   Comparison of PAC biotransformation processes

Based on the results of our group with enzymatic PAC production, a comparison of the different biotransformation processes was made by Rosche et al. (2002b) using four criteria, namely:

(1)   PAC concentrations (Figure 1.17),

(2)   Molar PAC yields (%) based on pyruvate and benzaldehyde consumed (Figure 1.18),

(3)   Overall volumetric PAC productivities (g l^{-1} day^{-1}) (Figure 1.19) and

(4)   Specific PAC production (mg PAC U^{-1} PDC) (Figure 1.20).

As can be seen in Figure 1.17, partitioning of benzaldehyde into the organic phase in a two-phase system produced greater than 667 mM (100 g l^{-1}) of PAC, even at low initial enzyme activity (0.9 U carboligase ml^{-1}) in the phase-separated process. The final PAC production from this process was almost seven times higher than the typical values for the fermentation-based biotransformation. Such improvements are the result of separating the inactivating substrate benzaldehyde away from the PDC. A lower PAC concentration level of 333 mM was observed in an aqueous phase benzaldehyde emulsion process (Rosche et al. 2002b) in which greater PDC stability was achieved by using a high concentration (2.5 M) MOPS buffer.

One advantage of enzymatic biotransformation over the traditional yeast-based process is shown in Figure 1.18. In absence of ADH and/or other oxidoreductases, enzymatic biotransformations achieved PAC molar yields (based on benzaldehyde utilized) of more than 95% without the formation of benzyl alcohol. Pyruvate loss and formation of by-products acetaldehyde and acetoin (depending on conditions) accounted for the PAC molar yields based on pyruvate utilized ranging from 60-93% (Rosche et al. 2002b).

Both benzaldehyde emulsion and two-phase emulsions with a high level of PDC activity (8.4-8.5 U ml^{-1}) carboligase demonstrated improved overall volumetric productivities over the estimated values for the traditional fermentation process (Figure

1.19). Mass transfer limitations of benzaldehyde from organic to the aqueous phase which are dependent on the partition coefficient, the degree of turbulence and the ratio of interfacial area to aqueous phase volume, are likely to influence productivities in the two-phase-separated system (Rosche et al. 2002b).

A reverse trend to overall volumetric productivities was evident when values of specific PAC production (expressed per U PDC activity) are compared (Figure 1.20). The specific PAC production was the most efficient for the phase-separated two-phase systems with a low degree of agitation with the values of more than 140 mg PAC U^{-1} PDC observed in a phase-separated systems using *C. utilis* PDC with an initial carboligase activity of 0.9 U ml^{-1} (Rosche et al. 2002b).
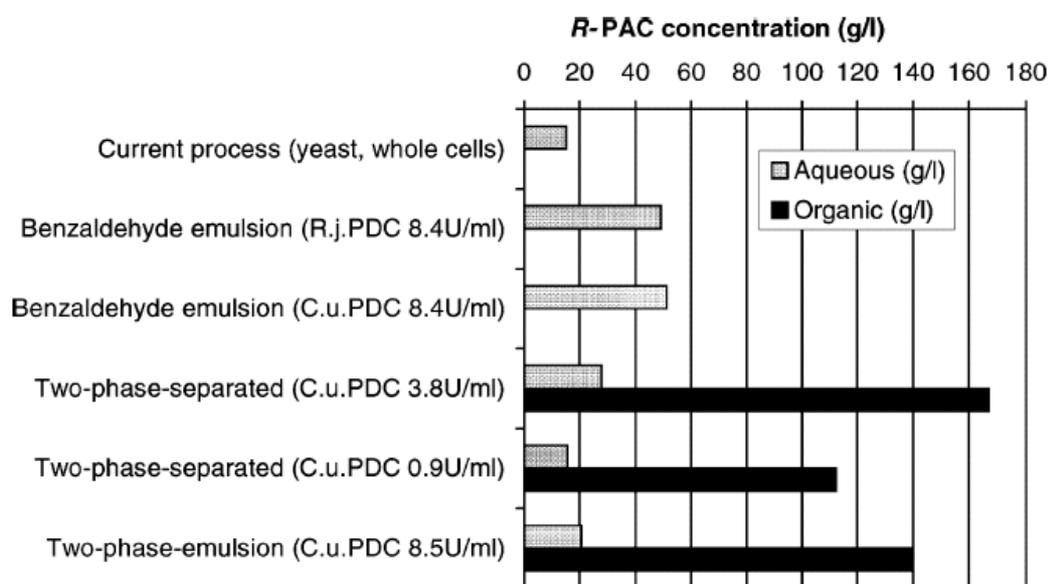
Figure 1.17: PAC concentrations of various processes (in both phases for two-phase systems). Enzyme activity is measured in from aqueous phase (yeast, *S. cerevisiae*; R.j., *R. javanicus*; C.u., *C. utilis*) (Rosche et al. 2002b).
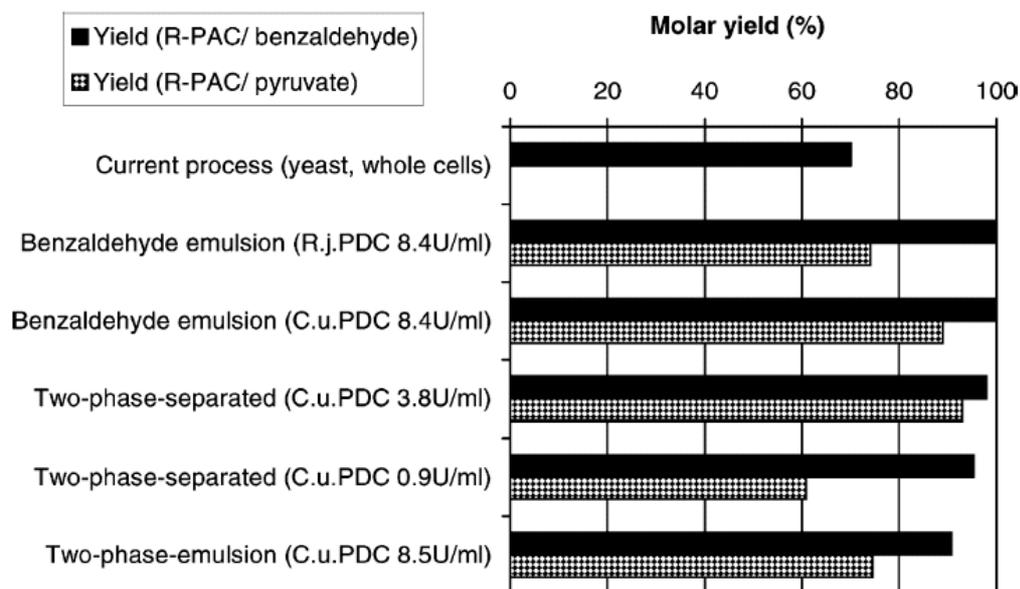
Figure 1.18: Molar PAC yields based on substrates benzaldehyde and pyruvate consumed. Yield on pyruvate for whole-cell-process is not available (see Figure 1.17 for abbreviations) (Rosche et al. 2002b).
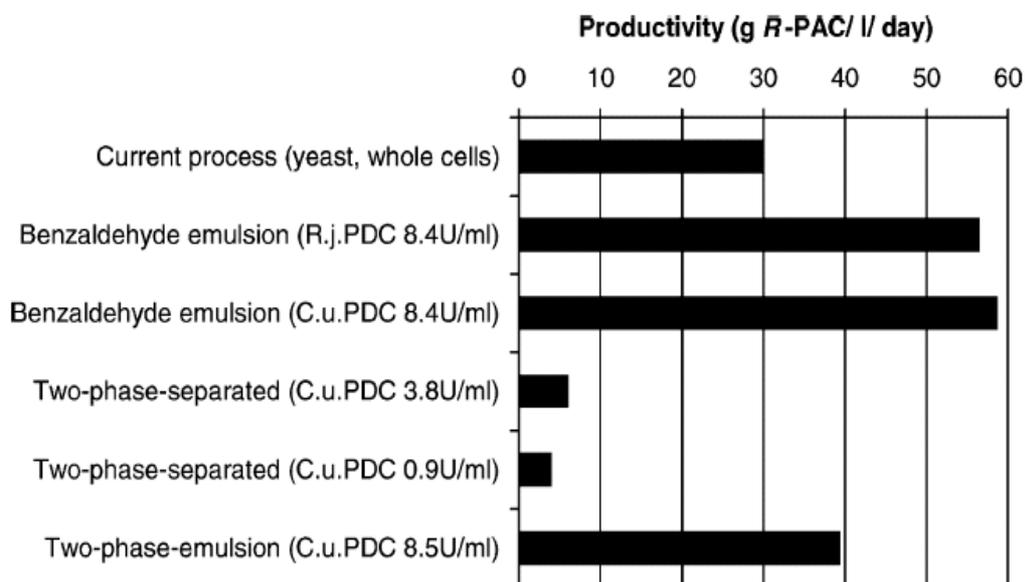
Figure 1.19: Overall volumetric PAC productivities (based on total reaction volume, see abbreviations on Figure 1.17) (Rosche et al. 2002b).
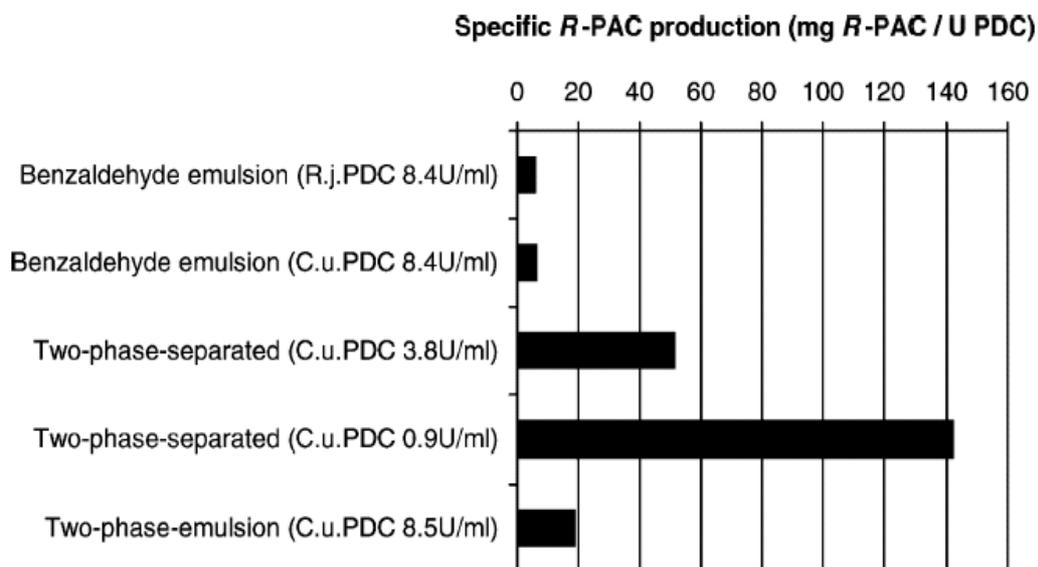
Figure 1.20: Specific PAC productivities based on added PDC (see abbreviations on Figure 1.17) (Rosche et al. 2002b).

1.5   NEW DEVELOPMENTS IN BIOTRANSFORMATION PROCESSES

1.5.1   Nonconventional media

A biotransformation reaction performed in an aqueous phase may be subjected to various limitations such as low solubilities of substrate and product, substrate and product toxicities, low yields, low productivities (Rogers et al. 1997) and product hydrolysis (Chen et al. 2001). To overcome these problems, numerous methods have been developed in nonconventional media (Hari Krishna 2002) by the use of organic cosolvent addition (Vinogradov et al. 2001, Wehbi et al. 2003, Yang et al. 2004), pure organic solvents (Stinson 2000, Klibanov 2001, Zaks 2001), micro-aqueous organic solvents (Giri et al. 2001, Panke and Wubbolts 2002, Thomas et al. 2002), reverse micelles (Ballesteros et al. 1995, de Carvalho and Cabral 2000), ionic liquids (Castro and Knubovets 2003, Rogers and Seddon 2003, Maruyama et al. 2004, Nara et al. 2004), supercritical fluids (Fontes et al. 2001, Da Cruz Francisco and Szwajcer Dey 2003, Knez et al. 2003), an aqueous-aqueous two-phase system (Sharma et al. 2003,

Cao et al. 2004, Katritzky et al. 2004), organic-aqueous two-phase systems (Panke et al. 2002, Schmid et al. 2002, Leon et al. 2003, de Carvalho et al. 2004, Hofstetter et al. 2004) and multiphase reaction media (Lamare and Legoy 1993, Straathof et al. 2002).

To select an appropriate system for a specific biotransformation process, one must consider a number of factors that usually vary from one process to another such as:

(1)   activity, specificity and stability of enzyme in a particular solvent (which solvent should be used?),

(2)   enzyme preparation (should the enzyme be lyophilized or dried in the presence of salts to improve catalytic activity (Ru et al. 2001) or immobilized in an appropriate type of support or matrix?),

(3)   properties of substrates and products (what is the volatility of the reactants in used?),

(4)   in addition, the biotransformation in multiphase reaction media involving a gas phase may be more attractive for the system involving highly volatile reactants than an organic-aqueous two-phase system (Halling 2001, Vulfson 2001).

According to Vulfson et al. (2001), several systems involving nonconventional media mentioned above are in the early stage of developments and their operational conditions have not yet been fully standardized. It is possible that media that are particularly efficient to one biotransformation system might not be suitable for another.

The application of nonconventional media opens the new production route for chemicals of interest which may include flavor esters, surfactants, emulsifiers, chiral drugs, biopolymers, proteins and various lipids. However due to a considerably lower activity exhibited by enzymes in such media relative to that in water, modification of the enzyme to suit a specific production system may become necessary (Hari Krishna 2002).

1.5.2   Enzyme developments/modification

De novo development of new biocatalysts may be possible through protein engineering (Burton et al. 2002, Breuer and Hauer 2003, Cherry and Fidantsef 2003) by directed evolution techniques (Iverson and Breaker 1998, Schmidt-Dannert and Arnold 1999, Kim et al. 2004) and enzyme engineering (Schmid et al. 2001). For example, production of *L*-methionine from hydantoinase was improved by five fold following random mutagenesis and saturation mutagenesis of the enzyme (May et al. 2000). Whereas molecular evolution focuses mainly on the modification of structure, selectivity and function of enzymes in aqueous media, modification of the enzyme microenvironment can also enhance its activity in the nonaqueous phase (Schmid et al. 2001).

In an evaluation of various methods for enhancing enzyme stability, Betancor et al. (2004) conjugated the surface of three different enzymes: namely glucose oxidase, *D*-amino acid oxidase and trypsin, with a low-cost dextran-aldehyde. This treatment was effective in enhancing the stability of all three enzymes. The coated enzymes remained fully active or highly active for more than 10 h in the presence of organic-aqueous and air-liquid interfaces while the unmodified oxidases lost at least 50% of activity in the first hour of experimentation. About 38% of activity for untreated trypsin remained after 12 h in comparison with 100% activity maintained over this period by the dextran-aldehyde conjugated trypsin.

1.5.3   Bioreactor design and operation

Extractive biotransformation described in the previous section is still in the early stage of large-scale development despite a number of research developments in this area. The industrial sector has been slow to adopt the technology because further studies on the feasibility of such processes are required to prevent a possible explosion hazard (in some cases) while maintaining optimum production efficiency (Leon et al. 1998). For volatile organic solvents, Schmid et al. (1998, 1999) proposed four strategies for safe operation of a two-phase aerobic cultivation of *Pseudomonas oleovorans* which included: decreasing the flammability of the organic solvent, operating within an

explosion proof reactor, maintaining the operating pressure above a minimum level and maintaining the oxygen concentration within the reactor headspace and exhaust below a critical value.

A recent example of new bioreactor design is the production of alkoxy phenylphosphine which was enhanced by up to 80,000 times using an ionic liquid phase (BASIL bioreactor) by comparison with the conventional process. This is the first industrial process based on room temperature ionic liquid technology and was developed by BASF (Figure 1.21) (Rogers and Seddon 2003, Seddon 2003). The term "ionic liquid" is used to describe a liquid that contains only ions at a temperature below 100°C. The advantages of such technology include the improvements of enzyme activity, stability and selectivity by employing the environmental-friendly ionic liquids ("green solvents") such as tetrafluoroborate and hexafluorophosphate (Hari Krishna 2002, Rogers and Seddon 2003).

Figure 1.21: A BASIL reactor. The upper phase contains the solvent-free pure product while the lower phase is ionic liquid (Rogers and Seddon 2003, Seddon 2003).

A dynamic model describing the growth-associated biotransformation of glucose to gluconic acid by an immobilised *Gluconobacter oxydans* was developed (Beschkov and Velizarov 2000). The model incorporated a product inhibition term and mass transfer equations that were subsequently used in the profiles prediction of substrates, products and biomass as well as performance evaluation of the process.

The need for high product concentrations in commercial processes often results in the investigation of several organic-aqueous two-phase systems on pilot scale (Schmid et al. 2002). An example of the successful pilot-scale application to an organic-aqueous two-phase system is the production of *S*-styrene oxide from epoxidation of styrene catalysed by recombinant *Escherichia coli* using 50% (v/v) dioctylphthalate/buffer two-phase system. An average productivity of 10.2 mM h^{-1} was obtained with 32.3 g *S*-styrene oxide l^{-1} recovered in the organic phase (Panke et al. 2002).

1.5.4   Economic considerations

Mathys et al. (1998a,b, 1999) performed an economic evaluation of a two-phase process for the bioconversion of n-octane to 1-octanol by a recombinant whole-cell catalyst from *P. oleovorans*. Figure 1.22 breaks the associated cost of such process down to costs of nutrients required for cell growth, cost of organic solvents and other expenses for an annual 1-octanol production of 10,000 tons. From this analysis it is evident that a significant proportion (more than 50%) of the costs are associated with the operation of the bioreactor through nutrients and water (42%) and organic solvents (11%). Thus this economic evaluation indicates the importance of operating the two-phase process at optimal or close to optimal conditions.
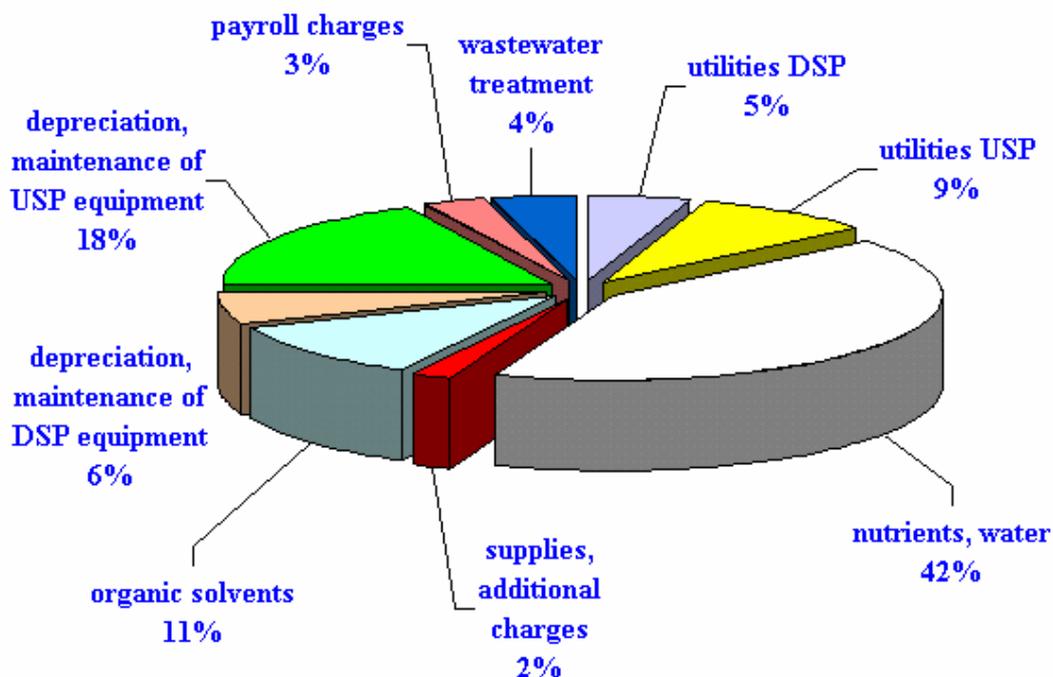
Figure 1.22: Breakdown of 1-octanol production costs from n-octane in a fed-batch two-phase system for an annual production of 10,000 tons; USP is up stream processing and DSP is down stream processing [adapted with modification from Schmid et al. (1998) and Mathys et al. (1999)].

Willeman et al. (2002a) developed a process model for the enzymatic production of (*R*)-cyanohydrins in an organic-aqueous two-phase batch system performed at pH 5.5 and 5°C with MTBE as the organic phase. This model approach was later extended by the same group (Willeman et al. 2002b) to calculate the optimum aqueous phase volume fraction (17% (v/v)) and required enzyme concentration (28.6 g l^{-1} aqueous phase) at 20°C for a batch-operated stirred tank reactor using cost estimations of enzyme and reactor use (Figure 1.23).
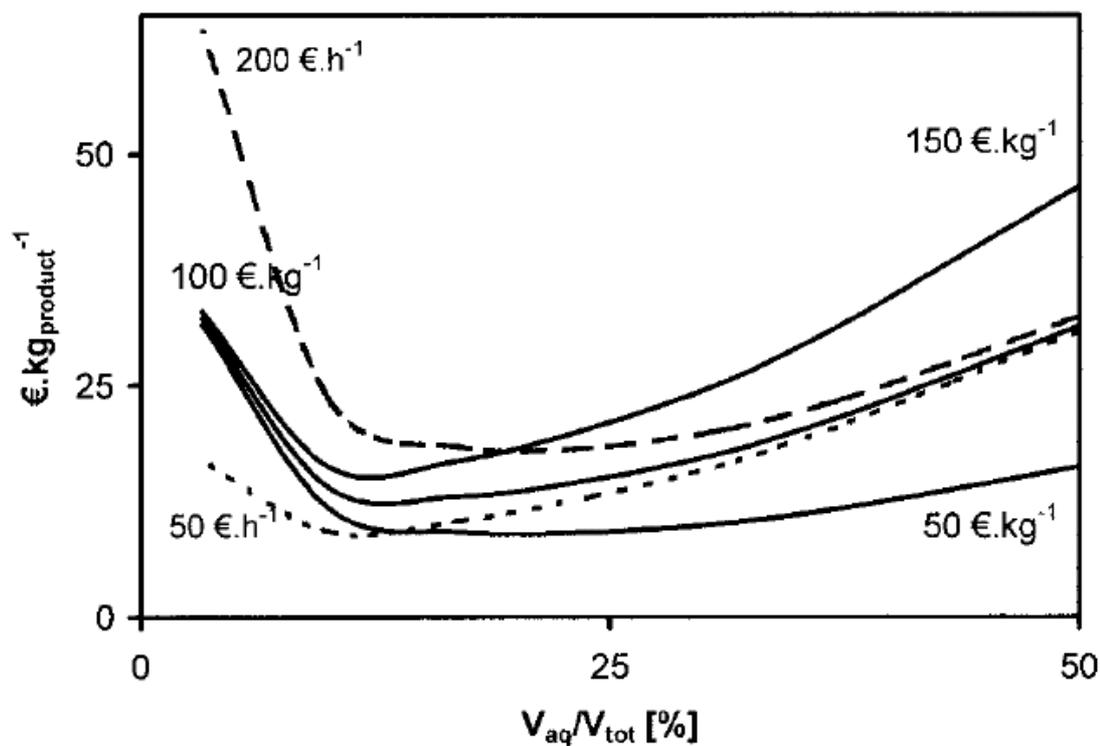
Figure 1.23: Costs estimation of the percentage of aqueous phase volume to the total volume (3.4-50% (v/v)) used in the organic-aqueous two-phase process of cyanohydrins production based on the enzyme costs and reactor use. The full lines illustrate the cases in which the reactor costs are 100 Euro h^{-1} and where the enzyme costs range from 50-150 Euro kg^{-1}. The dashed lines represent the cases in which the enzyme costs are 100 Euro kg^{-1} and the reactor costs are between 50-200 Euro h^{-1} (Willeman et al. 2002b).

Chapter 2

Materials and Methods

2.1   MICROORGANISMS

The filamentous fungal strain *Rhizopus javanicus* NRRL 13161 was kindly provided by Dr. R.J. Bothast and Dr. K. O'Donnell from the National Centre for Agricultural Utilization Research (Peoria, Ill.).

The yeast *Candida utilis* strain 70940 was obtained from the Culture Collection of the School of Biotechnology and Biomolecular Sciences, University of New South Wales, Sydney, Australia (World Culture Collection Number 248).

The stock cultures of both organisms were kept at -20°C.

2.2   CHEMICALS AND PROTEINS

Table 2.1: Sources of important chemicals and proteins used in the experiments

Names	Formula	Suppliers
2-[N-morpholino]ethanesulfonic acid (MES)	$C_6H_{13}NO_4S$	Sigma, Cat. No. M8250
3-[N-morpholino]propanesulfonic acid (MOPS)	$C_7H_{15}NO_4S$	Sigma, Cat. No. M1254
Acetaldehyde	C_2H_4O	Fluka, Cat. No. 00071
Acetic acid, glacial	CH_3COOH	APS, Cat. No. 10001
Acetoin	$C_4H_8O_2$	Fluka, Cat. No. 00540
Acetone	CH_3COCH_3	LAB-SCAN, Cat. No. A3501
Acetonitrile – 190 grade	CH_3CN	APS, Cat. No. 2315
Alcohol dehydrogenase (ADH)	-	Sigma, Cat. No. A7011
Ammonium sulphate	$(NH_4)_2SO_4$	APS, Cat. No. 56
Antifoam (polypropylene glycol)	-	Fluka, Cat. No. 81380
Azoalbumin	-	Sigma, Cat. No. A2382

Names	Formula	Suppliers
Bacteriological agar	-	Oxoid, Code L11
Benzaldehyde	C_6H_5CHO	APS, Cat. No. 781
Benzoic acid	$C_7H_6O_2$	Sigma, Cat. No. B7521
Bovine serum albumin (BSA), fraction V	-	Sigma, Cat. No. A3059
Calcium chloride dihydrate	$CaCl_2.2H_2O$	APS, Cat. No. 127
Citric acid, anhydrous	$C_6H_8O_7$	Sigma, Cat. No. C0759
Coloured coded buffer, pH 4	-	Merck, Cat. No. 19239.5W
Coloured coded buffer, pH 7	-	Merck, Cat. No. 19240.5H
Copper (II) sulphate, hydrated	$CuSO_4.5H_2O$	APS, Cat. No. 10091
Decyl alcohol	$C_{10}H_{22}O$	Aldrich, Cat. No. 15058-4
Dipropylene glycol (DPG)	$C_6H_{14}O_3$	Merck, Cat. No. 8.03265
Di-sodium hydrogen orthophosphate dodecahydrate	$Na_2HPO_4.12H_2O$	APS, Cat. No. 10248
EDTA-free cocktail tablets	-	Boehringer Mannheim, Cat. No. 1873580
Electrode cleaner, pepsin/HCl	-	Ingold, Order No. 209891250
Electrolyte viscolyt	-	Mettler Toledo, Order No. 20 9816 250
Electrolyte, 1 M LiCl in acetic acid	-	Mettler Toledo, Order No. 51340051
Ethanol, absolute	C_2H_5OH	APS, Cat. No. 214
Ethylenediaminetetra-acetic acid (EDTA) di-sodium salt	EDTA-$Na_2H_2.2H_2O$	APS, Cat. No. 180
Glucose (*D*-) anhydrous	$C_6H_{12}O_6$	APS, Cat. No. 783
Heptanol	$C_7H_{16}O$	Fluka, Cat. No. 51790

Names	Formula	Suppliers
Hexanol	$C_6H_{14}O$	Fluka, Cat. No. 52830
Hydrochloric acid	HCl	FSE, Cat. No. H/1100/PB17AU
Isopropanol (propan-2-ol)	C_3H_8O	APS, Cat. No. A425
Lactate dehydrogenase (LDH), from rabbit muscle suspension	-	Roche, Cat. No. 127876
Magnesium sulphate, hydrated	$MgSO_4.7H_2O$	APS, Cat. No. 302
Methanol	CH_3OH	APS, Cat. No. 318
Methanol (HPLC grade)	CH_3OH	APS, Cat. No. 2314
Methylcyclohexane	C_7H_{14}	BDH, Cat. No. 29221
Milli-Q (MQ) water	H_2O	Millipore, Cat. No. PF00671
n-heptane	C_7H_{16}	BDH, Cat. No. 28473
n-hexane	C_6H_{14}	APS, Cat. No. 2320
Nicotinamide adenine dinucleotide, reduced form, disodium salt, (NADH)	$C_{21}H_{27}N_7O_{14}P_2Na_2$	Roche, Cat. No. 92464233
n-octane	C_8H_{18}	Fluka, Cat. No. 74823
Octanol	$C_8H_{18}O$	APS, Cat. No. 2370
Paraffin	-	APS, Cat. No. 356
Pentanol	$C_5H_{12}O$	Aldrich, Cat. No. 13897-5
Pepstatin A	-	Boehringer Mannheim, Cat. No. 253286
Phosphoric acid	H_3PO_4	APS, Cat. No. 371
Potassium chloride	KCl	APS, Cat. No. 383
Potassium dihydrogen orthophosphate	KH_2PO_4	APS, Cat. No. 391
Potassium hydroxide pellets	KOH	APS, Cat. No. 10210
Proteinase K (40 U mg^{-1})	-	ICN Biomedicals, Cat. No. 193504

Names	Formula	Suppliers
Pyroneg	-	Diversey
Reactivation solution for glass electrodes (diluted HF/HCl)	-	Ingold, Order No. 9895
R-phenylacetylcarbinol (PAC)	$C_9H_{10}O_2$	BASF, Germany
Sodium hydrogen carbonate	$NaHCO_3$	APS, Cat. No. 475
Sodium hydroxide pellets	$NaOH$	APS, Cat. No. 482
Sodium pyruvate (pyruvic acid, sodium salt)	$C_3H_3NaO_3$	Fluka, Cat. No. 15990
Sulfuric acid	H_2SO_4	AlliedSignal, Cat. No. 30743
Thiamine pyrophosphate (TPP)	$C_{12}H_{19}ClN_4O_7P_2S$	Sigma, Cat. No. C8754
Trichloroacetic acid solution (TCA)	-	Sigma, Cat. No. T4396
Triethanolamine hydrochloride	$C_6H_{15}NO_3.HCl$	Sigma, Cat. No. T1502
Yeast extract	-	Oxoid, Code L21

2.3   MEDIA

All seed and cultivation media were prepared at a 1.1 fold concentration so that addition
of a 10% (v/v) inoculum resulted in the specified concentrations. Antifoam, 0.025%
(v/v) polypropylene glycol, was added separately for cultivations carried out in 5 and 30
l bioreactors. Reverse osmosis (RO) water was used in all preparations of media. All
media were sterilized at 121°C and 1 atm for 15 min using autoclave (Atherton) prior to
addition to sterilized bioreactors. Concentrated solutions of glucose, yeast extract and
salts were mixed aseptically in a laminar flow chamber (Email Westinghouse) after
cooling.

2.3.1   Agar medium for *R. javanicus*

Glucose	40.0	g l^{-1}
Yeast extract	10.0	g l^{-1}
KH$_2$PO$_4$	3.0	g l^{-1}
Na$_2$HPO$_4$.12H$_2$O	2.0	g l^{-1}
MgSO$_4$.7H$_2$O	1.0	g l^{-1}
(NH$_4$)$_2$SO$_4$	10.0	g l^{-1}
CaCl$_2$.2H$_2$O	0.05	g l^{-1}
Agar	15.0	g l^{-1}

2.3.2   Cultivation medium for *R. javanicus*

Glucose	90.0	g l^{-1}
Yeast extract	10.0	g l^{-1}
KH$_2$PO$_4$	3.0	g l^{-1}
Na$_2$HPO$_4$.12H$_2$O	2.0	g l^{-1}
MgSO$_4$.7H$_2$O	1.0	g l^{-1}
(NH$_4$)$_2$SO$_4$	10.0	g l^{-1}
CaCl$_2$.2H$_2$O	0.05	g l^{-1}

After solution mixing the pH of medium was 5.8-6.0 at 25°C. For the study on the effect
of yeast extract concentration, the yeast extract concentration was varied from 0-50 gl^{-1}.

2.3.3 Agar medium for *C. utilis*

Glucose	30.0	g l^{-1}
Yeast extract	5.0	g l^{-1}
KH$_2$PO$_4$	3.0	g l^{-1}
Na$_2$HPO$_4$.12H$_2$O	2.0	g l^{-1}
MgSO$_4$.7H$_2$O	1.0	g l^{-1}
(NH$_4$)$_2$SO$_4$	10.0	g l^{-1}
CaCl$_2$.2H$_2$O	0.05	g l^{-1}
Agar	15.0	g l^{-1}

2.3.4 Preseed and seed media for *C. utilis*

Glucose	10.0	g l^{-1}
Yeast extract	5.0	g l^{-1}
KH$_2$PO$_4$	3.0	g l^{-1}
Na$_2$HPO$_4$.12H$_2$O	2.0	g l^{-1}
MgSO$_4$.7H$_2$O	1.0	g l^{-1}
(NH$_4$)$_2$SO$_4$	10.0	g l^{-1}
CaCl$_2$.2H$_2$O	0.05	g l^{-1}
MES	39.0	g l^{-1} (pH adjusted to 6.0)

After solution mixing, the pH of each medium was 5.8-6.0 at 25°C.

2.3.5 Cultivation medium for *C. utilis*

The same cultivation medium as for *R. javanicus* was used for growth of *C. utilis* in the 5 and 30 l bioreactors.

2.3.6 Concentrated feed solution for *C. utilis*

Glucose	277	g l^{-1}
Yeast extract	61.5	g l^{-1}

2.4   BUFFERS

Reverse osmosis (RO) water was used in all buffer preparations. The pH adjustments were performed with 5 M H_2SO_4 or KOH unless stated otherwise. Inorganic salts and other chemicals used as additives in an aqueous phase for two-phase biotransformation were all Reagent Grade.

2.4.1   Breakage buffer for *R. javanicus*

MES	50	mM
$MgSO_4.7H_2O$	20	mM
TPP	0.5	mM

The pH was adjusted to 7.0 at 6°C.

2.4.2   Breakage buffer for *C. utilis*

Citric acid	200	mM
$MgSO_4.7H_2O$	20	mM
TPP	0.5	mM

The pH was adjusted to 6.5 at 6°C.

2.4.3   Deactivation buffer I

MOPS	600	mM
$MgSO_4.7H_2O$	20	mM (unless stated otherwise)
TPP	0.5	mM

The pH was adjusted to 7.0 at 6 or 25°C. For the study on the effect of pH on PDC half-life, the pH was varied from 3 and 5-8.

2.4.4 Deactivation buffer II

MOPS	2.5	M
$MgSO_4.7H_2O$	1	mM
TPP	1	mM
Benzaldehyde	varied concentrations	

The range of benzaldehyde concentrations investigated was between 0-200 mM. The pH was adjusted to 7.0 at $6^{°}C$ before use.

2.4.5 Biotransformation buffer

MOPS	2.5	M
$MgSO_4.7H_2O$	1	mM
TPP	1	mM
Sodium pyruvate	various concentrations, as specified	
Benzaldehyde	various concentrations, as specified	

The range of initial concentrations were 60-180 mM sodium pyruvate and 50-150 mM benzaldehyde. The pH was adjusted to 7.0 at $6^{°}C$ before use.

2.4.6 Aqueous phase biotransformation buffer

MOPS	20 mM or 2.5 M	
$MgSO_4.7H_2O$	1	mM
TPP	1	mM
Sodium pyruvate	various concentrations, as specified	
Chemical additives	various species and concentrations, as specified	

In the organic-aqueous two-phase biotransformation studies with pH control, the range of sodium pyruvate concentrations was 0.60-1.83 M with 2.5 M DPG as an chemical additive (where specified). Sodium pyruvate was not added to the aqueous phase biotransformation buffer used in benzaldehyde partitioning studies. The pH was adjusted to 7.0 at $6^{°}C$ before use.

2.4.7 Initial rate buffer for solvents/chemical additives selection

MOPS	20 mM or 2.5 M	
MgSO$_4$.7H$_2$O	1	mM
TPP	1	mM
DPG	0-2.5	M
Sodium pyruvate	120	mM
Benzaldehyde	100	mM

The pH was adjusted to 7.0 at 6°C.

2.4.8 Citrate buffer

Citric acid	200	mM

The pH was adjusted to 6.0 at 25°C.

2.4.9 Collection buffer

Citric acid	400	mM
MgSO$_4$.7H$_2$O	40	mM
TPP	4	mM

The pH was adjusted to 6.0 at 25°C.

2.4.10 Carboligase buffer

Citric acid	200	mM
MgSO$_4$.7H$_2$O	20	mM
TPP	2	mM
Sodium pyruvate	200	mM
Benzaldehyde	80	mM
Ethanol	3	M

The buffer was stored in 50 µl aliquot at 6°C for less than a week or at -20°C for a maximum of two weeks. The pH was adjusted to 6.4 at 25°C before use.

2.4.11 Triethanolamine buffer

Triethanolamine-HCl	250	mM
EDTA-disodium salt	2.5	mM

The pH was adjusted to 7.6 with 5 M NaOH at 25°C.

2.4.12 NADH buffer

NADH-disodium salt	7	mM
NaHCO$_3$	120	mM

The pH adjustment was not necessary for this buffer.

2.5 ORGANIC PHASES

Corresponding concentrations of benzaldehyde were dissolved in various types of Reagent Grade solvents, including: decyl alcohol, hexanol, heptanol, methylcyclohexane, n-heptane, n-hexane, n-octane, paraffin, octanol and pentanol, to form organic phases. Cooking oils (grapeseed oil, corn oil, canola oil and olive oil), used as alternative solvents in the studies, were purchased from a local supermarket.

2.6   PROTEASE INHIBITORS

One to two EDTA-free cocktail tablets per 10 ml buffer were used as serine and cysteine protease inhibitors. Pepstatin A, 0.7-7 μg ml^{-1} and 1 or 5 mM EDTA-disodium salt were employed to inhibit aspartate and metallo-proteases.

2.7   SPORE PRODUCTION AND HARVESTING

Spores of *R. javanicus* were produced by aseptically inoculating agar medium (approx. 5 mm thick) in wide neck flasks (5 cm neck dia. and 12 cm height) with 10 μl of spore suspension stock. The cultures were maintained at 30°C for 7 days. To harvest the spores from the mycelium, 30 ml sterile RO water was added aseptically to the flasks, the hyphae were then brushed lightly with a sterile spatula for 2 min to detach the spores. The concentrated spore suspensions were pooled and the spore concentration was determined microscopically by counting using a Thoma slide (Hawksley, England). For subsequent inoculation, the suspension was diluted with sterile RO water to give a final spore count of approximately 1.2×10^7 spores ml^{-1}. It was stored at -20°C in 10 ml aliquots. The spore inocula used in all cultivations were less than 30 days old.

2.8   GROWTH OF PRESEED AND SEED

The subculturing of *C. utilis* to a new agar medium incubated at 30°C was performed every 3-5 days. One inoculation loop of *C. utilis* colonies in the agar plate was aseptically transferred to a 250 ml baffled Erlenmeyer flask containing 50 ml of preseed medium. The preseed flask was agitated at 250 rpm and 30°C for 14 h in a temperature-controlled orbital shaker (Edwards Instrument, Model BL 4700). The seed culture was prepared in order to minimize the lag time at the beginning of cell cultivation in 5 and 30 l bioreactors. 2.5 ml of preseed culture was inoculated to a 1 l baffled Erlenmeyer flask containing 250 ml of seed medium. The seed culture was maintained in the same condition as preseed for 8.5 h, during which the exponential growth phase was achieved.

2.9   SHAKE FLASK STUDIES

Non-baffled cotton-stoppered Erlenmeyer flasks (500 ml) containing 90 ml concentrated cultivation medium were used for the shake flask studies. The frozen spore suspension harvested earlier was prewarmed at 30°C prior to dilution with sterile RO water so that inoculation with 10 ml concentrated spores would result in an approximate initial spore concentration of 1.2×10^6 spores ml^{-1}. The Erlenmeyer flasks were agitated at 340 rpm and 30°C in a bench-top orbital shaker incubator (Paton Scientific, Model OI 2116, Figure 2.1). After 24 h, the complete contents were harvested and analysed. The viabilities of the spores (%) following the various storage periods were calculated from the number of germinated spores after 6 h relative to the initial total spore count. There were four to five replicate flasks for each condition of yeast extract concentration (0, 2, 5, 10, 20, 30 and 50 g l^{-1}) investigated.

Figure 2.1: A bench-top orbital shaker incubator used in the shake flask studies of *R. javanicus*.

2.10   STUDIES IN 5 L BIOREACTOR

Four litres of cultivation medium (including 10% (v/v) spore inoculum) were stirred by double 6-blades Rushton impellers at 30°C, initial pH 6.0, 0.5 vvm initial airflow rate and initial spore concentration of 1.2×10^6 spores ml^{-1} in a 5 l bioreactor (Figure 2.2 and 2.3). The bioreactor was sterilized at 121°C and 1 atm for 15 min before addition of a sterile medium after cooling. For cultivation without dissolved oxygen (DO)- and pH-control, the stirrer speed was maintained constant at 340 rpm using a motor controller (Applikon$^{\circledR}$, Model No. ADI1012). For moderate aerobic cultivation and low aerobic cultivation, both with pH control at 6.0 (using 2 M HCl/NaOH), the DO level measured with a galvanic DO electrode (BABS, UNSW, Australia) was maintained above 20% air saturation by a cascade controller (Autoplex$^{\circledR}$, Australia), which varied the stirrer speed from 340 rpm to 800 rpm, during the initial aeration period (12 h for moderate aerobic and 10 h for low aerobic conditions). Following this initial time, with the DO close to 0% air saturation, the stirrer speed was set to a constant level of 340 rpm for moderate aerobic and 250 rpm for low aerobic cultivations. The airflow rate was also decreased to 0.25 vvm during this latter phase of growth for the low aerobic conditions.
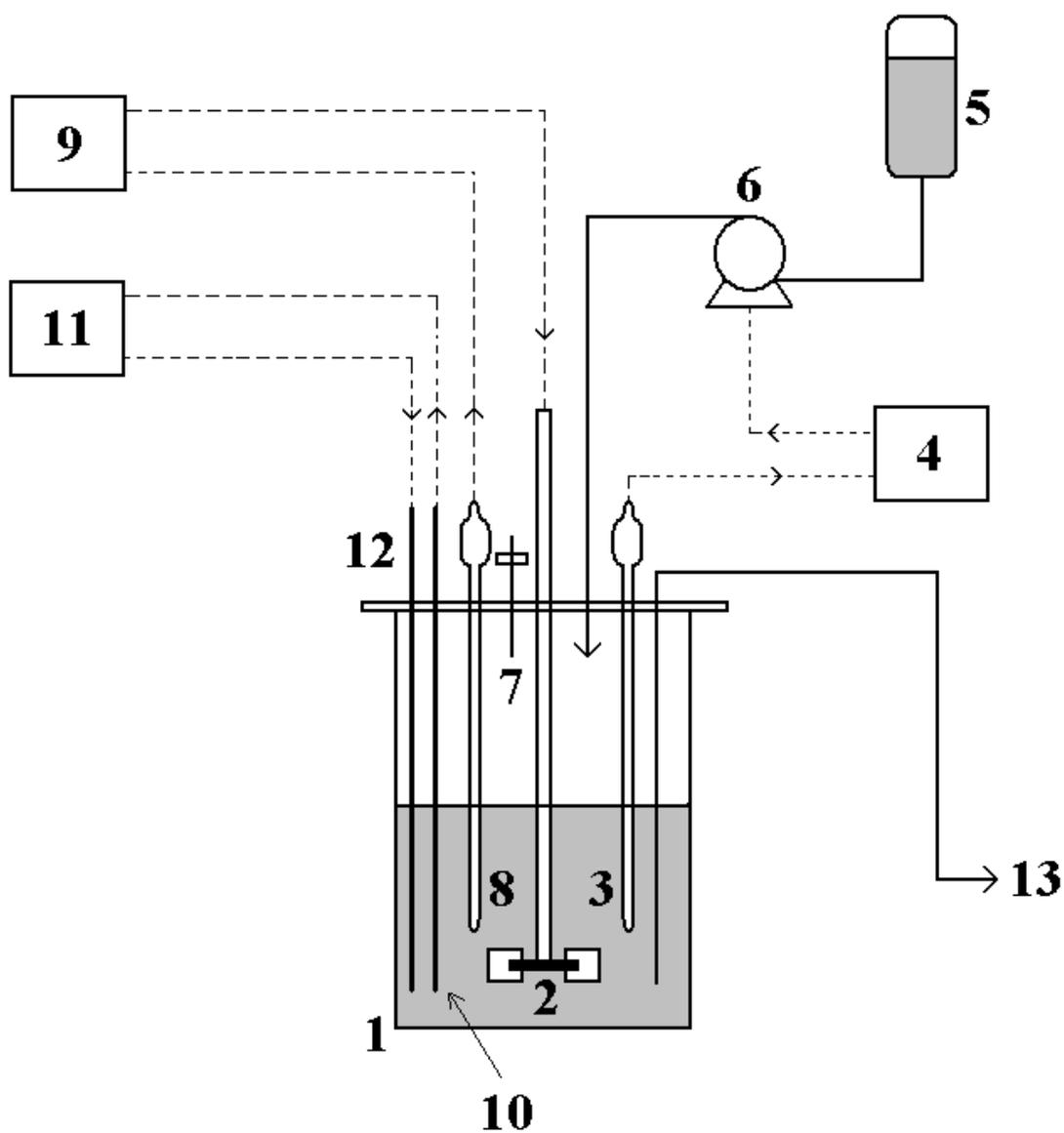
Figure 2.2: Schematic diagram of the 5 l batch cultivation system for *R. javanicus* (not to scale) (1) bioreactor vessel, (2) impeller, (3) pH electrode, (4) pH controller, (5) alkali reservoir (2 M NaOH), (6) alkaline pump, (7) air filter, (8) galvanic DO electrode, (9) cascade controller, (10) temperature electrode, (11) temperature controller, (12) heating element and (13) sampling port.

Figure 2.3: A 5 l bioreactor used in the studies of agitation/aeration effect for *R. javanicus*.

2.11 PRODUCTION OF PDC

2.11.1 Production of PDC for *C. utilis*

2.11.1.1 5 l bioreactor

C. utilis was grown in six batches of a 5 l bioreactor (B.Braun, Biostat®A, Figure 2.4) whose schematic diagram and operation details were similar to those described by Chow (1998) and Sandford (2002). The cultivation was started by inoculating 0.30 l of seed culture (exponential phase) into sterile 3.70 l cultivation medium (addition of inoculum resulted in concentrations specified previously). The culture conditions were controlled at 30°C, pH 6.0 (using 4 M H$_3$PO$_4$/KOH) and an airflow rate of 1.0 vvm. In the initial growth phase (11-13 h), the culture was maintained in fully aerobic conditions with a stirrer speed of 500 rpm. This was followed by switching to partially aerobic conditions with airflow rate and stirrer speed of 0.5 vvm and 300 rpm

respectively for the next 2.5-4.0 h, when the level of DO dropped below 5% air saturation, to induce PDC production. Concentrated feed solution (3.25 l) was added to the bioreactor one hour prior to harvesting, when glucose concentration had decreased below 20 g l^{-1}. The harvested cells were washed twice with RO water prior to resuspension in breakage buffer to give a cell dry weight of approximately 65 g l^{-1} which corresponded to an optical density at 660 nm (OD_{660}) of 184. The biomass of *C. utilis* generated in this section was further purified and used in the organic-aqueous two-phase biotransformation studies.

Figure 2.4: Biostat® A (5 l) used in the production of PDC from *C. utilis*.

2.11.1.2   30 l bioreactor

C. utilis was grown in a 30 l bioreactor (B.Braun, Biostat$^®$C, Figure 2.5). The cultivation was started by inoculating 1.5 l of seed culture (exponential phase) into sterile 18.5 l cultivation medium (addition of inoculum resulted in concentrations specified previously). The culture conditions were controlled at $30^°$C, pH 6.0 (using 4 M H_3PO_4/KOH) and an airflow rate of 0.5 vvm. In the initial growth phase (9 h), the culture was maintained in fully aerobic conditions with a respiratory quotient (RQ) = 1. This was followed by switching to partially aerobic conditions with RQ = 4 for the next 4 h to induce PDC production. RQ control was carried out by adjusting the stirrer speed between 275 to 780 rpm. The biomass was harvested at 13 h when glucose concentration had decreased below 20 g l^{-1}. The harvested cells were washed with RO water twice prior to resuspension in breakage buffer to give a cell dry weight of 65 g l^{-1} (OD_{660} = 184).

2.11.2   Production of PDC for *R. javanicus*

In the 30 l bioreactor, twenty litres cultivation medium (including 10% (v/v) spore inoculum) was used at $30^°$C, 300 rpm, pH 6.0 (using 2 M HCl/NaOH) and initial spore concentration of 1.2×10^6 spores ml^{-1}. During the cultivation time course, the airflow rate was reduced stepwise from 1.0 vvm (0-9 h) to 0.5 vvm (9-16 h) then 0.25 vvm (16-20 h) to allow an initial fully aerobic growth phase followed by fermentative conditions.

Figure 2.5: Biostat®C (30 l) used in the production of PDC.

2.12   SAMPLE COLLECTION FROM SHAKE FLASKS AND BIOREACTORS

Immediately before each sampling, 20 ml of mycelial or cell culture were withdrawn from a sampling port of the 5 or 30 l bioreactor and discarded to ensure a representative sample of the culture volume withdrawn afterwards.

2.12.1   *R. javanicus* sample

The culture broth samples of *R. javanicus* from the shake flasks (4-5 × 100 ml) and bioreactor studies (4 × 10 ml) were vacuum filtered through a 70 mm diameter filter paper (Whatman no. I, Cat. no. 1001 070) to separate mycelium from the supernatant. The filter was prewashed with RO water before use and dried to constant weight in an 105°C oven (Memmert GmbH + Co. KG, model UM400). Once the supernatant was removed and stored for further analysis of glucose and ethanol concentrations, each of the collected mycelium samples was rinsed twice with RO water. Two samples of the dried mycelium was placed in the oven at 105°C for 24 h for dry biomass weight measurement while the others were lyophilized in a freeze drier (Dynavac, model FD3, Figure 2.6) for subsequent preparation of crude extract as well as analyses of PDC activity and total protein concentration. A summary of sampling procedure is shown in Figure 2.7(a).

2.12.2   *C. utilis* sample

Forty-one ml of cell culture was collected, divided into three portions of 1 ml and 2 × 20 ml then stored in a 1.5 ml centrifuge tube and two McCartney bottles. One ml of the cell culture was used in the determination of optical density at 660 nm using a spectrophotometer (Pharmacia Biotech, Model Ultrospec 2000). Two of 10 ml cell culture from the first McCartney bottle were delivered to preweighed dry biomass tubes and centrifuged at 3,800 g for 15 min. The supernatant was removed and stored for further analysis of glucose and ethanol concentrations while the precipitated cells were washed twice with RO water. The rinsed cells were placed in the oven at 105°C for 24 h

for dry biomass weight measurement. Similar process of centrifugation and cell washing was applied to the second cell culture bottle except that the rinsed cells were resuspended in an appropriate volume of breakage buffer to prepare crude extract for subsequent analyses of PDC activity and total protein concentration as shown in Figure 2.7(b).

Figure 2.6: A Dynavac freeze drier (Model FD3).

2.13   CRUDE EXTRACT PREPARATION

2.13.1   *R. javanicus* crude extract

The frozen mycelial mats at -20°C were placed in a freeze drier for 24 h before grinding into powder with an equal weight of cold Ballotini glass beads grade 12. Cold breakage buffer for *R. javanicus* was later added to create a concentrated slurry. The mycelial debris was removed from the slurry mixture using a refrigerated centrifuge (Sorvall RC-5B, Du-Pont Instruments) at 6°C and 19,000 g for 7 min to obtain the crude extract.

(a)   Sample of mycelial culture

2 × 10 ml	1 × 10 ml	1 × 10 ml
Vacuum filter	Vacuum filter	Vacuum filter

Supernatant   Mycelial mat   Mycelial mat   Mycelial mat

Wash   Wash   Wash

Glucose and ethanol concentrations measurements   **Dry biomass weight measurement**   **Enzyme activity measurement**   **Total protein concentration measurement**

(b)   Sample of cell culture

1 ml	2 × 10 ml	2 × 5 ml	2 × 5 ml
Dilute	Centrifuge	Centrifuge	Centrifuge

Supernatant   Cells pellet   Cells pellet   Cells pellet

Wash   Wash   Wash

Optical density measurement measurement   **Glucose and ethanol concentrations measurements**   **Dry biomass weight measurement**   **Enzyme activity measurement**   **Total protein concentration**

Figure 2.7: Sampling procedures for (a) *R. javanicus* and (b) *C. utilis* cultivations in 5 and 30 l bioreactors.

2.13.2   *C. utilis* **crude extract**

The cells suspension in breakage buffer was frozen with an equal volume of liquid nitrogen and thawed at $30^{\circ}C$ three times before glass bead attrition to release intracellular PDC. Crude extract was obtained after clarification by centrifugation (3,800 g for 15 min).

2.14   ENZYME PURIFICATION

Acetone precipitation of the crude extract in the range of 40-50% (v/v) at $-10^{\circ}C$ was employed to obtain partially purified PDC. The enzyme paste was freeze-dried for 24 h, ground to a powder and stored at $-20^{\circ}C$. Before use, this partially purified PDC was dissolved in corresponding buffers and mixed by vertical rotation at 35 rpm and $6^{\circ}C$ for one hour. Then undissolved solid was removed by centrifugation at $6^{\circ}C$ and 19,000 g for 5 min.

2.15   DEACTIVATION STUDIES

2.15.1   **Deactivation studies of *R. javanicus* and *C. utilis***

All of the enzyme deactivation experiments were performed in 10 ml centrifuge tubes (dia. 1.2 cm and length 7 cm) with 5 ml enzyme solution in deactivation buffer I from either partially purified PDC or crude extracts of *R. javanicus* and *C. utilis*. The tubes were rotated vertically at 35 rpm. The relative decarboxylase activity was monitored regularly over the time course. The initial conditions were 7 U decarboxylase ml^{-1}, $6^{\circ}C$ and pH 7.0 unless stated otherwise. Table 2.2 summarizes all factors investigated.

A first order decay equation (Equation (2.1)) in a similar form to that which characterized the deactivation of *C. utilis* PDC (Chow et al. 1995, Leksawasdi et al. 2003) was applied to analyse the enzyme deactivation profiles of *R. javanicus* viz.,

$$E = E_0 \, e^{-k_{rj} \left(t - t_{lag} \right)}$$

(2.1)

where k_{rj} represents the enzyme deactivation constant in 0.6 M MOPS, t_{lag} indicates lag time period prior to enzyme deactivation (h), E_0 is the initial relative decarboxylase activity (100%), E is relative decarboxylase activity (%) and t is time (h).

Table 2.2: The type of enzyme and conditions used in the investigation of temperature, benzaldehyde, pH, initial decarboxylase activity, $MgSO_4$ and protease inhibitors on deactivation profiles of PDC obtained from *R. javanicus*.

	Type of enzyme		
Factors investigated	**Partially purified PDC**	**Crude extract**	**Conditions**
Temperature	✓	✓	At 6 and 25°C
Benzaldehyde	✓	✓	0 and 50 mM at 6 and 25°C
pH	-	✓	pH 3.0, 5.1, 6.1, 6.5, 7.0, 7.5, and 8.0
Initial enzyme level	-	✓	7, 13, 20, and 27 U decarboxylase ml^{-1}
$MgSO_4$	-	✓	0 and 20 mM
Protease inhibitor (PI)	-	✓	Serine and cysteine PI[!], aspartate PI[%] and metallo-PI[*]
Comparison with crude extract of *C. utilis*	-	✓	0 and 50 mM for *R. javanicus* and 0 and 73 mM for *C. utilis* at 6°C

[!] EDTA-free cocktail tablet, 1 or 2 tablets per 10 ml buffer

[%] Pepstatin A, 0.7-7 µg ml^{-1}

[*] EDTA-disodium salt, 1 and 5 mM

2.15.2   Deactivation studies of *C. utilis* for modelling purposes

Partially purified enzyme powder of *C. utilis* was suspended in a 15 ml centrifuge tube containing 6.3 ml of deactivation buffer II. The enzyme mixtures were rotated vertically at 35 rpm and 6°C for one hour to solubilize the PDC in the buffer. The activity of concentrated enzyme supernatant was kept between 28–32 U carboligase activity ml^{-1}.

Benzaldehyde of purity no less than 98% (w/w) was delivered to capped brown glass vials (inner dia. 1.25 cm, height 4.50 cm) containing deactivation buffer II and magnetic stirrer bars (dia. 0.65 cm, length 1.10 cm) to make up the desired benzaldehyde concentrations of approximately 0, 10, 20, 30, 40, 50, 60, 100, 150 and 200 mM. Three vial replicates were used for each benzaldehyde concentration. The vials were placed in a cold room ($6°C$) on a magnetic stirrer (Bibby, Model No. B292) for one hour to disperse benzaldehyde evenly throughout the deactivation buffer II. The stirrer speed was kept at 7.

Then 160 μl of concentrated enzyme supernatant was transferred to each glass vial to start the deactivation experiment. The final reaction volume was 1.6 ml with an enzyme activity in the range of 2.8–3.2 U carboligase ml^{-1}. The profile of enzyme activity was monitored at regular intervals for the period of 120 h.

2.16   INITIAL RATE AND BIOTRANSFORMATION STUDIES

2.16.1   Single-phase system without pH control for modelling purposes

As protons are consumed in the biotransformation (Rosche et al. 2002a), reactions were studied in 2.5 M MOPS buffer. Biotransformation buffer with benzaldehyde of purity no less than 98% (w/w) and sodium pyruvate were delivered to capped brown glass vials (inner dia. 1.25 cm, height 4.50 cm) with magnetic stirrer bars (dia. 0.65 cm, length 1.10 cm) for initial rate studies and to capped glass bottles (inner dia. 2.30 cm, height 5.70 cm) with magnetic stirrer bars (dia. 0.65 cm, length 2.00 cm) for biotransformation studies. Initial substrate and enzyme levels are given in the corresponding Figure captions. The vials were placed in a cold room ($6°C$) on a magnetic stirrer for one hour to disperse benzaldehyde evenly before reactions were started by the addition of PDC solution. The reaction volumes were 1.5 ml for initial rate studies and 10 ml for the biotransformation experiments. The stirrer speed was kept at 7 for the former and at 8.5 for the latter.

Reactions were stopped by transferring 100 µl of sample into 1.5 ml centrifuge tubes containing 10 µl of 100% (w/v) TCA. Precipitated protein was removed by centrifugation (19,000 g, 6°C for 2 min). In the initial rate studies, PAC formation was followed over time and the value for the initial rate was estimated from the tangent to the profile at time zero. For the biotransformations, pyruvate, benzaldehyde, PAC, acetaldehyde and acetoin concentrations and PDC activity were monitored at one hourly intervals over a period of 10 h.

2.16.2   Single-phase system with or without pH control for selection of solvents/chemical additives

The PAC production profiles without pH control for 2.5 M MOPS, 20 mM MOPS and 20 mM MOPS with 2.5 M DPG were obtained during a 30 min reaction time course. After dissolving the enzyme powder in the corresponding buffer for initial rate studies, 150 µl of a concentrated enzyme solution with 35 U carboligase activity ml^{-1} was delivered to a capped brown glass vial (inner dia. 1.25 cm, height 4.50 cm) containing 1.35 ml buffer with a magnetic stirrer bar (dia. 0.65 cm, length 1.10 cm). The reaction volume was 1.5 ml with initial carboligase activity of 3.5 U ml^{-1}.

A similar initial rate study with manual pH control of reaction mixture containing 20 mM MOPS with 2.5 M DPG was performed in a capped glass bottle (inner dia. 2.30 cm, height 5.70 cm) containing a magnetic stirrer bar (dia. 0.65 cm, length 2.00 cm). One ml of concentrated enzyme solution (35 U carboligase ml^{-1}) dissolved in 20 mM MOPS was added to 9 ml of 20 mM MOPS initial rate buffer with concentrated DPG to reach a final reaction volume of 10 ml, 2.5 M DPG and initial carboligase activity of 3.5 U ml^{-1}.

The reaction vials or bottles were placed in a cold room (6°C) on a magnetic stirrer for one hour before commencing the biotransformation by addition of concentrated enzyme. The stirrer speed was set at 7 for the studies without pH control and 8.5 for the study with pH control.

To stop the reaction, 100 μl of sample was transferred to 1.5 ml centrifuge tubes containing 10 μl of 100% (w/v) TCA followed by centrifugation at 19,000 g, 6°C for 2 min to remove the precipitated proteins. The initial rate was estimated from each PAC production profile by drawing a tangent from time zero. Manual pH control at 7.0 was performed by adding 5 or 10 μl of 0.36 M acetic acid.

2.16.3 Organic-aqueous two-phase system with pH control

Laboratory scale biotransformations in the two-phase system were performed in a 500 ml Quickfit reactor (dia. 7.3 cm, height 12.5 cm), see Figure 2.8. An overhead stirrer (IKA, Model RW 20n) with a R-1342 impeller (stirrer dia. 5 cm, shaft dia. 0.8 cm, shaft length 35 cm) was mounted on top. The stirrer speed was set at 255 rpm (setting I at level 5, 50 Hz). Acid addition was performed with a high precision digital pH-stat controller (Radiometer, Model PHM290, Figure 2.9(a)) and a 50 ml autoburette (Radiometer, Model ABU901, Figure 2.9(b)) fitted with an antidiffusion delivery tip (Radiometer, Cat. No. 956-309, Figure 2.9(c)). The autoburette was able to deliver a minimum dosing volume of 2.5 μl. A combination pH electrode (Mettler Toledo, Cat. No. 10 465 4505) with 1 M LiCl in acetic acid as an electrolyte (Mettler Toledo, Cat. No. 9828) was employed for pH measurement in the organic-aqueous emulsion condition. The pH was maintained at 7.0 with 3.6 M acetic acid. The horizon parameter in the adaptive addition algorithm (AAA) of the pH-stat controller was set at 10 for an aqueous phase biotransformation buffer containing 2.5 M MOPS and 62 for the system containing 20 mM MOPS. The default time constant value of 2 s was used. Four-fifth of the reactor was immersed in a cooling water bath (Thermoline, Model TBC-1-10) with a thermostat (Thermoline, Model TBC/TU4) to control the temperature at 4°C. Each experiment was performed in a fume cupboard (Conditionaire International, Model 2000 series).
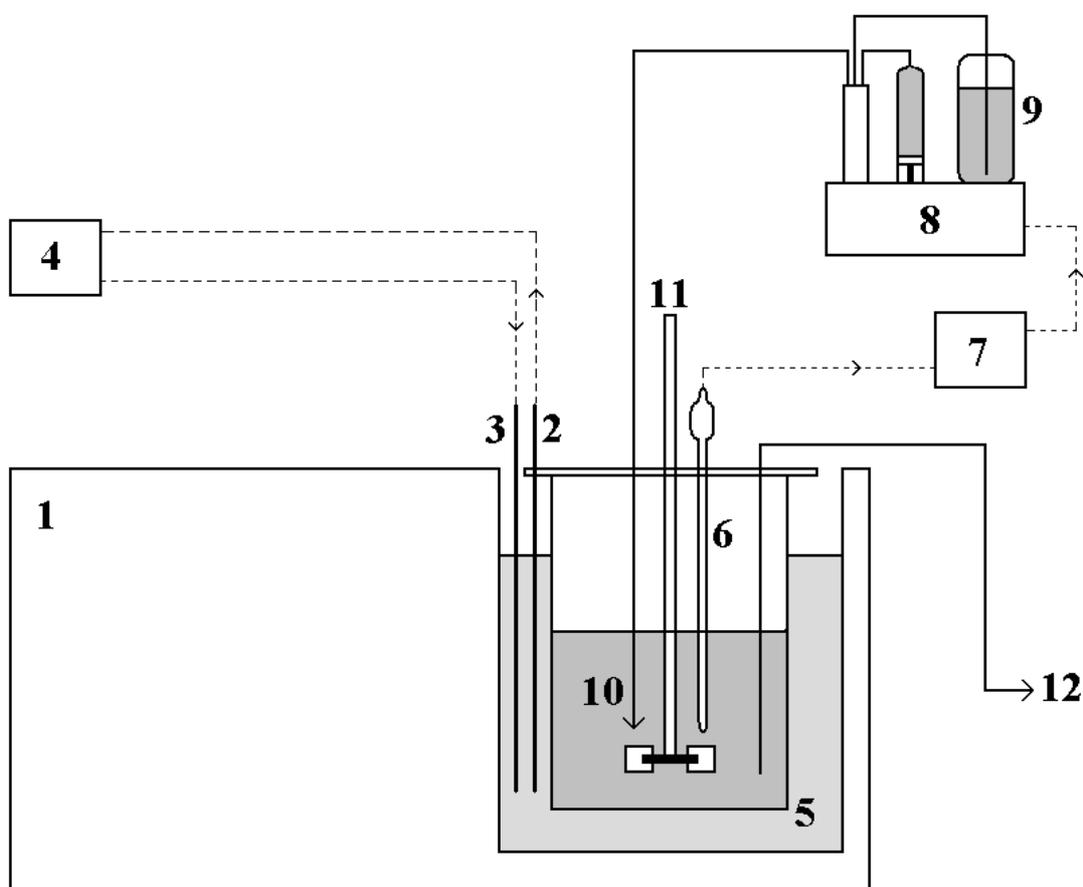
Figure 2.8: Schematic diagram of the laboratory scale batch biotransformation system (not to scale) (1) cooling water bath, (2)-(4) temperature electrode, heating element and temperature controller of TBC/TU4 thermostat respectively, (5) biotransformation reactor, (6) LiCl pH electrode, (7) digital pH controller PHM290, (8) autoburette ABU901, (9) 3.6 M acetic acid reservoir, (10) antidiffusion delivery tip, (11) R-1342 impeller and (12) sampling port.
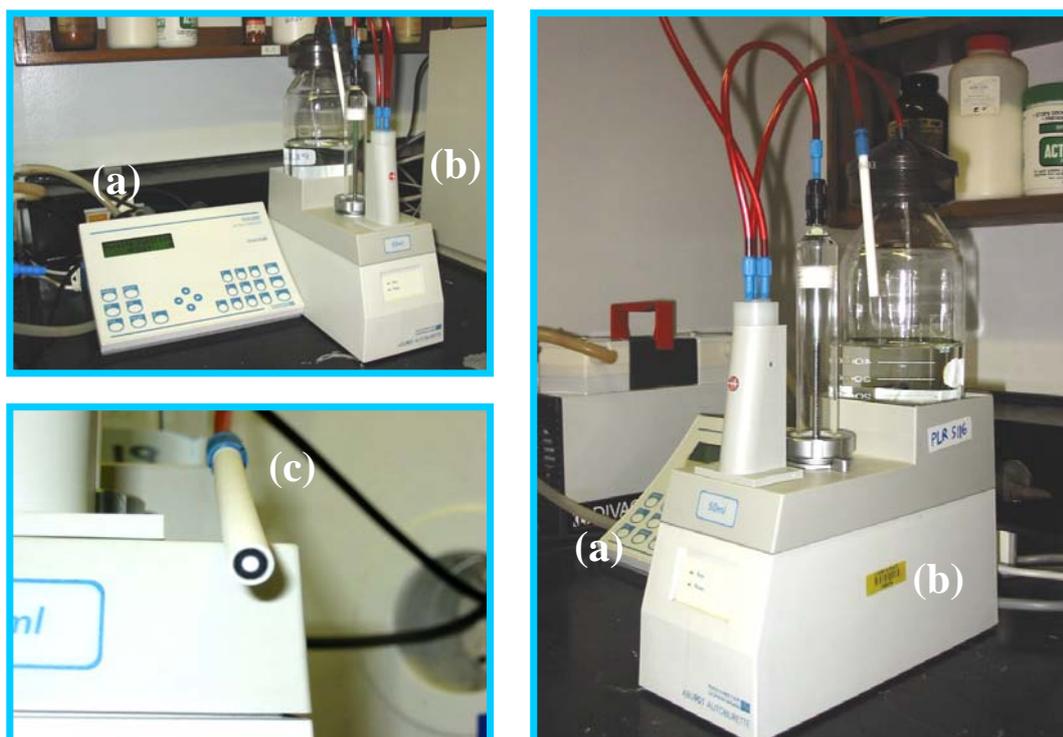
Figure 2.9: A high precision digital pH controller (PHM290, (a)) and autoburette (ABU901, (b)) equipped with an antidiffusion delivery tip (c) from Radiometer used in the organic-aqueous two-phase biotransformation studies.

Sixty ml of an aqueous phase biotransformation buffer was mixed with 75 ml of an organic octanol phase for at least half an hour to equilibrate the benzaldehyde concentrations in both phases. Fifteen ml of a concentrated PDC in aqueous phase biotransformation buffer was later added to initiate the biotransformation. The initial concentrations of substrates in each phase as well as initial enzyme activity are given in the corresponding Figure captions. The profiles of enzyme activity, substrates, product and by-products concentrations in each phase were monitored at regular intervals for the period of 81 h.

For the sampling, each phase was immediately separated from a 1.5 ml emulsion sample by centrifugation (19,000 g at 4°C for 5 min). Reactions in the aqueous phase were stopped by transferring 100 μl of aqueous solution into a 1.5 ml centrifuge tube containing 10 μl of 100% (w/v) TCA. Precipitated protein was removed by centrifugation (19,000 g at 4°C for 2 min). Proper dilutions of each phase with RO water

were made for concentrations analyses. A summary of sampling procedure is given in Figure 2.10. An appropriate calculation of dilution factor for each sample is shown in Appendix B, p. 230.

Sample of organic-aqueous two-phase biotransformation

↓

Centrifuge

Organic phase   Aqueous phase

Dilute   100 μl   3 × 55 μl

Addition of TCA   Gel filter

Centrifuge   Incubate

Supernatant

Dilute

PAC, benzaldehyde, benzoic acid, acetaldehyde and acetoin concentrations measurements   **PAC, benzaldehyde, benzoic acid, acetaldehyde, acetoin and pyruvate concentrations measurements**   **Carboligase activity measurements**

Figure 2.10: Sampling procedures for organic-aqueous two-phase biotransformation studies.

2.16.4   Separation of PDC from the reactions

To determine changes in PDC activity during each experiment, gel filtration columns (Micro Bio-Spin®6, Cat. No. 732-6200) were used to remove low molecular weight compounds from 55 μl (3 replicates) of the aqueous phase (Rosche et al. 2002a). PDC was recovered for each sample and mixed with 75 μl collection buffer at the lower end of the column while benzaldehyde was trapped in the column material. The collected enzyme was maintained on ice for 20 min and analysed for carboligase activity.

2.17   BENZALDEHYDE PARTITIONING STUDIES

In each study, equal volumes (0.75 ml) of aqueous phase biotransformation buffer and organic phase were transferred to a capped brown glass vial (inner dia. 1.25 cm, height 4.50 cm) with a short magnetic stirrer bar (dia. 0.65 cm, length 1.10 cm). Among the thirty-two types of chemicals investigated, some were either used as the alternative organic phase to octanol (pentanol, hexanol, heptanol, decyl alcohol, canola oil, corn oil, grapeseed oil, olive oil) or added directly to the aqueous phase (ethanol [2 M], isopropanol [2 M], butan-1-ol [2 M], benzyl alcohol [2 M], glycerol [2 M], DPG [2, 2.5, 3, 3.5, 4, 4.5 M], polyethyleneglycol (PEG)-6000 [10, 20, 26, 30, 35, 40% (w/v)], fructose [10% (w/v)], D-glucose [10% (w/v)], D-mannitol [7% (w/v)], lactose [2% (w/v)], maltose [10% (w/v)], sucrose [10% (w/v)], acetonitrile [2 M], tween-20 [10% (w/v)], tween-85 [10% (w/v)], $(NH_4)SO_4$ [1 M], KCl [1 M], urea [10, 18, 26, 30, 40% (w/v)]) while the others were mixed in different proportions with octanol and employed as organic phase (n-hexane [10, 50% (v/v)], methylcyclohexane [10, 50% (v/v)], n-heptane [10, 50% (v/v)], n-octane [10, 50% (v/v)], paraffin [10, 50% (v/v)]). The vials were either placed in a cold room at $6°$C or a $20°$C room on a magnetic stirrer for one hour to disperse benzaldehyde evenly between the two phases. The stirrer speed was set at 7.0. Duplicate samples from aqueous phase for each condition was analysed for the benzaldehyde concentrations.

2.18   ANALYTICAL METHODS

2.18.1   Determination of spore concentration

A Thoma slide chamber (Hawksley, England) was used for counting the spore concentration - it is one type of hemocytometer or Petroff-Hausser counting chamber. Ten μl of well-mixed suspension was transferred to the slide. The counting was carried out twice for each suspension. Figure 2.11 illustrates the determination of spore concentration using a Thoma slide under a microscope (Olympus BH).

Total number of squares	: 400
Area of each square (mm^2)	: 1/400
Area in counting region	: 1 mm^2
Depth	: 0.1 mm
Volume in counting region	: 0.1 mm^3 or
	: 10^{-4} ml
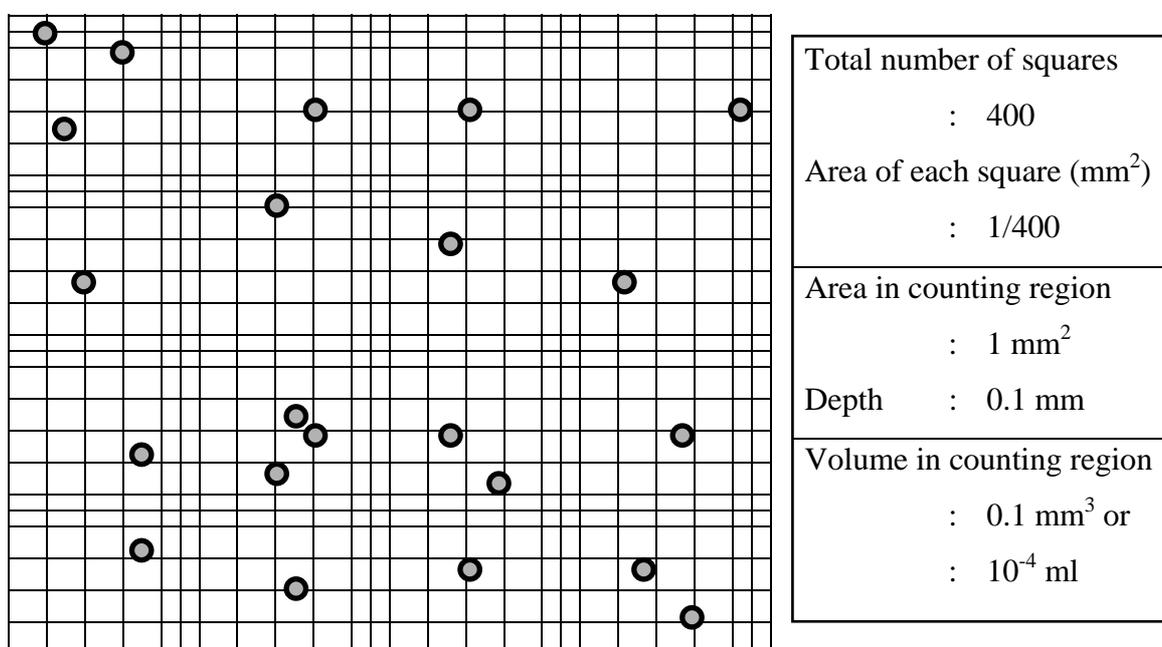
Figure 2.11: Determination of spore concentration using Thoma slide.

From Figure 2.11, total number of spore in the counting region are 22, hence the spore concentration is calculated from the number of spore in counting region divided by the volume in counting region = 22 spores/10^{-4} ml = 22×10^4 spores ml^{-1}. In this case, the spore suspension was diluted by 100 times hence the actual spore concentration from suspension was 2.2×10^7 spores ml^{-1}.

2.18.2   Determination of spore viability

Spore viability was estimated based on a direct counting procedure, the number of the spores in a given volume of sample was counted under microscope and used to calculate the concentration of spores in the original sample. The selected method is cheap, simple and relatively quick, it also gives details about the size and morphology of microorganisms (Atlas 1988, Prescott et al. 1996). The total spore concentration was estimated first after inoculating a concentrated spore suspension into cultivation medium using conditions previously described in Section 2.9, Shake Flask Studies, p.53 for 2 h. The spores were allowed to germinate for a further 4 h so that the enlarged live spores could be distinguished from non-germinating spores. The spore viability of a particular spore suspension was calculated from the percentage ratio of germinating spores at 6 h ((total number of spores at 2 h minus number of non-germinating spores at 6 h) over total number of spores at 2 h). A calculation example is shown in Table 2.3.

Table 2.3: Example for determination of spore viability

Age of spores	Number of spores	
	Total spores number after 2 h inoculation	**Number of non-germinating spores after 6 h inoculuation**
95 days	Count 1: 69, 78	Count 1: 41, 27
	Count 2: 62, 63	Count 2: 44, 53
	Count 3: 68, 64	Count 3: 53, 30
Average total number of spores	67.3	
Errors in total number of spores	2.4	
Average number of non-germinating spores	41.3	
Errors in number of non-germinating spores	4.5	
Percentage viability of spore inoculum	**38.6 ± 4.4 %**	

2.18.3   Determination of dissolved oxygen concentration

The dissolved oxygen concentration (DO) was measured as percentage air saturation using galvanic (BABS, UNSW, Australia) and polarographic oxygen electrodes (Ingold Cat. No. 341003047). Oxygen is reduced at the surface of a cathode after diffusing through the gas-permeable membrane. For galvanic electrode, a current generated from half-cell reactions at the cathode (Equation (2.2)) and anode (Equation (2.3)) provides a detectable voltage that can be correlated to DO level while the opposite is true for a polarographic electrode. A constant voltage is applied across the cathode and anode (Equation (2.4)) of the polarographic electrode resulting in a measurable current (Bailey and Ollis 1986).

Cathode $\quad\quad\quad\quad\quad \frac{1}{2} O_2 + H_2O + 2e^- \longrightarrow 2\ OH^- \quad\quad\quad\quad (2.2)$

Anode

$\quad\quad$ *Galvanic:* $\quad\quad\quad\quad Pb \longrightarrow Pb^{2+} + 2e^- \quad\quad\quad\quad (2.3)$

$\quad\quad$ *Polarographic:* $\quad\quad Ag + Cl^- \longrightarrow AgCl + e^- \quad\quad\quad (2.4)$
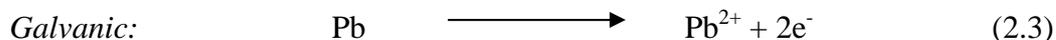
2.18.4   Determination of respiratory quotient

The respiratory quotient (RQ), calculated from the ratio of CO_2 evolution rate (CER) and O_2 uptake rate (OUR) both expressed as mmol l^{-1} h^{-1}, was determined as follows. The exhaust gas leaving the 5 and 30 l bioreactors was passed through a dehumidifier (Komatsu Electronics Inc., Model DH 1052 G) before entering the on-line gas analysers, which subsequently measured oxygen (Servomix type 1400A) and carbon dioxide (Servomix-R type 1410) concentrations in the exit gases. The RQ values were then calculated from these values and the gas flow rates as shown in Table 2.4.

Table 2.4: Algorithm for RQ calculation

Variables	Descriptions	Values
F_i	Flow inlet (l min^{-1})	F_i
O_i	Concentration of inlet O_2 (%)	20.9
C_i	Concentration of inlet CO_2 (%)	0.03
N_i	Concentration of inlet inert gas (%)	79.07
O_o	Concentration of outlet O_2 (%) {from gas analyser 1400A}	O_o
C_o	Concentration of outlet CO_2 (%){from gas analyser 1410}	C_o
V_f	Volume of bioreactor (l)	V_f
[*]K_{OUR}	Constant for OUR calculation (min × mmol l^{-1} h^{-1})	26.44
[*]K_{CER}	Constant for CER calculation (min × mmol l^{-1} h^{-1})	26.59
N_o	Concentration of outlet inert gas (%) = $100 - O_o - C_o$	
F_o	Flow outlet (l min^{-1}) = $F_i N_i / N_o$	
OUR	$(F_i \times O_i - F_o \times O_o) \times (K_{OUR}/V_f)$ mmol l^{-1} h^{-1}	
CER	$(F_o \times C_o - F_i \times C_i) \times (K_{CER}/V_f)$ mmol l^{-1} h^{-1}	
RQ	CER/OUR	

[*]Sandford (2002)

2.18.5 Determination of glucose concentration

The glucose concentration of the samples were detected by using a glucose and lactate analyser (YSI Model 2300 STAT PLUS, Figure 2.12). One ml of the sample was aliquot to a 1.5 ml centrifuge tube and centrifuged at 19,000 g for 5 min to remove insoluble solids before placing the supernatant on the analyser. The reaction of glucose with an immobilized enzyme, glucose oxidase, generates glucono-δ-lactone and hydrogen peroxide. The latter component diffuses across a membrane and reacts with a Pt anode to produce current which is proportional to the concentration of glucose in each sample. Because the linear concentration range of glucose is up to 27.8 mM, the samples with higher concentrations were diluted to this range before the measurement.

Figure 2.12: A glucose analyser YSI Model 2300 STAT PLUS.

2.18.6   Determination of ethanol concentration

Concentration of ethanol in the samples collected from culture broth were analysed by a gas chromatograph (Packard, Model 427). Three µl of sample was injected to the machine by a microinjector (Alltech, Part No. 001450SGE) through an injector port. The resulting chromatogram of eluting components were interpreted by an integrator (Spectra Physics, SP4270) for identification of each peak by retention time and concentration of components in the samples by area under the peak. The retention time of ethanol was between 2.70 to 2.90 min. The column and operating conditions used are listed in Table 2.5.

Table 2.5: The column and operating conditions of gas chromatograph for analysis of ethanol concentration.

Column material	¼ inch glass (Alltech)
Column length	1 m
Packing material	Porapak® type Q
Column mesh range	100-200 μm
Carrier gas	Nitrogen at 25 psig
Oven temperature	180°C
Injector temperature	220°C
Detector temperature	220°C
Detector type	Flame ionization detector (FID) with hydrogen (15 psig) and air (15 psig)
Operation	Isotherm
Total run time	6 min
Sample volume	3 μl

Six ethanol standards containing ethanol of known concentrations (1-50 g l^{-1}) were used to correlate the area under peak to the ethanol concentration. By using the correlation equation obtained from standard curve, ethanol concentration in the sample could be determined. For accurate results, the range of ethanol concentration in the standards should cover the concentration span of the samples.

2.18.7   Determination of pyruvate concentration

Concentration of pyruvate was determined spectrophotometrically by an established method of enzymatic NADH + H^+ coupled assay with lactate dehydrogenase (LDH) as indicated in Equation (2.5).

$$\text{Pyruvate} \xrightarrow{\text{LDH}} L\text{-lactate} \qquad (2.5)$$

$$NADH + H^+ \qquad NAD^+$$
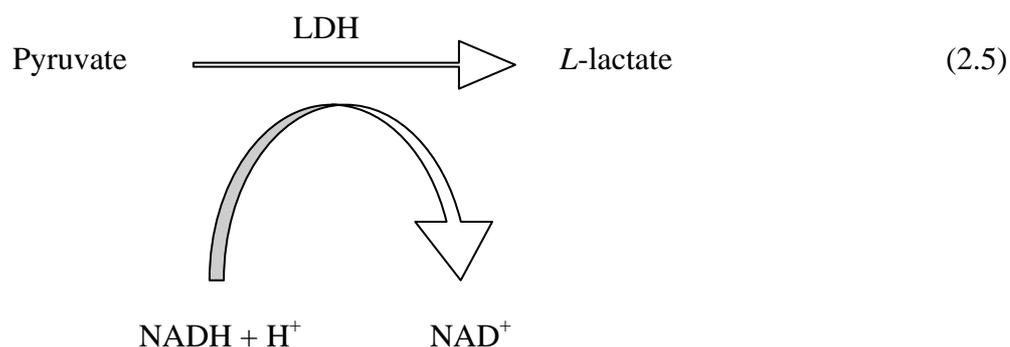
The pyruvate concentration was correlated to the disappearance of $NADH + H^+$ at wavelength of 340 nm in a 2.5 ml UV disposable cuvette (Kartell, Cat. No. 1941). The compositions of reaction mixture for pyruvate assay are listed in Table 2.6 (modified from Czok and Lamprecht 1974). The contents were thoroughly mixed with a spatula after the sample/blank was delivered to the cuvette. The initial absorbance of blank and sample were recorded prior to addition of LDH to begin the reaction. The final absorbance was measured after 8 min and the pyruvate concentration was quantified as stated in Table 2.7. The sample was diluted to a concentration range between 0.5 to 5 mM pyruvate.

Table 2.6: Compositions of pyruvate assay

Buffer/solution (in order)	Volume (μl)
Triethanolamine buffer	750
NADH buffer	25
Sample/blank	25
LDH (550 U mg^{-1})	5

Table 2.7: Quantification of pyruvate concentration

Variables	Descriptions
$A_{pyr,i}$	Initial absorbance of sample cuvette before LDH addition
$A_{bln,i}$	Initial absorbance of blank (RO water) cuvette before LDH addition
$A_{pyr,8}$	Absorbance of sample cuvette after LDH addition for 8 min
$A_{bln,8}$	Absorbance of blank cuvette after LDH addition for 8 min
A_{pyr}	$A_{pyr,i} - A_{pyr,8}$
A_{bln}	$A_{bln,i} - A_{bln,8}$
Abs	$A_{pyr} - A_{bln}$
V_{assay}	Final volume of assay $= 750 + 25 + 25 + 5 = 805$ μl
V_{sam}	Volume of blank/sample $= 25$ μl
λ	Light path length (1 cm)
ε	Extinction coefficient of NADH at 340 nm (6300 l mol^{-1} cm^{-1})
[Pyr]	Pyruvate concentration $= (V_{assay}/V_{sam}) \times \text{Abs} \times (1/\varepsilon\lambda) \times (1000 \text{ mmol mol}^{-1}) = 5.111 \times \text{Abs mM}$

2.18.8   Determination of acetaldehyde concentration

Concentrations of acetaldehyde in the aqueous and the organic phases were determined spectrophotometrically by enzymatic NADH + H$^+$ coupled assay method with alcohol dehydrogenase (ADH) as indicated in Equation (2.6). RO water was used to extract acetaldehyde from the organic phase.

$$\text{Acetaldehyde} \xrightarrow{\text{ADH}} \text{Ethanol} \qquad (2.6)$$

$$\text{NADH} + \text{H}^+ \longrightarrow \text{NAD}^+$$
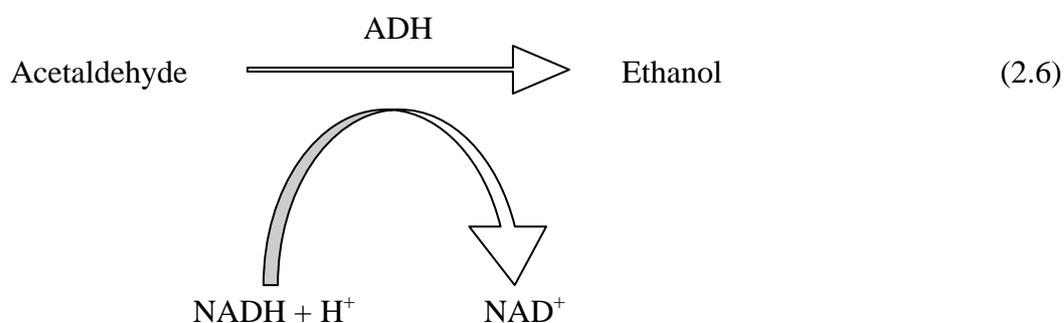
The amount of acetaldehyde present in the sample was proportional to the oxidation of $NADH + H^+$ to NAD^+ measured at wavelength of 340 nm in a 2.5 ml UV disposable cuvette. The compositions of reaction mixture for acetaldehyde assay are listed in Table 2.8 (modified from Bernt and Bergmeyer 1974). The contents were thoroughly mixed with a spatula after the sample/blank was delivered to the cuvette. The initial absorbance of blank and sample were recorded prior to addition of ADH to begin the reaction. The final absorbance was measured after 8 min and the acetaldehyde concentration was quantified as stated in Table 2.9. Sample was diluted to a concentration range between 1.0 to 2.5 mM acetaldehyde.

Table 2.8: Compositions of acetaldehyde assay

Buffer/solution (in order)	Volume (μl)
Triethanolamine buffer	750
NADH buffer	25
Sample/blank	25
ADH (200 U ml^{-1})	5

Table 2.9: Quantification of acetaldehyde concentration

Variables	Descriptions
$A_{ace,i}$	Initial absorbance of sample cuvette before ADH addition
$A_{bln,i}$	Initial absorbance of blank (RO water) cuvette before ADH addition
$A_{ace,8}$	Absorbance of sample cuvette after ADH addition for 8 min
$A_{bln,8}$	Absorbance of blank cuvette after ADH addition for 8 min
A_{ace}	$A_{ace,i} - A_{ace,8}$
A_{bln}	$A_{bln,i} - A_{bln,8}$
Abs	$A_{ace} - A_{bln}$
V_{assay}	Final volume of assay $= 750 + 25 + 25 + 5 = 805$ μl
V_{sam}	Volume of blank/sample $= 25$ μl
λ	Light path length (1 cm)
ε	Extinction coefficient of NADH at 340 nm (6300 l mol^{-1} cm^{-1})
[Ace]	Acetaldehyde concentration $= (V_{assay}/V_{sam}) \times Abs \times (1/\varepsilon\lambda) \times (1000$ mmol mol$^{-1}) = 5.111 \times Abs$ mM

2.18.9   Determination of PAC, benzaldehyde, benzyl alcohol and benzoic acid concentrations

PAC, benzaldehyde, benzyl alcohol and benzoic acid concentrations in aqueous and organic phases were determined using a Shimadzu high performance liquid chromatography (HPLC) system (Figure 2.13) with ultraviolet (UV) detection at 263 (for benzyl alcohol) and 283 nm as described by Rosche et al. (2001). RO water was used to extract PAC, benzaldehyde, benzyl alcohol and benzoic acid from the organic phase with at least 50 times dilution.

Figure 2.13: High performance liquid chromatography (HPLC) system for determination of PAC, benzaldehyde, benzyl alcohol and benzoic acid concentrations.

Table 2.10: The column and operating conditions of HPLC system for analysis of PAC, benzaldehyde, benzyl alcohol and benzoic acid concentrations.

Column material	Alltima^{TM} C8, 5 μm particle size (Alltech)
Column length	15 cm
Column diameter	4.6 mm (internal)
Guard column	Alltima All-guard^{TM} 5 μm particle size (Alltech)
Guard column length	7.5 mm
Guard column diameter	4.6 mm (internal)
Mobile phase	32% (v/v) acetonitrile, 0.5% (v/v) acetic acid in MQ water
Oven type	Column oven (Shimadzu, CTO-10AS VP)
Oven temperature	Room temperature
Detector type	Diode array detector (Shimadzu, SPD-M10A VP)
UV detection wavelength	263 nm (benzyl alcohol) and 283 nm (other species)
Injector type	Autoinjector (Shimadzu, SIL-10AD VP)
Pump unit	Liquid chromatograph (Shimadzu, LC-10AT VP)
Pump operation	Isocratic with flow rate of 1.0 ml min^{-1}
Total run time	20 min
Sample volume	5 μl

The preparation of a mobile phase was done using milli-Q (MQ) water with the compositions given in Table 2.10. The mobile phase was automatically degassed by a degasser (Shimadzu, DGU-14A) before passing through the HPLC system. All of the VP units listed in Table 2.10 were linked centrally to a system controller (Shimadzu, SCL-10A VP) whose user interface was a Class-VP^{TM} workstation software (Shimadzu version 5.031).

The quantification of PAC, benzaldehyde and benzoic acid concentrations in each sample was possible by a standard curve relating the peak area to a known concentration of each species. The concentration range of standards were 0.6-14.8 mM for PAC, 5-25 mM for benzaldehyde and 2-10 mM for benzoic acid. The chromatogram peak for benzyl alcohol was not detected in any of the analysed samples.

Note: Breuer et al. (2002) developed a novel assay for rapid detection of PAC using 2,3,5-triphenyltetrazolium chloride instead of a time consuming chromatographic method currently used by various authors (Shin and Rogers 1996a,b, Shukla and Kulkarni 1999, Rosche et al. 2001).

2.18.10   Determination of acetoin concentration

Concentration of acetoin in the samples collected from the aqueous and the organic phases of biotransformation system were analysed by a gas chromatograph (Packard, Model 427). RO water was used to extract acetoin from the organic phase with at least 25 times dilution. Three μl of sample was injected to the machine by a microinjector (Alltech, Part No. 001450SGE). The resulting chromatogram of eluting components was interpreted by an integrator (Spectra Physics, SP4270) for identification of each peak by retention time and concentrations of components in the samples by area under the peak. The retention time of acetoin was between 5.30 to 5.50 min. The column and operating conditions used are listed in Table 2.11.

Table 2.11: The column and operating conditions of gas chromatography for analysis of acetoin concentration.

Column material	Stainless steel (Alltech)
Column length	3.6 m
Packing material	10% carbowax® on chromsorb® W-AW
Column mesh range	80-100 μm
Carrier gas	Nitrogen at 25 psig
Oven temperature	150°C
Injector temperature	175°C
Detector temperature	175°C
Detector type	Flame ionization detector (FID) with hydrogen (15 psig) and air (15 psig)
Operation	Isotherm
Total run time	20 min
Sample volume	3 μl

Four acetoin standards containing acetoin of known concentrations (2-30 mM) were used to correlate the area under the peak to the acetoin concentration. By using the correlation equation obtained from standard curve, acetoin concentration in the sample could be determined. For accurate results, the range of acetoin concentration in the standards should cover concentration span of the samples.

2.18.11   Determination of PDC activity

2.18.11.1   Determination of carboligase activity

The sample (50 μl) was transferred to an equal volume of carboligase buffer, vortexed and incubated at 25°C for 20 min. After 20 min, the reaction was stopped by addition of 10 μl of 100% (w/v) TCA, resulting in a 1.1× dilution. The mixture was centrifuged at 19,000 g for 2 min before the removal of supernatant for further analysis of PAC formed by HPLC. One unit carboligase activity was defined as the amount of PDC which produces 1.0 μmol of PAC from benzaldehyde and pyruvate per min at pH 6.4 and 25°C (Rosche et al. 2002a). The linear assay range was 0.2-0.6 U carboligase ml^{-1}.

The carboligase activity was evaluated as follows:

Table 2.12: Computation of carboligase activity

Variables	Descriptions
V_{assay}	Final volume of assay = 50 + 50 + 10 = 110 μl
V_{sam}	Volume of sample = 50 μl
P_{assay}	PAC formed in the reaction assay after 20 min (mM or μmol ml^{-1})
t	Reaction time = 20 min
$E_{carboligase}$	Carboligase activity $= (V_{assay}/V_{sam}) \times P_{assay} \ \mu mol \ ml^{-1} \times (1/t) \ min^{-1}$ $= 0.11 \times P_{assay} \ U \ carboligase \ ml^{-1}$

2.18.11.2   *Determination of decarboxylase activity*

The assay of PDC decarboxylase activity was measured spectrophotometrically by the ADH-coupled assay as specified by Bergmeyer and Grabl (1983) and Sigma-Aldrich (St. Louis, Mo., USA). The activity of PDC was assayed by coupling the decarboxylation reaction with the ADH mediated reaction and monitoring the oxidation of $NADH + H^+$ to NAD^+ at 340 nm in a 4.5 ml UV cuvette (Kartell, Cat. No. 1939). The basic principle of the decarboxylase assay is shown in Figure 2.14.
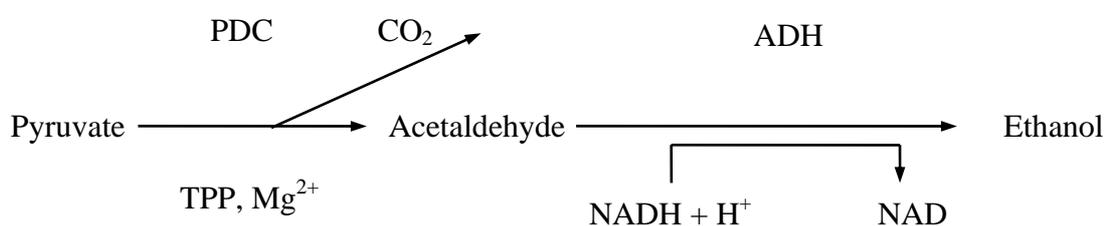
Figure 2.14: The basic principle of decarboxylase assay.

The assay compositions were as follows: 2.70 ml of 0.2 M citrate buffer (pH 6.0) at $28.5^{\circ}C$, 50 μl of cold 6.4 mM NADH sodium salt, 50 μl of cold ADH with activity of 200 U ml^{-1}, 100 μl of 1.0 M sodium pyruvate at $25^{\circ}C$ and 100 μl of blank/sample. One unit decarboxylase activity is defined as the amount of PDC which converts 1.0 μmol of pyruvate to acetaldehyde per min at pH 6.0 and $25^{\circ}C$ (Rosche et al. 2002a). The linear assay range was 0.3-0.6 U decarboxylase ml^{-1}. The reaction kinetics was monitored over the period of 2 min using Swift II$^{®}$ reaction kinetics software (Pharmacia Biotech) linked to the spectrophotometer. The rate of decrease in absorbance during 0.5-2 min was determined for further analysis of decarboxylase activity as shown in Table 2.13.

Table 2.13: Computation of decarboxylase activity

Variables	Descriptions
A_r	The rate of change in absorbance over time (min^{-1})
V_{assay}	Final volume of assay = $2700 + 50 + 50 + 100 + 100 = 3000$ μl
V_{sam}	Volume of blank/sample = 100 μl
λ	Light path length (1 cm)
ε	Extinction coefficient of NADH at 340 nm (6.3 ml μmol^{-1} cm^{-1})
$E_{decarbox}$	Decarboxylase activity $= (V_{assay}/V_{sam}) \times A_r\ min^{-1} \times (1/\varepsilon\lambda)$ μmol ml^{-1} $= 4.76 \times A_r$ U decarboxylase ml^{-1}

The possibility of interference by benzaldehyde of the decarboxylase assay was investigated by adding 100 μl of benzaldehyde at concentrations of 0, 20, 50, 80 and 100 mM to 2.6 ml PDC in citrate buffer prior to activity measurements. No interference of the enzyme assay by benzaldehyde was found for this concentration range.

An activity index (ratio of carboligase activity to decarboxylase activity) of the PDC used in the current study was 0.25.

2.18.12   Determination of protease activity

The protease activity was estimated at OD_{450} using the method of azoalbumin protease assay adapted from Tomarelli et al. (1949). Protease activity assay conditions were: 0.32 ml of 2% (w/v) azoalbumin substrate in 0.2 M $Na_2HPO_4.12H_2O$ or 0.6 M MOPS with corresponding concentration of $MgSO_4$, TPP, or EDTA (if any), pH 7.0 at room temperature and 80 μl of sample/blank/standard. The reaction carried out in a 1.5 ml centrifuge tube was stopped with addition of 400 μl of 10% (w/v) TCA after 30 min incubation at $35°C$, following by centrifugation at 19,000 g for 2 min, the final absorbance of supernatant was obtained by subtracting the blank value. One unit protease activity was defined as the amount of protease that catalyses the release of TCA-soluble azoalbumin equivalent to 50 μg per min at pH 7.0 and $35°C$. The linear

range of protease activity based on proteinase K activity was between 0.1-0.9 U protease ml^{-1}. The protease activity was quantified as shown in Table 2.14.

Table 2.14: Determination of protease activity

Variables	Descriptions
$A_{std,30}$	Absorbance of 4 mg ml^{-1} azoalbumin supernatant after 30 min reaction
$A_{sam,30}$	Absorbance of sample supernatant after 30 min reaction
$A_{bln,30}$	Absorbance of blank supernatant after 30 min reaction
A_{std}	$A_{std,30} - A_{bln,30}$
A_{sam}	$A_{sam,30} - A_{bln,30}$
V_{assay}	Final volume of assay = 320 + 80 + 400 = 800 µl
V_{sam}	Volume of sample = 80 µl
Azo_{sam}	Concentration of azoalbumin in sample $= 4$ mg ml$^{-1} \times (A_{sam} / A_{std}) \times (1000$ µg mg$^{-1})$ $= 4000 \times (A_{sam} / A_{std})$ µg ml^{-1}
t	Reaction time = 30 min
$E_{protease}$	Protease activity $= (V_{assay}/V_{sam}) \times Azo_{sam}$ µg ml$^{-1} \times (1/50t)$ U µg^{-1} $= (V_{assay}/V_{sam}) \times 4000 \times (A_{sam} / A_{std}) \times (1/50t)$ U ml^{-1} $= 26.7 \times (A_{sam} / A_{std})$ U ml^{-1}

2.18.13 Determination of total protein concentration

Protein concentrations were measured according to the biuret assay (Gornall et al. 1949) to account for the total protein with the following modifications: 0.6 ml of 30% (w/v) NaOH was mixed with 5 ml of crude extract and incubated at 25°C for 30 min before immersing the mixture in boiling RO water for another 15 min. After vortexing, the mixture was cooled on ice for 10 min before addition of 0.4 ml 25% (w/v) CuSO$_4$.5H$_2$O. The precipitate was removed by centrifugation at 3,800 g for 10 min and the absorbance of the supernatant was measured at 545 nm. The concentration of total protein in the sample was calculated from the comparison with a bovine serum albumin (BSA) standard curve.

2.19   MODELLING PROGRAM

2.19.1   Parameter estimation for deactivation studies

Computations to determine values of the enzyme deactivation constant and time lag were performed with a parameter-searching program (Joachimsthal 2001, Leksawasdi et al. 2001, 2003, 2004, Boonmee et al. 2003). The program was written in Microsoft Visual Basic for Application 6.3 under Microsoft EXCEL®2002 (see Appendix C, p. 235). The optimal parameter values were obtained when the minimum residual sum of squares (RSS) between predicted profile and experimental data was achieved. RSS was used further in the calculation of correlation coefficients (R^2).

For deactivation studies of *C. utilis* PDC;

$$RSS_{total} = \sum_{i=1}^{n} RSS_i \tag{2.7}$$

where: i = enzyme deactivation profile for a particular benzaldehyde concentration (0, 20, 30, 40, 50, 60, 100, 150, 200 mM); n = total number of enzyme deactivation profiles.

2.19.2   Parameter estimation for initial rates studies and biotransformations

The computations of parameter values from initial rate kinetic and batch biotransformation data were carried out using a similar parameter-searching program as that for the deactivation studies. The optimal parameter values were determined when the minimum total residual sum of squares (Σ RSS) was achieved between the predicted profiles and experimental data for three batch biotransformations, with RSS for each batch biotransformation defined as:

$$RSS = RSS_P + RSS_B + RSS_A + RSS_Q + RSS_R + RSS_E \tag{2.8}$$

where: P is the PAC, B is the benzaldehyde, A is the pyruvate, Q is the acetaldehyde, R is the acetoin and E is the carboligase activity and RSS_P, RSS_B, RSS_A, RSS_Q, RSS_R, as well as RSS_E are the residual sum of squares for each variable. Confidence intervals at 95% for all parameters were estimated using the method of linear approximation for nonlinear regression inference described in Bates and Watts (1988).

2.20   CALCULATIONS OF KINETIC PARAMETERS

2.20.1   Batch cultivation calculations

2.20.1.1   Specific rate of glucose consumption

The instantaneous specific rate of glucose consumption (q_s) was determined using:

$$q_s = \frac{1}{x} \frac{dGlu}{dt} \qquad (2.9)$$

where x is the dry biomass weight and dGlu/dt is the rate of glucose consumption.

The maximum value for the specific rate of glucose consumption (q_{smax}) was calculated over the exponential growth period with Equation (2.10).

$$q_{s,max} = \frac{1}{x_{average}} \frac{\Delta Glu}{\Delta t} \qquad (2.10)$$

where $x_{average}$ is the average dry biomass weight.

2.20.1.2   Specific rate of ethanol production

The instantaneous specific rate of ethanol production (q_p) was determined using:

$$q_p = \frac{1}{x} \frac{dEth}{dt} \qquad (2.11)$$

where x is the dry biomass weight and dEth/dt is the rate of ethanol production.

The maximum value for the specific rate of ethanol production ($q_{p,max}$) was calculated over the exponential growth period with Equation (2.12).

$$q_{p,max} = \frac{1}{x_{average}} \frac{\Delta Eth}{\Delta t} \qquad (2.12)$$

where $x_{average}$ is the average dry biomass weight.

2.20.1.3   Specific PDC production

$$\text{Specific PDC production} = \frac{\text{enzyme activity in the sample (U ml}^{-1})}{\text{mycelial dry biomass weight (g ml}^{-1})} \qquad (2.13)$$

2.20.1.4   Respiratory quotient

$$RQ = \frac{\text{carbon dioxide evolution rate (CER)}}{\text{oxygen evolution rate (OUR)}} \qquad (2.14)$$

The units of CER and OUR are in mmol l^{-1} h^{-1}.

2.20.2   Biotransformation calculations

2.20.2.1   Molar conversion yields

$$Y_{PAC/benzaldehyde} \left(Y_{P/BZ}\right) = \frac{\text{amount of PAC formed (mol)}}{\text{amount of benzaldehyde consumed (mol)}} \qquad (2.15)$$

$$Y_{PAC/pyruvate} \left(Y_{P/Pyr}\right) = \frac{\text{amount of PAC formed (mol)}}{\text{amount of pyruvate consumed (mol)}} \qquad (2.16)$$

$$Y_{acetaldehyde/pyruvate} \left(Y_{Q/Pyr}\right) = \frac{\text{amount of acetaldehyde formed (mol)}}{\text{amount of pyruvate consumed (mol)}} \qquad (2.17)$$

$$Y_{acetoin/pyruvate} \left(Y_{R/Pyr}\right) = \frac{\text{amount of acetoin formed (mol)}}{\text{amount of pyruvate consumed (mol)}} \qquad (2.18)$$

2.20.2.2   Percentage of substrates balance

Percentage of benzaldehyde balance $(BZ_{bal}) = 100 \times Y_{P/Bz}$ \qquad (2.19)

Percentage of pyruvate balance $(Pyr_{bal}) = 100 \times (Y_{P/Pyr} + Y_{Q/Pyr} + 2 \times Y_{R/Pyr}{}^{*})$ \qquad (2.20)

[*] Formation of 1 mole acetoin requires 2 moles of pyruvate

2.20.2.3   Specific PAC production

$$\text{Specific PAC production} = \frac{\text{PAC formed (mg ml}^{-1})}{\text{enzyme activity (U ml}^{-1})} \qquad (2.21)$$

2.20.2.4   Specific PAC productivity

$$\text{Specific PAC productivity} = \frac{\text{specific PAC production (mg U}^{-1})}{\text{time (h)}} \qquad (2.22)$$

2.21   CALCULATIONS OF EXPERIMENTAL ERRORS

When the number of replicates in each measurement was less than six, the calculated errors indicate the lowest and highest values of all replicates. For the measurement with six replicates or more, the standard error of a mean (s_m) was computed using sample standard deviation (s) and number of replicates (N) with a formula (Equation (2.23)) described by Skoog et al. (1996).

$$s_m = \frac{s}{\sqrt{N}} \qquad (2.23)$$

The error propagation in arithmetic calculations of more than one experimental data was determined using the relationships illustrated in Table 2.15 (Skoog et al. 1996).

Table 2.15: Error propagation in arithmetic calculations

Type of calculation	Example[*]	Standard deviation of Y
Addition or subtraction	$Y = A + B - C$	$s_Y = \sqrt{s_A^2 + s_B^2 + s_C^2}$
Multiplication or division	$Y = A \times B / C$	$\dfrac{s_Y}{Y} = \sqrt{\dfrac{s_A^2}{A} + \dfrac{s_B^2}{B} + \dfrac{s_C^2}{C}}$

[*]A, B and C are experimental variables with corresponding deviations of s_A, s_B and s_C

Chapter 3

Kinetic Model for Enzymatic PAC Production

3.1   NOMENCLATURE

Σ	sum of kappa products from all enzyme species for simplified model;
A	pyruvate;
B	benzaldehyde;
C	carbon dioxide;
E	free pyruvate decarboxylase (PDC) enzyme;
EA	binary enzyme complex between PDC and pyruvate;
E_o	initial activity of PDC enzyme (U carboligase ml^{-1});
EP	binary enzyme complex between PDC and PAC;
EQ	binary enzyme complex between PDC and 'active acetaldehyde';
EQB	ternary enzyme complex between PDC, 'active acetaldehyde' and benzaldehyde;
EQC	ternary enzyme complex between PDC, 'active acetaldehyde' and CO_2;
EQQ	ternary enzyme complex between PDC, 'active acetaldehyde' and acetaldehyde;
ER	binary enzyme complex between PDC and acetoin;
i	iteration loop identifier of each species to be used in numerical integration;
k_n	rate constant for forward reactions; n ranges from 1 to 10;
$k_{(-n)}$	rate constant for backward reactions; n ranges from 1 to 10;
k_{d1}	first order reaction time deactivation constant (h^{-1});
k_{d2}	first order benzaldehyde deactivation coefficient (mM^{-1} h^{-1});
K_{ma}	affinity constant for pyruvate (mM);
K_{mb}	affinity constant for benzaldehyde (mM);
K_r	rate constant product for the simplified model; r ranges from 1 to 19;
P	PAC;
Q	acetaldehyde;
R	acetoin;
t	time (h);
t_{lag}	lag time (h);
V_p	overall rate constant for the formation of PAC (μmol h^{-1} U^{-1});
V_q	overall rate constant for the formation of acetaldehyde (ml h^{-1} U^{-1});

V_r overall rate constant for the formation of acetoin (l^2 h^{-1} U^{-1} mol^{-1}).

3.2   INTRODUCTION

In a previous study, Chow (1998) combined the effect of pyruvate and benzaldehyde substrate limitation and inhibition, enzyme activity and PAC product inhibition to construct a rate equation for PAC formation in a biotransformation system containing 40 mM phosphate buffer. This equation covered the substrate concentrations range of 50-800 mM pyruvate and 5-300 mM benzaldehyde as well as 0.6-4.5 U carboligase ml^{-1}. An aggregate model consisting of six rate equations describing PAC, acetaldehyde and acetoin formation, pyruvate and benzaldehyde consumption as well as PDC deactivation was subsequently developed and employed in the simulation of existing enzymatic biotransformation profile reported by Shin and Rogers (1996b). The model fitting was in good agreement with experimental results at 150 mM (15.9 g l^{-1}) benzaldehyde and 225 mM (24.8 g l^{-1}) sodium pyruvate in 40 mM phosphate buffer at 4°C. Further simulation studies suggested that optimum benzaldehyde concentration should be maintained at 34 mM to achieve a maximum PAC concentration of 222 mM (33.3 g l^{-1}) at 14.7 h.

However this model was not validated over a range of initial substrate concentrations, it did not include the reaction mechanism involving the formation of by-products and did not describe the recently improved biotransformation process utilising 2-2.5 M MOPS as a buffering species (Rosche et al. 2002a,b, 2003a). The enzyme stability data reported by Chow et al. (1995) were subjected to major variations that were later found by Sandford (2002) to be strongly dependent on the benzaldehyde delivery method with PDC stability significantly increased when benzaldehyde was delivered as a solution rather than as droplets. The deactivation kinetics of PDC in benzaldehyde solution also showed a much higher degree of reproducibility. In the present research, a new model based on these improved conditions for initial rates and PDC stabilities has been developed and will be experimentally validated over a range of initial conditions.

The biotransformation of benzaldehyde and pyruvate to PAC and three by-products is a complex enzymatic process involving up to eight enzyme species including free enzyme, as well as binary and ternary enzyme complexes of enzyme-bound substrates, by-products and PAC. The general approach used in the classical Michaelis-Menten equation with only one substrate is not suitable for the current system due to its complexity. An alternative schematic method of deriving rate laws for complex enzyme-catalysed reactions developed previously by King and Altman (1956) has been employed in this Chapter to establish the requisite rate equations for the PAC biotransformation process. This set of non-linear differential equations provides a comprehensive mathematical model for the reactions. The model developed here includes also an equation describing the deactivation of PDC by benzaldehyde, which is tested experimentally (Leksawasdi et al. 2003) and described in Chapter 5. The combined rate equations can then be used to generate a profile of the batch biotransformation kinetics for PAC production and for future process optimization.

3.3   MODEL DEVELOPMENT

3.3.1   Proposed reaction mechanism

The proposed model for the enzymatic biotransformation of pyruvate and benzaldehyde to PAC and associated by-products (acetaldehyde, acetoin and CO_2) is shown in Figure 3.1. It consists of twenty composite reactions relating free PDC enzyme and its possible binary and ternary complexes. The transition mechanisms between binary (EA, EQ, ER and EP) and ternary complexes (EQB, EQC and EQQ) were expanded from the simple reaction mechanism involving two substrates and/or products proposed by Cornish-Bowden (1995).

The model shows the interaction of the substrate pyruvate (A) with the free PDC enzyme (E) to generate the enzyme complex EA. The decarboxylation function of the enzyme is illustrated via the formation of the ternary complex EQC from EA and its subsequent conversion to EQ with release of carbon dioxide (C). Also reverse reactions

are considered including the possibility of EQ formation from free enzyme (E) and acetaldehyde (Q).

Following decarboxylation of pyruvate, three fates are possible for EQ:

(1)   release of acetaldehyde from EQ as in the usual function of PDC for ethanol production. The free acetaldehyde is a by-product that may be used in the formation of acetoin,

(2)   reaction of EQ with free acetaldehyde through carboligase activity of PDC to create the ternary complex EQQ. Carboligation results in enzyme-bound by-product acetoin (ER). Acetoin (R) is released subsequently freeing PDC for further reaction,

(3)   complexing of EQ with benzaldehyde also through a carboligase reaction, resulting in the ternary complex EQB. Then PAC is formed leading to the binary complex EP. PAC is later released and the enzyme again becomes available.

The structure of this reaction mechanism is consistent with the widely accepted concept of the formation of an 'active acetaldehyde' or EQ at the PDC active site described previously in Section 1.4.2.4, Role of 'active acetaldehyde', p. 19. 'Active acetaldehyde' plays the central role in the carboligation reaction. According to Lobell and Crout (1996), the nucleophilic attack of 'active acetaldehyde' on the carbonyl carbon atom of aldehydes such as acetaldehyde and benzaldehyde results in the new compounds, acetoin and PAC. Alternatively, acetaldehyde can be released from the hydroxyethyl-TPP.

Figure 3.1: The proposed three-dimensional schematic diagram of PAC biotransformation and its related by-products for the determination of rate equations by the King and Altman method.

3.3.2   Simplification of the proposed reaction mechanism

The following reverse reactions have been assumed to be negligible, to simplify the proposed reaction mechanism:

(1)   the decarboxylation pathway of PDC was simplified by neglecting the reverse reactions, as this direction would involve ligation of CO_2 (EQC to EA) which was considered unfavourable ($k_{(-1)} = 0$, $k_{(-2)} = 0$, $k_{(-3)} = 0$),

(2)   the nucleophilic attacks of 'active acetaldehyde' within the ternary complexes EQB and EQQ, which lead to the formation of binary complexes EP and ER,

were assumed to be irreversible ($k_{(-6)} = 0$, $k_{(-9)} = 0$). Also the reverse reactions of the preceding association of benzaldehyde (B), or free acetaldehyde (Q) with EQ, were neglected ($k_{(-5)} = 0$, $k_{(-8)} = 0$). The assumption of $k_{(-9)} = 0$ is in consistent with the kinetic data for the forward reaction resulting in acetoin production by brewer's yeast PDC of Chen and Jordan (1984) and Stivers and Washabaugh (1993),

(3)   direct interactions of either the product PAC (P) or by-product acetoin (R) with the PDC enzyme were considered negligible, therefore $k_{(-7)} = 0$ and $k_{(-10)} = 0$ respectively. The assumption of $k_{(-10)} = 0$ is consistent also with the kinetic data which demonstrated acetoin production by brewer's yeast PDC of Chen and Jordan (1984) and Stivers and Washabaugh (1993).

The general simplified reaction mechanism is shown in Figure 3.2.

Special attention can be given to $k_{(-4)}$ which represents the rate constant for the formation of EQ from free PDC and free acetaldehyde. It has been suggested by Rosche et al. (2003b) that this reaction might be a characteristic of bacterial PDC as PAC formation from benzaldehyde and acetaldehyde was observed with *Z. mobilis* (Breuer et al. 1997, Goetz et al. 2001, Iwan et al. 2001, Rosche et al. 2004a) and *Zymobacter palmae* (Rosche et al. 2003b), while 97 species of yeast including *C. utilis* did not convert acetaldehyde and benzaldehyde to detectable concentrations of PAC (with the methods employed) even though PAC was produced from pyruvate and benzaldehyde (Rosche et al. 2003b). According to the investigation by Chen and Jordan (1984), brewer's yeast PDC (EC 4.1.1.1) was able to convert acetaldehyde, in absence of pyruvate, to acetoin but only to a limited extent. At 40°C and pH 6.0, these authors reported that acetoin was formed 60 to 100 times faster from pyruvate than from acetaldehyde. As k_8, k_9 and k_{10} are common to both reactions, it was suggested that EQ is produced 60 to 100 times faster from pyruvate than from acetaldehyde. Therefore, formation of EQ from free acetaldehyde could be neglected for *C. utilis* PDC ($k_{(-4)} = 0$). Any inhibition effects of substrates, PAC, or by-products have been assumed to be negligible at this stage of model development.

3.3.3 Rate equations for the general simplified reaction

The law of mass action has been applied to the general simplified reaction (Figure 3.2) which could apply to both bacteria and yeast PDC and the following rate equations have been obtained:

Rate of PAC production

$$\frac{d[P]}{dt}\bigg|_i = k_7 \, [EP_i] \tag{3.1}$$

Rate of benzaldehyde uptake

$$\frac{d[B]}{dt}\bigg|_i = -k_5 [EQ_i][B_i] \tag{3.2}$$

Rate of pyruvate uptake

$$\frac{d[A]}{dt}\bigg|_i = -k_1 [E_i][A_i] \tag{3.3}$$

Rate of acetoin production

$$\frac{d[R]}{dt}\bigg|_i = k_{10} \, [ER_i] \tag{3.4}$$

Rate of acetaldehyde production

$$\frac{d[Q]}{dt}\bigg|_i = k_4 \, [EQ_i] - k_{(-4)}[E_i][Q_i] - k_8[EQ_i][Q_i] \tag{3.5}$$

Rate of CO_2 production

$$\frac{d[C]}{dt}\bigg|_i = k_3 \, [EQC_i] \tag{3.6}$$
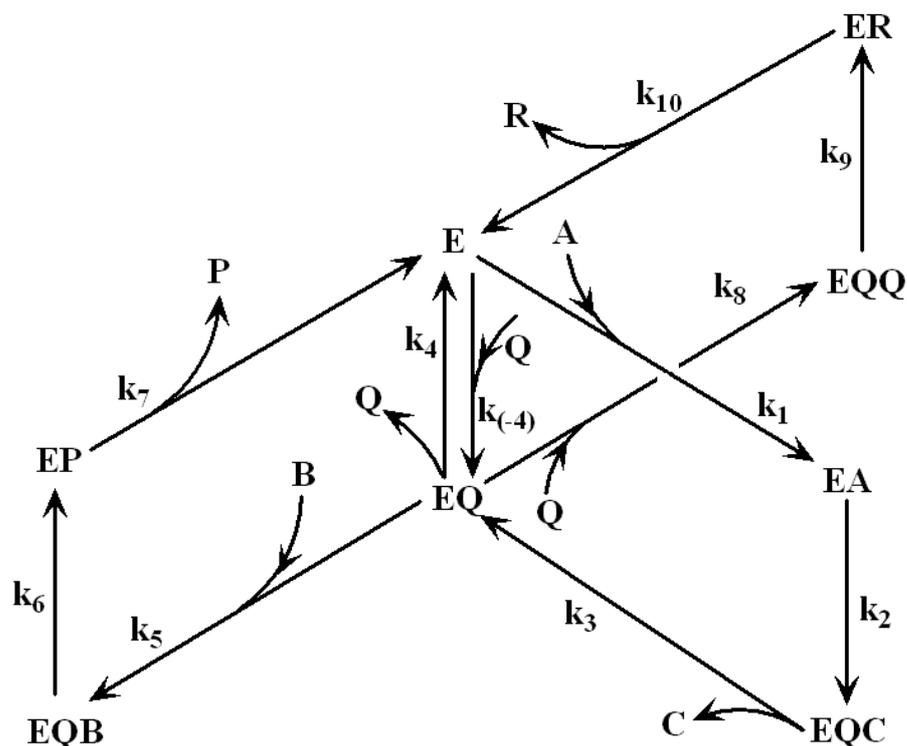
Figure 3.2: Simplification of the proposed three dimensional schematic diagram in Figure 3.1 by neglecting backward rate constants except $k_{(-4)}$.

An enzyme deactivation rate equation also needs to be included to take account of the deactivating influence of benzaldehyde on PDC. It describes the rate of enzyme deactivation based on 'total enzyme concentration' (E_o) and not 'free enzyme concentration' (E), which is one component of E_o. The distinction of these terms is necessary since in the current model development some of the rate equations (Equations (3.3) and (3.5)) include a term for free enzyme.

Rate of enzyme deactivation

$$\frac{d[E_o]}{dt}\bigg|_i = -\left(k_{d1} + k_{d2}.[B_i]\right)[E_{oi}] \qquad (3.7)$$

The rate equation describing PDC deactivation shown in Equation (3.7) is listed and confirmed in Chapter 5. It exhibits a first order deactivation of PDC by benzaldehyde

(B) up to a concentration of 200 mM. k_{d1} represents the inherent enzyme deactivation constant in 2.5 M MOPS buffer in absence of benzaldehyde and k_{d2} is a benzaldehyde deactivation coefficient in the range of 0–200 mM benzaldehyde.

3.3.4 The King and Altman procedure

The method of King and Altman (1956) was selected for the present study. This method has been used by other authors (Wong and Hanes 1962, Volkenstein and Goldstein 1966) as a basis for development of further methods for analysis and derivation of rate equations for complex enzymatic systems.

From the proposed simplified PAC biotransformation mechanism shown in Figure 3.2, there are eight enzyme species: free enzyme (E), four binary enzyme-substrate or enzyme-product complexes (EA, EQ, EP and ER) and three ternary complexes (EQB, EQQ and EQC). A reaction is represented by an arrow directed to or away from the specified enzyme complex. The rate constant and accompanying substrate (where applicable) for the reaction are also given on each arrow. Reaction patterns were established according to the King and Altman (1956) procedure.

For a pattern to be valid, it must satisfy the following criteria:

(1)   arrows must connect all forms of enzyme complexes in the reaction mechanism, a pattern that visits all eight enzyme species therefore consists of seven arrows

(2)   connected arrows must not form closed loop(s)

(3)   all arrows in the pattern must be pointing in the direction that leads to the formation of the enzyme complex under investigation.

A combinatorial theorem was applied with the above criteria using the subroutines designed in Visual Basic 6.3 of Microsoft® EXCEL 2002 to select the valid reaction patterns (see Appendix A, p. 220).

3.4   RESULTS

3.4.1   Application of King and Altman procedure

The patterns derived from the general simplified reaction (Figure 3.2) corresponding to each enzyme complex are presented in Figure 3.3.

These patterns were then used in further model development. Equations (3.1) to (3.6) are not particularly useful because they contain the various enzyme complexes (EQ, ER, EP and EQC) whose concentrations are not measurable experimentally. For obtaining a usable set of rate equations based on experimental data, the King and Altman procedure uses patterns to create expressions for each enzyme complex related to measurable concentrations of pyruvate, acetaldehyde and benzaldehyde.

The term 'kappa product' was used by King and Altman (1956) to define the multiplication of the product of all rate constants (known as 'rate constant product') with the substrate concentration variables for all arrows of a specific pattern. As an example, the kappa product derivation is illustrated for the enzyme complex EP in Figure 3.4.

Palmer (1991) illustrated clearly the application of King and Altman procedure in the derivation of the rate equations for single-substrate Michaelis-Menten kinetics and other more complicated reactions. The following relationship was used in the present study as a simplified version of determinant solutions from King and Altman:

$$\frac{[\textit{Enzyme complex species}]}{[E_o]} = \frac{\textit{Sum of kappa products for a particular enzyme species}}{\textit{Sum of all kappa products for all enzyme species}} \qquad (3.8)$$

After determination of the kappa products sum for each enzyme species, an expression for the concentration of each enzyme complex related to the concentrations of pyruvate, benzaldehyde and acetaldehyde can be obtained from Equation (3.8).

Enzyme species (pattern designation)	King and Altman pattern of Figure 3.2
E (K_1, K_2, K_3)	
EQ (K_4, K_5)	
EP (K_6, K_7)	
EA (K_8, K_9, K_{10})	
ER (K_{11}, K_{12})	
EQB (K_{13}, K_{14})	
EQC (K_{15}, K_{16}, K_{17})	
EQQ (K_{18}, K_{19})	

Figure 3.3: The patterns for each enzyme species derived with the King and Altman procedure from the general simplified reaction mechanism in Figure 3.2.

Substitution of these revised enzyme complex expressions derived from the King and Altman procedure in Equations (3.1) to (3.6) resulted in a theoretical model representing the biotransformation of PAC and its related by-products based on the simplified mechanism.

The summation of kappa products derived for each complex for both bacterial and yeast PDC are listed in Table 3.1. The last row of Table 3.1 is the summation expression of all kappa products from the top rows. The symbols K_1 to K_{19} are the abbreviations of rate constant products as listed in Table 3.2.

Using Equation (3.8) and the kappa product expressions given in Table 3.1 (column 3), the new expressions for the concentrations of the various enzyme complexes expressed as fractions of total enzyme activity were derived for yeast PDC. These now consist only of rate constants and concentrations of measurable species.
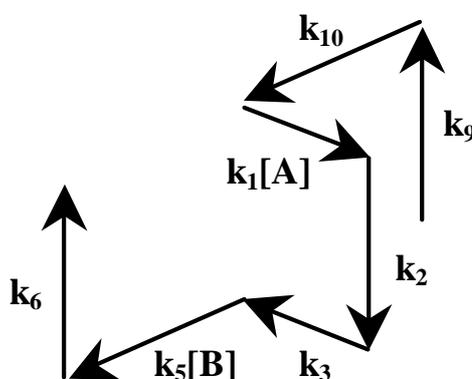
Figure 3.4: As an example of kappa product derivation, the procedure is explained for the sixth entry of Figure 3.3, a pattern for EP. The corresponding rate constant product and kappa product of this pattern are $k_1k_2k_3k_5k_6k_9k_{10}$ and $k_1k_2k_3k_5k_6k_9k_{10}[A][B]$ or $K_6[A][B]$ respectively. K_6 is the abbreviated term for the rate constant product derived from this Figure.

Table 3.1: The sum of kappa products corresponding to each enzyme species for the simplified model (Figure 3.2) and the simplified model for yeast PDC ($k_{(-4)} = 0$).

Enzyme Species	Sum of kappa products	
	General simplified model	**Simplified model for yeast[*] ($k_{(-4)} = 0$)**
E	$K_1 + K_2[Q_i] + K_3[B_i]$	$K_1 + K_2[Q_i] + K_3[B_i]$
EQ	$K_4[A_i] + K_5[Q_i]$	$K_4[A_i]$
EP	$K_6[A_i][B_i] + K_7[Q_i][B_i]$	$K_6[A_i][B_i]$
EA	$K_8[A_i] + K_9[A_i][B_i] + K_{10}[Q_i][A_i]$	$K_8[A_i] + K_9[A_i][B_i] + K_{10}[Q_i][A_i]$
ER	$K_{11}[Q_i][A_i] + K_{12}[Q_i][Q_i]$	$K_{11}[Q_i][A_i]$
EQB	$K_{13}[A_i][B_i] + K_{14}[Q_i][B_i]$	$K_{13}[A_i][B_i]$
EQC	$K_{15}[A_i] + K_{16}[A_i][B_i] + K_{17}[Q_i][A_i]$	$K_{15}[A_i] + K_{16}[A_i][B_i] + K_{17}[Q_i][A_i]$
EQQ	$K_{18}[Q_i][A_i] + K_{19}[Q_i][Q_i]$	$K_{18}[Q_i][A_i]$
Σ	$K_1 + (K_4 + K_8 + K_{15})[A_i] + K_3[B_i] +$ $(K_2 + K_5)[Q_i] +$ $(K_6 + K_9 + K_{13} + K_{16})[A_i][B_i] +$ $(K_{10} + K_{11} + K_{17} + K_{18})[Q_i][A_i] +$ $(K_7 + K_{14})[Q_i][B_i] + (K_{12} + K_{19})[Q_i][Q_i]$	$K_1 + (K_4 + K_8 + K_{15})[A_i] + K_3[B_i] +$ $K_2[Q_i] +$ $(K_6 + K_9 + K_{13} + K_{16})[A_i][B_i] +$ $(K_{10} + K_{11} + K_{17} + K_{18})[Q_i][A_i]$

[*] For the simplified model of yeast PDC, $K_5 = K_7 = K_{12} = K_{14} = K_{19} = 0$, because $k_{(-4)} = 0$.

Table 3.2: The corresponding rate constant products of K_1 to K_{19} symbols.

Symbol	Rate constant product	Symbol	Rate constant product
K_1	$k_2k_3k_4k_6k_7k_9k_{10}$	K_{11}	$k_1k_2k_3k_6k_7k_8k_9$
K_2	$k_2k_3k_6k_7k_8k_9k_{10}$	K_{12}	$k_2k_3k_6k_7k_8k_9k_{(-4)}$
K_3	$k_2k_3k_5k_6k_7k_9k_{10}$	K_{13}	$k_1k_2k_3k_5k_7k_9k_{10}$
K_4	$k_1k_2k_3k_6k_7k_9k_{10}$	K_{14}	$k_2k_3k_5k_7k_9k_{10}k_{(-4)}$
K_5	$k_2k_3k_6k_7k_9k_{10}k_{(-4)}$	K_{15}	$k_1k_2k_4k_6k_7k_9k_{10}$
K_6	$k_1k_2k_3k_5k_6k_9k_{10}$	K_{16}	$k_1k_2k_5k_6k_7k_9k_{10}$
K_7	$k_2k_3k_5k_6k_9k_{10}k_{(-4)}$	K_{17}	$k_1k_2k_6k_7k_8k_9k_{10}$
K_8	$k_1k_3k_4k_6k_7k_9k_{10}$	K_{18}	$k_1k_2k_3k_6k_7k_8k_{10}$
K_9	$k_1k_3k_5k_6k_7k_9k_{10}$	K_{19}	$k_2k_3k_6k_7k_8k_{10}k_{(-4)}$
K_{10}	$k_1k_3k_6k_7k_8k_9k_{10}$		

3.4.2 Rate equations from the simplified reaction mechanism for yeast PDC

3.4.2.1 PAC Production

Algebraic rearrangement of Equation (3.9) obtained from Equation (3.1) and the expression of EP from column three of Table 3.1, results in Equation (3.10).

$$
\frac{d[P]}{dt}\bigg|_i = \frac{k_7 K_6 [A_i][B_i][E_{oi}]}{\Sigma} \tag{3.9}
$$

$$
\frac{d[P]}{dt}\bigg|_i = \frac{[A_i][B_i][E_{oi}]}{\left(\frac{1}{k_1}+\left(\frac{1}{k_2}+\frac{1}{k_3}\right)[A_i]\right)\left(\frac{k_4}{k_5}+[B_i]+\frac{k_8}{k_5}[Q_i]\right)+[A_i]\left(\frac{1}{k_5}+\left(\frac{1}{k_6}+\frac{1}{k_7}\right)[B_i]+\frac{k_8}{k_5}\left(\frac{1}{k_9}+\frac{1}{k_{10}}\right)[Q_i]\right)} \tag{3.10}
$$

The following assumptions have been made to simplify Equation (3.10):

(1)   from the biotransformation profiles obtained experimentally (Rosche et al. 2003a), the concentration of acetaldehyde $[Q_i]$ was significantly lower than those of benzaldehyde and pyruvate. Thus $[Q_i]$ was neglected in the above PAC rate equation,

(2)   the decarboxylation pathway of pyruvate (k_1, k_2 and k_3), which leads to the formation of 'active acetaldehyde' was considered rate limiting in the pathways of PAC and acetoin formation. Assuming the rate constants leading to PAC (k_5, k_6, k_7) to be large, allows further simplification by neglecting the third term of the denominator in Equation (3.10).

After simplification and rearrangement, Equation (3.11) is obtained. This has the form of an equation with two-substrate Michaelis-Menten type kinetics for each substrate as illustrated in Equation (3.12).

$$\frac{d[P]}{dt}\bigg|_i = \frac{\left(\dfrac{k_2 k_3}{k_2 + k_3}\right)[A_i][B_i][E_{oi}]}{\left(\dfrac{1}{k_1}\dfrac{k_2 k_3}{(k_2 + k_3)} + [A_i]\right)\left(\dfrac{k_4}{k_5} + [B_i]\right)} \tag{3.11}$$

$$\frac{d[P]}{dt}\bigg|_i = \frac{V_p [A_i][B_i][E_{oi}]}{\left(K_{ma} + [A_i]\right)\left(K_{mb} + [B_i]\right)} \tag{3.12}$$

where: $V_p = \dfrac{k_2 k_3}{k_2 + k_3}$, $K_{ma} = \dfrac{1}{k_1}\dfrac{k_2 k_3}{k_2 + k_3}$, $K_{mb} = \dfrac{k_4}{k_5}$

A double substrate kinetic model had been applied also by Goetz et al. (2001) and Iwan et al. (2001) to predict a profile of continuous PAC production in an enzyme membrane reactor using a potent mutant of *Z. mobilis* PDC.

3.4.2.2 Benzaldehyde Consumption

Equation (3.2) and the expression for EQ in Table 3.1 are used in solving for rate equation of benzaldehyde consumption. The resulting equation is shown as Equation (3.13).

$$\frac{d[B]}{dt}\bigg|_i = -\frac{k_5 K_4 [A_i][B_i][E_{oi}]}{\Sigma} \tag{3.13}$$

Because $k_5 K_4/\Sigma$ is in fact $k_7 K_6/\Sigma$ (from information in Tables 3.1 and 3.2), Equation (3.13) can then be rearranged as shown in Equation (3.14).

$$\frac{d[B]}{dt}\bigg|_i = -\frac{k_7 K_6 [A_i][B_i][E_{oi}]}{\Sigma} = -\frac{d[P]}{dt}\bigg|_i \tag{3.14}$$

3.4.2.3   Acetoin Production

Substitution of Equation (3.4) with kappa product expression for ER given in Table 3.1 results in Equation (3.15). The term V_r is introduced in Equation (3.16) to replace $k_{10}K_{11}/\Sigma$.

$$\left.\frac{d[R]}{dt}\right|_i = \frac{k_{10}K_{11}[Q_i][A_i][E_{oi}]}{\Sigma} \tag{3.15}$$

$$\left.\frac{d[R]}{dt}\right|_i = V_r[Q_i][A_i][E_{oi}] \tag{3.16}$$

3.4.2.4   Acetaldehyde Production

The rate equation describing the formation of acetaldehyde (Equation (3.17)) can be obtained from Equation (3.5) and from Table 3.1 for [E] and [EQ]. The term V_q for acetaldehyde formation replaces k_4K_4/Σ.

$$\left.\frac{d[Q]}{dt}\right|_i = \frac{k_4K_4[A_i][E_{oi}] - k_8K_4[Q_i][A_i][E_{oi}]}{\Sigma} \tag{3.17}$$

As k_8K_4/Σ is in fact $k_{10}K_{11}/\Sigma$ (Tables 3.1 and 3.2) or V_r, Equation (3.17) can be rewritten as Equation (3.18).

$$\left.\frac{d[Q]}{dt}\right|_i = V_q[A_i][E_{oi}] - V_r[Q_i][A_i][E_{oi}] \tag{3.18}$$

3.4.2.5   Pyruvate Consumption

By inserting the expression of E from Table 3.1 to Equations (3.3), Equation (3.19) is obtained.

$$\left.\frac{d[A]}{dt}\right|_i = -\frac{k_1K_1[A_i][E_{oi}] + k_1K_2[Q_i][A_i][E_{oi}] + k_1K_3[A_i][B_i][E_{oi}]}{\Sigma}$$ (3.19)

Writing k_1K_1/Σ as V_q and k_1K_2/Σ as V_r and expressing k_1K_3/Σ as k_7K_6/Σ (Tables 3.1 and 3.2), Equation (3.19) can be rewritten then as Equation (3.20).

$$\left.\frac{d[A]}{dt}\right|_i = -V_q[A_i][E_{oi}] - V_r[Q_i][A_i][E_{oi}] - \left.\frac{d[P]}{dt}\right|_i$$ (3.20)

Further rearrangements of Equation (3.20) using Equations (3.16) and (3.18) results in Equation (3.21).

$$\left.\frac{d[A]}{dt}\right|_i = -\left.\frac{d[P]}{dt}\right|_i - \left.\frac{d[Q]}{dt}\right|_i - 2\left.\frac{d[R]}{dt}\right|_i$$ (3.21)

The coefficient of 2 in the rate equation for acetoin reflects the fact that it requires two moles of pyruvate for one mole of its production.

3.4.2.6 CO₂ Production

Equation (3.22) is obtained after combination of Equation (3.6) with the expression for EQC given in Table 3.1.

$$\left.\frac{d[C]}{dt}\right|_i = \frac{k_3K_{15}[A_i][E_{oi}] + k_3K_{17}[Q_i][A_i][E_{oi}] + k_3K_{16}[A_i][B_i][E_{oi}]}{\Sigma}$$ (3.22)

As k_3K_{15}/Σ can be written as V_q, k_3K_{17}/Σ as V_r and k_3K_{16}/Σ as k_7K_6/Σ (Tables 3.1 and 3.2), Equation (3.22) can be rewritten as Equation (3.23).

$$\left.\frac{d[C]}{dt}\right|_i = V_q[A_i][E_{oi}] + V_r[Q_i][A_i][E_{oi}] + \left.\frac{d[P]}{dt}\right|_i$$ (3.23)

The modification of Equation (3.23) is performed then in similar way to that for Equation (3.20) to obtain Equation (3.24).

$$\frac{d[C]}{dt}\bigg|_i = \frac{d[P]}{dt}\bigg|_i + \frac{d[Q]}{dt}\bigg|_i + 2\frac{d[R]}{dt}\bigg|_i \tag{3.24}$$

The system of differential equations developed here forms the basis of a time profile for a batch biotransformation process of PAC production. Simultaneous numerical integration of Equations (3.7), (3.12), (3.14), (3.16), (3.18) and (3.21) with the Euler-Cauchy method (Kreyszig 1993) results in concentration-time profiles for PAC production, decrease in PDC activity, benzaldehyde consumption, pyruvate consumption, acetoin and acetaldehyde formation. Equation (3.24) for the CO_2 production profile may be relevant for the future design of a feedback control strategy for substrate feeding based on the rate of CO_2 emission.

3.5 DISCUSSION

The method of King and Altman used in the current study has been applied by various other authors for the derivation of rate equations from complex reaction systems. These include the reaction of acetylcholine esterase to break down the neurotransmitter acetylcholine to acetate and choline (Principato et al. 1979), the hydrolysis of ATP by (Na,K)-ATPase (Moczydlowksi and Fortes 1981), the reduction of cytochrome-c with reductase (Motilva et al. 1988), the inhibition of xanthine oxidase by uric acid in the reduction of xanthine (Radi et al. 1992) and endocytosis of sucrose lipoprotein by Hep-G2 cells (Harwood and Pellarin 1997). An alternative procedure for evaluating King and Altman diagrams was also suggested by Myers and Palmer (1985).

The computer algorithm for King and Altman method was given by Olavarria (1986) to calculate all patterns, including those containing cycles. Further extension of the method has been made by Zhao (1992) to the analysis of relaxation times of enzyme-catalysed reactions and by Mogi (1993) to "a graphic transformation method" in obtaining the steady-state distribution of a coupled system. Mazur and Kuchinski (1992) related the similarity of King and Altman procedure to probabilistic enzyme kinetics in

avoiding the use of the mass action law for deriving rate equations. Topham and Brocklehurst (1992) used a King and Altman schematic diagram in an evaluation of the general validity of the Cha method (Cha 1968), an alternative method for deriving rate equations.

The advantage of constructing a model from its overall reaction mechanisms is that all neglected variables and rate constants can be recovered if evidence negating the validity of one or more of the assumptions emerges. For example, the application of the more complicated forms of rate equations is possible in case of inadequate fitting of the data with the more simplified forms.

Detailed experimental determination of kinetic parameters and validation studies over a range of initial benzaldehyde and pyruvate concentrations are reported in Chapter 6. The potential of such modelling is that it provides a more complete analysis of the reaction mechanisms as well as the basis for future process optimization.

3.6   CONCLUSIONS

In the present Chapter, a simplified mathematical model has been developed which describes the enzymatic conversion of pyruvate and benzaldehyde by PDC to PAC and associated by-products acetaldehyde and acetoin. The model incorporates the accepted mechanism of PAC production involving pyruvate decarboxylation by PDC to form an 'active acetaldehyde' enzyme complex, followed by its subsequent reaction with benzaldehyde (or acetaldehyde to form by-product acetoin). It also accounts for the experimental observation that PDC from some bacteria (e.g. *Zymomonas* sp.) can efficiently convert acetaldehyde and benzaldehyde to PAC (Rosche et al. 2004a), while PDC from various yeasts and fungi require pyruvate rather than acetaldehyde for the biotransformation (Rosche et al. 2003b).

Chapter 4

Enzyme Selection: Comparison of Characteristics of PDC from Fungal and Yeast Sources

4.1   NOMENCLATURE

E   relative enzyme activity at time t;

E_0 initial relative enzyme activity (100%);

k_{rj} enzyme deactivation constant (h^{-1});

k_{sv} spore viability decay constant (day^{-1});

R^2 correlation coefficient;

t   time (h or day);

t_{lag} lag time (h);

V   percentage of spore viability at time t;

V_0 initial percentage of spore viability (100%).

4.2   INTRODUCTION

PDC is found in a wide range of ethanol-producing bacteria, yeasts and filamentous fungi. *In vivo*, PDC decarboxylates pyruvate, the end product of glycolysis, to produce acetaldehyde and CO_2. Acetaldehyde is further reduced by alcohol dehydrogenase and $NADH + H^+$ to ethanol. *In vitro*, PDC from the filamentous fungus *R. javanicus* may be used to catalyse the biotransformation of pyruvate and benzaldehyde to PAC.

Evaluation of a number of ethanol-producing filamentous fungi (19 *Aspergillus* sp. and 10 *Rhizopus* sp.) by Skory et al. (1997) suggested that strains of *R. oryzae* and *R. javanicus* were relatively efficient at converting simple sugars to ethanol. Subsequent screening by our group of *Ascomycota*, *Zygomycota* and *Basidiomycota* have identified strains of *Rhizopus* sp. and *Fusarium* sp. as potential sources of PDC for PAC production (Rosche et al. 2001) and have established that an enzymatic process based on PDC from *R. javanicus* can produce up to 50.6 g PAC l^{-1} (337 mM) in 29 h at 6°C from initial concentrations of 396 mM benzaldehyde and 600 mM pyruvate (Rosche et al. 2002a,b). It was further shown that the molar yield of PAC on consumed pyruvate from *R. javanicus* could be improved (from 59% to 74%) by lowering the concentration of Mg^{2+} in the biotransformation buffer from 20 to 0.5 mM (Rosche et al. 2003a).

Cultivation of filamentous fungi can be more difficult relative to yeast or bacteria due to changes in morphology during growth resulting in the formation of long filaments, pellets or fungal mats (Papagianni and Moo-Young 2002). Many factors have been reported to affect their morphology, including the strain type, inoculum concentration, medium composition, pH, presence of surfactants, polymer additives, agitation speed and presence of particulate matter in the medium (Byre and Ward 1989, Prosser and Tough 1991, Du et al. 2003). For example, shake flask experiments with *R. javanicus* have shown that inoculum concentrations of 10^5 spores ml^{-1} and lower resulted in the formation of large mycelial aggregates with hollow centres indicating mycelial degradation, while inoculation with 10^6 spores ml^{-1} resulted in homogeneously dispersed mycelia (Rosche et al. 2001).

In this Chapter, the growth of a strain of the filamentous fungus *R. javanicus* has been investigated for a range of cultivation conditions and various key factors influencing the production of PDC were identified. The characteristics of *R. javanicus* PDC were assessed to determine the effects of temperature (6 and 25°C), benzaldehyde concentration (50 mM), degree of enzyme purification (partially purified and crude extract), pH, initial enzyme activity and magnesium sulphate concentration (0 and 20 mM) and addition of protease inhibitors on PDC deactivation kinetics. The study provides the basis for a comparison of the characteristics of PDC produced from various sources for further process optimization.

4.3   RESULTS AND DISCUSSION

4.3.1   Viability of frozen spore suspension

The inoculation of cultivation medium with spores is more convenient than using vegetative cells because spores can tolerate more adverse conditions and can be stored in frozen form without the need for immediate cultivation prior to inoculation. Germination and growth can resume rapidly once inoculated into a suitable environment (Smith 1975). The viability-time profile for a frozen spore suspension of *R. javanicus* stored at -20°C is shown in Figure 4.1. A first order decay equation (Equation (4.1)) was fitted to the experimental data (Figure 4.1) resulting in a spore viability decay constant (k_{sv}) of 7.35 x 10^{-3} day^{-1} with a correlation coefficient (R^2) of 0.98:

$$ V = V_0 \ e^{(-k_{sv}t)} \tag{4.1} $$

where: V is the percentage of spore viability at time t relative to total spore concentration, V_0 is the initial percentage of spore viability (100%), k_{sv} is the spore viability decay constant (day^{-1}) and t is the storage time of frozen spore suspension (day).

Based on this result, the spore inoculum could be stored at –20°C for a month while maintaining spore viability above 80%. The half-life of the frozen spore suspension was 94 days.

Other authors have reported on the effects of storage conditions on the viability of spores from various fungi. For example, the spores of *Aspergillus ochraceus* could be stored without any detectable loss of hydroxylating activity for 3 months at 4°C and 1 year at -20°C (Singh et al. 1992). A slight decline in spore viability of *Penicillium bilaii* in the period of 3 months under refrigeration was observed when the spores were evenly-coated with instant skim milk powder in a fluidized bed dryer (Tadayyon et al.

1997). The spore viability of green macroalga *Enteromorpha intestinalis* in a reduced saline medium (75% (v/v) seawater and 5-10% (v/v) dimethyl sulphoxide (DMSO)) was above 40% when stored at -20°C for up to 35 days (Taylor and Fletcher 1999). The spore half-lives of 2.0 years (stored at 24°C) and 3.5 years (stored at 4°C) has been reported for *Glomus claroideum* (Wagner et al. 2001).
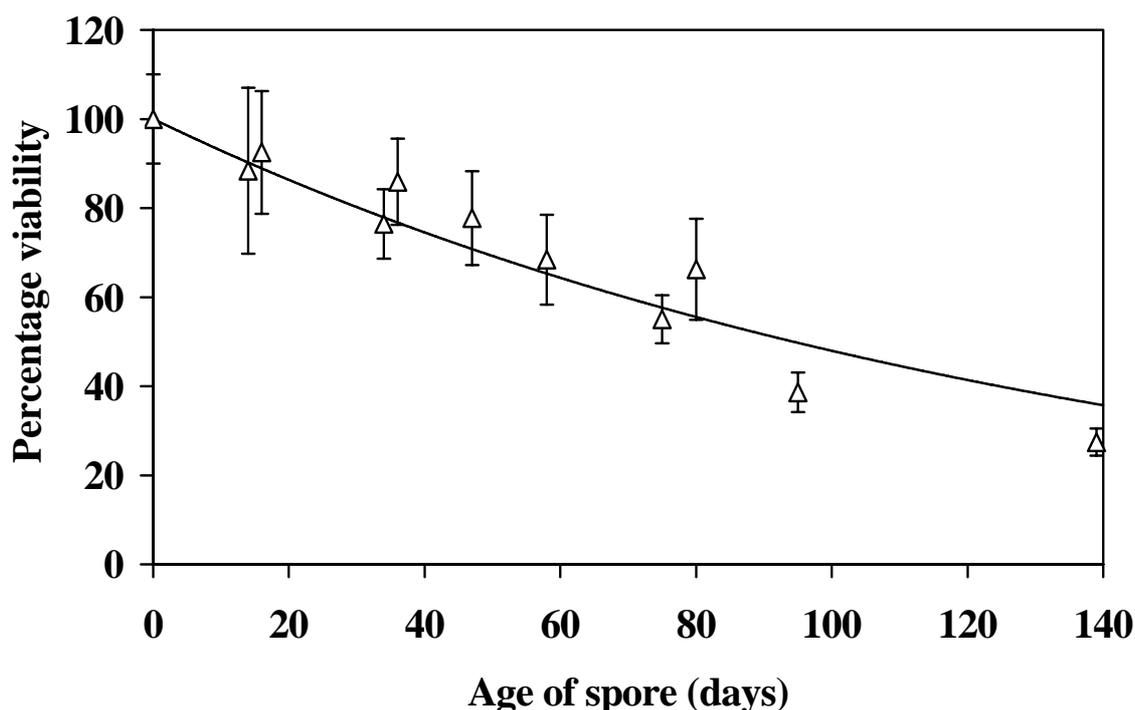
Figure 4.1: The percentage viability of *R. javanicus* spores during storage at -20°C. The viability of the spore suspension was calculated from the number of germinated spores after 6 h relative to total spores in cultivation medium. The error bar of each data point shows lowest and highest value of three to five counts.

4.3.2   Effect of nitrogen source on PDC production

The effect of two different nitrogen sources in the cultivation medium was evaluated. In the presence of only inorganic nitrogen (10 g (NH$_4$)$_2$SO$_4$ l^{-1}), growth was very low with 4.1 g dry biomass l^{-1} produced. The effect of yeast extract addition on ethanol and specific PDC production by *R. javanicus* in 500 ml Erlenmeyer flasks is shown in

Figure 4.2. Addition of 2, 5 and 10-50 g yeast extract l^{-1} resulted in an average of 6.2, 10.6 and 12.4 g biomass l^{-1} respectively. Ethanol formation increased with increasing yeast extract concentration up to 10 g l^{-1}, reaching a maximum of 35 g ethanol l^{-1} at this concentration. The ethanol concentrations remained similar (31–35 g l^{-1}) when higher levels of yeast extract (up to 50 g l^{-1}) were used. Skory et al. (1997) reported the production of 23.5 and 19.6 g ethanol l^{-1} at day 3 from the same strain of *R. javanicus*, which was cultivated in YPM media (3 g yeast extract l^{-1}, 5 g peptone l^{-1} and 3 g malt extract l^{-1}) supplemented with 50 and 100 g glucose l^{-1} respectively.

In the present experiments, PDC production peaked at 20 g yeast extract l^{-1} with specific PDC activity levels of 286 U decarboxylase g^{-1} mycelium and 3.48 U decarboxylase ml^{-1} culture (Figure 4.2). PDC activities were found to decrease at higher yeast extract levels. As a more economical choice for further investigation of *R. javanicus* cultivation, 10 g yeast extract l^{-1} addition to the medium was selected. An acceptable level of PDC production (244 U decarboxylase g^{-1} mycelium and 2.92 U decarboxylase ml^{-1} culture) was achieved with 10 g yeast extract l^{-1}.
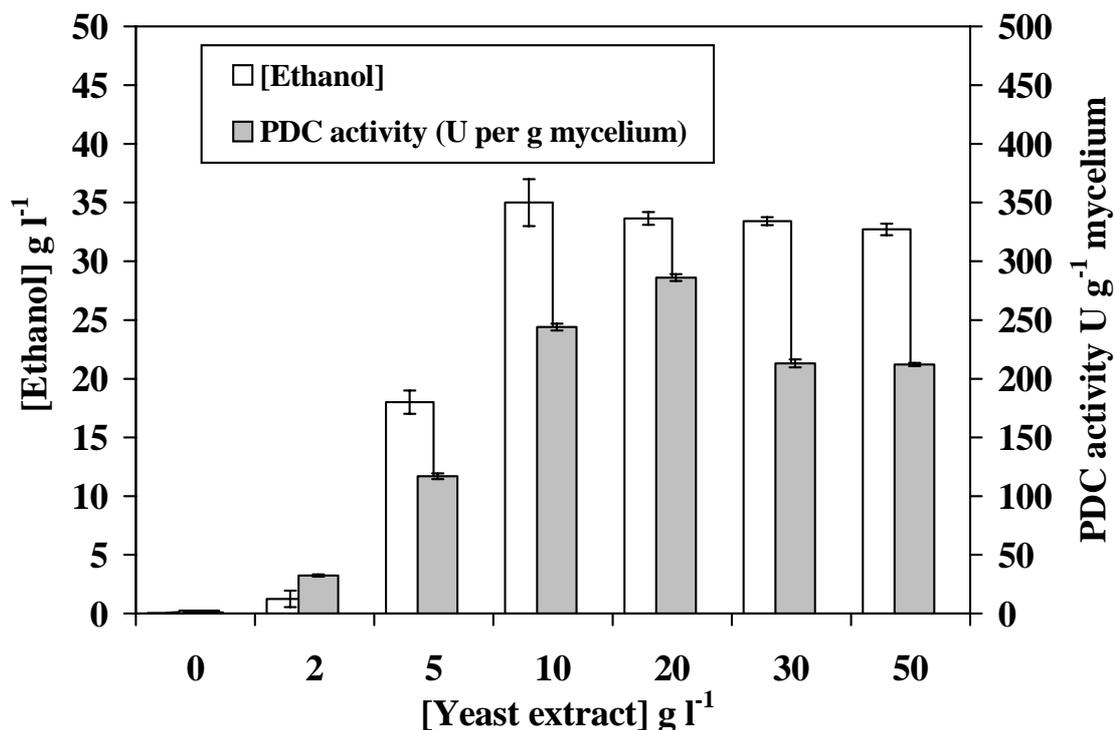
Figure 4.2: The effect of yeast extract concentration in the range of 0 to 50 g l^{-1} on ethanol production (g l^{-1}) and specific PDC activity (U decarboxylase g^{-1} mycelium) of *R. javanicus* after 24 h. The error bars (maximum and minimum values) for of each data point were computed from two to three replicates of experiments in Erlenmeyer flasks.

4.3.3 Effect of growth conditions on mycelial morphology

Dispersed mycelial cultures are desirable because:

(1)   mass transfer limitations of nutrients and products are less likely to occur for dispersed mycelia than for clumps or pellet forms of growth,

(2)   for experimental studies, the samples withdrawn should be representative of the whole cultivation batch.

A dispersed mycelial form of growth of *R. javanicus* is illustrated in Figure 4.3 for a shake flask culture. The increases in yeast extract concentration in Erlenmeyer flask did not alter the morphology of its growth.
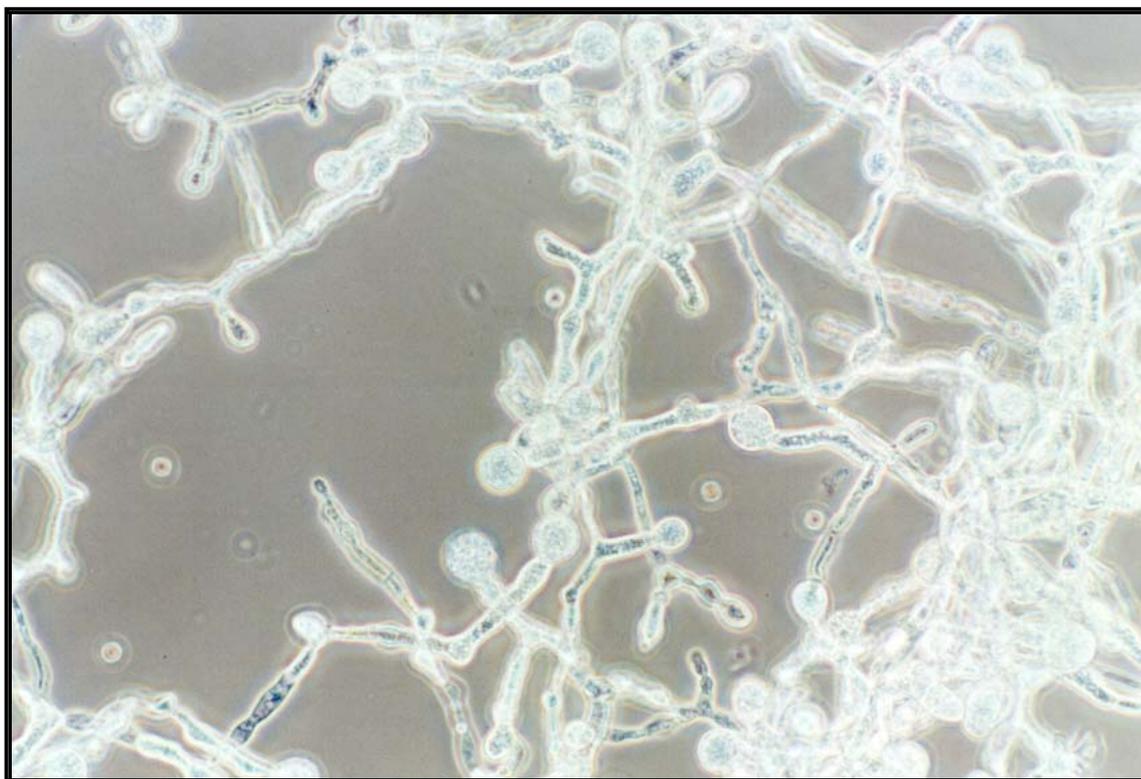
Figure 4.3: Growth morphology of *R. javanicus* at 24 h (250× magnification) in 500 ml non-baffled Erlenmeyer flask with 100 ml cultivation medium.

In 5 l controlled bioreactor experiments, high levels of agitation and aeration were found to play significant roles in heterogeneous formation by *R. javanicus* while the moderate or lower agitation and aeration levels generated a more homogeneous morphology. Figure 4.4(a) provides evidence of homogeneous dispersed fungal growth under conditions of low to moderate agitation and aeration. However, when the dissolved oxygen was maintained at 20% air saturation or higher by increasing agitation ($\geq$ 340 rpm) throughout the cultivation period with airflow rate of 0.75 vvm, the fungal culture was highly heterogeneous with thick mycelial mats floating in the culture broth and attaching to surfaces (Figure 4.4(b)).
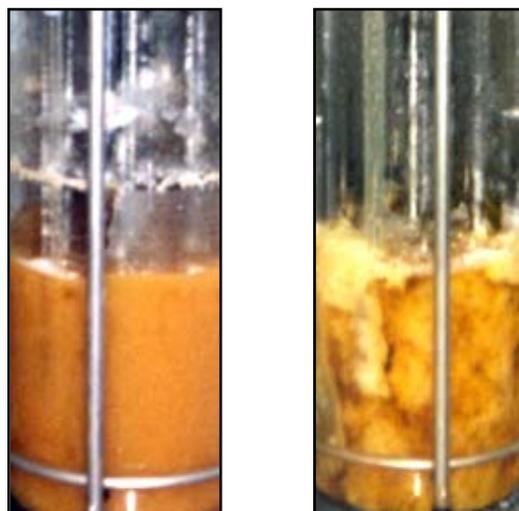
(a) **(b)**

Figure 4.4: Growth morphology of *R. javanicus* in 5 l bioreactor at 30°C with pH control at 6.0 for 24 h: (a) homogeneous dispersed growth was observed with low (0–10 h: DO $\geq$ 20%, 0.5 vvm, variable rpm ($\geq$ 340 rpm); 10-24 h: DO = 0%, 0.25 vvm, 250 rpm) to moderate degree of aeration (0-12 h: DO $\geq$ 20%, 0.5 vvm, variable rpm ($\geq$ 340 rpm); 12-24 h: DO = 0%, 0.5 vvm, 340 rpm) and (b) heterogeneous growth with clump formation occurred when the culture was subjected to high level of aeration (DO $\geq$ 20%, 0.75 vvm, variable rpm ($\geq$ 340 rpm)).

Other authors have reported that agitation speed and dissolved oxygen level are among several parameters affecting the morphology of filamentous fungi (Cui et al. 1997, Pazouki and Panda 2000). Using *A. awamori* CBS 115.52 as a model, a "shaving mechanism" for the effects of agitation on the morphology of pellets formation was proposed (Cui et al. 1997). The effect of aeration on the morphology of *A. niger* B1-D in continuous cultivation, 500 rpm, pH 4, 25°C and 1.0 vvm gas flow rate was reported by Wongwicharn et al. (1999). Long filamentous growth was observed by these authors when air or air enriched with 10% oxygen was used, while air enriched with 30% and 50% oxygen resulted in short hyphal elements with multiple branching. A similar phenomenon was observed in cultivation of *P. chrysogenum* (Dion et al. 1954). However mycelial mats formation was not reported in any of these studies. Also for

Mucor circinelloides, filamentous dispersed morphology was found in batch cultivation with 600 rpm, pH 5, 28°C and 1.0 vvm airflow rate (McIntyre et al. 2002).

4.3.4 Strategies for enhanced PDC production

A controlled process for PDC production in the yeast *C. utilis* has been described previously by our group (Shin and Rogers 1996a,b). Variation of stirrer speed was used to control the respiratory quotient (RQ) of the yeast. An RQ of 1 during the initial period of cultivation was indicative of full respiratory growth and was used to generate biomass for later PDC production. Maintaining the RQ at 4 during the latter stages of cultivation was indicative of significant fermentation with resultant increased PDC production.

Table 4.1 shows the results of PDC production by *R. javanicus* under various cultivation conditions.

All processes listed in Table 4.1 gave rise to a homogeneous morphology of *R. javanicus*. To simulate the conditions obtained in the shake flask, a 5 l process at 30°C with minimal control (no pH control, final pH 3.3, constant agitation speed of 340 rpm and airflow rate of 0.50 vvm) was performed. A similar maximum activity of PDC to that determined for the shake flask culture was obtained (Condition (a) in Table 4.1).

Various control strategies were implemented in 5 and 30 l bioreactors. The degree of agitation/aeration was decreased from (b) to (c) and (d) as shown in Table 4.1. While similar levels of biomass were formed (9-11.4 g l^{-1}), the processes clearly differed in maximum specific rates of ethanol production (q$_{p,max}$) and specific PDC production (U decarboxylase g^{-1} mycelium). In the moderate agitation/aeration conditions in the 5 l bioreactor (b), q$_{p,max}$ = 0.18 g ethanol g^{-1} biomass h^{-1} and 197 U decarboxylase g^{-1} mycelium was produced. In the low agitation/aeration conditions in the same bioreactor (c), q$_{p,max}$ = 0.23 g ethanol g^{-1} biomass h^{-1} with 228 U decarboxylase g^{-1} mycelium, while also for lower agitation/aeration conditions in the 30 l bioreactor (d), q$_{p,max}$ = 0.30

Table 4.1: Comparison of *R. javanicus* cultivation data and PDC production for 500 ml Erlenmeyer flask, 5 and 30 l bioreactors. The variables measured include: t (time point (h)), [biomass] (dry biomass concentration (g l^{-1})), [protein] (total protein concentration from biuret assay (g l^{-1})), $q_{s,max}$ (maximum specific rate of glucose consumption (g glucose g^{-1} biomass h^{-1})), $q_{p,max}$ (maximum specific rate of ethanol production (g ethanol g^{-1} biomass h^{-1})), PDC (specific PDC production (U decarboxylase g^{-1} mycelium)) and RQ_{avg} (average RQ during fermentative phase).

	Uncontrolled pH		Controlled pH at 6.0		
Variables	**500 ml shake flask**	**(a) 5 l bioreactor: no DO control**	**(b) 5 l bioreactor: moderate agitation/ aeration conditions after growth**	**(c) 5 l bioreactor: low agitation/ aeration conditions after growth**	**(d) 30 l bioreactor: lower agitation/ aeration conditions after growth**
t (h)	24	24	24	24	20
[biomass] (g l^{-1})	12.0	9.75	11.4	9.00	10.7
[protein] (g l^{-1})	6.18	5.99	5.54	5.25	4.83
$q_{s,max}$ (g g^{-1} h^{-1})	0.30[*]	0.36[*]	0.50	0.54	0.81
$q_{p,max}$ (g g^{-1} h^{-1})	0.12[*]	0.15[*]	0.18	0.23	0.30
PDC (U g^{-1}_{myc})	244	281	197	228	328
RQ_{avg}	N/a	N/a	3.7	11	21

[*] The calculations were made from 0 and 24 h time points

(a)   0-24 h   : 0.5 vvm, 340 rpm (DO = 0% at 9 h)

(b)   0-12 h   : DO ≥ 20%,   0.5 vvm, variable rpm (≥ 340)
        12-24 h : DO = 0 %,   0.5 vvm, 340 rpm

(c)   0-10 h   : DO ≥ 20%,   0.5 vvm, variable rpm (≥ 340)
        10-27 h : DO = 0 %,   0.25 vvm, 250 rpm

(d)   300 rpm; 0-9 h : 1.0 vvm, 9-16 h : 0.5 vvm, 16-20 h : 0.25 vvm
        (DO was higher than 20% in the first 7 h and zero after the first 9 h.

Note: A value of PDC activity of 214 U decarboxylase g^{-1} mycelium was reported previously by Rosche et al. (2002a) for the 30 l bioreactor at 30°C, pH = 6.0, 300 rpm and 0.5 vvm.

g ethanol g^{-1} biomass h^{-1} was achieved with 328 U decarboxylase g^{-1} mycelium. The increased specific ethanol production rate and the highest average RQ values are illustrative of the most fermentative conditions in the 30 l bioreactor.

It is interesting to note also that when comparing the bioreactor without DO and pH control (a) in which the pH decreased from 6.0 to 3.3 with the pH-controlled process at moderate agitation/aeration conditions (b), a higher specific activity of PDC was obtained for the former (281 U decarboxylase g^{-1} mycelium) when compared to that for the latter (197 U decarboxylase g^{-1} mycelium).

A detailed cultivation time course for *R. javanicus* at low agitation/aeration with pH-control in the 5 l bioreactor (c) is shown in Figure 4.5. The shift towards fermentative conditions at 10 h, PDC activity increased rapidly during a period of 9-12 h, after which the level of PDC remained in the region of 175-230 U decarboxylase g^{-1} mycelium. The increase of ethanol concentration after 10 h clearly marked the beginning of enhanced PDC production. Two thirds of the fungal biomass were accumulated in the first 10 h of high aeration with a maximum specific growth rate of 0.26 h^{-1}.

The cultivation profile of *R. javanicus* in the 30 l bioreactor (d) is given in Figure 4.6. The average RQ during the fermentative phase was 21 ± 6 in this cultivation, which compares to 3.7 ± 0.6 in process (b) and 11 ± 2 in process (c), which suggests that oxygen limitation was likely to have been greatest for the control strategy used in the 30 l bioreactor. The low agitation/aeration conditions in this system resulted in a specific PDC activity of 328 U decarboxylase g^{-1} mycelium and $q_{p,max}$ of 0.30 g ethanol g^{-1} biomass h^{-1}, the highest for the various control strategies (Table 4.1).
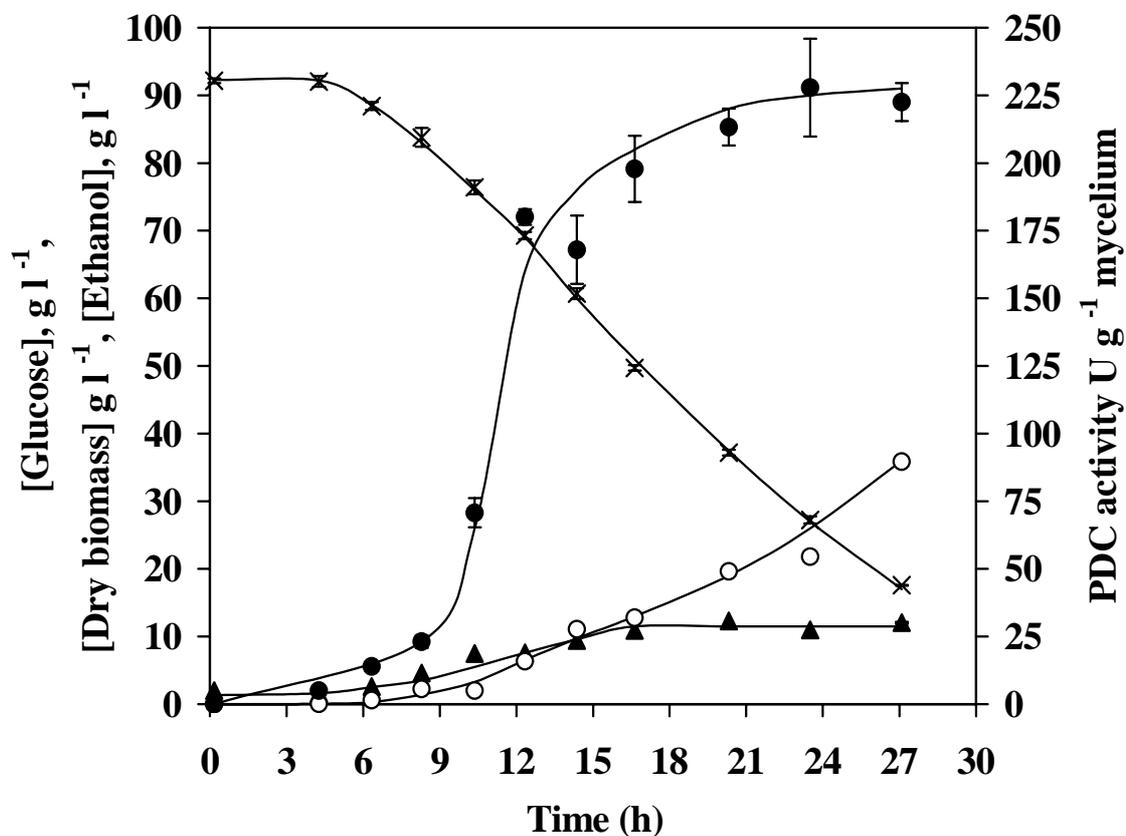
Figure 4.5: The cultivation profile of *R. javanicus* in a 5 l bioreactor containing 4 l of cultivation media at 30°C and pH 6.0 (bioreactor (c) in Table 4.1). The following cultivation conditions were applied; 0–10 h: DO $\geq$ 20%, 0.5 vvm, variable rpm ($\geq$ 340 rpm); 10-27 h: DO = 0%, 0.25 vvm, 250 rpm; ($\times$) glucose, ($\bullet$) PDC decarboxylase activity, ($\blacktriangle$) dry biomass and ($\bigcirc$) ethanol.
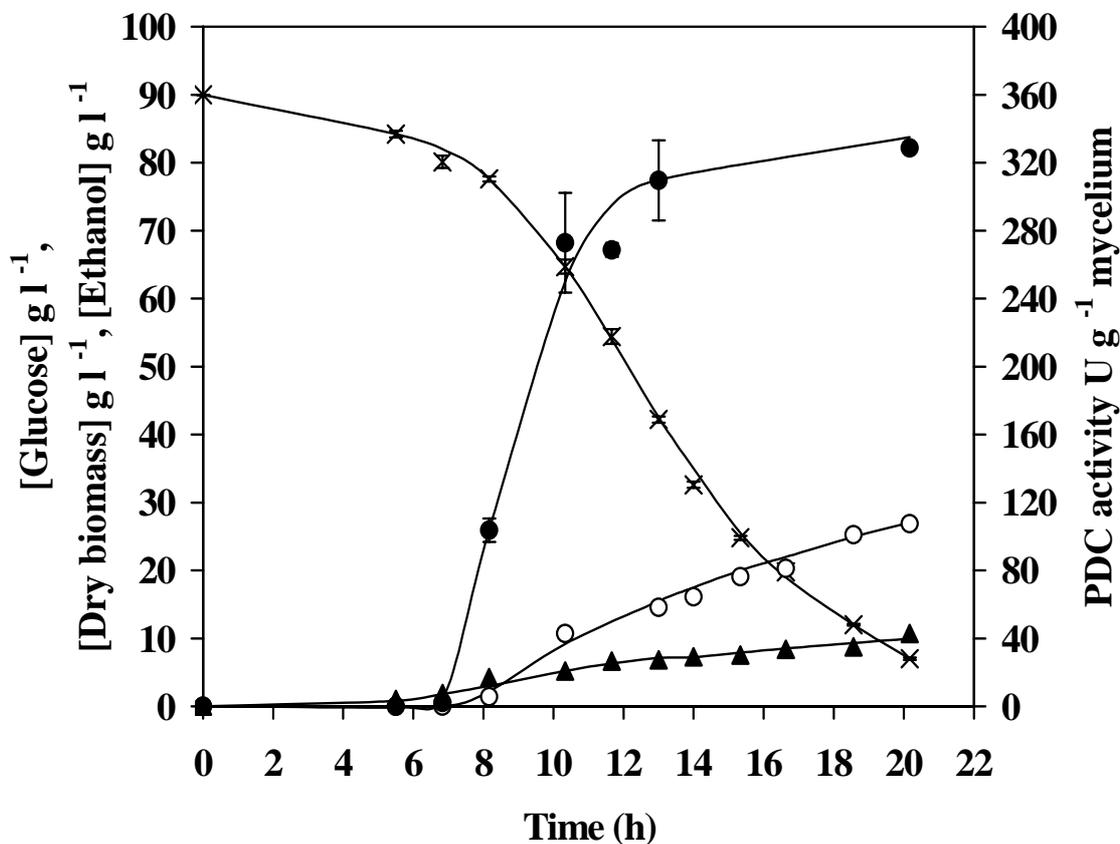
Figure 4.6: The cultivation profile of *R. javanicus* in a 30 l bioreactor containing 20 l of cultivation medium at 30°C, 300 rpm and pH 6.0 (bioreactor (d) in Table 4.1). The airflow rate was reduced stepwise from 1.0 vvm (0-9 h) to 0.5 vvm (9-16 h) then 0.25 vvm (16-20 h); glucose ($\times$), PDC decarboxylase activity ($\bullet$), dry biomass ($\blacktriangle$) and ethanol ($\bigcirc$).

4.3.5 PDC deactivation studies

The effects of temperature, benzaldehyde concentration (50 mM) and degree of enzyme purification on PDC stability over time are shown in Figures 4.7(a)-(b). Table 4.2(a)-(c) summarizes the corresponding deactivation kinetics parameters, PDC half-life and R^2 values. It is evident from this data that PDC stability is enhanced at the lower temperature and also in the crude extract form. Addition of 50 mM benzaldehyde decreases its stability as expected from earlier PDC studies (Chow et al. 1995, Leksawasdi et al. 2003).

The deactivation kinetics of PDC from the alternative source *C. utilis* in buffers containing 40 mM phosphate at 4°C and 2.5 M MOPS at 6°C have been reported previously (Chow et al. 1995, Leksawasdi et al. 2003) and demonstrated strong deactivation by benzaldehyde with the application of high concentration MOPS buffer (2-2.5 M) resulting in increased PDC stability.

Due to the greater enzyme stability of the crude extract, this preparation was used to examine the effects of pH and initial enzyme level at 6°C. The pH optimum for crude extract stability was found to be in the range 6.5-7.0 (Figure 4.8). This optimal pH range for PDC from *R. javanicus* was in agreement with that reported by others for PDC from various sources (Lowe and Zeikus 1992, Pohl et al. 1995, Goetz et al. 2001, Iwan et al. 2001). At pH 3 the PDC half-life was 61% of the optimum value, however at pH 8 the half-life was only 19%, demonstrating higher sensitivity of PDC at alkaline rather than acidic conditions. This might reflect the ability of *R. javanicus* to withstand low pH conditions in the late fermentative phase. This corresponds well to the pH profile for PAC production by *R. javanicus* PDC (Rosche et al. 2002a), which shows a large decrease in final PAC concentration at pH higher than 7.0 while 90% concentration was still attainable at pH 5.5 although at a slower rate of PAC formation.

(a)

(b)
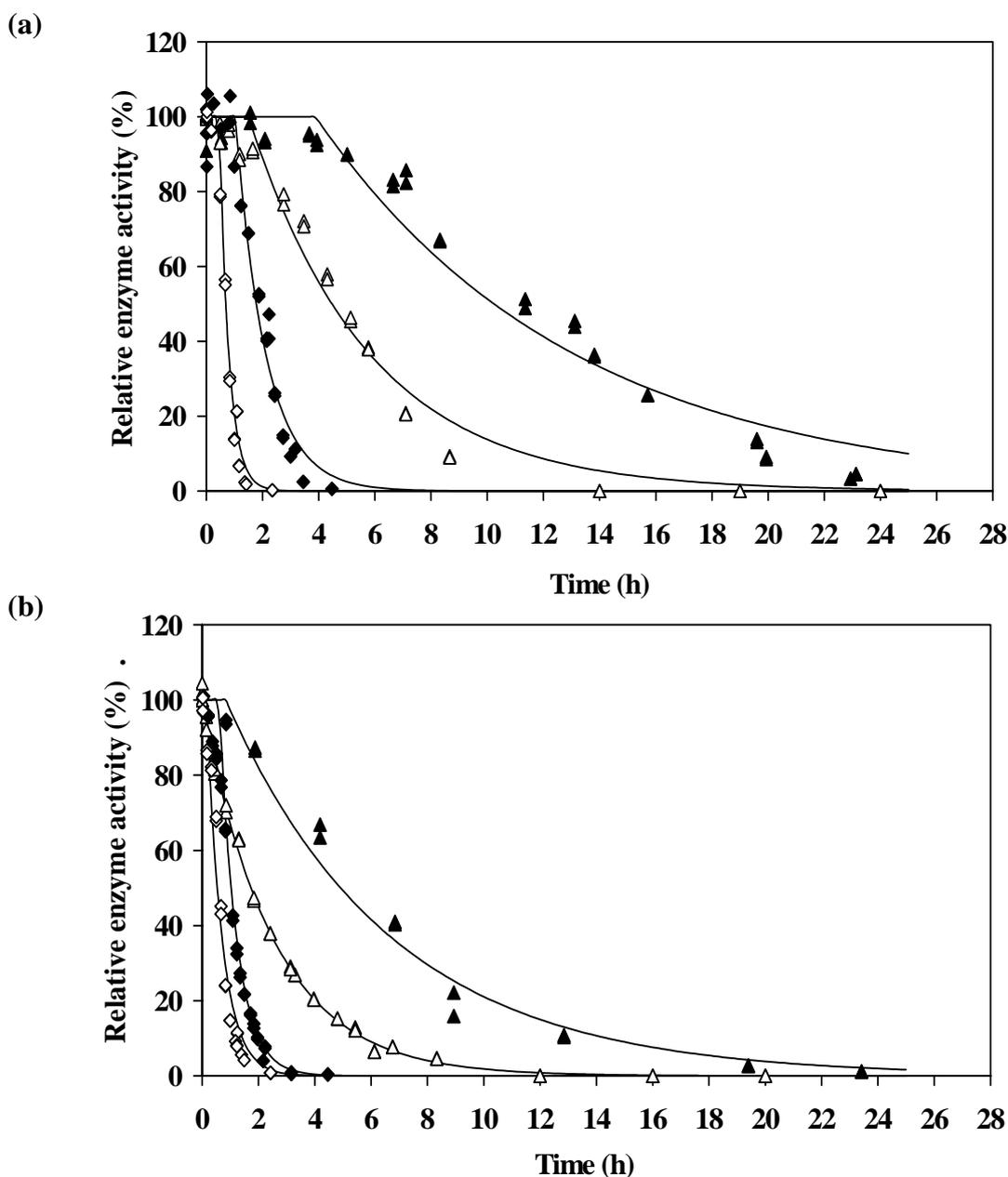
Figure 4.7: Effect of temperature (6 and 25°C) and degree of enzyme purification (partially purified and crude extract) on deactivation kinetics of PDC obtained from *R. javanicus* in the (a) absence and (b) presence of benzaldehyde. The deactivation buffer contained 0.6 M MOPS buffer, 20 mM $MgSO_4$ and 1 mM TPP with initial enzyme activity of 7.0 U decarboxylase ml^{-1}, pH 7.0, ($\diamond$) partially purified PDC at 25°C, ($\triangle$) partially purified PDC at 6°C, ($\blacklozenge$) crude extract at 25°C and ($\blacktriangle$) crude extract at 6°C. Deactivation model fittings are shown as lines.

Table 4.2: The enzyme deactivation parameters and half-life corresponding to the effect of enzyme purification degree, benzaldehyde and temperature for *R. javanicus* PDC (Figure 4.7(a)-(b)).

(a)

Parameters	No benzaldehyde (Figure 4.7(a))			
	Crude extract		Partially purified PDC	
	6°C	25°C	6°C	25°C
k_{rj} (h^{-1})	0.11	0.87	0.23	3.2
t_{lag} (h)	3.9	1.0	1.5	0.5
R^2	**0.9916**	**0.9912**	**0.9930**	**0.9931**

(b)

Parameters	50 mM benzaldehyde (Figure 4.7(b))			
	Crude extract		Partially purified PDC	
	6°C	25°C	6°C	25°C
k_{rj} (h^{-1})	0.17	1.3	0.39	2.6
t_{lag} (h)	0.84	0.57	0.00	0.23
R^2	**0.9926**	**0.9796**	**0.9991**	**0.9794**

(c)

Presence of 50 mM benzaldehyde	Half-life (h) (Figure 4.7(a)-(b))			
	Crude extract		Partially purified PDC	
	6°C	25°C	6°C	25°C
Absence	10.2	1.8	4.4	0.68
Presence	5.0	1.1	1.8	0.50
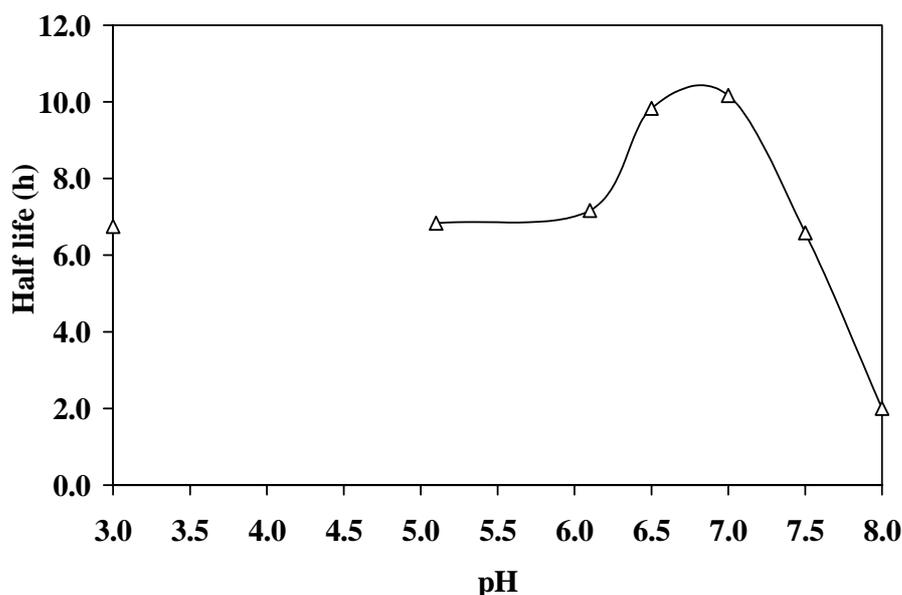
Figure 4.8: Effect of pH on the half-life of crude extract from *R. javanicus* at 6°C. The deactivation buffer contained 0.6 M MOPS buffer, 20 mM $MgSO_4$ and 1 mM TPP with initial enzyme activity of 7.0 U decarboxylase ml^{-1}.
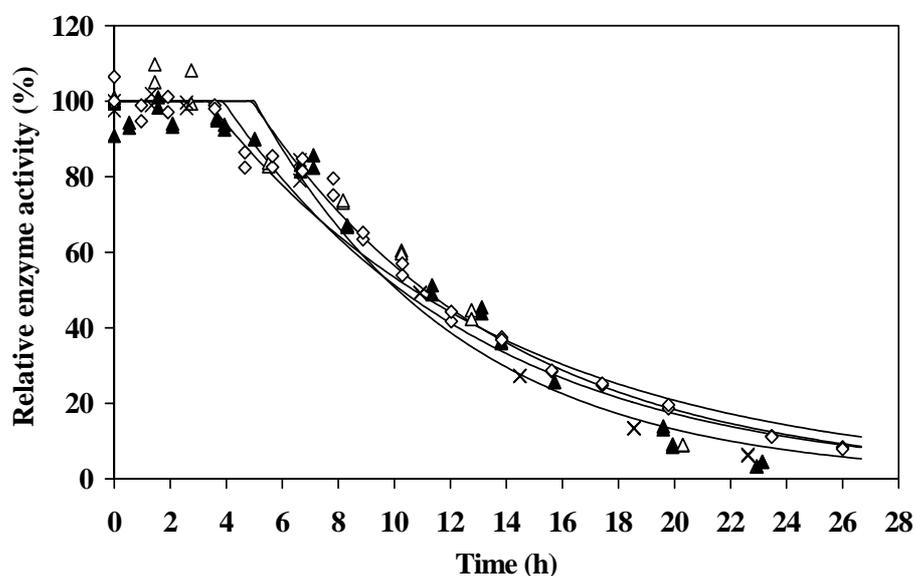
Figure 4.9: Effect of initial enzyme activity on PDC deactivation kinetics at 6°C of crude extract obtained from *R. javanicus*. The deactivation buffer contained 0.6 M MOPS buffer, 20 mM $MgSO_4$, 1 mM TPP with pH 7.0 and decarboxylase activity of, (▲) 7 U ml^{-1}, (△) 13 U ml^{-1}, (×) 20 U ml^{-1} and (◇) 27 U ml^{-1}. Deactivation model fittings are shown as lines.

The deactivation kinetics profiles of PDC in the crude extract preparation with various initial enzyme activities (7-27 U decarboxylase ml^{-1}) indicated no obvious effect of initial enzyme activity on PDC stability (Figure 4.9). The deactivation constant and half-life values were in the range of 0.11 ± 0.03 h^{-1} and 10.6 ± 0.6 h respectively at 0.6 M MOPS and 6°C. However, for partially purified *R. javanicus* PDC in 2 M MOPS at 4°C, it has been reported that the enzyme stability was lower at a higher PDC concentration with 35% activity remaining after 18 h at 42 U ml^{-1} decarboxylase activity in comparison to 50% residual activity at 6 U ml^{-1} (Rosche et al. 2002a). Furthermore the authors found that high concentrations of MOPS buffer strongly increased the stability of partially purified *R. javanicus* PDC (investigated at initial decarboxylase activity of 42 U ml^{-1}, 4°C) with a half-life of 2 h in 0.6 M MOPS and 14 h in 2 M MOPS (Rosche et al. 2002a).

The protease activity index (ratio of protease:decarboxylase activity) was determined for *R. javanicus* PDC and found to be $2.40 \times 10^{-1} \pm 2.8\%$ for crude extract and $5.79 \times 10^{-2} \pm 4.5\%$ for partially purified enzyme. The decreased PDC stability might indicate the presence of higher protease activities in *R. javanicus*. The filamentous fungi of genus *Rhizopus* are commonly used in the production of tempeh and lipases and others have reported that *Rhizopus* sp. could produce high levels of aspartic and serine proteases (Heskamp and Barz 1997, Sang-Duk et al. 2002) in different isoforms (Heskamp and Barz 1998). However as shown in previous experiments (see Table 4.2(c)), the PDC crude extract has much greater stability than partially purified PDC despite the higher protease activity index of the crude extract.

The addition of an EDTA-free protease inhibitor cocktail (1-2 tablets per 10 ml buffer) and 0.7-7 μg ml^{-1} pepstatin A protease inhibitor did not have any stabilising effect on PDC at 6°C. The deactivation profiles of PDC for the addition of an EDTA-free protease inhibitor cocktail (1 tablet per 10 ml buffer) and 0.7 μg ml^{-1} pepstatin A protease inhibitors are shown in Figure 4.10. The half-life of PDC crude extract in the presence of these protease inhibitors was about 11.0 h.

However omission of Mg^{2+} from deactivation buffer resulted in a lower protease activity relative to a control, with a similar trend being observed when 1 or 5 mM EDTA was added to deactivation buffer containing 20 mM Mg^{2+} and 1 mM TPP. The complete omission of Mg^{2+} is not recommended, as it is one of the essential cofactors necessary for the proper functioning of PDC.

As shown in Figure 4.10, addition of 1 mM EDTA increased the half-life of PDC crude extract at $6^{\circ}C$ by 5 h (increased concentration of 5 mM EDTA showed no further enhancement of the stability) and removal of Mg^{2+} from the deactivating buffer increased the half-life by 3.2 h (Figure 4.11) suggesting a role of metallo-proteases in decreasing PDC stability or an adverse effect of possible impurities of heavy metal ions in the $MgSO_4$-salt. Ghorbel et al. (2003) found on removal of 2 mM Ca^{2+}, that the activity of metallo-protease present in *Bacillus cereus* BG1 was reduced by 500%. In the current study, a lower level of Mg^{2+} in the buffer might have been used as Rosche et al. (2003a) reported an adverse effect of Mg^{2+} on pyruvate stability and observed increased pyruvate stability and unaffected PAC production after lowering the concentration of $MgSO_4$ from 20 to 0.5 mM.

The relative stabilities of PDC in crude extracts from *R. javanicus* and *C. utilis* are compared in Figure 4.12, in the presence and absence of benzaldehyde at $25^{\circ}C$. Even though the conditions applied to *C. utilis* PDC were harsher (73 mM benzaldehyde) than to *R. javanicus* (50 mM benzaldehyde), the stability of *C. utilis* PDC was still much greater. The deactivation profile for *C. utilis* PDC in crude extract at $25^{\circ}C$ could be separated into two stages as shown in Figure 4.12, although this was not found in deactivation studies on partially purified PDC from *C. utilis* at $6^{\circ}C$ (Chow et al. 1995, Leksawasdi et al. 2003). The protease activity index of the crude extract for PDC of *C. utilis* was $1.94 \times 10^{-3} \pm 7.0\%$ at $25^{\circ}C$ which was appreciably lower than that of *R. javanicus*. By comparison, Gierhart and Potter (1979) observed extended crude extract stability with lower protease activities for *C. utilis* relative to *S. cerevisiae* and Shin and Rogers (1996b) found low protease activity in *C. utilis*. The protease activity index of *S. cerevisiae* determined recently in our group (unpublished result) was $3.53 \times 10^{-2} \pm 6.0\%$.
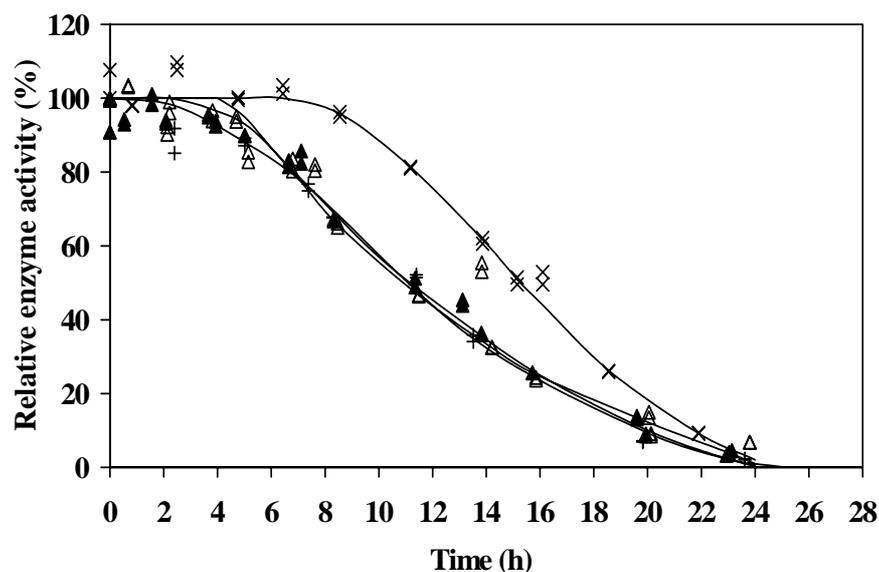
Figure 4.10: Effect of various protease inhibitors on deactivation kinetics of crude extract obtained from *R. javanicus* at 6°C. The deactivation buffer contained 0.6 M MOPS buffer, 20 mM $MgSO_4$ and 1 mM TPP with initial enzyme activity of 7 U decarboxylase ml^{-1}, pH 7.0, ($\times$) 1 mM EDTA, ($\triangle$) 0.7 μg ml^{-1} pepstatin A, ($+$) cocktail inhibitor (1 tablet per 10 ml buffer) and ($\blacktriangle$) control.
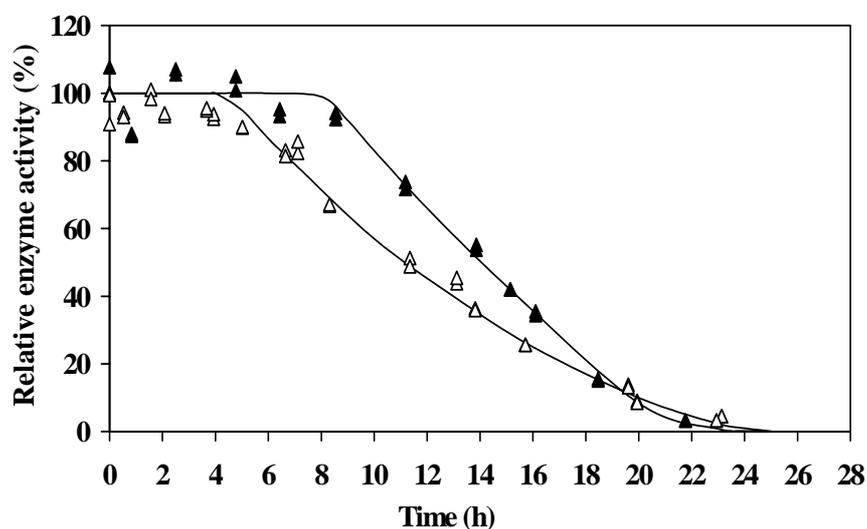
Figure 4.11: Effect of magnesium sulphate concentration (0 and 20 mM) on deactivation kinetics of crude extract obtained from *R. javanicus* at 6°C. The deactivation buffer contained also 0.6 M MOPS buffer and 1 mM TPP with initial enzyme activity of 7.0 U decarboxylase ml^{-1}, pH 7.0, ($\blacktriangle$) 0 mM $MgSO_4$ and ($\triangle$) 20 mM $MgSO_4$.
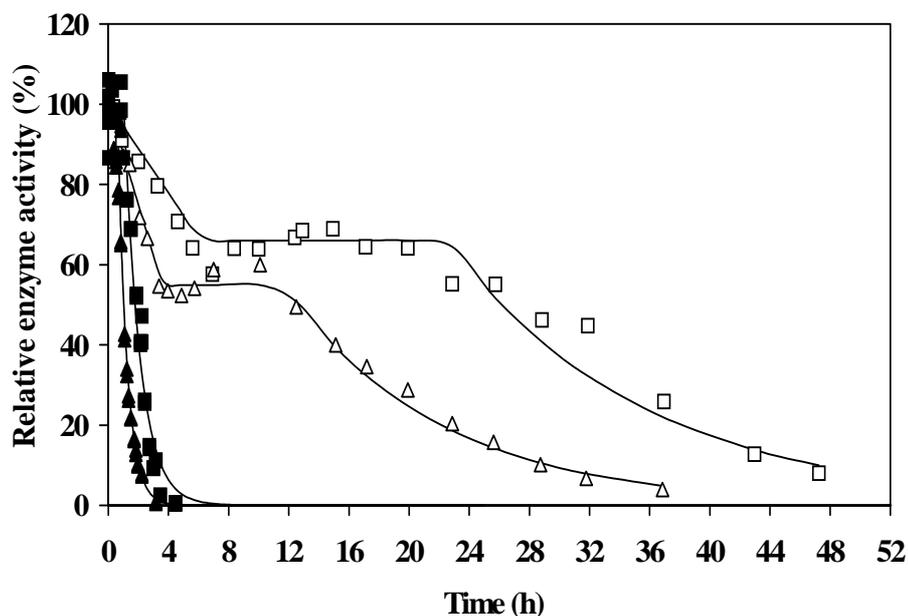
Figure 4.12: Stability comparison of crude extract obtained from the yeast *C. utilis* and the filamentous fungi *R. javanicus* with or without the presence of benzaldehyde (50 mM for *R. javanicus* and 73 mM for *C. utilis*). The deactivation buffer contained 0.6 M MOPS buffer, 20 mM $MgSO_4$ and 1 mM TPP with initial enzyme activity of 27 U decarboxylase ml^{-1}, pH 7.0 and 25°C, ($\square$) *C. utilis* crude extract in the absence of benzaldehyde, ($\triangle$) *C. utilis* crude extract in 73 mM benzaldehyde, ($\blacksquare$) *R. javanicus* crude extract in the absence of benzaldehyde and ($\blacktriangle$) *R. javanicus* crude extract in 50 mM benzaldehyde.

The PDC half-lives of various microorganisms are listed in Table 4.3 from literature values and present results and ranked in order of descending stability. The source of PDC, purification steps, type and concentration of buffer species, temperature, pH, chemical additives, cofactors and benzaldehyde concentrations, all play significant roles in the stability of PDC. It is interesting to note that a highly purified PDC (purity > 95%) from *S. cerevisiae* showed an exceptional stability in 10 mM phosphate buffer (Farrenkopf and Jordan 1992). The PDC half-life of 0.2 U ml^{-1} initial activity of this enzyme at 4°C was reported to be more than 8 months, however 99% of the original PDC activity was lost in the purification process. Pohl et al. (1998) found that the half-life of purified *Z. mobilis* PDC was greater than 20 h.

Table 4.3: Comparison of published PDC half-lives from *C. utilis*, *R. javanicus*, *S. cerevisiae* and *Z. mobilis*. BZ is benzaldehyde.

Microorganism	Half-life	Conditions
S. cerevisiae [a]	> 252 d	10 mM phosphate, pH 6.8, 4°C, 0.2 U ml^{-1}, no BZ
C. utilis [b]	268 h	2.5 M MOPS, pH 7.0, 6°C, 12 U ml^{-1}, no BZ
C. utilis [b]	60.5 h	2.5 M MOPS, pH 7.0, 6°C, 12 U ml^{-1}, 50 mM BZ
S. cerevisiae [c]	36.7 h	1 M phosphate, pH 6.3, 5°C, 17.3 U ml^{-1}, no BZ
C. utilis [b]	36.1 h	2.5 M MOPS, pH 7.0, 6°C, 12 U ml^{-1}, 100 mM BZ
C. utilis [d]	26.3 h	0.6 M MOPS, pH 7.0, 25°C, 27 U ml^{-1}, no BZ
Z. mobilis [e]	> 20 h	50 mM MES, pH 6.5, 25°C, 0.1 mg PDC ml^{-1}, no BZ
R. javanicus [f]	17.8 h	2.5 M MOPS, pH 6.5, 6°C, 33.6 U ml^{-1}, 400 mM BZ
R. javanicus [g]	15.3 h	0.6 M MOPS, pH 7.0, 6°C, 7 U ml^{-1}, no BZ
R. javanicus [h]	13.9 h	2.0 M MOPS, pH 7.0, 4°C, 42 U ml^{-1}, no BZ
C. utilis [d]	12.9 h	0.6 M MOPS, pH 7.0, 25°C, 27 U ml^{-1}, 73 mM BZ
S. cerevisiae [c]	11.7 h	100 mM phosphate, pH 7.0, 5°C, 16.7 U ml^{-1}, no BZ
R. javanicus [d]	11.2 h	0.6 M MOPS, pH 7.0, 6°C, 27 U ml^{-1}, no BZ

[a] purified (purity > 95%) (Farrenkopf and Jordan 1992)

[b] partially purified by acetone precipitation (Leksawasdi et al. 2003)

[c] UV mutant, partially purified by $(NH_4)_2SO_4$ precipitation (Juni and Heym 1968b)

[d] crude extract, current study

[e] wild type, purified (Pohl et al. 1998)

[f] partially purified by acetone precipitation (Rosche et al. 2003a)

[g] crude extract + 1 mM EDTA, current study

[h] partially purified by acetone precipitation (Rosche et al. 2002a)

4.4   CONCLUSIONS

The present study with *R. javanicus* has shown that both cell morphology and PDC activity are strongly dependent on the growth conditions. For low to moderate agitation/aeration following the growth phase, a dispersed homogeneous fungal culture was evident with a maximum of 328 U decarboxylase g^{-1} mycelium achieved in a 30 l controlled bioreactor, while with increased agitation/aeration intensity, decreased enzyme activity and a heterogeneous culture with significant clump formation were evident. The relatively high specific PDC activity was associated with increased fermentative metabolism as evidenced by a higher respiratory quotient (RQ) and a higher specific rate of ethanol production. The half-life of *R. javanicus* PDC from crude extract was found to be greater than that of partially purified enzyme in 0.6 M MOPS buffer, pH 7.0 at 6 and $25^{\circ}C$ in both the presence and absence of benzaldehyde. From deactivation kinetic studies, *R. javanicus* PDC stability was much lower by comparison with *C. utilis* PDC confirming that the latter would be more suitable for the enzymatic biotransformation of benzaldehyde and pyruvate to *R*-phenylacetylcarbinol.

Chapter 5 137

Experimental determination of model relationships:
Kinetics of deactivation by benzaldehyde of PDC from *C. utilis*

Chapter 5

Experimental Determination of Model Relationships: Kinetics of Deactivation by Benzaldehyde of PDC from *C. utilis*

Experimental determination of model relationships:
Kinetics of deactivation by benzaldehyde of PDC from *C. utilis*

5.1   NOMENCLATURE

b   benzaldehyde concentration (mM);

E   PDC activity at time t (U ml^{-1});

E_0 initial PDC activity at time zero (U ml^{-1});

k   benzaldehyde deactivation coefficient developed by Chow et al. (1995)
                (mM^{-1} h$^{-0.5}$);

k_{d1} first order reaction time deactivation constant (h^{-1});

k_{d2} first order benzaldehyde deactivation coefficient (mM^{-1} h^{-1});

K_d overall deactivation parameter (h^{-1} or h^{-n} in general form);

n   time exponent constant;

t   time (h);

$t_{0.5}$ half-life of PDC (h);

$t_{0.8}$ eighty percent life of PDC (h);

t_{lag} lag time (h).

5.2 INTRODUCTION

Benzaldehyde which supplies the aromatic ring to PAC is toxic (Goetz et al. 2001, Iwan et al. 2001). Continuous exposure of the enzyme to benzaldehyde results in irreversible deactivation of PDC (Long and Ward 1989b). Understanding the deactivation kinetics of PDC by benzaldehyde is necessary in the optimization of this enzymatic PAC biotransformation process as sufficient enzyme activity must be maintained for an extended period so that the production of PAC can be maximized.

Previous studies by our group (Chow et al. 1995) evaluated PDC deactivation kinetics in a biotransformation buffer containing 40 mM phosphate, cofactors 1 mM Mg^{2+} and 1 mM TPP and 2 M ethanol at pH 7.0, $4^°C$ with various initial concentrations of benzaldehyde in the range 100-300 mM. A first order effect of benzaldehyde on the deactivation kinetics and a square root time dependency for these conditions were reported. Subsequently Rosche et al. (2002a) reported the pH-dependency of the biotransformation and improved buffering (2-2.5 M MOPS, pH 6.5, $6^°C$) in order to perform small scale studies without the need for pH adjustments. Under these latter conditions, stability of *R. javanicus* PDC increased and significant enhancement of PAC production was achieved with both *R. javanicus* and *C. utilis* PDC. These improved conditions are the basis for the enzyme deactivation kinetic studies in this Chapter.

5.3 RESULTS AND DISCUSSION

5.3.1 Experimental deactivation kinetics

The experimental profiles of PDC deactivation for various benzaldehyde concentrations are shown in Figure 5.1(a)-(j). The initial relative enzyme activity of all profiles at 100% corresponded to enzyme activities ranging between 2.8-3.2 U carboligase ml^{-1}. A lag period of more than 10 h occurred before enzyme deactivation when benzaldehyde concentrations were less than 40 mM. At higher concentrations of benzaldehyde, the lag time was shortened but still existed at 200 mM (about 5 h). The deactivation profile of

Chapter 5   **140**

Experimental determination of model relationships:
Kinetics of deactivation by benzaldehyde of PDC from *C. utilis*

PDC by 50 mM benzaldehyde (Figure 5.1(f)) shows results from two different batches of enzyme (current study and Sandford (2002)). The similarity of both profiles suggests good experimental data reproducibility between enzyme batches.

5.3.2   Equations for PDC deactivation

Chow et al. (1995) adopted the general deactivation equation proposed by Han and Levenspiel (1988). The deactivation kinetics of PDC by benzaldehyde in this earlier study with phosphate buffer was:

$$E = E_0 \, e^{-K_d \, t^n}$$

(5.1)

where n was 0.5 and K_d was a linear function of benzaldehyde concentration ($K_d = k.b$ where $k = 6.74 \times 10^{-3}$ mM^{-1} h$^{-0.5}$). This equation was developed for prediction of PDC deactivation kinetics with benzaldehyde concentrations ranging from 100–300 mM in 40 mM phosphate buffer containing 2 M ethanol at pH 7.0 and 4°C.

However application of high concentration MOPS buffer (2.5 M) instead of 40 mM phosphate buffer for pH control has been found to result in significant improvement of PAC formation and enhanced PDC stability (Rosche et al. 2002a). It was shown that PDC deactivated more slowly in the MOPS buffer with evidence of an initial period of constant or slightly elevated enzyme activity. This initial phase of constant (or elevated) stability has been discussed previously (Rosche et al. 2002a) as possibly being due to enzyme refolding following its solubilization from the PDC acetone precipitate.

An additional term (t_{lag}) was included in the equation to take into account this phenomenon. Furthermore it was shown that PDC deactivation in 2.5 M MOPS buffer in the absence of benzaldehyde followed linear kinetics and it was determined that the time exponent n in Equation (5.1) should be taken as 1. In the present study, the overall deactivation kinetics given in Equation (5.2) incorporates the effect of t_{lag}, the first order

Chapter 5   141

Experimental determination of model relationships:
Kinetics of deactivation by benzaldehyde of PDC from *C. utilis*

time dependency and the first order benzaldehyde deactivation to give a typical pattern
of exponential enzyme decay as described by Bailey and Ollis (1986), viz:

$$E = E_0 \, e^{-\left(k_{d1} + k_{d2}.b\right)\left(t - t_{lag}\right)}$$

(5.2)

In Equation (5.2), k_{d1} represents the time-related enzyme deactivation constant in 2.5 M
MOPS buffer in the absence of benzaldehyde, k_{d2} is the first order deactivation rate due
to benzaldehyde, b is the benzaldehyde concentration and t_{lag} indicates the lag time
period prior to enzyme deactivation.

The optimal values of the kinetic constants derived from the modelling program after
fitting Equation (5.2) to experimental data points are listed in Table 5.1. The
corresponding correlation coefficient (R^2), Residual Sum of Squares (RSS) and Mean
Sum of Square for Residuals (MS) for each benzaldehyde concentration profile are
given in Table 5.2. The resultant simulation curves from the equation are shown in
Figure 5.1(a)–(j) for comparison with experimental data points. As evident from Figure
5.1 and Table 5.2, the equation was found to provide very acceptable fitting of the data
for the benzaldehyde concentration range 0–200 mM.

Table 5.1: Constants and coefficient for optimal fitting of PDC deactivation equation at
6°C in deactivation buffer containing 2.5 M MOPS (pH 7.0), 1 mM $MgSO_4$ and 1 mM
TPP with initial PDC activity between 2.8–3.2 U carboligase ml^{-1}.

Constants/ Coefficient	Unit	Values
E_o	%	105.5
k_{d1}	h^{-1}	2.64×10^{-3}
k_{d2}	$mM^{-1} \, h^{-1}$	1.98×10^{-4}
t_{lag}	h	5.23
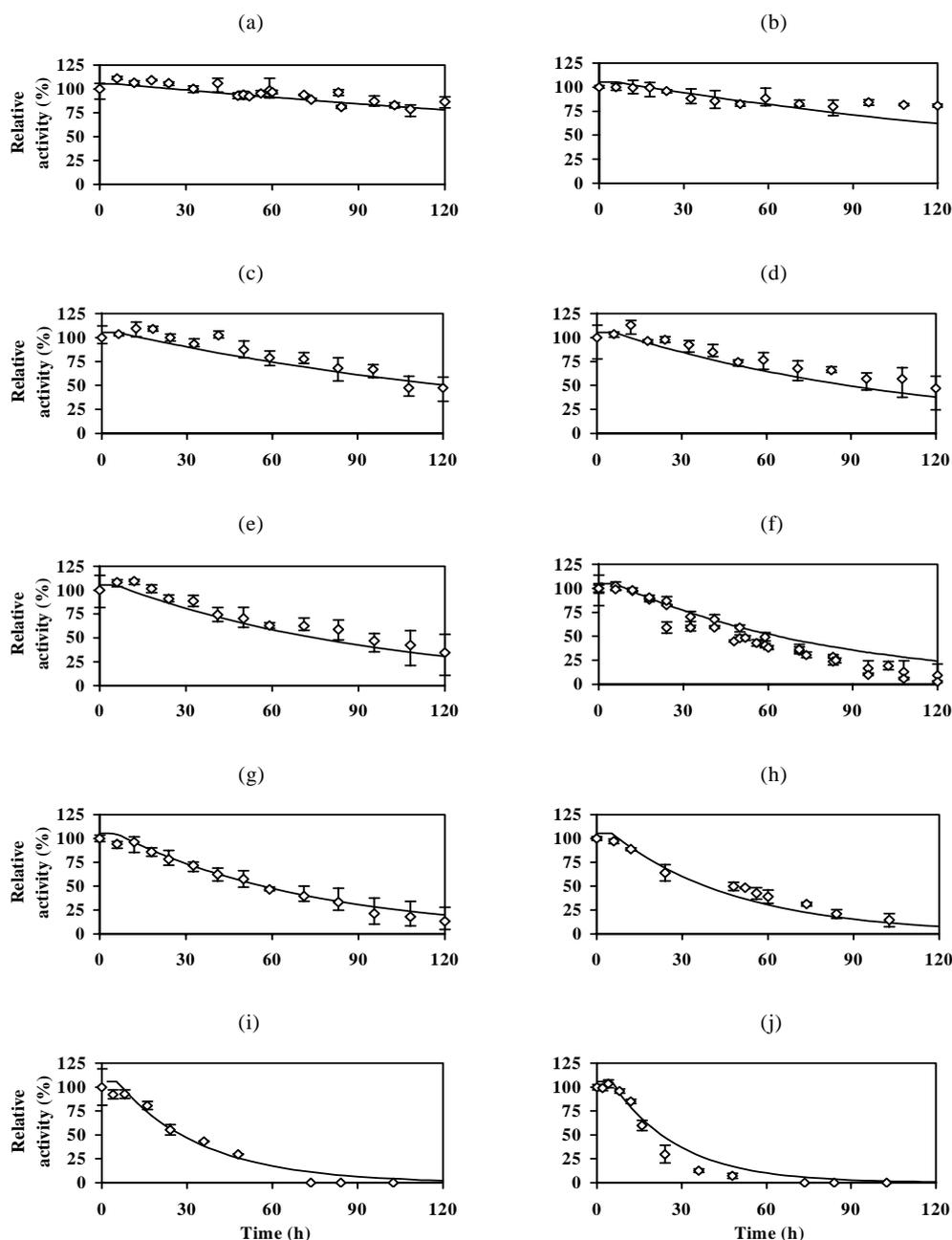
Figure 5.1: Enzyme deactivation profile ($\diamondsuit$) with model fitting (line) in the absence of benzaldehyde (a) and in the presence of benzaldehyde of various concentrations: (b) 9.49 mM, (c) 19.0 mM, (d) 31.6 mM, (e) 41.1 mM, (f) 51.4 mM, (g) 60.0 mM, (h) 101 mM, (i) 153 mM and (j) 202 mM. The experiment was performed in glass vials containing 2.5 M MOPS buffer (pH 7.0), 1 mM $MgSO_4$ and 1 mM TPP with initial enzyme activity in the range of 2.8–3.2 U carboligase ml^{-1} at $6°C$. The enzyme activity of each data point was an average from three replicates. Error bars show the lowest and highest values.

Chapter 5   **143**

Experimental determination of model relationships:
Kinetics of deactivation by benzaldehyde of PDC from *C. utilis*

A family of deactivation profiles constructed from Equation (5.2) with constant and coefficient values listed in Table 5.1 are plotted in Figure 5.2.

Table 5.2: Summary of RSS, MS and R^2 results after fitting deactivation equation to experimental data.

Benzaldehyde concentration (mM)	RSS	MS	R^2
0.00	2783	44.9	0.9952
9.49	3709	97.6	0.9892
19.0	4342	114	0.9850
31.6	5770	152	0.9772
41.1	5586	147	0.9758
51.4	16828	157	0.9685
60.0	2708	71.3	0.9861
101	2261	38.3	0.9819
153	2437	43.5	0.9813
202	2939	48.2	0.9829
Average	**4936**	**91.4**	**0.9823**

For comparison with the previously published PDC deactivation kinetics (Chow et al. 1995), Figure 5.3 shows experimental data for PDC deactivation in the presence of 100 mM benzaldehyde in the two buffers. The data confirm the significant improvement of long term PDC stability in 2.5 M MOPS buffer when compared to that in 40 mM phosphate buffer. With both buffers a lag phase was observed.

Chapter 5   144

Experimental determination of model relationships:
Kinetics of deactivation by benzaldehyde of PDC from *C. utilis*
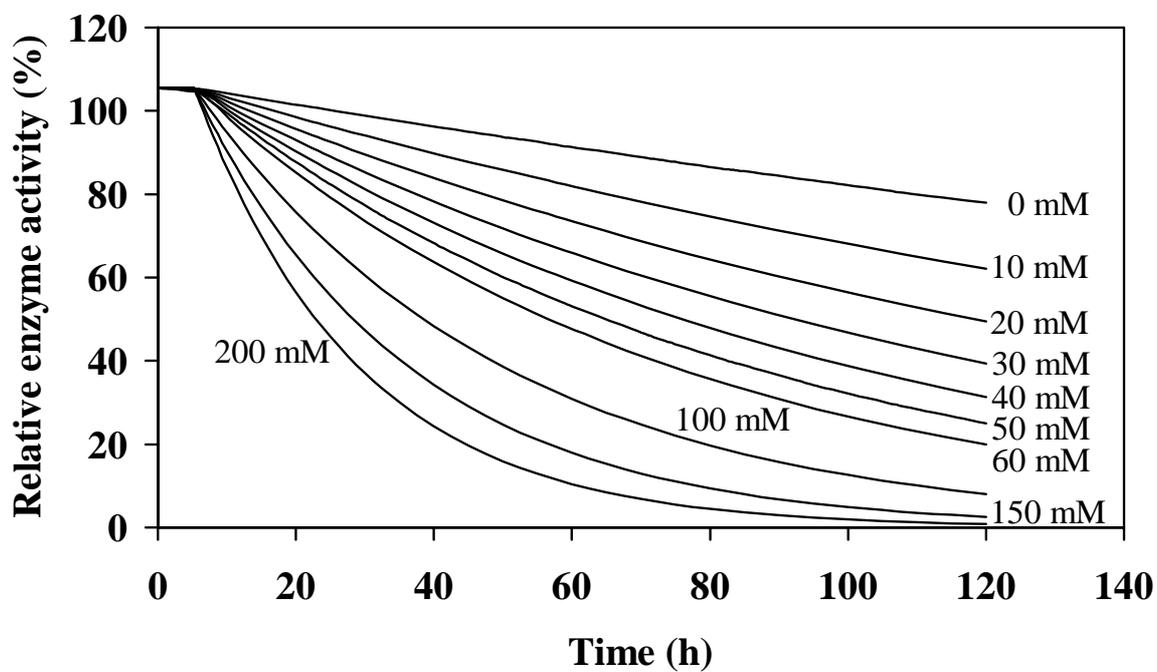
Figure 5.2: Summary of PDC deactivation profiles generated by the equation for various benzaldehyde concentrations.
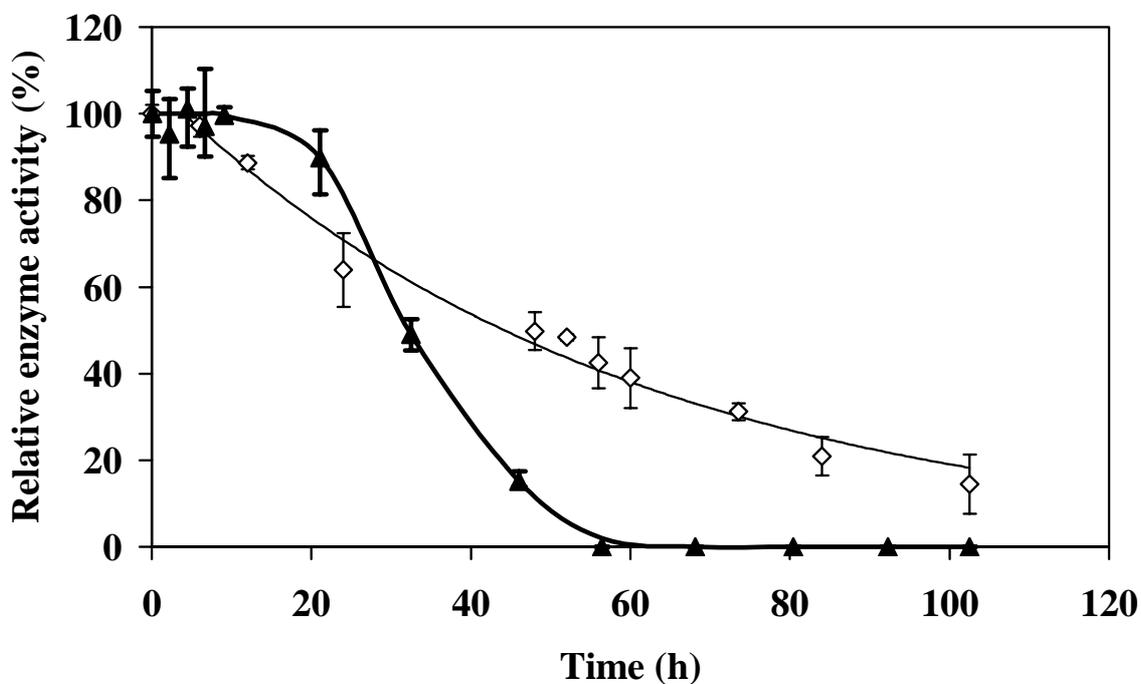
Figure 5.3: Effect of buffer on PDC inactivation in the presence of 100 mM benzaldehyde: ($\diamond$) 2.5 M MOPS and ($\blacktriangle$) 40 mM phosphate buffer, 1 mM $MgSO_4$ and 1 mM TPP with initial enzyme activity in the range of 2.8–3.2 U carboligase ml^{-1} at 6°C (pH 7.0). The enzyme activity of each data point was an average from three replicates. Error bars show the lowest and highest values.

Chapter 5   **146**

Experimental determination of model relationships:
Kinetics of deactivation by benzaldehyde of PDC from *C. utilis*

5.3.3   Half-life determinations

The PDC half lives were determined graphically for each individual experimental data set shown in Figure 5.1. These half-life values are shown as data points in Figure 5.4(a) and compared with the curve of half-life values derived from the deactivation equation. This curve was determined by inserting E_o, k_{d1}, k_{d2} and t_{lag} (Table 5.1) into Equation (5.3), the rearranged Equation (5.2).

$$t_{0.5} = \frac{\ln\left(\dfrac{1}{0.5}\right)}{\left(k_{d1} + k_{d2}.b\right)} + t_{lag} \tag{5.3}$$

For benzaldehyde concentrations lower than 20 mM, the experimental data points taken over 120 h were not sufficient to determine half-life. Therefore, further comparison for the time of retention of 80% enzyme activity (80% life) is shown in Figure 5.4(b) to illustrate the model fitting for benzaldehyde concentrations below 20 mM. Acceptable overall fitting for both data sets was obtained with R^2, RSS and MS of 0.9840, 298 and 49.7 for Figure 5.4(a) and 0.9683, 1406 and 352 respectively for Figure 5.4(b).

5.3.4   PDC deactivation rate equation

Differentiated from Equation (5.2), the rate of deactivation of PDC by benzaldehyde can be described in Equation (5.4). This equation will be used later to describe PDC deactivation kinetics as one of a series of differential equations for the overall modelling and simulation of PAC batch biotransformation profiles in Chapter 6. Such a model can then be the basis for designing feeding profiles for optimized fed batch PAC biotransformations.

$$\left.\frac{dE}{dt}\right|_i = \left\{ \begin{array}{ll} 0 & ; \quad t \leq t_{lag} \\ -\left(k_{d1} + k_{d2}.b\right)E_i & ; \quad t > t_{lag} \end{array} \right\} \tag{5.4}$$

Experimental determination of model relationships:
Kinetics of deactivation by benzaldehyde of PDC from *C. utilis*

(a)

$$t_{0.5} = \frac{\ln\left(\dfrac{1}{0.5}\right)}{\left(k_{d1} + k_{d2}.b\right)} + t_{lag}$$

Half life (h) vs Benzaldehyde concentration (mM)

(b)

$$t_{0.8} = \frac{\ln\left(\dfrac{1}{0.8}\right)}{\left(k_{d1} + k_{d2}.b\right)} + t_{lag}$$

Eighty percent life (h) vs Benzaldehyde concentration (mM)
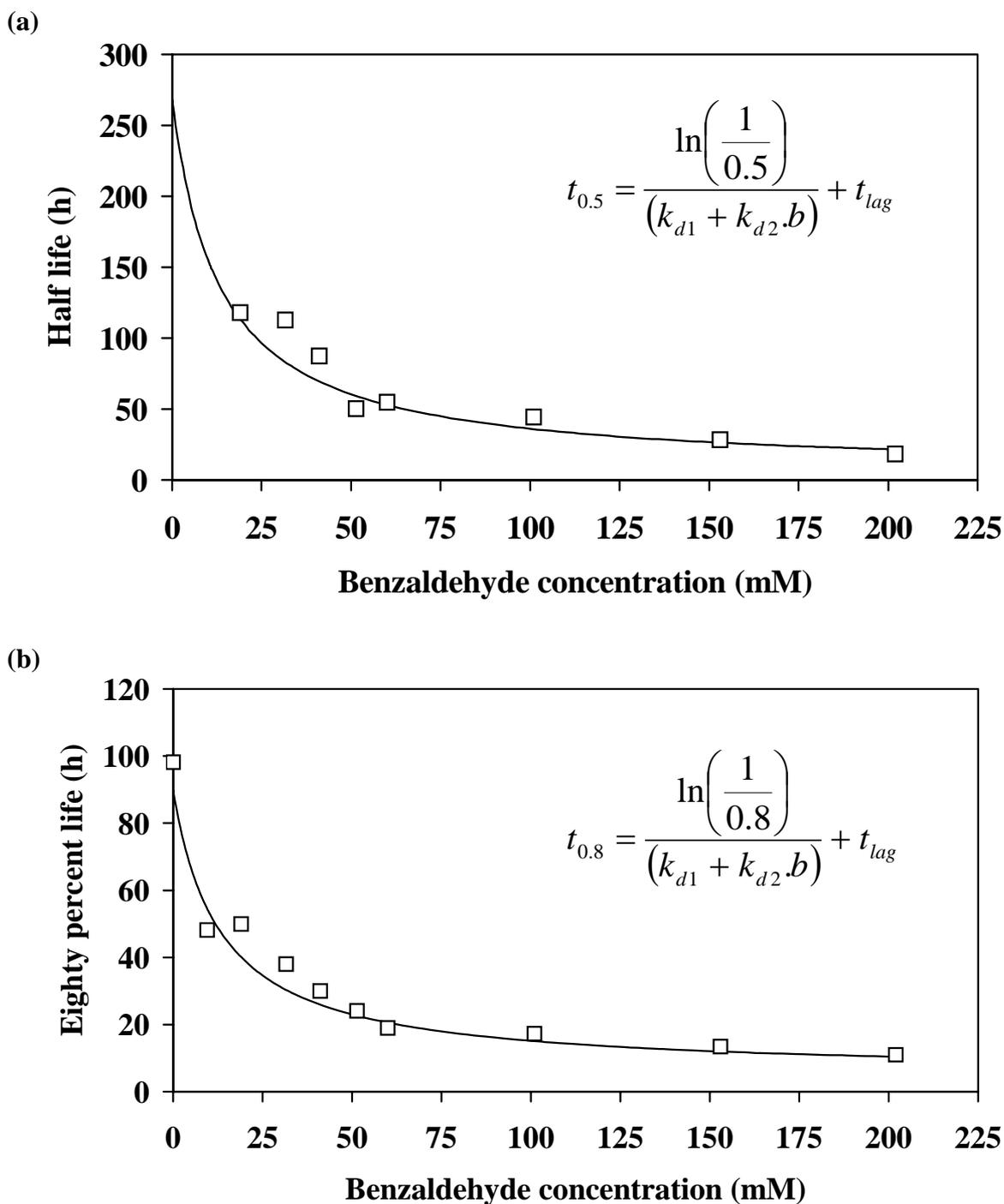
Figure 5.4: Half-life (a) and eighty percent life (b) of PDC. Comparison of deactivation equation (line) and values derived from each experimental data set of Figure 5.1. The half-life values of PDC without benzaldehyde and with 10 mM benzaldehyde were not included because the remnant relative activities after 120 h in both conditions were higher than 75%.

Chapter 5   **148**

Experimental determination of model relationships:
Kinetics of deactivation by benzaldehyde of PDC from *C. utilis*

5.4   CONCLUSIONS

A kinetic equation has been developed which provides good fitting to the experimental deactivation of PDC in 2.5 M MOPS, 1 mM MgSO$_4$, 1 mM TPP, pH 7.0 at 6°C with various initial concentrations of benzaldehyde up to 200 mM. Using standard statistical analyses, it was established that the equation provided a good overall fit for these deactivation profiles. The rate equation for PDC deactivation derived from this study will be used with other differential equations in modelling the enzymatic production of PAC from pyruvate and benzaldehyde.

The results of this Chapter has already been published in:

Leksawasdi, N., Breuer, M., Hauer, B., Rosche, B. and Rogers, P.L. (2003). Kinetics of pyruvate decarboxylase deactivation by benzaldehyde, Biocatalysis and Biotransformation 21: 315-320.

Chapter **6**

Model Development and Validation

6.1 NOMENCLATURE

A   pyruvate concentration (mM);

B   benzaldehyde concentration (mM);

E   PDC activity at time t (U carboligase ml^{-1});

E_o initial concentration of PDC enzyme (U carboligase ml^{-1});

EQ   binary enzyme complex between PDC and 'active acetaldehyde';

h   exponent with similar functionality to Hill coefficient for benzaldehyde (no units);

i   iteration loop identifier of each species to be used in numerical integration;

k_{d1} first order reaction time deactivation constant (h^{-1});

k_{d2} first order benzaldehyde deactivation coefficient (mM^{-1} h^{-1});

K_b intrinsic or microscopic binding constant for benzaldehyde (mM^{1-h});

K_{ma} affinity constant for pyruvate (mM);

K_{mb} affinity constant for benzaldehyde (mM);

P   PAC concentration (mM);

Q   acetaldehyde concentration (mM);

R   acetoin concentration (mM);

R^2 correlation coefficient;

RQ   respiratory quotient;

RSS   residual sum of squares;

t   time (h);

t_{lag} lag time (h);

U   carboligase enzyme activity unit;

V_p overall rate constant for the formation of PAC (μmol h^{-1} U^{-1});

V_q overall rate constant for the formation of acetaldehyde (ml h^{-1} U^{-1});

V_r overall rate constant for the formation of acetoin (l^2 h^{-1} U^{-1} mol^{-1});

Δt step size constant of Euler-Cauchy numerical integration (0.01 h).

6.2   INTRODUCTION

Mathematical modelling and simulation, supported by detailed kinetic experimentation, offers an important strategy for enhancing productivities and yields of enzymatic and microbial cultivation processes (Tholudur et al. 1999, d'Anjou and Daugulis 2000).

Previous kinetic equations developed in studies of the PAC biotransformation have either described PDC deactivation by benzaldehyde (Chow et al. 1995 and Chapter 5 of this thesis) or were simplified rate equations for PAC formation involving only one or two variables (Shin and Rogers 1996b, Goetz et al. 2001, Iwan et al. 2001).

Recent improvements of enzymatic PAC production by PDC extracted from yeast (*C. utilis*) or filamentous fungi (*R. javanicus*) in benzaldehyde emulsion systems (Rosche et al. 2001, 2002a,b, 2003a) have stimulated an interest in a systematic approach for analysing and optimizing this process. In this Chapter, an overall model is developed for PAC production. For this purpose initial rate experiments are performed on ranges of substrate concentrations and enzyme activity levels. Furthermore four independent batch biotransformations with different initial substrate concentrations are presented with complete profiles (pyruvate, benzaldehyde, PAC, acetaldehyde, acetoin and enzyme activity). Three of these are used for the estimation of overall and by-products rate constants and the refinement of estimated parameter constants from the initial rate studies. The fourth set of biotransformation data is used for model validation.

6.3   RESULTS

6.3.1   Model Structure

A kinetic model developed in Chapter 3 has been used as a basis for further analysis of the relationships influencing the formation of PAC and related by-products. The model provides a simplified description of the actual reactions.

6.3.2   Effect of enzyme activity on initial rate

The time profiles of PAC formation over the first 30 min with excess pyruvate and benzaldehyde and enzyme activities from 0.5–10.0 U carboligase ml^{-1} using partially purified PDC from *C. utilis* are plotted in Figure 6.1(a). As can be seen from Figure 6.1(b), the initial rates of PAC formation were directly proportional to the enzyme activities up to 5.0 U carboligase ml^{-1} after which the relationship declined from linearity. Equation (6.1) expresses the linear relationship between initial rate and enzyme activity level, with the R^2 for the linear fitting from 0 to 5.0 U carboligase ml^{-1} being 0.9977.

$$\frac{d[P]}{dt} \propto [E] \tag{6.1}$$

6.3.3   Effect of pyruvate concentration on initial rate

For determination of initial rate data, the time profiles for PAC formation with pyruvate concentrations from 10-250 mM in the presence of 102 mM benzaldehyde are shown in Figure 6.2(a). Significant rate differences were evident for pyruvate concentrations in the range 10-50 mM, however there was little difference in the data for 100-250 mM over the initial 30 min. The relationship between initial rates and pyruvate concentrations is shown in Figure 6.2(b), which indicates that Michaelis-Menten kinetics best fits experimental data with K_{ma} of 6.59 mM, RSS of 0.0393 and R^2 of 0.9975. The relationship between initial rate and pyruvate concentration is given in Equation (6.2).

$$\frac{d[P]}{dt} \propto \frac{[A]}{K_{ma} + [A]} \tag{6.2}$$

where: K_{ma} = 6.59 mM.

(a)

(b)
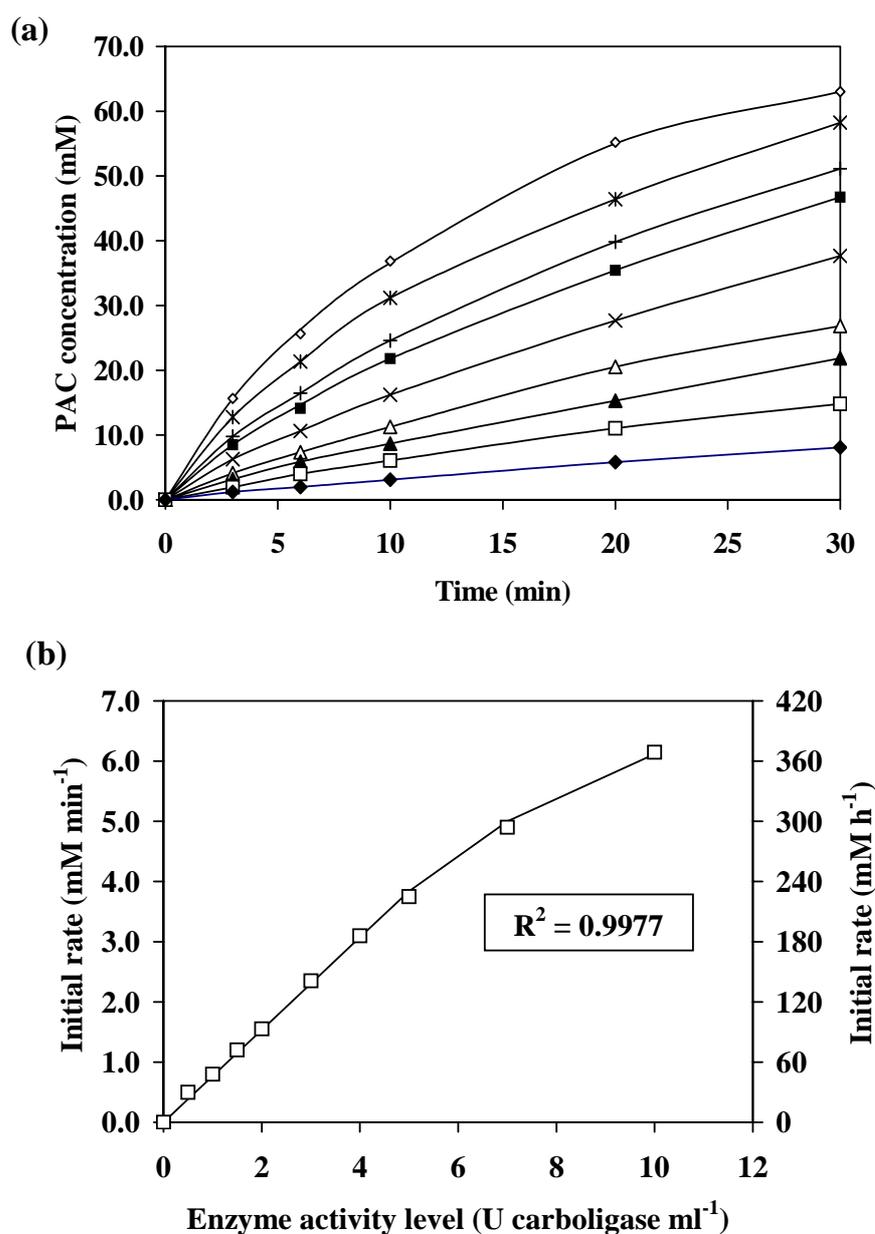
Figure 6.1: Time and initial rate profiles of PAC formation with variation of enzyme activity from 0.5–10.0 U carboligase ml^{-1}. Reaction mixture contained 100 mM sodium pyruvate, 103 mM benzaldehyde, 2.5 M MOPS, 1 mM MgSO$_4$, 1 mM TPP, at 6°C (pH 7.0), (a) time profiles of PAC formation for the first 30 min of reaction with enzyme activity levels of (U carboligase ml^{-1}): ($\diamondsuit$) 10.0, ($*$) 7.0, ($+$) 5.0, ($\blacksquare$) 4.0, ($\times$) 3.0, ($\triangle$) 2.0, ($\blacktriangle$) 1.5, ($\square$) 1.0 and ($\blacklozenge$) 0.5, (b) initial rate profile of PAC formation (mM min^{-1} and mM h^{-1}) taken at time zero by tangential method. The R^2 was calculated from linear fitting of initial rate and enzyme activity up to 5.0 U carboligase ml^{-1}.

(a)

(b)
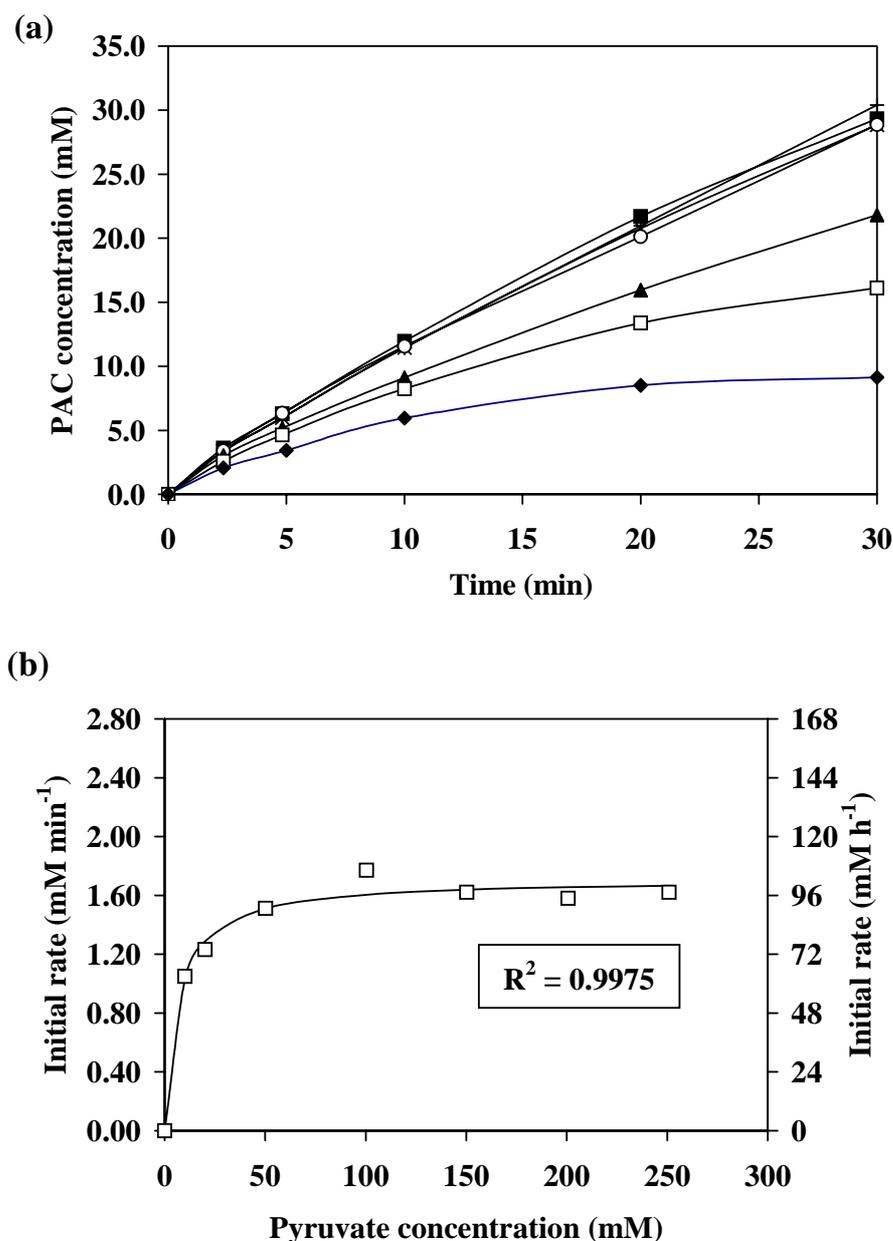
Figure 6.2: Time and initial rate profiles of PAC formation with variation of sodium pyruvate concentrations from 10–250 mM. Reaction mixture contained 102 mM benzaldehyde, 3.0 U carboligase ml^{-1}, 2.5 M MOPS, 1 mM MgSO$_4$, 1 mM TPP, at 6°C (pH 7.0), (a) time profiles of PAC formation for the first 30 min of reaction with sodium pyruvate concentrations of (mM): ($+$) 251, ($\bigcirc$) 201, ($\times$) 150, ($\blacksquare$) 100, ($\blacktriangle$) 50.2, ($\square$) 20.1 and ($\blacklozenge$) 10.0, (b) initial rate profile of PAC formation (mM min^{-1} and mM h^{-1}) taken at time zero by tangential method.

6.3.4 Effect of benzaldehyde concentration on initial rate

Time profiles describing the influence of the benzaldehyde concentration (10–150 mM) on PAC formation are presented in Figure 6.3(a). There was a sigmoidal type relationship between initial rates and benzaldehyde concentrations as shown in Figure 6.3(b).

A kinetic relationship based on the Michaelis-Menten equation did not adequately describe the experimental data with affinity constant (K_{mb}) of 67.7 mM, RSS of 0.232 and R^2 of 0.9874 . As a result, the Monod-Wyman-Changeux (MWC) equation (Palmer 1991) was employed and the line prediction created by this equation is shown in Figure 6.3(b). In this case the RSS and R^2 were 0.0896 and 0.9951 respectively. The binding constant (K_b) and Hill coefficient-like exponent (h) were determined as 1.00×10^{-4} mM$^{-1.61}$ and 2.61 (no unit) respectively. Equation (6.3) describes this relationship:

$$\frac{d[P]}{dt} \propto \frac{K_b[B]^h}{1 + K_b[B]^h}$$

(6.3)

where: $K_b = 1.00 \times 10^{-4}$ mM$^{-1.61}$ and h = 2.61 (no unit).

Relative low value for K_b (with magnitude of $5.5 \pm 0.2 \times 10^{-4}$) has been reported also by Changeux et al. (1968) who investigated the binding of aspartate transcarbamylase (ATCase) catalytic subunit with a substrate, succinate.

6.3.5 Modification of model based on initial rate studies

The rate equation for PAC production developed in Chapter 3 had the form given in Equation (6.4). However modification of this equation is necessary to account for the sigmoidal relationship between benzaldehyde and initial rates as described in Equation (6.3). The relationships between initial rates and pyruvate concentrations and enzyme activities used in the model have been confirmed in the present experimental analysis. The modified PAC rate equation is given in Equation (6.5):

(a)

(b)
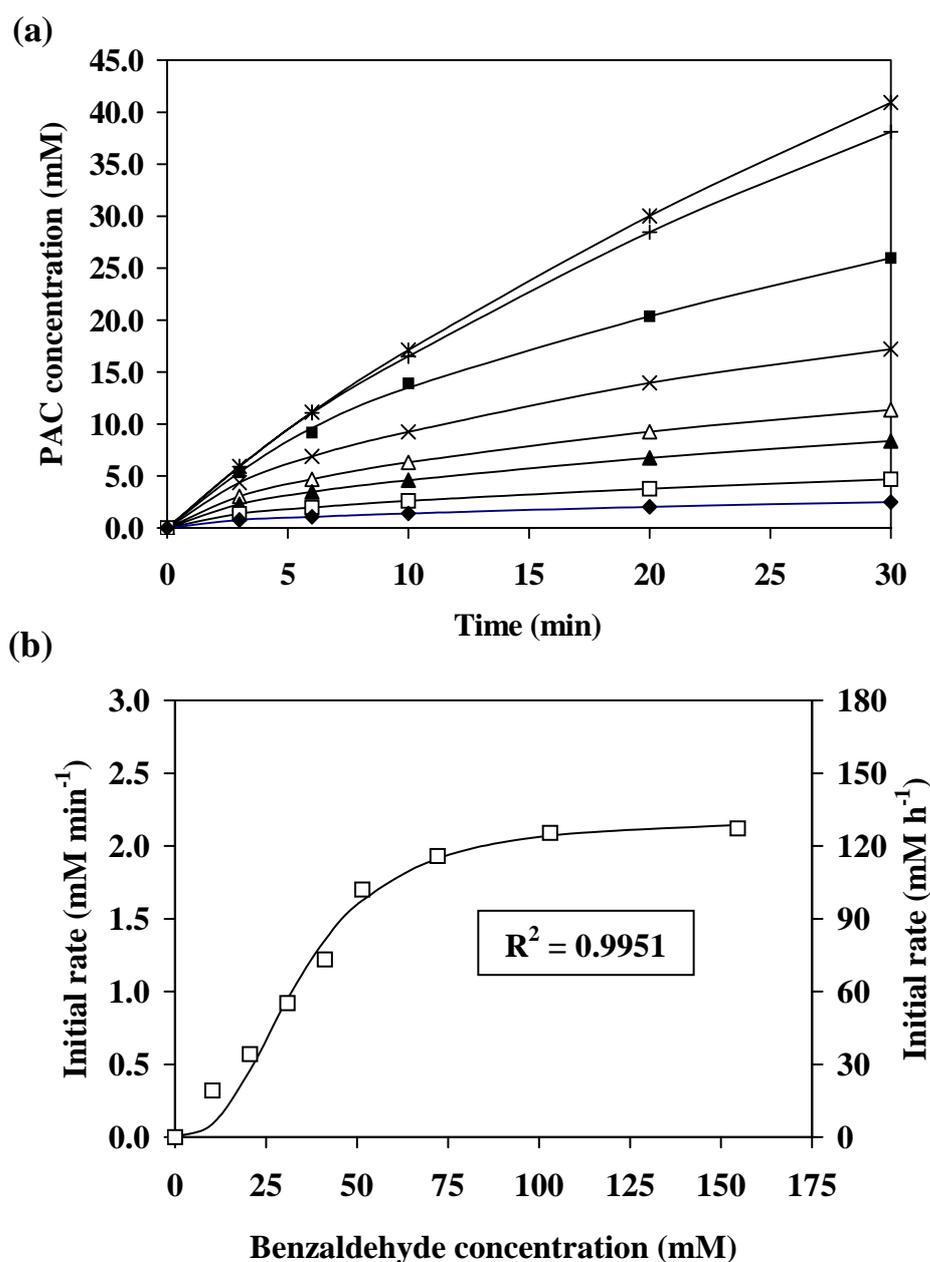
Figure 6.3: Time and initial rate profiles of PAC formation with variation of benzaldehyde concentrations from 10–150 mM. Reaction mixture contained 99.9 mM sodium pyruvate, 3.0 U carboligase ml^{-1}, 2.5 M MOPS, 1 mM MgSO$_4$, 1 mM TPP, at 6°C (pH 7.0), (a) time profiles of PAC formation for the first 30 min of reaction with benzaldehyde concentrations of (mM): ($*$) 155, ($+$) 103, ($\blacksquare$) 72.1, ($\times$) 51.5, ($\triangle$) 41.2, ($\blacktriangle$) 30.9, ($\square$) 20.6 and ($\blacklozenge$) 10.3, (b) initial rate profile of PAC formation (mM min^{-1} and mM h^{-1}) taken at time zero by tangential method.

$$\frac{d\,[P]}{d\,t}\bigg|_i = V_p \left[\frac{[B_i]}{K_{mb}+[B_i]}\right]\left[\frac{[A_i]}{K_{ma}+[A_i]}\right][E_i] \tag{6.4}$$

$$\frac{d\,[P]}{d\,t}\bigg|_i = V_p \left[\frac{K_b\,[B_i]^h}{1+K_b\,[B_i]^h}\right]\left[\frac{[A_i]}{K_{ma}+[A_i]}\right][E_i] \tag{6.5}$$

Other rate equations representing the consumption of pyruvate (6.6) and benzaldehyde (6.7) and the formation of by-products, acetaldehyde (6.8) and acetoin (6.9), were as derived previously from Chapter 3. Equation (6.8) and (6.9) can also be derived from the experimental observation that PDC from various yeasts and fungi require pyruvate rather than acetaldehyde for PAC formation (Rosche et al. 2003b) and that any acetaldehyde produced can only be converted to acetoin and not to PAC.

$$\frac{d\,[A]}{d\,t}\bigg|_i = -\frac{d\,[P]}{d\,t}\bigg|_i - \frac{d\,[Q]}{d\,t}\bigg|_i - 2\frac{d\,[R]}{d\,t}\bigg|_i \tag{6.6}$$

$$\frac{d\,[B]}{d\,t}\bigg|_i = -\frac{d\,[P]}{d\,t}\bigg|_i \tag{6.7}$$

$$\frac{d\,[Q]}{d\,t}\bigg|_i = V_q\,[A_i][E_i] - V_r\,[A_i][Q_i][E_i] \tag{6.8}$$

$$\frac{d\,[R]}{d\,t}\bigg|_i = V_r\,[A_i][Q_i][E_i] \tag{6.9}$$

The equation for enzyme deactivation (6.10) has been described in Chapter 5 for partially purified PDC in 2.5 M MOPS buffer for the benzaldehyde concentration range 0-200 mM.

$$\frac{d\,[E]}{d\,t}\bigg|_i = -(k_{d1}+k_{d2}\,[B_i])[E_i]\,;\,if\ t\le t_{lag}\ (5.23\ h)\,;\,\frac{d\,[E]}{d\,t}\bigg|_i = 0 \tag{6.10}$$

Numerical integration based on the Euler-Cauchy method (Kreyszig 1993) with a time increment (Δt) of 0.01 h has been employed to construct the simulation profiles. Equations (6.11)–(6.16) are used in the determination of the concentrations of each

chemical species and enzyme activity from the assigned time increment and rate equations.

$$[P_i] = [P_{i-1}] + \frac{d[P]}{dt}\bigg|_{i-1} \Delta t \tag{6.11}$$

$$[A_i] = [A_{i-1}] - \left(\frac{d[P]}{dt}\bigg|_{i-1} + \frac{d[Q]}{dt}\bigg|_{i-1} + 2\frac{d[R]}{dt}\bigg|_{i-1}\right)\Delta t \tag{6.12}$$

$$[B_i] = [B_{i-1}] - \frac{d[P]}{dt}\bigg|_{i-1} \Delta t \tag{6.13}$$

$$[Q_i] = [Q_{i-1}] + \frac{d[Q]}{dt}\bigg|_{i-1} \Delta t \tag{6.14}$$

$$[R_i] = [R_{i-1}] + \frac{d[R]}{dt}\bigg|_{i-1} \Delta t \tag{6.15}$$

$$[E_i] = [E_{i-1}] + \frac{d[E]}{dt}\bigg|_{i-1} \Delta t \tag{6.16}$$

6.3.6   Experimental determination of overall rate constants for PAC, acetaldehyde and acetoin formation

Three batch biotransformation studies - initial substrate concentrations of 50 mM benzaldehyde / 60 mM sodium pyruvate and 150 mM benzaldehyde / 180 mM sodium pyruvate with initial PDC of 3.4 U carboligase ml^{-1} as well as 100 mM benzaldehyde / 120 mM sodium pyruvate with initial PDC of 1.1 U carboligase ml^{-1} - have been used in the estimation of the overall rate constants in the complete model using the parameter-searching method as described. The optimal values of overall rate constants for the formation of PAC, acetaldehyde and acetoin were determined as $V_p = 34.7$ μmol h^{-1} U^{-1}, $V_q = 0.0163$ ml h^{-1} U^{-1}, $V_r = 0.00261$ l^2 h^{-1} U^{-1} mol^{-1} based on the model with these parameters providing the 'best fit' between the experimental and predicted values of

pyruvate, benzaldehyde, acetaldehyde, acetoin, PAC and enzyme activity profiles for the three sets of data. The statistical analysis (RSS, R^2) corresponding to each fitting was (385, 0.9873) for 50 mM benzaldehyde / 60 mM sodium pyruvate with initial PDC of 3.4 U carboligase ml^{-1}, (665, 0.9955) for 100 mM benzaldehyde / 120 mM sodium pyruvate with initial PDC of 1.1 U carboligase ml^{-1}, (772, 0.9971) for 150 mM benzaldehyde / 180 mM sodium pyruvate with initial PDC of 3.4 U carboligase ml^{-1}. Both experimental data and model fitting for the kinetic profiles are given in Figure 6.4(a)–(c). The values of all kinetic parameters used in the modelling of the batch biotransformation kinetics are listed in Table 6.1.
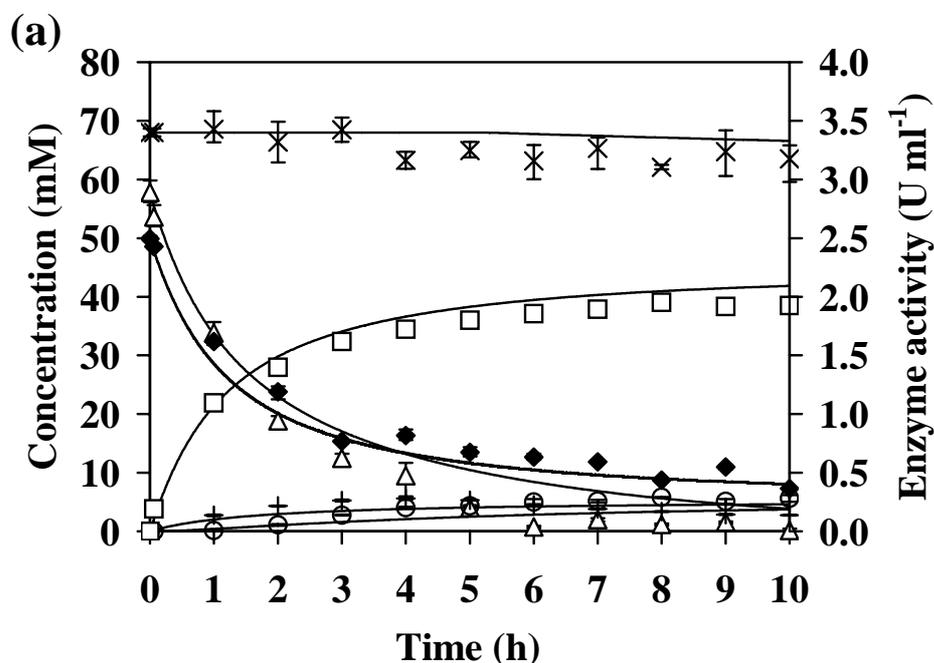
Figure 6.4(a): Batch biotransformation kinetics and model fitting for determination of overall rate constants for the formation of PAC, acetaldehyde and acetoin (V_p, V_q and V_r) at 50 mM benzaldehyde / 60 mM sodium pyruvate with initial PDC activity of 3.4 U carboligase ml^{-1}. Reaction mixture contained 2.5 M MOPS, 1 mM $MgSO_4$, 1 mM TPP at $6^{\circ}C$ (pH 7.0): ($\triangle$) pyruvate, ($\blacklozenge$) benzaldehyde, ($+$) acetaldehyde, ($\bigcirc$) acetoin, ($\square$) PAC and ($\times$) enzyme activity. Error bars show the lowest and highest values of three replicates. Line of best fit through each data profile was created from the optimal value of $V_p = 34.7$ µmol h^{-1} U^{-1}, $V_q = 0.0163$ ml h^{-1} U^{-1} and $V_r = 0.00261$ l^2 $h^{-1}U^{-1}mol^{-1}$.
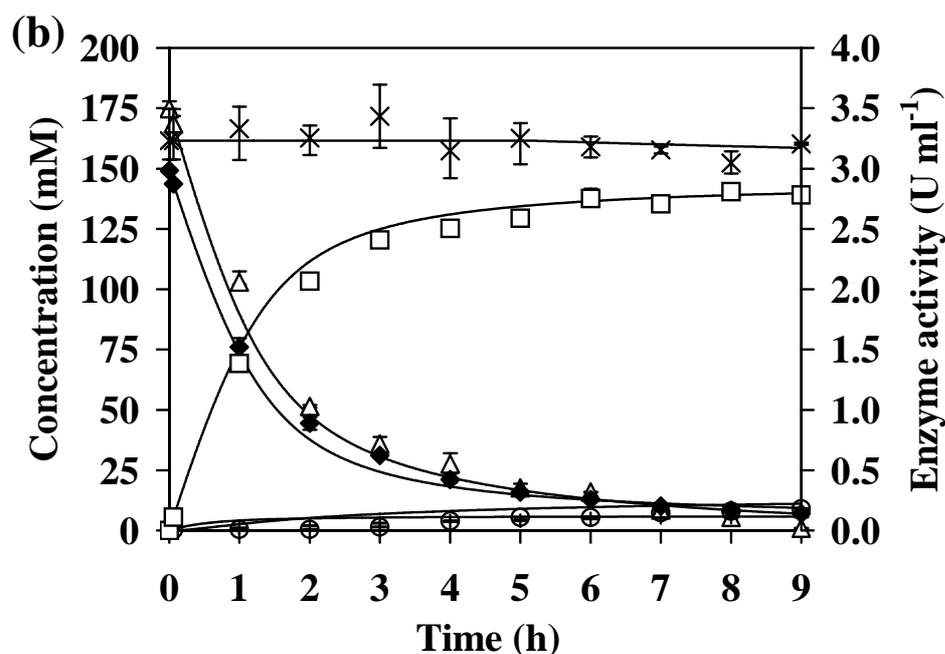
Figure 6.4(b): Batch biotransformation kinetics and model fitting for determination of overall rate constant for the formation of PAC, acetaldehyde and acetoin (V_p, V_q and V_r) at 150 mM benzaldehyde / 180 mM sodium pyruvate with initial PDC activity of 3.4 U carboligase ml^{-1}. Reaction mixture contained 2.5 M MOPS, 1 mM $MgSO_4$, 1 mM TPP at $6°C$ (pH 7.0): ($\triangle$) pyruvate, ($\blacklozenge$) benzaldehyde, ($+$) acetaldehyde, ($\bigcirc$) acetoin, ($\square$) PAC and ($\times$) enzyme activity. Error bars show the lowest and highest values of three replicates. Line of best fit through each data profile was created from the optimal value of $V_p = 34.7$ μmol h^{-1} U^{-1}, $V_q = 0.0163$ ml h^{-1} U^{-1} and $V_r = 0.00261$ $l^2 h^{-1} U^{-1} mol^{-1}$.
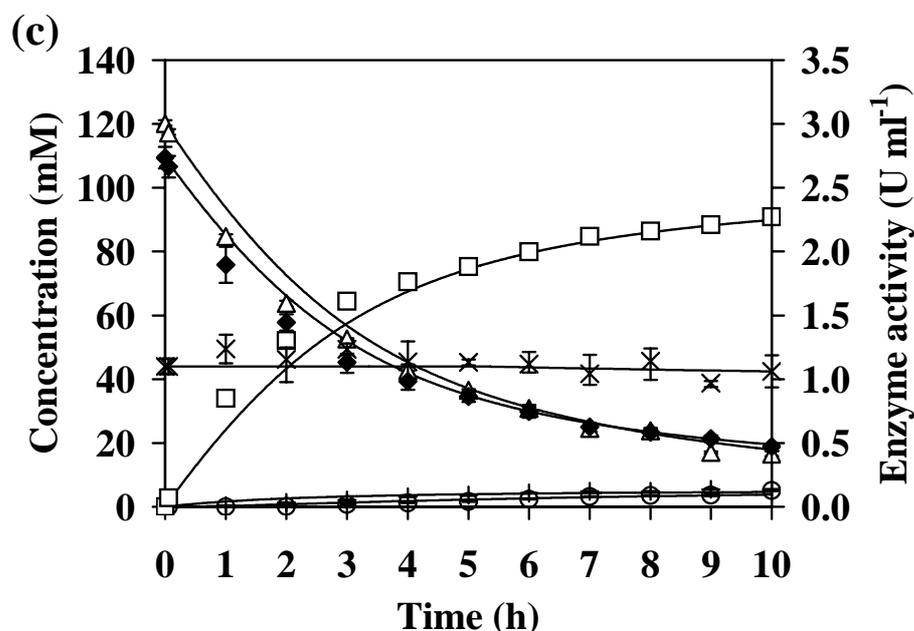
Figure 6.4(c): Batch biotransformation kinetics and model fitting for determination of overall rate constant for the formation of PAC, acetaldehyde and acetoin (V_p, V_q and V_r) at 100 mM benzaldehyde / 120 mM sodium pyruvate with initial PDC activity of 1.1 U carboligase ml^{-1}. Reaction mixture contained 2.5 M MOPS, 1 mM MgSO$_4$, 1 mM TPP at 6°C (pH 7.0): ($\triangle$) pyruvate, ($\blacklozenge$) benzaldehyde, ($+$) acetaldehyde, ($\bigcirc$) acetoin, ($\square$) PAC and ($\times$) enzyme activity. Error bars show the lowest and highest values of three replicates. Line of best fit through each data profile was created from the optimal value of V_p = 34.7 μmol h^{-1} U^{-1}, V_q = 0.0163 ml h^{-1} U^{-1} and V_r = 0.00261 l^2 h^{-1}U^{-1}mol^{-1}.

Table 6.1: Constants for the complete model for PAC biotransformation process at $6^{\circ}C$ in biotransformation buffer containing 2.5 M MOPS (pH 7.0), 1 mM MgSO$_4$ and 1 mM TPP with initial PDC activity between 1.1–3.4 U carboligase ml^{-1}.

Constants	Unit	Values	Error, (95% C.I.)
V_p [1]	µmol h^{-1} U^{-1}	34.7	0.55, (33.6, 35.8)
K_b [2]	mM$^{-1.18}$	1.00×10^{-4}	5.20 x 10^{-8}, (9.99×10^{-5}, 1.00×10^{-4})
h [2]	(no unit)	2.18	0.58, (1.02, 3.34)
K_{ma} [2]	mM	7.91	8.21, (-8.63, 24.4)
V_q [1]	ml h^{-1} U^{-1}	1.63×10^{-2}	5.91×10^{-6}, (7.34×10^{-3}, 2.52×10^{-2})
V_r [1]	l^2 h^{-1} U^{-1} mol^{-1}	2.61×10^{-3}	4.04×10^{-6}, (2.51×10^{-3}, 2.71×10^{-3})
k_{d1} [3]	h^{-1}	2.64×10^{-3}	2.53×10^{-4}, (2.13×10^{-3}, 3.15×10^{-3})
k_{d2} [3]	mM^{-1} h^{-1}	1.98×10^{-4}	1.91×10^{-8}, (Small interval)
t_{lag} [3]	h	5.23	6.54×10^{-5}, (Small interval)

(1)   Batch biotransformation kinetics

(2)   Initial rate study and batch kinetics

(3)   Enzyme deactivation study

6.3.7   Model validation by prediction of independent batch biotransformation kinetics

Model validation was performed by using the model and the calculated kinetic parameters to determine simulation profiles for consumption of substrates, enzyme deactivation, product and by-products formation for the initial concentrations of benzaldehyde and pyruvate of 100 and 120 mM and enzyme activity level of 3.0 U carboligase ml^{-1}. An experimental batch biotransformation at the same initial conditions was carried out for comparison with the model predictions. The simulation profile shown in Figure 6.5 was in close agreement with the experimental data with RSS and R^2 values of 451 and 0.9963 respectively. It provided strong evidence that the model could accurately predict experimental results within this range of initial conditions, although some overestimation of PDC activity was evident in Figure 6.5 in the latter stages of the biotransformation.
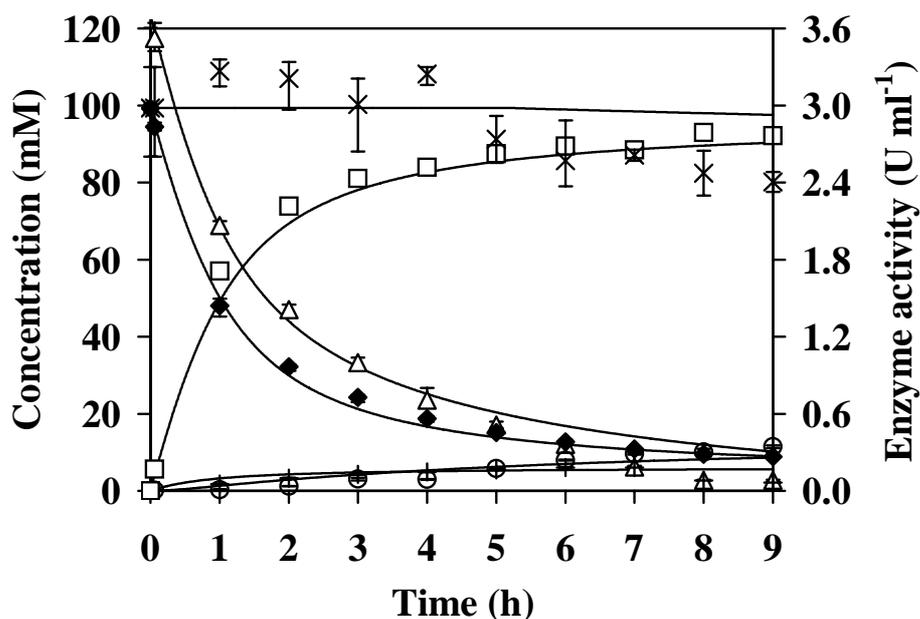
Figure 6.5: Model prediction of batch biotransformation kinetics for 100 mM benzaldehyde / 120 mM sodium pyruvate with 3.0 U carboligase ml^{-1}. Model prediction using V_p, V_q and V_r from Figure 6.4 (line) and experimental data points (2.5 M MOPS, 1 mM MgSO$_4$, 1 mM TPP at 6°C, pH 7.0): ($\triangle$) pyruvate, ($\blacklozenge$) benzaldehyde, ($+$) acetaldehyde, ($\bigcirc$) acetoin, ($\square$) PAC, ($\times$) enzyme activity. Each data point was an average from three replicates. Error bars show the lowest and highest values of three replicates.

6.3.8   Mass balance and yield analysis on batch biotransformation experiments

Mass balances based on molarity were performed at all time points for all four biotransformation studies and showed 2.50 ± 0.50% loss of pyruvate and a closing molarity balance for benzaldehyde. The molar yields of PAC based on substrates consumed were 0.99 ± 0.07 mol PAC / mol benzaldehyde and 0.78 ± 0.11 mol PAC / mol pyruvate. The by-products yields were 0.058 ± 0.039 mol acetaldehyde / mol pyruvate and 0.073 ± 0.024 mol acetoin / mol pyruvate. Benzyl alcohol, a by-product of PAC production, was not detected. The formation of benzoic acid by oxidation of benzaldehyde was less then 0.4 mM for all batch biotransformations.

6.3.9   Extended model fitting to the batch biotransformation kinetics with initial benzaldehyde and pyruvate concentrations of 400 and 600 mM

In order to extend the model fitting beyond the concentration range of substrates and PDC activity previously investigated, the kinetic parameters in Table 6.1 were modified as indicated in Table 6.2 to accommodate for different biotransformation conditions in the emulsion batch biotransformation previously published for production of PAC using PDC from *C. utilis* (Rosche et al. 2003a). The initial benzaldehyde and pyruvate concentrations were 400 and 600 mM in 2.5 M MOPS with initial enzyme activity of 8.4 U carboligase ml^{-1}, pH 6.5 at 6°C. The parameters searching program was applied to obtain the optimal fitting value for each constant to best fit the previously published experimental data of this biotransformation (Rosche et al. 2003a).

As seen from Figure 6.6, the generated profiles of pyruvate (A) and benzaldehyde (B) consumption, PAC (P) and by-products acetaldehyde (Q) and acetoin (R), as well as the enzyme deactivation provided acceptable fitting to the experimental data with RSS and R^2 values of 4.49 × 10^3 and 0.9980 respectively.
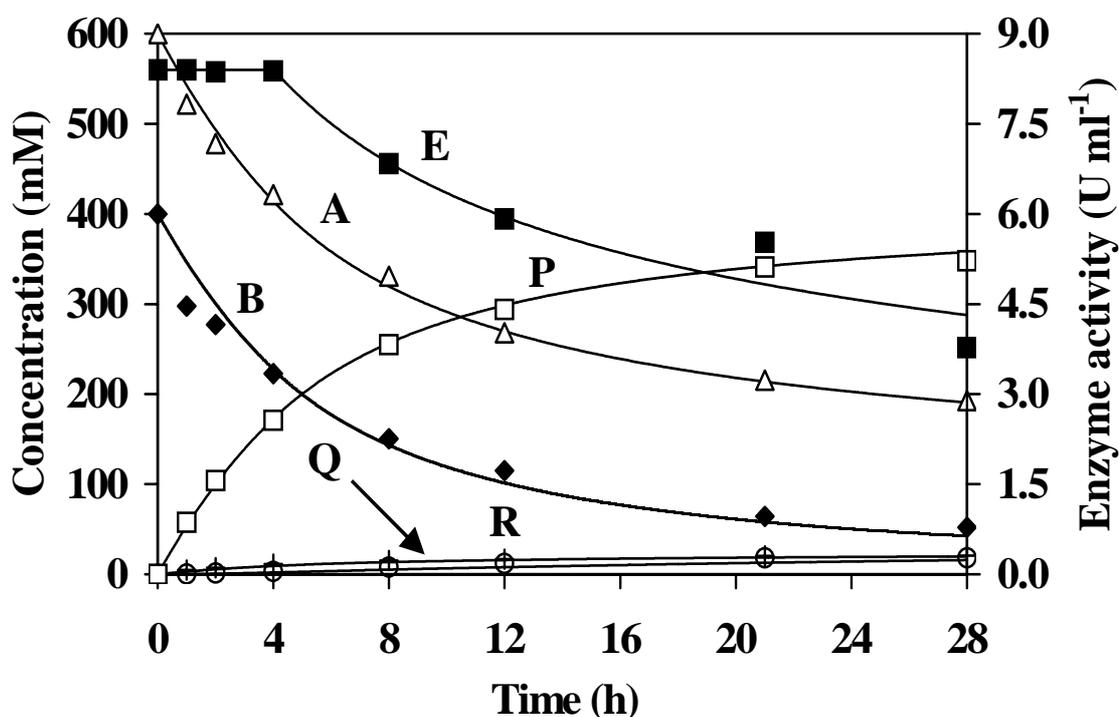
Figure 6.6: Fitting of PAC production profiles using the complete model with modified constants listed in Table 6.2 for PAC biotransformation process with initial substrates concentration of 600 mM sodium pyruvate and 400 mM benzaldehyde. The experimental data for partially purified *C. utilis* PDC in 2.5 M MOPS, 0.5 mM MgSO$_4$, 1 mM TPP, initial pH and carboligase activity of 6.5 and 8.4 U carboligase ml^{-1} at 6°C were given by Rosche et al. (2003a); ($\triangle$) pyruvate, ($\blacklozenge$) benzaldehyde, ($+$) acetaldehyde, ($\bigcirc$) acetoin and ($\square$) PAC. Each capital letter represents substrate, product, or by-product; pyruvate (A), benzaldehyde (B), PAC (P), acetaldehyde (Q), acetoin (R) and relative carboligase activity (E).

Table 6.2: Kinetic parameters used in the construction of PAC simulation profile in Figure 6.6. They were obtained by best fit parameter searching within a specified boundary.

Kinetic parameters	Unit	Values	Values listed in Table 6.1
$V_p^{(1)}$	μmol h^{-1} U^{-1}	23.7	34.7
*$K_b^{(1)}$	mM$^{-0.39}$	9.00×10^{-5}	1.00×10^{-4}
$h^{(1)}$	(no unit)	1.39	2.18
*$K_{ma}^{(1)}$	MM	8.70	7.91
$V_q^{(1)}$	ml h^{-1} U^{-1}	6.70×10^{-4}	1.63×10^{-2}
$V_r^{(1)}$	l^2 h^{-1} U^{-1} mol^{-1}	2.46×10^{-5}	2.61×10^{-3}
$k_{d1}^{(2)}$	h^{-1}	2.64×10^{-3}	2.64×10^{-3} (unchanged)
$k_{d2}^{(1)}$	mM^{-1} h^{-1}	2.70×10^{-4}	1.98×10^{-4}
$t_{lag}^{(1)}$	h	4.01	5.23

(1)   Batch biotransformation kinetics from Figure 6.6

(2)   Enzyme deactivation study

Note: K_b reached the 10% lower bound and K_{ma} reached the 10% upper bound during the search for optimal fitting parameter values

6.4   DISCUSSION

From the relatively good fit achieved by the model for the three complete data sets for PAC production and from its predictive value for a fourth data set, it is evident that the model provides an acceptable description of the enzymatic biotransformation over a range of enzyme activities and substrate concentrations. In addition, the initial rate studies have provided some interesting insights into enzyme behaviour. For example, the effect of pyruvate on initial rate of PAC formation was found to follow Michaelis-Menten kinetics while sigmoidal-shape kinetics were determined for the effect of benzaldehyde. As PDC is a tetrameric enzyme consisting of four protein subunits and binding sites (Flatau et al. 1988), complex interactions between PDC and substrate benzaldehyde might account for such sigmoidal behaviour. However, while Boiteux and

Hess (1970) and Palmer (1991) suggested that a sigmoidal-shape profile might be evidence of the allosteric behaviour of an enzyme containing more than one subunit, Stivers and Washabaugh (1993) recommended caution in the interpretation of such sigmoidicity, which they suggested may be unrelated to the reaction mechanism.

In the development of the overall model for the biotransformation profiles, it is also significant to recognize that six of the nine constants used were derived from kinetic studies, which provided values of initial rate constants (K_b, h, K_{ma}) and enzyme deactivation constants (k_{d1}, k_{d2}, t_{lag}). The overall product rate constants (V_p, V_q, V_r) were determined from the experimental data and computer curve fitting. Modifications (within $\pm$ 20% of the original values) of h and K_{ma} were allowed during parameter searching to improve fitting to the biotransformation profiles.

From the comparison of the simulation curves generated by the model and the experimental data obtained from the various biotransformations in the ranges of initial 50-150 mM benzaldehyde, 60-180 mM pyruvate and 1.1-3.4 U carboligase ml^{-1}, there is evidence of some minor under/over estimations of the experimental data. However these variations were not considered to be systematic in nature and appeared to be due to experimental variations/errors within particular studies. It is possible that some inhibitory effects (not currently included in the model structure) may have had some influence on the biotransformation kinetics. The initial rate profiles for the effect of pyruvate and benzaldehyde on PAC production (see Figures 6.2(b) and 6.3(b)) suggest that these substrates are not likely to cause PDC inhibition for the above substrate ranges. Product inhibition by PAC may be possible at the higher concentration levels (140 mM); however Iwan et al. (2001) and Goetz et al. (2001) found no evidence for *Z. mobilis* PDC inhibition by PAC in the concentration range 20-100 mM. Acetoin is not likely to cause inhibition at low concentrations of less than 10 mM (unpublished results); however acetaldehyde has been reported to inhibit *C. utilis* PDC with an estimated K_p of 20 mM at 4°C (Shin and Rogers 1996b) and may cause some inhibition (acetaldehyde concentrations up to 5.7 mM). This was in contrary with the study by Sandford (2002) who reported a minimal impact of 30 mM acetaldehyde to *C. utilis* PDC in 50 mM MES buffer at 4°C over 15 h. The strategy of using complete

biotransformation profiles for the determination of optimal kinetic constant values had the advantage of incorporating minor inhibitory or even synergistic effects due to the presence of PAC and/or by-products.

The complete model developed in Section 6.3.6 was extended further to batch biotransformation kinetics with 400 mM benzaldehyde and 600 mM pyruvate as shown in Figure 6.6. The modification of the constants were relatively small (within 10%) for K_b and K_{ma} while moderate for t_{lag} (24% changes). The parameters which were more sensitive to high substrate concentrations include V_p, h and k_{d2} with up to 40% changes from the original values. A significant decrease of by-products formation in the experimental data also decreased the overall rate constants for the formation of acetaldehyde and acetoin by 24 and 106 times respectively relative to the values listed in Table 6.1. The reaction time deactivation constant (k_{d1}) was not altered because it reflects an inherent enzyme deactivation that is independent to the level of benzaldehyde concentration in use. The elevated value of pyruvate affinity constant (K_{ma}) may suggest a decreased efficiency of PDC-pyruvate binding at high substrate concentration level. In addition, the increase benzaldehyde deactivation coefficient (k_{d2}) in association with a shorter time lag (t_{lag}) were as expected since 400 mM benzaldehyde posed a much stronger deactivating effect to PDC. The optimal fitting of previously published experimental data (Rosche et al. 2003a) at these higher initial substrate concentrations required some changes in the kinetic constants, however the basic model structure remained the same and good fitting was obtained. The changes in the kinetic parameters might result from inhibition effects due to the higher concentrations of benzaldehyde and possible inhibitory products (e.g. PAC, acetoin, acetaldehyde) and future model development at higher initial substrate concentrations may need to incorporate substrate and product inhibition terms.

In this Chapter, a kinetic model has been developed based on the use of traditional equations for enzyme kinetic relationships. This can be compared to a more complex approach investigated in Chapter 3 which followed the procedure outlined originally by King and Altman (1956).

6.5   CONCLUSIONS

A mathematical model describing the formation of PAC and its related by-products has been refined and validated for the enzymatic reaction performed by *C. utilis* PDC in 2.5 M MOPS buffer, 1 mM MgSO$_4$, 1 mM TPP, 6°C and pH 7.0. It is based on a theoretical model that reflects the complex reaction mechanism and on experimental initial rate studies, batch biotransformation kinetics, as well as deactivation kinetics of PDC by benzaldehyde. The concentration range of model prediction covers 60-180 mM sodium pyruvate and 50-150 mM benzaldehyde at a molar pyruvate/benzaldehyde ratio of 1.2, PAC up to 140 mM, by-products up to 10 mM and enzyme activity levels of 1.1-3.4 U carboligase ml^{-1}. Model validation was confirmed in an independent batch biotransformation with 120/100 mM initial pyruvate/benzaldehyde with 3.0 U carboligase ml^{-1}. The model was used also to describe the kinetic profiles for higher initial substrate concentrations (e.g. 600 mM pyruvate and 400 mM benzaldehyde). The value of this model is that it provides both a more complete understanding of the kinetics of PAC production, as well as a rationale for process optimization in the selection of optimal PDC activities and substrate concentrations for future batch, fed-batch or continuous processes.

The major part of this Chapter has already been published in;

Leksawasdi, N., Chow, Y.Y.S., Breuer, M., Hauer, M., Rosche, B. and Rogers, P.L. (2004). Kinetic studies and model validation of enzymatic (*R*)-phenylacetylcarbinol batch biotransformation process, Journal of Biotechnology, 111: 179-189.

Chapter **7**

Cost Effective Development of Two-Phase Biotransformation for PAC Production

7.1   NOMENCLATURE

Bz_{bal} percentage of benzaldehyde accounted for from PAC;

Cost   Australian dollars spent on buffering and chemical additives for the production of 1 g PAC ($ g^{-1});

E_{act} relative enzyme activity at time t (%);

E_{ini} initial carboligase activity in the aqueous phase (U carboligase ml^{-1});

P   PAC;

PAC_{aq} concentration of PAC in the aqueous phase (g l^{-1} aqueous phase);

$PAC_{max\ rate}$ maximum rate of PAC production (mM h^{-1});

PAC_{or} concentration of PAC in the organic phase (g l^{-1} organic phase);

$PAC_{productivity}$ overall volumetric PAC productivity (g l^{-1} day^{-1});

PAC_{spec} specific PAC production (mg U^{-1} initial carboligase activity);

$PAC_{spec\ prod}$ specific PAC productivity (mg U^{-1} initial carboligase activity h^{-1});

PAC_{tot} overall concentration of PAC (g l^{-1} emulsion);

Pyr_{bal} percentage of pyruvate accounted for from PAC, acetaldehyde and acetoin;

Q   acetaldehyde;

R   acetoin;

t   time point when PAC production reached stationary phase (h);

$V_{aq}:V_{or}$ volume ratio of the aqueous to organic phase at equilibrium (l aqueous phase l^{-1} organic phase);

$Y_{P/BZ}$ yield of PAC produced over consumed benzaldehyde (mol PAC mol^{-1} benzaldehyde);

$Y_{P/Pyr}$ yield of PAC produced over consumed pyruvate (mol PAC mol^{-1} pyruvate);

$Y_{Q/Pyr}$ yield of acetaldehyde produced over consumed pyruvate (mol acetaldehyde mol^{-1} pyruvate);

$Y_{R/Pyr}$ yield of acetoin produced over consumed pyruvate (mol acetoin mol^{-1} pyruvate).

7.2   INTRODUCTION

Enzymatic production of PAC in a single phase process with partially purified *C. utilis* PDC in phosphate buffer (40 mM) resulted in a final PAC concentration of 28 g l^{-1} in 8 h (Shin and Rogers 1996b). By the use of high concentration buffer (2 M MOPS) in a benzaldehyde emulsion (6°C, initial pH of 6.5, 400 mM benzaldehyde and 600 mM pyruvate), Rosche et al. (2003a) demonstrated with *R. javanicus* and *C. utilis* PDC the achievement of increased PAC concentrations of 50.6 g l^{-1} in 29 h and 51.2 g l^{-1} in 21 h respectively. More recently, development of an organic-aqueous two-phase process for PAC production has resulted in increased final PAC concentrations in the organic phase (octanol) to more than 160 g PAC l^{-1} (Rosche et al. 2002b, Sandford 2002).

As the biotransformation for PAC production is a proton consuming process, the pH will rise and eventually results in the irreversible deactivation of PDC (Rosche et al. 2001, 2002a,b). High buffer capacity in the aqueous phase (2.0-2.5 M MOPS, initial pH 6.5) was employed to reduce the pH increase (Rosche et al. 2002a,b, 2003a). In addition, MOPS was found to have a beneficial effect on enhancing PDC stability as were a number of other solutes at high concentrations (e.g. 1 M KCl, 2 M glycerol and 0.75 M sorbitol) (Rosche et al. 2002a). The application of high buffer concentration and additives to stabilise PDC had been proposed also by other authors and are described in Section 1.4.3.4, p. 24.

The aim of the present Chapter is to develop an optimal two-phase biotransformation process with pH control and identify a low cost medium component which can still maintain PDC stability while eliminating the major cost of high concentration MOPS addition.

7.3   RESULTS AND DISCUSSION

7.3.1   Kinetics of PAC production with pH control and 2.5 M MOPS

Previous studies of the PAC biotransformation in a two-phase emulsion system utilised 2.5 M MOPS to stabilise PDC in the aqueous phase and maintain a relatively constant pH during the early stages of the biotransformation (Sandford 2002). However, as the reaction progressed, the pH gradually rose as protons were consumed (see Figure 1.14, p. 22) with the pH reaching 8.5 at the end of the reaction. Under these conditions the residual PDC carboligase activity was 23% initial activity (see Table 7.1).

To determine the effect of pH control, an experiment was set up using similar initial conditions to those described by Rosche et al. (2002b) and Sandford (2002). The time profiles of relative carboligase activity and relevant chemical species for a pH-controlled two-phase biotransformation with 2.5 M MOPS in the aqueous phase are given in Figures 7.1(a)-(b) and the data are summarized in Table 7.1. Final PAC concentrations were 1053 mM (158 g l^{-1}) and 137 mM (20.5 g l^{-1}) in the organic and aqueous phases respectively at 34 h with residual PDC carboligase activity of 84%. This compares with 940 mM PAC (organic phase) and 123 mM PAC (aqueous phase) after 49 h with residual PDC carboligase activity of 23% when the pH was not controlled. Most of the PAC was produced during the first 22 h of biotransformation with an average rate of PAC formation of 51.3 ± 0.2 mM h^{-1} in the organic phase and 6.7 ± 0.5 mM h^{-1} in the aqueous phase over this time period. The formation of by-products was considerably lower in the pH-controlled system, with the acetoin concentration being 14 and 13 mM in the organic and aqueous phases at 81 h respectively and less than 3 mM acetaldehyde in either phase. Oxidation of benzaldehyde to benzoic acid was negligible as indicated by a constant level of benzoic acid being maintained at less than 3 mM in the organic phase and 10 mM in the aqueous phase. This concentration was due to the presence of low concentrations of benzoic acid in the original benzaldehyde.

(a)

(b)
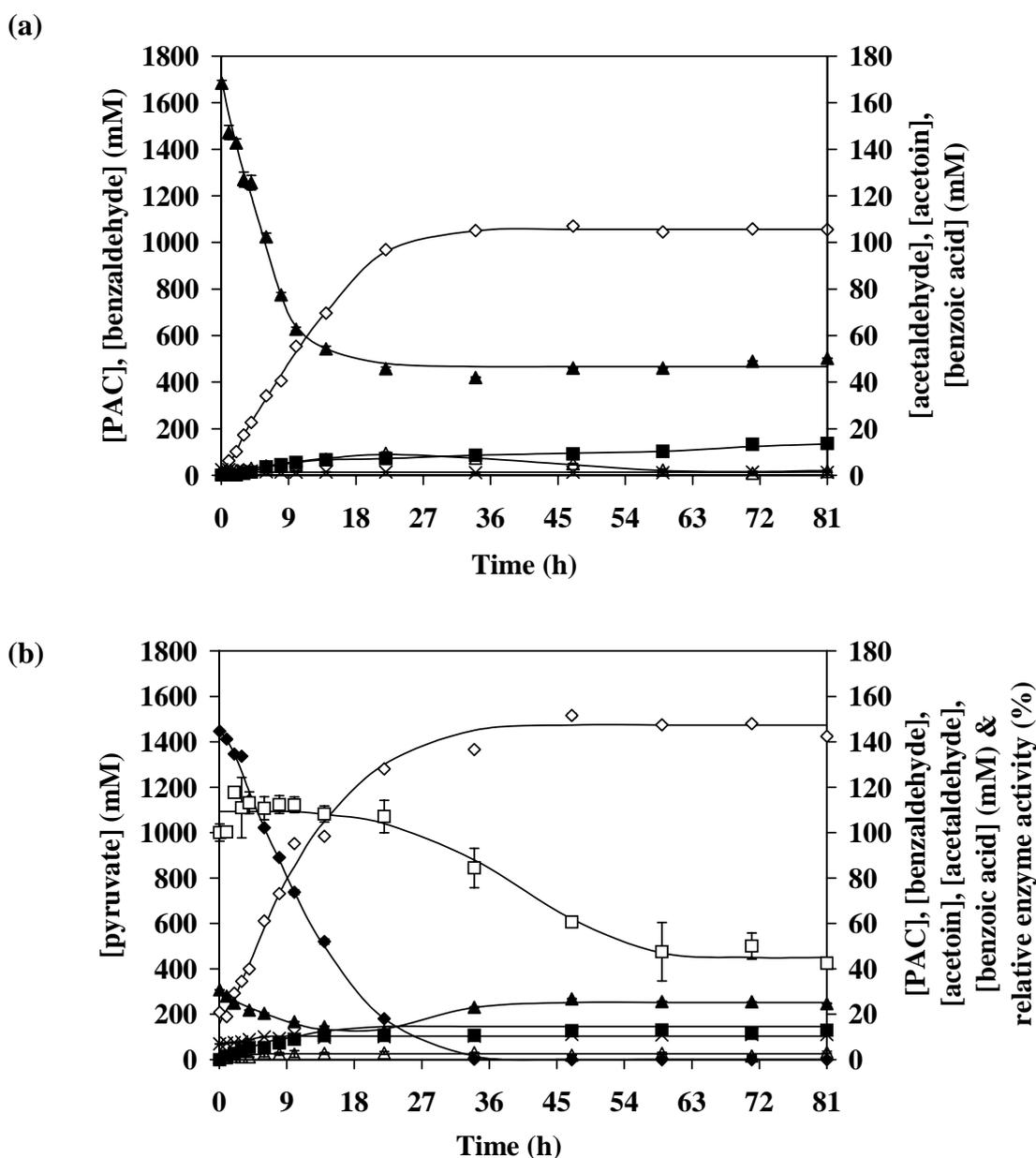
Figure 7.1: Time profiles of relative carboligase activity and chemical species in the (a) organic and (b) aqueous phases for the pH controlled (using 3.6 M acetic acid to maintain pH at 7.0) organic-aqueous two-phase biotransformation system at $4°C$ and stirring speed of 255 rpm. Organic phase contained 1.75 M benzaldehyde in octanol. The aqueous phase contained 2.5 M MOPS, 1 mM TPP, 1 mM $MgSO_4$, 1.48 M pyruvate and 8.80 U carboligase ml^{-1} with initial pH of 6.7. The initial volume used in each phase was 75 ml, (◆) pyruvate, (▲) benzaldehyde, (◇) PAC, (□) enzyme activity, (×) benzoic acid, (△) acetaldehyde and (■) acetoin.

The benefits of implementing pH control in the organic-aqueous two-phase process are clearly illustrated in Table 7.1. These include (1) an approximate 10% increase in final PAC concentrations in both organic and aqueous phases, (2) an approximate 60% increase in specific productivity, $PAC_{spec\ prod}$, (based on initial PDC activity) and in overall volumetric productivity ($PAC_{productivity}$) due to the significant decrease in reaction time, (3) decreased yields of by-products acetaldehyde and acetoin, and (4) a 3.6 fold increase in residual PDC activity (E_{act}) due to maintaining the pH at its optimal activity during the biotransformation. Some substrate losses were evident from the material balance, particularly for pyruvate (13% loss). This phenomenon has been noted previously by Rosche et al. (2002a) and was attributed to possible polymerisation of pyruvate.

7.3.2   Kinetics of PAC production with pH control and decreased MOPS

With constant pH, the requirement for high buffering capacity (2.5 M MOPS) in the aqueous phase becomes unnecessary, and this was decreased to 20 mM MOPS (to maintain some slight buffering capacity) for the following experiment. The time profiles are given in Figure 7.2(a)-(b) and the results are summarized in Table 7.1. It was found that the lowering of MOPS concentration resulted in a major decrease in final PAC concentration as well as in specific and overall volumetric PAC productivities. Yield on pyruvate decreased also due to greatly increased acetoin production (192 mM) in the aqueous phase. Interestingly, the final PDC activity after 81 h was 76%, almost 1.7 fold higher than that for 2.5 M MOPS (pH controlled, 81 h). This is likely to result from the lower level of benzaldehyde partitioning in the aqueous phase at the lower MOPS concentration.

The average benzaldehyde level in the aqueous phase with 2.5 M MOPS was 22.7 mM (Figure 7.1(b)) compared to 13.4 mM for 20 mM MOPS (Figure 7.2(b)). A separate benzaldehyde partitioning study on a range of MOPS concentrations from 20 mM-2.5 M MOPS confirmed that high MOPS concentrations increased benzaldehyde levels in the aqueous phase with 56.6 ± 2.2 mM at 2.5 M compared to 33.9 ± 1.2 mM benzaldehyde at 20 mM (see Appendix F, p. 246).
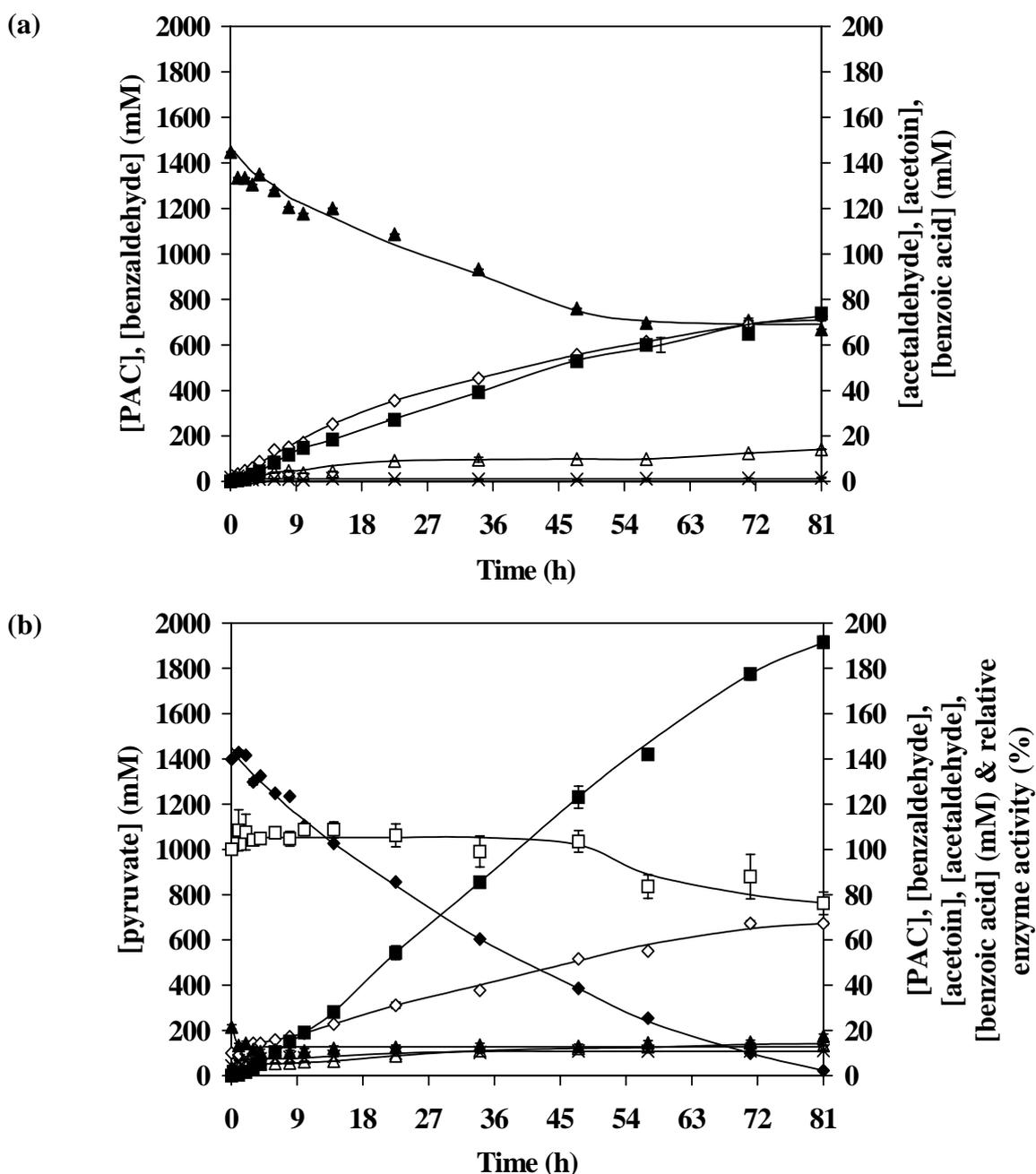
Figure 7.2: Time profiles of relative carboligase activity and chemical species in the (a) organic and (b) aqueous phases for the pH controlled (using 3.6 M acetic acid to maintain pH at 7.0) organic-aqueous two-phase biotransformation system at $4°C$ and stirring speed of 255 rpm. Organic phase contained 1.49 M benzaldehyde in octanol. The aqueous phase contained 20 mM MOPS, 1 mM TPP, 1 mM $MgSO_4$, 1.43 M pyruvate and 6.92 U carboligase ml^{-1} with initial pH of 6.8. The initial volume used in each phase was 75 ml, ($\blacklozenge$) pyruvate, ($\blacktriangle$) benzaldehyde, ($\diamondsuit$) PAC, ($\square$) enzyme activity, ($\times$) benzoic acid, ($\triangle$) acetaldehyde and ($\blacksquare$) acetoin.

From Figure 7.2(b) it might have been expected that the relatively high acetoin production in the aqueous phase (final concentration of 192 mM) would result in appreciable PDC inhibition, as previous studies (Sandford 2002) indicated that 60 mM acetoin caused a 50% inhibition of PDC activity. However this was not evident for the conditions of the present experiment with PDC activity being maintained at 100% for the first 50 h and only declining to 76% initial activity after 81 h. It is possible that the negative effects of acetoin inhibition on PDC stability were counteracted by the lower benzaldehyde concentration as well as the high pyruvate concentration in the biotransformation experiment (Rosche et al. 2004b).

7.3.3 Strategies for enhancing PAC production with pH control and 20 mM MOPS

The benzaldehyde concentration in the aqueous phase may be elevated by either increasing the benzaldehyde concentration in the organic phase or by addition of solvents/solutes to the aqueous phase, as illustrated by previous results with addition of 2.5 M MOPS.

7.3.3.1 Effect of increasing benzaldehyde concentrations in the organic phase

The partitioning of benzaldehyde from the organic to the aqueous phase containing 20 mM MOPS in the two-phase system was investigated by varying the benzaldehyde concentration in octanol from 0 to 8.5 M at 6°C (see Appendix G, p. 247). The benzaldehyde concentration in the aqueous phase was found to be proportional to the initial benzaldehyde concentration in the organic phase up to 7.1 M with a saturated benzaldehyde level of 73 mM in the aqueous phase. To sustain the same level of benzaldehyde in the aqueous phase as a system with 2.5 M MOPS (56.6 mM), the organic phase would need to contain an initial benzaldehyde concentration of at least 4.2 M. However an experiment with 20 mM MOPS using initial 5.5 M benzaldehyde in the organic phase (initial 1.48 M pyruvate in aqueous phase) with pH control resulted in an overall PAC concentration of 27.4 g l^{-1} after 14 h with specific PAC productivity of 0.60 mg U^{-1} h^{-1}. This compared with 59.6 g PAC l^{-1} after 14 h and 0.97 mg U^{-1} h^{-1} with

2.5 M MOPS for the same conditions. The decreasing in specific and overall volumetric productivity presumably resulted from the increased benzaldehyde inhibitory effects on PDC activity at low MOPS.

7.3.3.2   *Effect of solute addition to the aqueous phase*

From the previous results (Figure 7.1(a)-(b)), it was evident that a high concentration of MOPS (at 2.5 M) was important in maintaining PAC productivity and yield (on pyruvate) and that its role was both that of increasing benzaldehyde partitioning into the aqueous phase and enhancing PDC stability. The problem with the use of MOPS at high concentration is that it is very expensive. For this reason, a number of alternative solutes were investigated for both their potential to increase benzaldehyde partitioning and also for maintaining PDC activity under these conditions.

Experiments were carried out with an initial benzaldehyde concentration of 1.5 M in the octanol organic phase and 20 mM MOPS in the aqueous phase at $6°C$. The most successful results from this study are presented in Table 7.2 (see full results in Appendix D, p. 240).

Benzaldehyde partitioning similar to that of 2.5 M MOPS was achieved with addition of DPG (2.5 M), urea (26% (w/v)) or PEG-6000 (30% (w/v)). DPG was chosen for the subsequent kinetic study of PAC production using pH control because both urea and PEG-6000 resulted in significantly decreased PAC formation (see Appendix I, p. 249).

The specific PAC production profiles during the first 14 h at $4°C$ for the pH-controlled two-phase system containing 20 mM MOPS in the absence and presence of 2.5 M DPG are shown in Figure 7.3 together with data for 2.5 M MOPS. The results with 2.5 M MOPS and 2.5 M DPG were almost identical over the first 10 h, indicating that DPG may be a suitable low cost replacement for MOPS in the biotransformation reaction mixture (see Appendix H, p. 248 for another experimental confirmation with initial rate studies).

According to Fagain (1997), the presence of a number of compounds with concentrations of 1 M or higher can have a positive effect on stabilizing solubilized proteins. The high concentration of DPG is likely to achieve this by decreasing the water activity in the aqueous phase in the same manner as glycerol addition used in many processes for enzyme stabilization (Scopes 1994). Glycerol was not found to be suitable in the present study. Its addition (2 M glycerol) did not enhance the benzaldehyde partitioning (Table 7.2).
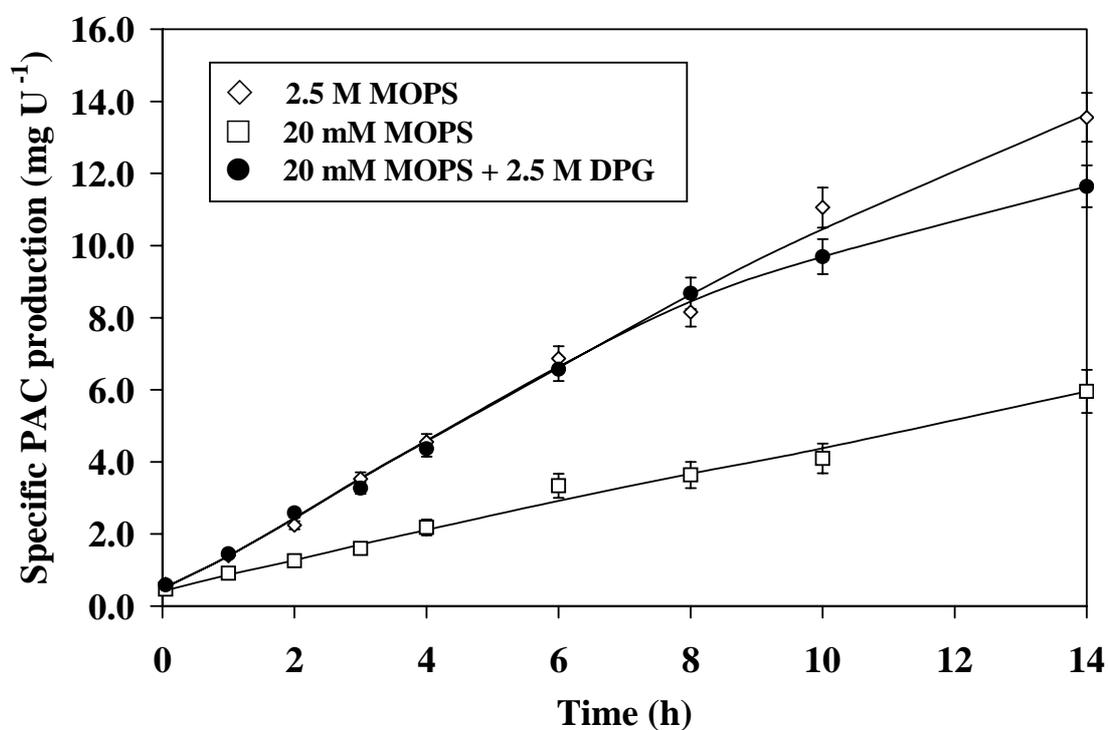
Figure 7.3: Time profiles of specific PAC production (mg PAC U^{-1} carboligase activity) of various pH controlled organic-aqueous two-phase systems in the first 14 h at 4°C, 255 rpm and pH 7.0.

7.3.4 Kinetics of PAC production with pH control and 20 mM MOPS, 2.5 M DPG

The kinetic profiles for the two-phase system containing 20 mM MOPS and 2.5 M DPG in the aqueous phase are shown in Figure 7.4 and the summarized results are included in Table 7.1 for comparison with the other systems. From a comparison of the data for 2.5 M DPG with that of 2.5 M MOPS it is evident that: (1) final PAC concentrations in both phases are similar, although about a 25% reduction in specific PAC productivity and overall volumetric productivity has occurred with 2.5 M DPG, presumably due to the less protective effect of DPG on the enzyme compared to 2.5 M MOPS, (2) the less protective effect of DPG is evident also from the decreased PDC activity at the end of the biotransformation although 74% activity still remains after 47 h, (3) the concentrations of by-products acetaldehyde and acetoin are of similar magnitude with final yields of PAC based on pyruvate utilized ($Y_{P/Pyr}$) virtually the same. The mass balance on benzaldehyde is excellent although again there is some loss of pyruvate (about 10%). The main advantage of the former system is that 2.5 M MOPS addition at \$AUD 1.21 g^{-1} has been replaced by 2.5 M DPG at the much lower \$AUD 0.09 g^{-1} PAC.
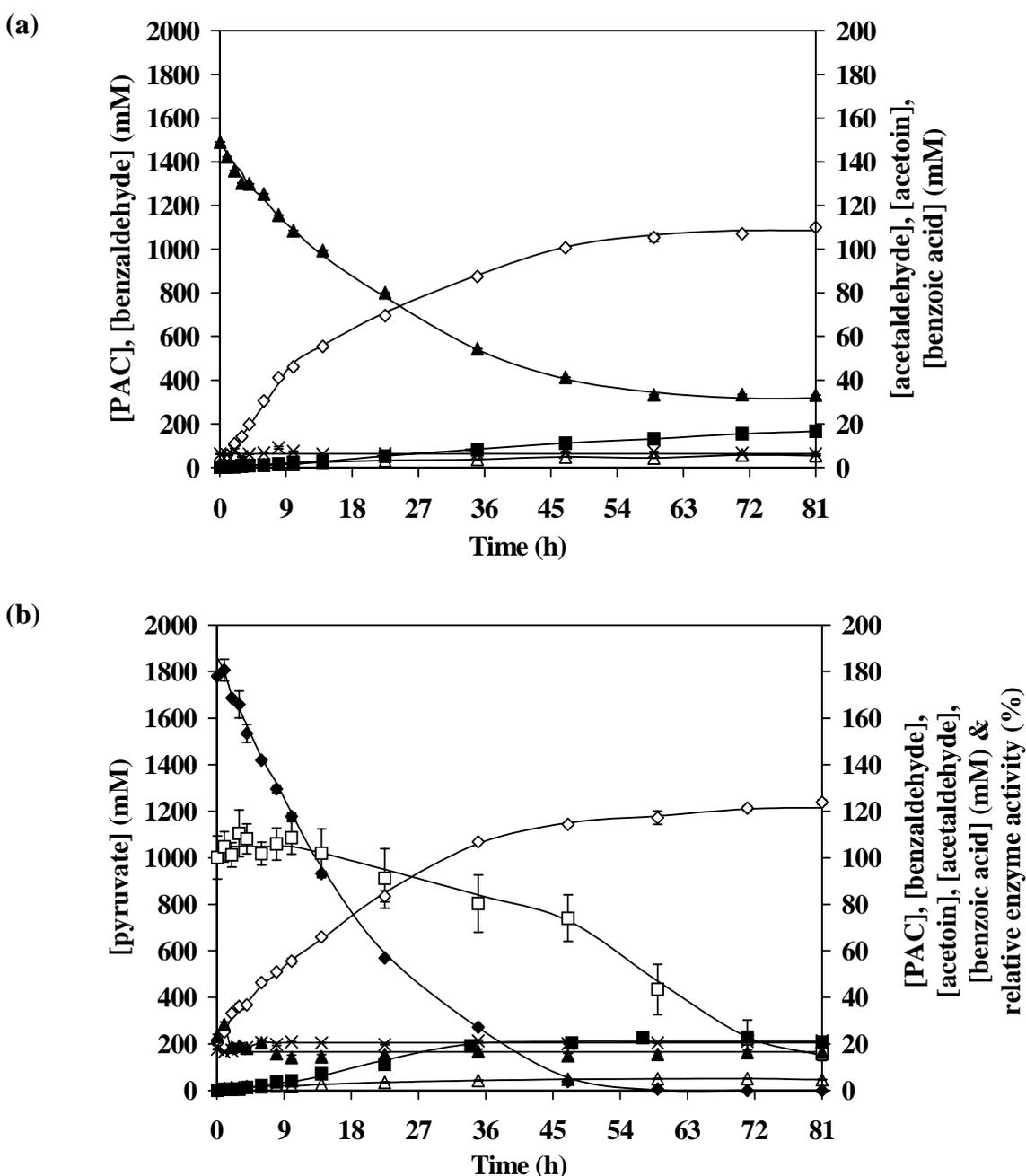
Figure 7.4: Time profiles of relative carboligase activity and chemical species in the (a) organic and (b) aqueous phases for the pH controlled (using 3.6 M acetic acid to maintain pH at 7.0) organic-aqueous two-phase biotransformation system at $4°C$ and stirring speed of 255 rpm. Organic phase contained 1.55 M benzaldehyde in octanol. The aqueous phase contained 20 mM MOPS, 2.5 M DPG, 1 mM TPP, 1 mM MgSO$_4$, 1.83 M pyruvate and 10.0 U ml^{-1} carboligase activity with initial pH of 7.0. The initial volume used in each phase was 75 ml, ($\blacklozenge$) pyruvate, ($\blacktriangle$) benzaldehyde, ($\Diamond$) PAC, ($\square$) enzyme activity, ($\times$) benzoic acid, ($\triangle$) acetaldehyde and ($\blacksquare$) acetoin.

Cost effective development of two-phase biotransformation for PAC production

Table 7.1: Comparison of PAC production in stirred emulsion two-phase systems without pH control (a) and controlled pH at 7.0 (b)-(d) using 3.6 M acetic acid. The details description of each variable measured is given in Section 7.1, Nomenclature, p.171.

Variables	No pH control[*] 2.5 M MOPS (a)	Controlled pH at 7.0 with 3.6 M acetic acid		
		2.5 M MOPS (b), Figure 7.1	20 mM MOPS (c), Figure 7.2	20 mM MOPS + 2.5 M DPG (d), Figure 7.4
t (h)	49	34	81	47
PAC_{aq} (g l^{-1})	18.5	20.5	10.1	17.2
PAC_{or} (g l^{-1})	141	158	109	151
V_{aq}:V_{or} (l l^{-1})	1:1	1:1	1:1	0.88:1.12
PAC_{tot} (g l^{-1})	79.8	89.3	59.6	92.1
E_{ini} (U ml^{-1})	8.50	8.80	6.92	10.0
E_{act} (%)	23	84	76	74
PAC_{spec} (mg U^{-1} initial carboligase activity)	18.8	20.3	17.2	20.9
$PAC_{spec\ prod}$ (mg U^{-1} h^{-1})	0.38	0.60	0.21	0.45
$PAC_{productivity}$ (g l^{-1} day^{-1})	39.1	63.0	17.7	47.0
$PAC_{max\ rate}$ (mM h^{-1})	47.7	58.0	24.4	48.9
Cost ($AUD g^{-1})[#]	1.35	1.21	0.01	0.09
$Y_{P/BZ}$ (mol mol^{-1})	0.90	0.98	0.99	0.99
$Y_{P/Pyr}$ (mol mol^{-1})	0.73	0.82	0.56	0.84
$Y_{Q/Pyr}$ (mol mol^{-1})	3.1×10^{-2}	8.4×10^{-3}	2.4×10^{-2}	6.8×10^{-3}
$Y_{R/Pyr}$ (mol mol^{-1})	6.2×10^{-2}	2.0×10^{-2}	0.19	2.4×10^{-2}
Pyr_{bal} (%)	89	87	96	90
Bz_{bal} (%)	90	98	99	99

[*]   Rosche et al. (2002b), Sandford (2002)

[#]   Australian dollars spent on buffering and chemical additives per g PAC produced

Note: Details of calculations of this Table are given in Appendix E, p. 242.

Table 7.2: Comparison of benzaldehyde partitioning in an aqueous phase for various types of organic-aqueous two-phase biotransformation systems.

Compositions of aqueous phase	Benzaldehyde partitioning in aqueous phase (mM)
2.5 M MOPS	56.6
20 mM MOPS, 1 M $(NH_4)_2SO_4$	14.9
20 mM MOPS, 1 M KCl	27.5
20 mM MOPS	33.9
20 mM MOPS, 2 M ethanol	35.1
20 mM MOPS, 2 M glycerol	35.8
20 mM MOPS, 30% (w/v) PEG-6000	53.2
20 mM MOPS, 2.5 M DPG	54.2
20 mM MOPS, 26% (w/v) urea	63.2

7.4   CONCLUSIONS

The two-phase PAC biotransformation process has been further developed using pH control and addition of 2.5 M DPG to replace 2.5 M MOPS in the more expensive and highly buffered system. By comparison with this system in the absence of pH control, improved final PAC concentrations (15%), productivities (20%) and pyruvate yield (approx. 15%) was achieved for the lower cost process.

Chapter **8**

Overall Conclusions and Future Work

8.1 MODELLING OF ENZYMATIC PAC PRODUCTION BASED ON REACTION MECHANISMS

A mathematical model for the enzymatic biotransformation of benzaldehyde and pyruvate to *R*-phenylacetylcarbinol (PAC) and its associated by-products has been developed using a schematic method devised by King and Altman (1956) for deriving the rate equations for a complete enzyme-catalysed reaction. PAC is the commercial intermediate for the production of ephedrine and pseudoephedrine. A combinatorial theorem was applied using Visual Basic to create all of the possible reaction patterns for a simplified form of the pyruvate decarboxylase (PDC) biotransformation mechanism. The rate equations for substrates, product, and by-products have been derived from the patterns for yeast PDC and combined with a deactivation model for PDC from *Candida utilis*.

8.2 CHARACTERISTICS OF PDC FROM FUNGAL AND YEAST SOURCES

With the objective of developing an optimized enzymatic process for the pharmaceutical intermediate PAC, the production of PDC by a strain of *R. javanicus* was studied in 5 and 30 l bioreactors. A maximum specific decarboxylase activity of 328 U g^{-1} mycelium was achieved when aeration/agitation were reduced in the later stages of cultivation. The morphology of *R. javanicus* was found to be influenced by the degree of aeration/agitation with heterogeneous clump formation at high aeration/agitation conditions and homogeneous dispersed mycelia at low levels. The stabilities of partially purified PDC and crude extract preparations were evaluated by enzyme deactivation kinetics which followed a conventional first order exponential decay profile after an initial lag phase. The initial enzyme activity had no effect on stability of crude extract PDC in the region of 7-27 U decarboxylase ml^{-1}. Although the crude extract enzyme preparation had a higher protease activity than the partially purified PDC, it was found to be more stable both in the presence or absence of 50 mM benzaldehyde. By comparison, a crude extract preparation of *C. utilis* PDC was found to be much more stable than the PDC from *R. javanicus* under similar conditions.

8.3   DEACTIVATION KINETICS OF *C. UTILIS* PDC BY BENZALDEHYDE

Based on experimental data, a kinetic model for the deactivation of partially purified PDC by benzaldehyde (0–200 mM) in 2.5 M MOPS buffer has been developed. An initial lag period prior to deactivation was found to occur. With first order dependencies of PDC deactivation on exposure time and on benzaldehyde concentration, a reaction time deactivation constant of 2.64×10^{-3} h^{-1} and a benzaldehyde deactivation coefficient of 1.98×10^{-4} mM^{-1}h^{-1} were determined for benzaldehyde concentrations up to 200 mM. The PDC deactivation kinetic equation established (Equation (8.1)) is an essential component in an overall model being developed to describe the enzymatic biotransformation of benzaldehyde and pyruvate to produce PAC.

$$\left. \frac{dE}{dt} \right|_i = \begin{cases} 0 & ; \quad t \leq t_{lag} \\ -\left(k_{d1} + k_{d2}.b\right)E_i & ; \quad t > t_{lag} \end{cases} \qquad (8.1)$$

8.4   MODEL DEVELOPMENT AND VALIDATION

Initial rate and biotransformation studies were applied to refine and validate a mathematical model for enzymatic PAC production from pyruvate and benzaldehyde using *C. utilis* PDC. The rate of PAC formation was directly proportional to the enzyme activity level up to 5.0 U carboligase ml^{-1}. Michaelis-Menten kinetics was determined for the effect of pyruvate concentration on the reaction rate. The effect of benzaldehyde followed the sigmoidal shape of the Monod-Wyman-Changeux (MWC) model. The biotransformation model, which also included Equation (8.1) for PDC inactivation by benzaldehyde, was used to determine the overall rate constants for the formation of PAC, acetaldehyde and acetoin. These values were determined from data for three batch biotransformations performed over a range of initial concentrations (viz 50-150 mM benzaldehyde, 60-180 mM pyruvate, 1.1-3.4 U carboligase ml^{-1}). The finalised model was then used to predict a batch biotransformation profile at 120/100 mM initial pyruvate/benzaldehyde (initial enzyme activity 3.0 U carboligase ml^{-1}). The simulated kinetics gave acceptable fitting ($R^2 = 0.9963$) to the time courses of these latter

experimental data for substrates pyruvate and benzaldehyde, product PAC, by-products acetaldehyde and acetoin as well as enzyme activity level. The batch biotransformation profile generated by the model validated previously for a data set at initial substrate concentrations 50-150 mM benzaldehyde and 60-180 mM pyruvate, provided an acceptable fit for published data at initial concentrations of 400 mM benzaldehyde and 600 mM pyruvate.

8.5 COST EFFECTIVE DEVELOPMENT OF TWO-PHASE BIOTRANSFORMATION FOR PAC PRODUCTION

An organic-aqueous two-phase process for production of PAC has been developed further through optimal pH control and addition of a low cost solute to maintain PDC activity in the aqueous phase. The specific rate of PAC production in the pH controlled system (pH = 7.0) with 2.5 M MOPS was 0.60 mg U^{-1} h^{-1} (reaction completed at 34 h), a 1.6 times improvement over the same system without pH control (0.38 mg U^{-1} h^{-1} at 49 h). An improved stability of PDC was evident at the end of biotransformation for the pH controlled system with 84% residual carboligase activity, while 23% of enzyme activity remained in the absence of pH control. The positive effect of maintaining a constant pH during two-phase biotransformation included also a higher yield of PAC for pyruvate consumed of 0.82 mol mol^{-1}. This compared to 0.73 mol mol^{-1} when the pH control was not applied due to increased production of by products acetaldehyde and acetoin in the latter case.

Screening for a lower cost solute to replace the expensive 2.5 M MOPS identified dipropylene glycol (DPG) as a suitable candidate. The addition of 2.5 M DPG to the reaction mixture containing 20 mM MOPS increased benzaldehyde partitioning in the aqueous phase from a concentration of 33.9 to 54.2 mM. Subsequent biotransformation with 20 mM MOPS and 2.5 M DPG resulted in a similar level of PAC production (151 g l^{-1} in the organic phase and 17.2 g l^{-1} in the aqueous phase after 47 h) to that with 2.5 M MOPS (158 g l^{-1} in the organic phase and 20.5 g l^{-1} in the aqueous phase after 34 h). However the specific PAC productivity was higher in the latter system presumably due to the greater PDC protective effect of MOPS.

8.6 RECOMMENDED FUTURE WORK

Future research following from the present study could include:

8.6.1 Enzyme stabilization

- enzyme immobilization or cross-linking to further enhance the stability of *C. utilis* PDC in the presence of benzaldehyde while maintaining PAC productivity,

- identification of other key factors influencing PDC deactivation in the two-phase system such as agitation rate, presence of soluble octanol and benzaldehyde in the aqueous phase, interfacial area between the organic and aqueous phases as well as enzyme concentration.

8.6.2 Optimal environmental conditions

- investigation of temperature effect in the range of $6\text{-}30^{\circ}\text{C}$ on PAC production and by-products formation for the two-phase system to identify optimal temperature conditions,

- enhancement of PDC production by varying culture conditions such as replacement of complex media with minimal media and manipulation of pH. An improved PDC production process (e.g. fed-batch, optimal environmental control) might be simpler than the current method of RQ control.

8.6.3 Process development

- investigation of the use of resting whole cells in biotransformation to avoid the cost relating to enzyme purification,

- development of a continuous enzyme membrane reactor for the continuous removal of PAC and by-products (acetaldehyde and acetoin) in the aqueous phase of the organic-aqueous two-phase biotransformation, in order to maximize PAC production and productivity,

- sourcing of a cheaper pyruvate, for example, a commercial pyruvate producer, *C. glabrata* or a recombinant *E. coli*, where concentrations of more than 50 g l^{-1} are now reported,

- investigation of PDC characteristics from other yeast sources such as *S. cerevisiae*, *C. tropicalis* and *Kluyvermyces marxianus*, in order to select a system with higher PDC stability and less by-product(s) formation while maintaining similar levels of PAC production and productivity during biotransformation to that of *C. utilis*. This would be important if by-products such as acetoin cause major problems in PAC separation and purification.

8.6.4   Further modelling/optimization

- extension of mathematical modelling developed in this thesis to describe two-phase biotransformation profiles and design optimal substrates feeding strategies to maximize PAC production,

- enhancement of PAC production in a single-phase biotransformation process by designing optimal feeding of pyruvate and/or benzaldehyde, based on simulation results from the present modelling studies.

8.6.5   Economic analysis

- economic evaluation of the two-phase biotransformation process including the fully-stirred and phase-separated systems, in order to identify a more cost effective system.

As shown in Chapter 1, Section 1.4.4, p. 27, the enzymatic two-phase PAC biotransformation has many advantages over the traditional baker's yeast fermentation process used by industry, and the further modelling and optimization of this process will only further enhance its commercial potential. A patent application on this two-phase process has been filed (Hauer et al. 2003) and the two-phase strategy is likely to have application to a number of other enzyme-based processes for fine chemicals and pharmaceuticals.

References

Agarwal, S.C., Basu, S.K., Vora, V.C., Mason, J.R. and Pirt, S.J. (1987). Studies on the production of *L*-acetylphenylcarbinol by yeast employing benzaldehyde as precursor. Biotechnology and Bioengineering 29: 783-785.

AHRQ (Agency for Healthcare Research and Quality). (2003). Ephedra and ephedrine for weight loss and athletic performance enhancement: clinical efficacy and side effects. Evidence Report/Technology Assessment No 76, pp. 3-4.

Alvarez, F.J., Ermer, J., Hubner, G., Schellenberger, A. and Schowen, R.L. (1991). Catalytic power of pyruvate decarboxylase. Rate-limiting events and microscopic rate constants from primary carbon and secondary hydrogen isotope effects. Journal of the American Chemical Society 113: 8402-8409.

Arjunan, P., Umland, T., Dyda, F., Swaminathan, S., Furey, W., Sax, M., Farrenkopf, B., Gao, Y., Zhang, D. and Jordan, F. (1996). Crystal structure of the thiamin diphosphate-dependent enzyme pyruvate decarboxylase from the yeast *Saccharomyces cerevisiae* at 2.3 A resolution. Journal of Molecular Biology 256: 590-600.

Astrup, A., Breum, L., Toubro, S., Hein, P. and Quaade, F. (1992a). The effect and safety of an ephedrine-caffeine compound compared to ephedrine, caffeine and placebo in obese objects on an energy restricted diet: a double blind trial. International Journal of Obesity 16: 269-277.

Astrup, A., Buemann, B., Christensen, N.J., Toubro, S., Thoebek, G., Victor, O.J. and Quaade, F. (1992b). The effect of ephedrine/caffeine mixture on energy expenditure and body composition in obese women. Metabolism 41: 686-688.

Astrup, A., Breum, L. and Toubro, S. (1995). Pharmacological and clinical studies of ephedrine and other thermogenic agonists. Obesity Research 3: 537S-540S.

References

Atlas, R.M. (1988). Microbiology: Fundamentals and Applications, 2nd edn. Macmillan Publishing: New York, pp. 102-103.

Baburina, I, Gao, Y., Hu, Z., Jordan, F., Hohmann, S. and Furey, W. (1994). Substrate activation of brewer's yeast pyruvate decarboxylase is abolished by mutation of cysteine 221 to serine. Biochemistry 33: 5630-5635.

Bailey, J.E. and Ollis, D.F. (1986). Biochemical Engineering Fundamentals, 2nd edn. McGraw-Hill: Singapore, pp. 136-137, 661-664.

Ballesteros, A., Bornscheuer, U., Capewell, A., Combes, D., Condoret, J.S., Koenig, K., Kolisis, F.N., Marty, A., Menge, U., Scheper, T., Stamatis, H. and Xenakis, A. (1995). Enzymes in non-conventional phases. Biocatalysis and Biotransformation 13: 1-42.

BASF. (2004). (Accessed 22nd April 2004).
http://www.basf.com/pharma/0105.htm

Bates, D.M. and Watts, D.G. (1988). Nonlinear regression analysis and its applications. John Wiley and Sons: New York, pp. 52-78.

Becvarova, H., Hane, O. and Macek, K. (1963). Course of transformation of benzaldehyde by *Saccharomyces cerevisiae*. Folia Microbiologica 8: 165-169.

Bernt, E. and Bergmeyer, H.U. (1974). Acetaldehyde: determination with alcohol dehydrogenase from yeast. In: *Methods of enzymatic analysis, Vol. 3, 2nd edn* (H.U. Bergmeyer, ed.) Academic Press: New York, pp. 1506-1509.

Bergmeyer, H.U. and Grabl, M. (1983). Pyruvate decarboxylase from yeast. In: *Methods of enzymatic analysis, Vol. 2, 3rd edn* (H.U. Bergmeyer, J. Bergmeyer, M. Grabl, eds.) Verlag Chemie: Florida, pp. 302-303.

Beschkov, V. and Velizarov, S. (2000). Dynamic modelling of aerobic bioprocesses in gel particles with immobilised cells: Part 1: Growth associated biotransformation. Bioprocess Engineering 22: 233-241.

References

Betancor, L., Lopez-Gallego, F., Hidalgo, A., Alonso-Morales, N., Fuentes, M., Fernandez-Lafuente, R. and Guisan, J.M. (2004). Prevention of interfacial inactivation of enzymes by coating the enzyme surface with dextran-aldehyde. Journal of Biotechnology 110: 201-207.

Boesten, W.H.J., Moody, H.M. and Roos, E.C. (1996). Process for the recovery of ampicillin from enzymatic acylation of 6-aminopenicillanic acid (Chemferm; patent no. WO. 9630376; The Netherlands).

Boiteux, A. and Hess, B. (1970). Allosteric properties of yeast pyruvate decarboxylase. FEBS Letters 9: 293-296.

Boonmee, M., Leksawasdi, N., Bridge, W. and Rogers, P.L. (2003). Batch and continuous culture of Lactococcus lactis NZ133: experimental data and model development. Biochemical Engineering Journal 14: 127-135.

Breslow, R. (1957). Rapid deuterium exchange in thiazolium salts. Journal of the American Chemical Society 79: 1762-1763.

Breslow, R. (1958). On the mechanism of thiamine action. IV. Evidence from studies on model systems. Journal of the American Chemical Society 80: 3719-3726.

Breslow, R. and McNelis, E. (1959). Studies on model systems for thiamine action. Synthesis of reactive intermediates and evidence on the function of the pyrimidine ring. Journal of the American Chemical Society 81: 3080-3082.

Breuer, M. and Hauer, B. (2003). Carbon-carbon coupling in biotransformation. Current Opinion in Biotechnology 14: 570-576.

Breuer, M., Hauer, B. and Friedrich, T. (2003). Novel pyruvate decarboxylase, production and use thereof. Patent Application No: WO 03/020921 A2.

Breuer, M., Hauer, B., Mesch, K., Goetz, G., Pohl, M. and Kula, M-R. (1997). Method for producing enatiomer-free phenylacetylcarbinols from acetaldehyde and

benzaldehyde in the presence of pyruvate decarboxylase from *Zymomonas*. German Patent 19 736 104 A1.

Breuer, M., Pohl, M., Hauer, B. and Lingen, B. (2002). High-throughput assay of (*R*)-phenylacetylcarbinol synthesized by pyruvate decarboxylase. Analytical and Bioanalytical Chemistry 374: 1069-1073.

Bringer-Meyer, S. and Sahm, H. (1988). Acetoin and phenylacetylcarbinol formation by the pyruvate decarboxylases of *Zymomonas mobilis* and *Saccharomyces carlsbergensis*. Biocatalysis 1: 321-331.

Bringer-Meyer, S., Schimz, K.-L. and Sahm, H. (1986). Pyruvate decarboxylase from *Zymomonas mobilis* isolation and partial characterization. Archives of Microbiology 146: 105-110.

Bruhn, H., Pohl, M., Grotzinger, J. and Kula, M-R. (1995). The replacement of Trp392 by alanine influences the decarboxylase/carboligase activity and stability of pyruvate decarboxylase from *Zymomonas mobilis*. European Journal of Biochemistry 234: 650-655.

Burton, S.G., Cowan, D.A. and Woodley, J.M. (2002). The search for the ideal biocatalyst. Nature Biotechnology 20: 37-44.

Byrne, G.S. and Ward, O.P. (1989). Effect of nutrition on pellet formation by *Rhizopus arrhizus*. Biotechnology and Bioengineering 33: 912-914.

Cao, X.J., Wu, X.Y., Fonseca, L.J., Cabral, J.M. and Marcos, J.C. (2004). Production of 6-aminopenicillanic acid in aqueous two-phase systems by recombinant *Escherichia coli* with intracellular penicillin acylase. Biotechnology Letters 26: 97-101.

Cardillo, R., Servi, S. and Tinti, C. (1991). Biotransformation of unsaturated aldehydes by microorganisms with pyruvate decarboxylase activity. Applied Microbiology and Biotechnology 36: 300-303.

Castro, G.R. and Knubovets, T. (2003). Homogeneous biocatalysis in organic solvents and water-organic mixtures. Critical Reviews in Biotechnology 23: 195-231.

Cha, S. (1968). A simple method for derivation of rate equations for enzyme-catalysed reactions under the rapid equilibrium assumption or combined assumptions of equilibrium and steady state. Journal of Biological Chemistry 243: 820-825.

Changeux, J.-P., Gerhart, J.C. and Schachman, H.K. (1968). Allosteric interactions in aspartate transcarbamylase. I. Binding of specific ligands to the native enzyme and its isolated subunits. Biochemistry 7: 531-538.

Chen, G.C. and Jordan, F. (1984). Brewers' yeast pyruvate decarboxylase produces acetoin from acetaldehyde: a novel tool to study the mechanism of steps subsequent to carbon dioxide loss. Biochemistry 23: 3576-3582.

Chen, K.K. and Schmidt, C.F. (1930). Ephedrine and related substances. Medicine 9: 1-117.

Chen, K.K., Wu, C-K. and Henrikesen, E. (1929). Relationship between the pharmacological action and the chemical constitution and configuration of the optical isomers of ephedrine and related compounds. Journal of Pharmacology and Experimental Therapeutics 36: 363-400.

Chen, S.-T., Sookkheo, B., Phutrahul, S. and Wang, K.-T. (2001). Enzymes in nonaqueous solvents. In: *Methods in Biotechnology. Vol 15: Enzymes in nonaqueous solvents: Methods and Protocols* (E.N. Vulfson, P.J. Halling, H.L. Holland, eds.) Humana Press: New Jersey, p. 373.

Cherry, J.R. and Fidantsef, A.L. (2003). Directed evolution of industrial enzymes: an update. Current Opinion in Biotechnology 14: 438-443.

Chow, Y.S., Shin, H.S., Adesina, A.A. and Rogers, P.L. (1995). A kinetic model for the deactivation of pyruvate decarboxylase (PDC) by benzaldehyde. Biotechnology Letters 17: 1201-1206.

References

Chow, Y.Y.S. (1998). Modelling of biotransformation kinetics for *L*-phenylacetylcarbinol (*L*-PAC) production from pyruvate and benzaldehyde by pyruvate decarboxylase from *Candida utilis*. Department of Biotechnology. Sydney, University of New South Wales, Ph.D. Thesis.

Cornish-Bowden, A. (1995). Fundamentals of enzyme kinetics, revised edn. Portland Press: London, pp. 21-22, 73-92.

Crout, D.H., Dalton, H., Hutchinson, D.W. and Miyagoshi, M. (1991). Studies on pyruvate decarboxylase acyloin formation from aliphatic aromatic and heterocyclic aldehydes. Journal of the Chemical Society. Perkin Transactions 1: 1329-1334.

Cui, Y.Q., van der Lans, R.G.J.M. and Luyben, K.C.A.M. (1997). Effect of agitation intensities on fungal morphology of submerged fermentation. Biotechnology and Bioengineering 55: 715-726.

Culic, K., Ulbrecht, S., Vojtisek, V. and Vodnansky, M. (1984). Method of the cost reduction in the production of *D*-(-)-1-phenyl-1-hydroxy-2-propane for the preparation of *L*-(-)-ephedrine. Czech 22941 (Cl. C07C 49/24).

Czok, R. and Lamprecht, W. (1974). Pyruvate, phosphoenolpyruvate and *D*-glycerate-2-phosphate. In: *Methods of enzymatic analysis, Vol. 3, 2nd edn* (H.U. Bergmeyer, ed.) Academic Press: New York, pp. 1446-1451.

d'Anjou, M.C. and Daugulis, A.J. (2000). Mixed-feed exponential feeding for fed-batch culture of recombinant methylotrophic yeast. Biotechnology Letters 22: 341-346.

Da Cruz Francisco, J. and Szwajcer Dey, E. (2003). Supercritical fluids as alternative, safe, food-processing media: an overview. Acta Microbiologica Polonica 52: 35-43.

de Carvalho, C.C.C.R., Cruz, A., Angelova, B., Fernandes, P., Pons, M.N., Pinheiro, H.M., Cabral, J.M.S. and de Fonseca, M.M.R. (2004). Behaviour of *Mycobacterium* sp. NRRL B-3805 whole cells in aqueous, organic-aqueous and

organic media studied by fluorescence microscopy. Applied Microbiology and Biotechnology 64: 695-701.

de Carvalho, C.M.L. and Cabral, J.M.S. (2000). Reverse micelles as reaction media for lipases. Biochimie 82: 1063-1085.

Dion, W.M., Carilli, A., Sermonti, G. and Chain, E.B. (1954). The effect of mechanical agitation on the morphology of *Penicillium chrysogenum (Thom)* in stirred fermenters. Rendiconti 1st Superiore Sanita Pubblica 17: 187.

Dissara, Y. (1996). Evaluation of mutants of *Candida utilis* for *L*-PAC production from benzaldehyde. Department of Biotechnology. Sydney, University of New South Wales, Ph.D. Thesis.

Du, L.X., Jia, S.J. and Lu, F.P. (2003). Morphological changes of *Rhizopus chinesis* 12 in submerged culture and its relationship with antibiotic production. Process Biochemistry 38: 1643-1646.

Dyda, F., Furey, W., Swaminathan, S., Sax, M., Farrenkopf, B. and Jordan, F. (1993). Catalytic centres in the thiamin diphosphate dependent enzyme pyruvate decarboxylase at 2.4 A resolution. Biochemistry 32: 6165-6170.

Engel, S., Vyazmensky, M., Geresh, S., Barak, Z. and Chipman, D.M. (2003). Acetohydroxyacid synthase: A new enzyme for chiral synthesis of *R*-phenylacetylcarbinol. Biotechnology and Bioengineering 83: 833-840.

Elvers, B., Hawkins, S. and Schulz, G. (Eds.) (1990). Ullmann's Encyclopedia of Industrial Chemistry, Vol A16: Magnetic Materials to Mutagenic Agents, 5th edn. VCH: Germany, pp. 543-550.

Fagain, C.O. (1997). Stabilizing protein function. Springer: New York, p. 69.

Farrenkopf, B.C. and Jordan, F. (1992). Resolution of brewer's yeast pyruvate decarboxylase into multiple isoforms with similar subunit structure and activity

using high-performance liquid chromatography. Protein Expression and Purification 3: 101-107.

FDA. (2003a). (Accessed 22nd April 2004).

http://www.fda.gov/oc/initiatives/ephedra/december2003/

FDA. (2003b). (Accessed 22nd April 2004).

http://www.hhs.gov/news/press/2003pres/20031230.html

Flatau, S., Fischer, G., Kleinpeter, E. and Schellenberger, A. (1988). 31P NMR investigations on free and enzyme bound thiamine pyrophosphate. FEBS Letters 233: 379-382.

Fontes, N., Almeida, M.C., Garcia, S., Peres, C., Partridge, J., Halling, P.J. and Barreiros, S. (2001). Supercritical fluids are superior media for catalysis by cross-linked enzyme microcrystals of *Subtilisin Carlsberg*. Biotechnology Progress 17: 355-358.

Furey, W., Arjunan, P., Chen, L., Sax, M., Guo, F. and Jordan, F. (1998). Structure-function relationships and flexible tetramer assembly in pyruvate decarboxylase revealed by analysis of crystal structures. Biochimica et Biophysica Acta 1385: 253-270.

Ghorbel, B., Sellami-Kamoun, A. and Nasri, M. (2003). Stability studies of protease from *Bacillus cereus* BG1. Enzyme and Microbial Technology 32: 513-518.

Gierhart, D.L. and Potter, N.N. (1979). Effects of RNA removal methods on proteolytic activity and protein solubility in *Candida utilis*. Biotechnology and Bioengineering 21: 1963-1980.

Giri, A., Dhingra, V., Giri, C.C., Singh, A., Ward, O.P. and Narasu, M.L. (2001). Biotransformations using plant cells, organ cultures and enzyme systems: current trends and future prospects. Biotechnology Advances 19: 175-199.

Goetz, G., Iwan, P., Hauer, B., Breuer, M. and Pohl, M. (2001). Continuous production of (*R*)-phenylacetylcarbinol in an enzyme-membrane reactor using a potent mutant of pyruvate decarboxylase from *Zymomonas mobilis*. Biotechnology and Bioengineering 74: 317–325.

Gornall, A.G., Bardawill, C.J. and David, M.M. (1949). Determination of serum proteins by means of the biuret reaction. Journal of Biological Chemistry 177: 751-766.

Groger, G., Schmauder, H.P. and Mothes, K. (1966). Untersuchung uber die gewinnung von *L*-phenylacetylcarbinol. Zeitschrift fur Allgemeine Mikrobiologie 6: 275-287.

Gruber, M. and Wassenaar, J.S. (1960). Inhibition of yeast carboxylase by acetaldehyde. Biochimica et Biophysica Acta 38: 355-357.

Halling, H.L. (2001). Control of enzyme activity in nonaqueous solvents. In: *Methods in Biotechnology. Vol 15: Enzymes in nonaqueous solvents: Methods and Protocols* (E.N. Vulfson, P.J. Halling, H.L. Holland, eds.) Humana Press: New Jersey, p. 1.

Han, K. and Levenspiel, O. (1988). Extended Monod kinetics for substrate, product and cell inhibition. Biotechnology and Bioengineering 32: 430-437.

Hanc, O. and Karac, B. (1956). Yeast carboxylase and formation of phenyl acetyl carbinol. Naturwissenschaft 43: 498.

Hari Krishna, S. (2002). Developments and trends in enzyme catalysis in nonconventional media. Biotechnology Advances 20: 239-267.

Hari Krishna, S., Srinivas, N.D., Raghavarao, K.S.M.S. and Karanth, N.G. (2002). Reverse micellar extraction for downstream processing of proteins/enzymes. Advances in Biochemical Engineering Biotechnology 75: 119-183.

Harwood, H.J. Jr and Pellarin, L.D. (1997). Kinetics of low-density lipoprotein receptor activity in Hep-G2 cells: Derivation and validation of a Briggs-Haldane-based

kinetic model for evaluating receptor-mediated endocytotic processes in which receptors recycle. Biochemical Journal 323: 649-659.

Hauer, B., Breuer, M., Rogers, P.L., Sandford, V. and Rosche, B. (2003). Process for production of *R*-phenylacetylcarbinol by an enzymatic process in a two-phase system. Patent application No: WO 03/020942.

Hedges, A.R. (1998). Industrial applications of cyclodextrins. Chemical Reviews 98: 2035-2044.

Heskamp, M.L. and Barz, W. (1997). Characterization of proteases from *Rhizopus* species after growth on soybean protein. Zeitschrift Fur Naturforschung Ca Journal of Biosciences 52: 595-604.

Heskamp, M.L. and Barz, W. (1998). Expression of proteases by *Rhizopus* species during tempeh fermentation of soybeans. Nahrung 42: 23-28.

Hildebrandt, G. and Klavehn, W. (1932). Verfahren zur Herstellung von 1-1-Phenyl-2-methylaminopropan-1-ol. German patent 548 459.

Hildebrandt, G. and Klavehn, W. (1934). 1-phenyl-2-methylamino-1-propanol, May 1. USP 1,956,930.

Hofstetter, K., Lutz, J., Lang, I., Witholt, B. and Schmid, A. (2004). Coupling of biocatalytic asymmetric epoxidation with NADH regeneration in organic-aqueous emulsions. Angewandte Chemie-International Edition 43: 2163-2166.

Holzer, H. and Beaucamp, K. (1959). Nachweis und charakterisierung von zwischenprodukten der decarboxylierung und oxydation von pyruvat-aktiviertes pyruvat und aktivierter acetaldehyd. Angewandte Chemie-International Edition 71: 776-776.

Hu, S.Y. (1969). Ephedra (Ma-Huang) in the new Chinese materia medica. Economic Botany 23: 346-351.

Hubner, G., Weidhase, R. and Schellenberger, A. (1978). The mechanism of substrate activation of pyruvate decarboxylase. A first approach. European Journal of Biochemistry 92: 175-181.

Iding, H., Siegert, P., Mesch, K. and Pohl, M. (1998). Application of α-keto acid decarboxylases in biotransformations (Review). Biochimica et Biophysica Acta 1385: 307-322.

Iverson, B.L. and Breaker, R.R. (1998). Be careful what you wish for. Trends in Biotechnology 16: 52-53.

Iwan, P., Goetz, G., Schmitz, S., Hauer, B., Breuer, M. and Pohl, M. (2001). Studies on the continuous production of R-(-)-phenylacetylcarbinol in an enzyme-membrane reactor. Journal of Molecular Catalysis B: Enzymatic 11: 387-396.

Joachimsthal, E.L. (2001). Kinetic characterization of recombinant *Zymomonas mobilis* for the production of ethanol fuel from lignocellulosics. Department of Biotechnology. Sydney, University of New South Wales, Ph.D. Thesis.

Jordan, F. (1999). Interplay of organic and biological chemistry in understanding coenzyme mechanisms: example of thiamin diphosphate-dependent decarboxylations of 2-oxo-acids (Review). FEBS Letters 457: 298-301.

Juni, E. (1961). Evidence for a two-site mechanism for decarboxylation of α-keto acids by α-carboxylase.The Journal of Biological Chemistry 236: 2302-2308.

Juni, E. and Heym, G.A. (1968a). Properties of yeast pyruvate decarboxylase and their modification by proteolytic enzyme I: Stability of decarboxylases from wild-type and mutant strains. Archives of Biochemistry and Biophysics 127: 79-88.

Juni, E. and Heym, G.A. (1968b). Properties of yeast pyruvate decarboxylase and their modification by proteolytic enzyme II: Selective alteration by yeast proteases. Archives of Biochemistry and Biophysics 127: 89-100.

References

Kanayama, G., Gruber, A.J., Pope, H.G. Jr, Borowiecki, J.J. and Hudson, J.I. (2001). Over-the-counter drug use in gymnasiums: an underrecognized substance abuse problem?. Psychotherapie und Psychosomatik 70: 137-140.

Katritzky, A.R., Tamm, K., Kuanar, M. and Fara, D.C. (2004). Aqueous biphasic systems, partitioning of organic molecules: A QSPR treatment. Journal of Chemical Information and Computer Sciences 44: 136-142.

Kern, D., Kern, G., Neef, H., Tittmann, K., Killenberg-Jabs, M., Wikner, C., Scheider, G. and Hubner, G. (1997). How Thiamin Diphosphate Is Activated in Enzymes. Science 275: 67-70.

Kheradmandy, M. (1990). Synthesis of *L*-ephedrine and norephedrine with transformation of benzaldehyde by yeast. Iran Amirkabir 4: 19-24.

Kim, J.-H., Choi, G.-S., Kim, S.-B., Kim, W.-H., Lee, J.-Y., Ryu, Y.-W. and Kim, G.-J. (2004). Enhanced thermostability and tolerance of high substrate concentration of an esterase by directed evolution. Journal of Molecular Catalysis B: Enzymatic 27: 169-175.

King, E.L. and Altman, C. (1956). A schematic method of deriving the rate laws for enzyme catalysed reactions. Journal of Physical Chemistry 60: 1375–1378.

Klibanov, A.M. (2001). Improving enzymes by using them in organic solvents. Nature 409: 241-246.

Knez, Z., Habulin, M. and Primozic, M. (2003). Hydrolases in supercritical CO_2 and their use in a high-pressure membrane reactor. Bioprocess and Biosystem Engineering 25: 279-284.

Knight, J. (2004). Safety concerns prompt US ban on dietary supplement. Nature 427: 90.

References

Konig, S. (1998). Subunit structure, function and organisation of pyruvate decarboxylases from various organisms (Review). Biochimica et Biophysica Acta 1385: 307-322.

Kostraby, M.M., Smallridge, A.J. and Trewhella, M.A. (2002). Yeast-mediated preparation of *L*-PAC in an organic solvent. Biotechnology and Bioengineering 77: 827-831.

Krampitz, L.O. (1969). Catalytic functions of thiamin diphosphate. Annual Reviews Biochemistry 38: 213-240.

Kren, V., Crout, D.H.G., Dalton, H., Hutchinson, D.W., Konig, W., Turner, M.M., Dean, G. and Thomson, N. (1993). Pyruvate decarboxylase: a new enzyme for the production of acyloins by biotransformation. Journal of the Chemical Society, Chemical Communications 4: 341-343.

Kreyszig, E. (1993). Advanced Engineering Mathematics, 7th edn. John Wiley and Sons: New York, pp. 1035-1036.

Kyte, J. (1995). Mechanism in protein chemistry. Garland Publishing: New York, pp. 62-69.

Lamare, S. and Legoy, M.-D. (1993). Biocatalysis in the gas phase. Trends in Biotechnology 11: 413-418.

Laurence, G., Smallridge, A.J. and Trewhella, M.A. (2002). Lactate as an alternative to pyruvate in the yeast mediated preparation of PAC. Journal of Molecular Catalysis B: Enzymatic 19-20: 399-403.

Leksawasdi, N., Breuer, M., Hauer, B., Rosche, B. and Rogers, P.L. (2003). Kinetics of pyruvate decarboxylase deactivation by benzaldehyde. Biocatalysis and Biotransformation 21: 315-320.

Leksawasdi, N., Chow, Y.Y.S., Breuer, M., Hauer, B., Rosche, B. and Rogers, P.L. (2004). Kinetic analysis and modelling of enzymatic (*R*)-phenylacetylcarbinol batch biotransformation process. Journal of Biotechnology 111: 179-189.

Leksawasdi, N., Joachimsthal, E.L. and Rogers, P.L. (2001). Mathematical modelling of ethanol production from glucose/xylose mixtures by recombinant *Zymomonas mobilis*. Biotechnology Letters 23: 1087-1093.

Leon, R., Fernandes, P., Pinheiro, H.M. and Cabral, J.M.S. (1998). Whole-cell biocatalysis in organic media. Enzyme and Microbial Technology 23: 483-500.

Leon, R., Martin, M., Vigara, J., Vilchez, C. and Vega, J.M. (2003). Microalgae mediated photoproduction of β-carotene in aqueous-organic two phase systems. Biomolecular Engineering 20: 177-182.

Leung, A.Y. and Foster, S. (1996). Ephedra. In: Encyclopedia of Common Natural Ingredients Used in Foods, Drugs and Cosmetics. John Wiley and Sons: New York, p. 227.

Liese, A. and Filho, M.V. (1999). Production of fine chemicals using biocatalysis. Current Opinion in Biotechnology 10: 595-603.

Lilly, M.D. (1994). Advances in biotransformation processes. Food and Bioproducts Processing: Transactions of the Institution of Chemical Engineers, Part C 72: 27-34.

Liu, C.L., Nikas, Y.J. and Blankschtein, D. (1996). Bioprocess Technologies: Novel bioseparations using two-phase aqueous micellar systems. Biotechnology and Bioengineering 52: 185-192.

Lobell, M. and Crout, D.H.G. (1996). Pyruvate decarboxylase: A molecular modelling study of pyruvate decarboxylation and acyloin formation. Journal of the American Chemical Society 118: 1867-1873.

Lohmann, K. and Schuster, P. (1937). Untersuchungen über die Cocarboxylase. Biochemische Zeitschrift 294: 188-214.

Long, A., James, P. and Ward, O.P. (1989). Aromatic aldehydes as substrates for yeast and yeast alcohol dehydrogenase. Biotechnology and Bioengineering 33: 657-660.

Long, A. and Ward, O.P. (1989a). Biotransformation of aromatic aldehydes by *Saccharomyces cerevisiae* investigation of reaction rates. Journal of Industrial Microbiology 4: 49-53.

Long, A. and Ward, O.P. (1989b). Biotransformation of benzaldehyde by *Saccharomyces cerevisiae*: characterization of the fermentation and toxicity effects of substrates and products. Biotechnology and Bioengineering 34: 933-941.

Lowe, S.E. and Zeikus, J.G. (1992). Purification and characterization of pyruvate decarboxylase from *Sarcina ventriculi.* Journal of General Microbiology 138: 803-807.

Maddison, D.R. (1995). Tree of life web project. (Accessed 22nd April 2004). http://tolweb.org/tree?group=Ephedraandcontgroup=Gnetales

Mahmoud, W.M., El-Sayed, A.M.M. and Coughlin, R.W. (1990a). Effect of β-cyclodextrin on production of *L*-phenylacetylcarbinol by immobilized cell of *Saccharomyces cerevisiae*. Biotechnology and Bioengineering 36: 256-262.

Mahmoud, W.M., El-Sayed, A.M.M. and Coughlin, R.W. (1990b). Production of *L*-phenylacetylcarbinol by immobilized yeast cell: I. Batch fermentation. Biotechnology and Bioengineering 36: 47-54.

Mahmoud, W.M., El-Sayed, A.M.M. and Coughlin, R.W. (1990c). Production of *L*-phenylacetylcarbinol by immobilized yeast cell: II. Semicontinuous fermentation. Biotechnology and Bioengineering 36: 55-63.

Malandrinos, G., Louloudi, M., Deligiannakis, Y. and Hadjiliadis, N. (2001). Complexation of Cu^{2+} by HETPP and the pentapeptide Asp-Asp-Asn-Lys-Ile: A structural model of the active site of thiamin-dependent enzymes in solution. Inorganic Chemistry 40: 4588-4596.

Martinek, K., Levashov, A.V., Klyachko, N., Khmelnitski, Y.L. and Berezin, I.V. (1986). Micellar enzymology. European Journal of Biochemistry 155: 453-468.

Maruyama, T., Yamamura H., Kotani, T., Kamiya, N. and Goto, M. (2004). Poly(ethylene glycol)-lipase complexes that are highly active and enatioselective in ionic liquids. Organic and Biomolecular Chemistry 2: 1239-1244.

Mathews, C.K. and van Holde, K.E. (1990). Biochemistry. Benjamin/Cummings Publishing: California, pp. 475-477.

Mathys, R.G., Kut, O.M. and Witholt, B. (1998a). Alkanol removal from the apolar phase of a two-liquid phase bioconversion system. Part 1: comparison of a less volatile and a more volatile in-situ extraction solvent for the separation of 1-octanol by distillation. Journal of Chemical Technology and Biotechnology 71: 315-325.

Mathys, R.G., Schmid, A., Kut, O.M. and Witholt, B. (1998b). Alkanol removal from the apolar phase of a two-liquid phase bioconversion system. Part 2: effect of fermentation medium on batch distillation. Journal of Chemical Technology and Biotechnology 71: 326-334.

Mathys, R.G., Schmid, A. and Witholt, B. (1999). Integrated two-liquid phase bioconversion and product-recovery processes for the oxidation of alkanes: process design and economic evaluation. Biotechnology and Bioengineering 64: 459-477.

May, O., Nguyen, P.T. and Arnold, F.H. (2000). Inverting enantioselectivity by directed evolution of hydantoinase for improved production of *L*-methionine. Nature Biotechnology 18: 317-320.

May, S.W. (1992). Biocatalysis in the 90s: a perspective. Enzyme and Microbial Technology 14: 80–84.

May, S.W. (1997). New applications for biocatalysts. Current Opinion in Biotechnology 8: 181-186.

Mazur, A.K. and Kuchinski, A.V. (1992). Schematic methods for probabilistic enzyme kinetics. Journal of Theoretical Biology 155: 387-407.

McCoy, M. (2000). Novozymes emerges. Chemical Engineering News 19: 23-25.

McIntyre, M., Breum, J., Arnau, J. and Nielsen, J. (2002). Growth physiology and dimorphism of *Mucor circinelloides* (syn. *racemosus*) during submerged batch cultivation. Applied Microbiology and Biotechnology 58: 495-502.

Moczydlowksi, E.G. and Fortes, P.A.G. (1981). Inhibition of sodium potassium ATPase by 2' 3'-O 2 4 6 trinitrocyclohexadienylidene adenine nucleotides implications for the structure and mechanism of sodium potassium pump. Journal of Biological Chemistry 256: 2357-2366.

Mogi, K. (1993). Graphic analysis of coupling in biological systems. Journal of Theoretical Biology 162: 337-352.

Moran, L.A., Scrimgeour, K.G., Horton, H.R., Ochs, R.S. and Rawn, J.D. (1994). Biochemistry, 2nd edn. Neil Patterson: New Jersey, pp. 8.21-8.23.

Motilva, P., Del Arco, A., Usero, J.L., Izquierdo, C. and Casado, J. (1988). Kinetic study of the enzyme NADPH cytochrome-C P-450 reductase non-Michaelian behaviour. International Journal of Biochemistry 20: 41-48.

Myers, D. and Palmer, G. (1985). Microcomputer tools for steady-state enzyme kinetics. Computer Application in Biosciences 1: 105-110.

Nara, S.J., Mohile, S.S., Harjani, J.R., Naik, P.U. and Salunkhe, M.M. (2004). Influence of ionic liquids on the rates and regioselectivity of lipase-mediated

biotransformations on 3,4,6-tri-O-acetyl-D-glucal. Journal of Molecular Catalysis B: Enzymatic 28: 39-43.

Netrval, J. and Vojtisek, V. (1982). Production of phenyl acetyl carbinol in various yeast species. European Journal of Applied Microbiology and Biotechnology 16: 35-38.

Neuberg, C. and Hirsch, J. (1921). Uber ein kohlenstoffketten knupfendes ferment (Carboligase). Biochemische Zeitschrift 115: 282-310.

Neuberg, C. and Karczag, L. (1911). Uber zuckerfreie Hefegarungen. IV. Carboxylase, ein neues Enzym der Hefe. Biochemische Zeitschrift 36: 68-81.

Neuberg, C. and Ohle, H. (1922). Biosynthetic carbon chain union in fermentation processes. Biochemische Zeitschrift 128: 610-618.

Neuser, F., Zorn, H. and Berger, R.G. (2000). Generation of odorous acyloins by yeast pyruvate decarboxylases and their occurrence in sherry and soy sauce. Journal of agricultural and food chemistry 48: 6191-6195.

Nikolova, P. and Ward, O.P. (1991). Production of *L*-phenylacetylcarbinol by biotransformation: product and by-product formation and activation of the key enzymes in wild-type and ADH isoenzyme mutants of *Saccharomyces cerevisiae*. Biotechnology and Bioengineering 38: 493-498.

Olavarria, J.M. (1986). A systematic method for the compilation of the King and Altman graphs of a steady-state enzyme model suitable for manual or computer use. Journal of Theoretical Biology 122: 269-276.

Oliver, A.L., Anderson, B.N. and Roddick, F.A. (1999). Factors affecting the production of *L*-phenylacetylcarbinol by yeast: A case study. Advances in Microbial Physiology 41: 1-45.

References

Ose, S. and Hironaka, J. (1957). Studies on production of phenyl acetyl carbinol by fermentation. Proceedings of the International Symposium on Enzyme Chemistry 2: 457-460.

Palmer, T. (1991). Understanding enzymes, 3rd edn. Ellis Horwood: Great Britain, pp. 93, 94, 106, 118-120, 135-137, 221-222, 247-253.

Panke, S., Held, M., Wubbolts, M.G., Witholt, B. and Schmid, A. (2002). Pilot-scale production of (*S*)-styrene oxide from styrene by recombinant *Escherichia coli* synthesizing styrene monooxygenase. Biotechnology and Bioengineering 80: 33-41

Panke, S. and Wubbolts, M.G. (2002). Enzyme technology and bioprocess engineering. Current Opinion in Biotechnology 13: 111-116.

Papagianni, M. and Moo-Young, M. (2002). Protease secretion in glucoamylase producer *Aspergillus niger* cultures: fungal morphology and inoculum effects. Process Biochemistry 37: 1271-1278.

Patel, R.N. (2001). Biocatalytic synthesis of intermediates for the synthesis of chiral drug substances. Current Opinion in Biotechnology 12: 587-604.

Pazouki, M. and Panda, T. (2000). Understanding the morphology of fungi. Bioprocess Engineering 22: 127-143.

Pohl, M. (1997). Protein design on pyruvate decarboxylase (PDC) by site-directed mutagenesis. Application to mechanistical investigations and tailoring PDC for the use in organic synthesis. Advanced Biochemical Engineering and Biotechnology 58: 15-43.

Pohl, M., Kathrin, M., Anja, R. and Maria-Regina, K. (1995). Stability investigations on the pyruvate decarboxylase from *Zymomonas mobilis*. Biotechnology and Applied Biochemistry 22: 95-105.

References

Pohl, M., Siegert, P., Mesch, K., Bruhn, H. and Grotzinger, J. (1998). Active site mutants of pyruvate decarboxylase from *Zymomonas mobilis*: A site directed mutagenesis study of L112, I472, I476, E473 and N482. European Journal of Biochemistry 257: 538-546.

Prescott, L.M., Harley, J.P., Klein, D.A. (1996). Microbiology, 3rd edn. Wm. C. Brown Publishers: New York, pp. 118-119.

Principato, G.B., Giovannini, E., Mallone, L. and Menghini, A.R. (1979). Derivation of a velocity equation for a model of the reaction of acetylcholin esterase with 2 binding sites. Bollettino-Societa Italiana Biologia Sperimentale 55: 757-761.

Prosser, J.I. and Tough, A.J. (1991). Growth mechanisms and growth kinetics of filamentous microorganisms. Critical Reviews in Biotechnology 10: 252-274.

Radi, R., Tan, S., Prodanov, E., Evans, R.A. and Parks, D.A. (1992). Inhibition of xanthine oxidase by uric acid and its influence on superoxide radical production. Biochimica et Biophysica Acta 1122: 178-182.

Ragsdale, S.W. (2003). Pyruvate ferredoxin oxidoreductase and its radical intermediate. Chemical Reviews 103: 2333-2346.

Rogers, P.L., Shin, H.S. and Wang, B. (1997). Biotransformation for *L*-ephedrine production. Advances in Biochemical Engineering/Biotechnology 56: 33-59.

Rogers, R.D. and Seddon, K.R. (2003). Ionic liquids – solvents of the future ?. Science 302: 792-793.

Rosche, B., Breuer, M., Hauer, B. and Rogers, P.L. (2003a). Increased pyruvate efficiency in enzymatic production of (*R*)-phenylacetylcarbinol. Biotechnology Letters 25: 847-851.

Rosche, B., Breuer, M., Hauer, B. and Rogers, P.L. (2003b). Screening of yeasts for cell-free production of (*R*)-phenylacetylcarbinol. Biotechnology Letters 25: 841-845.

Rosche, B., Breuer, M., Hauer, B. and Rogers, P.L. (2004a). Biphasic aqueous/organic biotransformation of acetaldehyde and benzaldehyde by *Zymomonas mobilis* pyruvate decarboxylase. Biotechnology and Bioengineering 86: 788-794.

Rosche, B., Breuer, M., Hauer, B. and Rogers, P.L. (2004b). Roles of pyruvate in enhancing pyruvate decarboxylase stability towards benzaldehyde. Journal of Biotechnology (in press).

Rosche, B., Sandford, V., Breuer, M., Hauer, B. and Rogers, P.L. (2001). Biotransformation of benzaldehyde into (*R*)-phenylacetylcarbinol by filamentous fungi or their extracts. Applied Microbiology and Biotechnology 57: 309-315.

Rosche, B., Leksawasdi, N., Sandford, V., Breuer, M., Hauer, B. and Rogers, P. (2002a). Enzymatic (*R*)-phenylacetylcarbinol production in benzaldehyde emulsions. Applied Microbiology and Biotechnology 60: 94-100.

Rosche, B., Sandford, V., Breuer, M., Hauer, B. and Rogers, P.L. (2002b). Enhanced production of *R*-phenylacetylcarbinol (*R*-PAC) through enzymatic biotransformation. Journal of Molecular Catalysis B: Enzymatic 19-20: 109-115.

Rose, A.H. (1980). Microbial enzymes and bioconversion. In Economic Microbiology, vol. 5. Academic Press: New York, pp. 6-10.

Ru, M.T., Dordick, J.S., Reimer, J.A. and Clark, D.S. (2001). Salt-induced activation of enzyme in organic solvents: optimizing the lyophilization time and water content. In: *Methods in Biotechnology. Vol 15: Enzymes in nonaqueous solvents: Methods and Protocols* (E.N. Vulfson, P.J. Halling, H.L. Holland, eds.) Humana Press: New Jersey, p. 3.

Sandford, V.M. (2002). Enzymatic bioprocess development for *R*-PAC: an intermediate for ephedrine/pseudoephedrine production. Department of Biotechnology. Sydney, University of New South Wales, Ph.D. Thesis.

Sang-Duk, Y., Jong-Saeng, K., Gyu-Hee, L., Jae-Hong, J. and Man-Jin, O. (2002). Changes of amylase and protease activities in soybean powder and flour koji prepared with *Rhizopus* sp. Journal of the Korean Society of Agricultural Chemistry and Biotechnology 45: 51-55.

Schellenberger, A. (1998). Sixty years of thiamin diphosphate biochemistry. Biochimica et Biophysica Acta 1385: 173.

Schorken, U. and Sprenger, G.A. (1998). Thiamin-dependent enzymes as catalysts in chemoenzymatic syntheses. Biochimica et Biophysica Acta 1385: 229-243.

Schmid, A., Dordick, J.S., Hauer, B., Kiener, A., Wubbolts, M. and Witholt, B. (2001). Industrial biocatalysis today and tomorrow. Nature 409: 258-268.

Schmid, A., Hollmann, F., Park, J.B. and Buhler, B. (2002). The use of enzymes in the chemical industry in Europe. Current Opinion in Biotechnology 13: 359-366.

Schmid, A., Kollmer, A., Mathys, R.G. and Witholt, B. (1998). Developments toward large-scale bacterial bioprocesses in the presence of bulk amounts of organic solvents. Extremophiles 2: 249-256.

Schmid, A., Kollmer, A., Sonnleitner, B. and Witholt, B. (1999). Development of equipment and procedures for the safe operation of aerobic bacterial bioprocesses in the presence of bulk amounts of flammable organic solvents. Bioprocess Engineering 20: 91-100.

Schmidt-Dannert, C. and Arnold, F.H. (1999). Directed evolution of industrial enzymes. Trends in Biotechnology 17: 135-136.

Schulze, B. and Wubbolts, M.G. (1999). Biocatalysis for industrial production of fine chemicals. Current Opinion in Biotechnology 10: 609-615.

Scopes, R.K. (1994). Protein purification: principles and practice, 3rd edn. Springer-Verlag: New York, p. 323.

Seddon, K.R. (2003). Ionic liquids: a taste of the future. Nature Materials 2: 363-365.

Seely, R.J., Hageman, R.V., Yarus, M.J. and Sullivan, S.A. (1989a). US Patent No. PCT/US 89/04423.

Seely, R.J., Hageman, R.V., Yarus, M.J. and Sullivan, S.A. (1990). (Synergen Inc.) Process for making phenyl acetyl carbinol (PAC): Microorganism for use in the process and method for preparing the microorganism PCT Int. Patent Application No: WO 9004 831 (Cl.C12N1/B) 03 May 1990 US Patent Application No: 261010 21 Oct. 1988.

Seely, R.J., Heefner, D.L., Hageman, R.W., Yarus, M.J. and Sullivan, S.A. (1989b). US Patent No. PCT/US 89/04421.

Sergienko, E.A. and Jordan, A. (2002). New Model for activation of yeast pyruvate decarboxylase by substrate consistent with the alternating sites mechanism: demonstration of the existence of two active forms of the enzyme. Biochemistry 41: 3952-3967.

Sharma, S., Teotia, S. and Gupta, M.N. (2003). Bioconversion in an aqueous two-phase system using a smart biocatalyst: casein hydrolysis by a α-chymotrypsin derivative. Enzyme and Microbial Technology 32: 337-339.

Shekelle, P.G., Hardy, M.L., Morton, S.C., Maglione, M., Mojica, W.A., Suttorp, M.J., Rhodes, S.L., Jungvig, L. and Gagne, J. (2003). Efficacy and safety of ephedra and ephedrine for weight loss and athletic performance. The Journal of the American Medical Association 289: 1537-1545.

Shin, H.S. and Rogers, P.L. (1995). Biotransformation of benzaldehyde to *L*-phenylacetylcarbinol, an intermediate in *L*-ephedrine production, by immobilized *Candida utilis*. Applied Microbiology and Biotechnology 44: 7-14.

Shin, H.S. and Rogers, P.L. (1996a). Kinetic evaluation of biotransformation of benzaldehyde to *L*-phenylacetylcarbinol by immobilized pyruvate decarboxylase from *Candida utilis*. Biotechnology and Bioengineering 49: 429-436.

Shin, H.S. and Rogers, P.L. (1996b). Production of *L*-Phenylacetylcarbinol (*L*-PAC) from benzaldehyde using partially purified pyruvate decarboxylase (PDC). Biotechnology and Bioengineering 49: 52-62.

Shukla, V.B. and Kulkarni, P.R. (1999). Downstream processing of biotransformation broth for recovery and purification of *L*-phenylacetylcarbinol (*L*-PAC). Journal of Scientific and Industrial Research 58: 591-593.

Shukla, V.B. and Kulkarni, P.R. (2000). *L*-Phenylacetylcarbinol (*L*-PAC): biosynthesis and industrial applications. World Journal of Microbiology and Biotechnology 16: 499-506.

Silverman, M. and Werkman, C.H. (1941). The formation of acetylmethylcarbinol from pyruvic acid by a bacterial enzyme preparation. Journal of Biological Chemistry 138: 35-48.

Singh, A., Kumar, P.K.R. and Schugerl, K. (1992). Bioconversion of cellulosic materials to ethanol by filamentous fungi. Advanced in Biochemical Engineering /Biotechnology 45: 29-55.

Skoog, D.A., West, D.M. and Holler, F.J. (1996). Fundamentals of analytical chemistry, 7th edn. Saunders College Publishing, New York, pp. 30, 34.

Skory, C.D., Freer, S.N. and Bothast, R.J. (1997). Screening for ethanol producing filamentous fungi. Biotechnology Letters 19: 203-206.

Smith, J.E. (1975). The structure and development of filametous fungi. In: *The Filamentous Fungi, Vol. 1: Industrial Mycology* (J.E. Smith, D.R. Berry, eds.) Edward Arnold, Great Britain, pp. 1-14.

Smith, P.F. and Hendlin, D. (1953). Mechanism of phenylacetylcarbinol synthesis by yeast. Journal of Bacteriology 65: 440-445.

Sola, S., Helmy, T. and Kacharava, A. (2004). Coronary dissection and thrombosis after ingestion of ephedra. The American Journal of Medicine 116: 645-646.

References

Soni, M.G., Carabin, I.G., Griffiths, J.C. and Burdock, G.A. (2004). Safety of ephedra: lessons learned. Toxicology Letters 150: 97-110.

Sorensen, G.G. and Spenser, I.D. (1988). Biosynthesis of ephedrine. Journal of the American Chemical Society 110: 3714-3715.

Sprenger, G.A. and Pohl, M. (1999). Synthetic potential of thiamin diphosphate-dependent enzymes (Review). Journal of Molecular Catalysis B: Enzymatic 6: 145-159.

Stinson, S.C. (1993). Chiral drugs. Chemical Engineering News, September 27: 38-65.

Stinson, S.C. (2000). Chiral drugs. Science/Biotechnology 78: 55-78.

Stivers, J.T. and Washabaugh, M.W. (1993). Catalysis of acetoin formation by brewers' yeast pyruvate decarboxylase isozymes. Biochemistry 32: 13472-13482.

Straathof, A.J.J., Panke, S. and Schmid, A. (2002). The production of fine chemicals by biotransformations. Current Opinion in Biotechnology 13: 548-556.

Szejtli, J. (1998). Introduction and general overview of cyclodextrin chemistry. Chemical Reviews 98: 1743-1753.

Tadayyon, A., Hill, G.A., Ingledew, W.M. and Sokhansanj, S. (1997). Contact-sorption drying of *Penicillium bilaii* in a fluidized bed dryer. Journal of Chemical Technology and Biotechnology 68:277-282.

Taylor, R. and Fletcher, R.L. (1999). A simple method for the freeze-preservation of zoospores of the green macroalga *Enteromorpha intestinalis*. Journal of Applied Phycology 11: 257-262.

Tholudur, A., Ramirez, W.F. and McMillan, J.D. (1999). Mathematical modelling and optimisation of cellulase protein production using *Trichoderma reesei* RL-P37. Biotechnology and Bioengineering 66: 1-16.

References

Thomas, S.M., DiCosimo, R. and Nagarajan, A. (2002). Biocatalysis: applications and potentials for the chemical industry. Trends in Biotechnology 20: 238-242.

Thome, O.W. (1885). Image of *Ephedra distachya* (Ephedraceae). In: MPI fur Zuchtungsforschung. (K. Stubers Online Library) (Accessed 22nd April 2004). http://caliban.mpiz-koeln.mpg.de/~stueber/thome/band1/tafel_028.html

Tilston, J. (1988). ICI to build plant for Exports, Sydney Morning Herald, September 22, Investment Issue, p. 25.

Tomarelli, R.M., Charney, J. and Harding, M.L. (1949). The use of azoalbumin as a substrate in the colourimetric determination of peptic and tryptic activity. Journal of Laboratory and Clinical Medicine 34: 428-433.

Topham, C.M. and Brocklehurst, K. (1992). In defence of the general validity of the Cha method of deriving rate equations: the importance of explicit recognition of the thermodynamic box in enzyme kinetics. Biochemical Journal 282: 261-265.

Tripathi, C.K.M., Basu, S.K., Vora, V.C., Mason, J.R. and Pirt, S.J. (1988). Continuous cultivation of a yeast strain for biotransformation of *L*-phenylacetylcarbinol (*L*-PAC) from benzaldehyde. Biotechnology Letters 10: 635-636.

Tripathi, C.K.M., Basu, S.K., Vora, V.C., Mason, J.R. and Pirt, S.J. (1991). Biotransformation of benzaldehyde to *L*-acetylphenylcarbinol (*L*-PAC) by immobilized yeast cell. Research and Industry 36: 159-160.

Turner, N.J. (2003). Controlling chirality. Current Opinion in Biotechnology 14: 401-406.

Ullrich, J. and Donner, I. (1970). Fluorimetric study of 2-p-toluidinonaphthalene-6-sulphonate binding to cytoplasmic yeast pyruvate decarboxylase. Hoppe-Seyler's Zeitschrift fur Physiologische Chemie 351: 1030-1034.

Van Dijken, J.P. and Scheffers, W.A. (1986). Redox balances in the metabolism of sugars by yeasts. FEMS Microbiology Reviews 32: 199–224.

References

Van Urk, H., Schipper, D., Breedveld, G.J., Mak, P.R., Scheffers, W.A. and Van Dijken, J.P. (1989). Localization and kinetics of pyruvate-metabolizing enzymes in relation to aerobic alcoholic fermentation in *Saccharomyces cerevisiae* CBS 8066 and *Candida utilis* CBS 621. Biochimica et Biophysica Acta 992: 78-86.

Vinogradov, A.A., Kudryashova, E.V., Grinberg, V.Y., Grinberg, N.V., Burova, T.V. and Levashov, A.V. (2001). The chemical modification of alpha-chymotrypsin with both hydrophobic and hydrophilic compounds stabilizes the enzyme against denaturation in water-organic media. Protein Engineering 14: 683-689.

Voets, D. and Voets, J.G. (1990). Biochemistry. John Wiley and Sons: New York, pp. 446-447.

Voets, J.P., Vandamme, E.J. and Vlerick, C. (1973). *L*-phenyl acetyl carbinol biosyntheis by *Saccharomyces cerevisiae*. Zeitschrift fur Allgemeine Mikrobiologie 13: 355-365.

Vojtisek, V. and Netrval, J. (1982). Effect of pyruvate decarboxylase EC-4.1.1.1 activity and of pyruvate concentration on the production of 1-hydroxy-1-phenyl-propanone in *Saccharomyces carlsbergensis*. Folia Microbiologica 27: 173-177.

Volkenstein, M.V. and Goldstein, B.N. (1966). A new method for solving the problems of the stationary kinetics of enzymological reactions. Biochimica et Biophysica Acta 115: 471.

Vulfson, E.N. (2001). Reaction systems and bioreactor design. In: *Methods in Biotechnology. Vol 15: Enzymes in nonaqueous solvents: Methods and Protocols* (E.N. Vulfson, P.J. Halling, H.L. Holland, eds.) Humana Press: New Jersey, p. 469.

Vulfson, E.N., Halling, P.J. and Holland, H.L., (Eds.) (2001). Methods in Biotechnology. Vol 15: Enzymes in Nonaqueous Solvents: Methods and Protocols. Humana Press: New Jersey, pp. v,vi.

References

Wagner, S.C., Skipper, H.D., Walley, F. and Bridges, W.B.J. (2001). Long-term survival of *Glomus claroideum* propagules from soil pot cultures under simulated conditions. Mycologia 93: 815-820.

Wandrey, C., Liese, A. and Kihumbu, D. (2000). Industrial biocatalysis: past, present and future. Organic Process Research and Development 4: 286-290.

Wang, B. (1993). Kinetic study of fed-batch and continuous bioconversion processes for *L*-phenylacetylcarbinol (*L*-PAC) production by the yeast *Candida utilis*. Department of Biotechnology. Sydney, University of New South Wales, Ph.D. Thesis.

Ward, O.P. and Singh, A. (2000). Enzymatic asymmetric synthesis by decarboxylases. Current Opinion in Biotechnology 11: 520–526.

Wehbi, H., Feng, J. and Roberts, M. (2003). Water-miscible organic cosolvents enhance phosphatidylinositol-specific phospholipase C phosphotransferase as well as phosphodiesterase activity. Biochimica et Biophysica Acta 1613: 15-27.

WHO. (1999). Herba Ephedra. WHO Monographs on Selected Medicinal Plants, vol. 1. World Health Organization, Geneva, pp. 145-153.

Wijono, D. (1991). Kinetics of phenylacetylcarbinol (PAC) production by the yeast *C. utilis*. Department of Biotechnology. Sydney, University of New South Wales, Ph.D. Thesis.

Willeman, W.F, Gerrits, P.J., Hanefeld, U., Brussee, J., Straathof, A.J., van der Gen, A. and Heijnen, J.J. (2002a). Development of a process model to describe the synthesis of (*R*)-mandelonitrile by *Prunus amygdalus* hydroxynitrile lyase in an aqueous-organic biphasic reactor. Biotechnology and Bioengineering 77: 239-247.

Willeman, W.F., Neuhofer, R., Wirth, I., Pochlauer, P., Straathof, A.J. and Heijnen, J.J. (2002b). Development of (*R*)-4-hydroxymandelonitrile synthesis in an aqueous-

organic biphasic stirred tank batch reactor. Biotechnology and Bioengineering 79: 154-164.

Wong, J.T. and Hanes, C.S. (1962). Kinetic formulations for enzymic reactions involving two substrates. Canadian Journal of Biochemistry and Physiology 40: 763-804.

Wongwicharn, A., McNeil, B. and Harvey, L.M. (1999). Effect of oxygen enrichment on morphology, growth and heterologous protein production in chemostat cultures of *Aspergillus niger* B1-D. Biotechnology and Bioengineering 65: 416-424.

Yang, Z.W., Tendian, S.W., Carson, W.M., Brouillette, W.J., Delucas, L.J. and Brouillette, C.G. (2004). Dimethyl sulfoxide at 2.5% (v/v) alters the structural cooperativity and unfolding mechanism of dimeric bacterial NAD$^+$ synthetase. Protein Science 13: 830-841.

Zaks, A. (2001). Industrial biocatalysis. Current Opinion in Chemical Biology 5: 130-136.

Zeng, X.P., Farrenkopf, B., Hohmann, S., Dyda, F., Furey, W. and Jordan, F. (1993). Role of cysteines in the activation and inactivation of brewers' yeast pyruvate decarboxylase investigated with a pdc1-pdc6 fusion protein. Biochemistry 32: 2704-2709.

Zhao, M. (1992). Graphic analysis of relaxation times of enzyme-catalysed reactions: an extension of the graphic method of King and Altman. Biochemical Journal 287: 391-393.

Zijlstra, G.M., de Gooijer, C.D. and Tramper, J. (1998). Extractive bioconversions in aqueous two-phase systems. Current Opinion in Biotechnology 9: 171-176.

Appendix A

Rate Constant Products Derived From The Proposed Reaction Mechanisms

Table A.1: Input list to King and Altman search program designed in Visual Basic for Applications (VBA) of Microsoft EXCEL[®] spreadsheet

Reaction	From complex	To complex	Rate constant
1	EP	E	k_7
2	E	EP	$k_{(-7)}[P]$
3	EQB	EP	k_6
4	EP	EQB	$k_{(-6)}$
5	EQ	EQB	$k_5[B]$
6	EQB	EQ	$k_{(-5)}$
7	EQ	E	k_4
8	E	EQ	$k_{(-4)}[Q]$
9	EQ	EQC	$k_{(-3)}[C]$
10	EQC	EQ	k_3
11	EA	EQC	k_2
12	EQC	EA	$k_{(-2)}$
13	EA	E	$k_{(-1)}$
14	E	EA	$k_1[A]$
15	EQ	EQQ	$k_8[Q]$
16	EQQ	EQ	$k_{(-8)}$
17	ER	EQQ	$k_{(-9)}$
18	EQQ	ER	k_9
19	ER	E	k_{10}
20	E	ER	$k_{(-10)}[R]$

Appendix A

Table A.2(a): Rate constant products from the proposed and simplified mechanisms

Complex	One	Two	Three	Four	Five	Six	Seven	Time passed	Current Time	Valid pattern for all 20 reactions	Simplify Level 1 k(-3) = k(-7) = k(-10) = 0	Simplify Level 2 All reverse = 0, except k(-4)	Simplify Level 3 All reverse = 0
E	1	3	5	10	11	16	17	1.57 min	23:56:39	k2k3k5k6k7k(-8)k(-9)[B]	k2k3k5k6k7k(-8)k(-9)[B]		
E	7	4	6	10	11	16	17	3.19 min	23:58:17	k2k3k4k(-5)k(-6)k(-8)k(-9)	k2k3k4k(-5)k(-6)k(-8)k(-9)		
E	13	4	6	9	12	16	17	4.82 min	23:59:54	k(-1)k(-2)k(-3)k(-5)k(-6)k(-8)k(-9)[C]			
E	19	4	10	10	11	15	18	Restart Timing		k2k3k8k9k10k(-5)k(-6)[Q]	k2k3k8k9k10k(-5)k(-6)[Q]		
E	1	7	3	10	11	16	17	1.41 min	00:01:32	k2k3k4k6k7k(-8)k(-9)	k2k3k4k6k7k(-8)k(-9)		
E	1	7	6	10	11	16	17	1.41 min	00:02:57	k2k3k4k7k(-5)k(-8)k(-9)	k2k3k4k7k(-5)k(-8)k(-9)		
E	1	13	3	5	10	16	17	2.82 min	00:02:57	k5k6k7k(-1)k(-8)k(-9)[B]	k3k5k6k7k(-1)k(-8)k(-9)[B]		
E	1	13	3	5	12	16	17	2.82 min	00:04:22	k6k7k(-1)k(-2)k(-8)k(-9)[B]	k5k6k7k(-1)k(-2)k(-8)k(-9)[B]		
E	1	13	3	9	12	16	17	2.83 min	00:04:22	k6k7k(-1)k(-2)k(-3)k(-8)k(-9)[C]			
E	1	13	6	9	12	16	17	2.83 min	00:04:22	k7k(-1)k(-2)k(-3)k(-5)k(-8)k(-9)[C]			
E	1	19	3	5	10	11	16	4.23 min	00:05:46	k2k3k5k6k7k10k(-8)[B]	k2k3k5k6k7k10k(-8)[B]		
E	1	19	3	5	10	11	18	4.23 min	00:05:46	k2k3k5k6k7k9k10[B]	k2k3k5k6k7k9k10[B]	k2k3k5k6k7k9k10[B]	k2k3k5k6k7k9k10[B]
E	1	19	3	10	11	15	18	4.23 min	00:05:46	k2k3k6k7k8k9k10[Q]	k2k3k6k7k8k9k10[Q]	k2k3k6k7k8k9k10[Q]	k2k3k6k7k8k9k10[Q]
E	1	19	6	10	11	15	18	4.23 min	00:05:46	k2k3k7k8k9k10k(-5)[Q]	k2k3k7k8k9k10k(-5)[Q]		
E	7	13	4	6	10	16	17	5.66 min	00:07:12	k3k4k(-1)k(-5)k(-6)k(-8)k(-9)	k3k4k(-1)k(-5)k(-6)k(-8)k(-9)		
E	7	13	4	6	12	16	17	5.66 min	00:07:12	k4k(-1)k(-2)k(-5)k(-6)k(-8)k(-9)	k4k(-1)k(-2)k(-5)k(-6)k(-8)k(-9)		
E	7	19	4	6	10	11	16	7.07 min	00:08:36	k2k3k4k10k(-5)k(-6)k(-8)	k2k3k4k10k(-5)k(-6)k(-8)		
E	7	19	4	6	10	11	18	7.07 min	00:08:36	k2k3k4k9k10k(-5)k(-6)	k2k3k4k9k10k(-5)k(-6)		
E	13	19	4	6	9	12	16	8.53 min	00:10:04	k10k(-1)k(-2)k(-3)k(-5)k(-6)k(-8)[C]			
E	13	19	4	6	9	12	18	8.53 min	00:10:04	k9k10k(-1)k(-2)k(-3)k(-5)k(-6)[C]			
E	13	19	4	6	10	15	18	8.53 min	00:10:04	k8k9k10k(-1)k(-2)k(-5)k(-6)[Q]	k3k8k9k10k(-1)k(-2)k(-5)k(-6)[Q]		
E	1	7	13	3	10	16	17	9.42 min	00:10:58	k3k4k6k7k(-1)k(-8)k(-9)	k3k4k6k7k(-1)k(-8)k(-9)		
E	1	7	13	3	12	16	17	9.42 min	00:10:58	k4k6k7k(-1)k(-2)k(-8)k(-9)	k4k6k7k(-1)k(-2)k(-8)k(-9)		
E	1	7	13	6	12	16	17	9.42 min	00:10:58	k3k4k7k(-1)k(-5)k(-8)k(-9)	k3k4k7k(-1)k(-5)k(-8)k(-9)		
E	1	7	13	6	12	16	18	9.42 min	00:10:58	k4k7k(-1)k(-2)k(-5)k(-8)k(-9)	k4k7k(-1)k(-2)k(-5)k(-8)k(-9)		
E	1	7	19	3	10	11	16	10.3 min	00:11:53	k2k3k4k6k7k10k(-8)	k2k3k4k6k7k10k(-8)		
E	1	7	19	3	10	11	18	10.3 min	00:11:53	k2k3k4k6k7k9k10	k2k3k4k6k7k9k10	k2k3k4k6k7k9k10	k2k3k4k6k7k9k10
E	1	7	19	6	10	11	18	10.3 min	00:11:53	k2k3k4k7k10k(-5)k(-8)	k2k3k4k7k10k(-5)k(-8)		
E	1	7	19	6	10	11	18	10.3 min	00:11:53	k2k3k4k7k9k10k(-5)	k2k3k4k7k9k10k(-5)		
E	1	13	19	3	5	10	16	11.2 min	00:12:47	k3k5k6k7k10k(-1)k(-8)[B]	k3k5k6k7k10k(-1)k(-8)[B]		
E	1	13	19	3	5	10	18	11.2 min	00:12:47	k3k5k6k7k9k10k(-1)[B]	k3k5k6k7k9k10k(-1)[B]		
E	1	13	19	3	5	12	16	11.2 min	00:12:47	k5k6k7k10k(-1)k(-2)k(-8)[B]	k5k6k7k10k(-1)k(-2)k(-8)[B]		
E	1	13	19	3	5	12	18	11.2 min	00:12:47	k5k6k7k9k10k(-1)k(-2)[B]	k5k6k7k9k10k(-1)k(-2)[B]		
E	1	13	19	3	9	12	16	11.2 min	00:12:47	k6k7k10k(-1)k(-2)k(-3)k(-8)[C]			
E	1	13	19	3	9	12	18	11.2 min	00:12:47	k6k7k9k10k(-1)k(-2)k(-3)[C]			
E	1	13	19	3	12	15	18	11.2 min	00:12:47	k6k7k8k9k10k(-1)k(-2)[Q]	k6k7k8k9k10k(-1)k(-2)[Q]		
E	1	13	19	6	9	12	16	11.2 min	00:12:47	k7k10k(-1)k(-2)k(-3)k(-5)k(-8)[C]			
E	1	13	19	6	9	12	18	11.2 min	00:12:47	k7k9k10k(-1)k(-2)k(-3)k(-5)[C]			
E	1	13	19	6	9	12	18	11.2 min	00:12:47	k7k8k9k10k(-1)k(-5)[Q]	k3k7k8k9k10k(-1)k(-5)[Q]		
E	1	13	19	6	12	15	18	11.3 min	00:12:47	k7k8k9k10k(-1)k(-2)k(-5)[Q]	k7k8k9k10k(-1)k(-2)k(-5)[Q]		
E	7	13	19	4	6	10	16	12.2 min	00:13:42	k3k4k10k(-1)k(-5)k(-6)k(-8)	k3k4k10k(-1)k(-5)k(-6)k(-8)		
E	7	13	19	4	6	10	18	12.2 min	00:13:42	k3k4k9k10k(-1)k(-5)k(-6)	k3k4k9k10k(-1)k(-5)k(-6)		
E	7	13	19	4	6	12	16	12.2 min	00:13:42	k4k10k(-1)k(-2)k(-5)k(-6)k(-8)	k4k10k(-1)k(-2)k(-5)k(-6)k(-8)		
E	7	13	19	4	6	12	18	12.2 min	00:13:42	k4k9k10k(-1)k(-2)k(-5)k(-6)	k4k9k10k(-1)k(-2)k(-5)k(-6)		
E	1	7	13	19	3	10	16	12.6 min	00:14:09	k3k4k6k7k10k(-1)k(-8)	k3k4k6k7k10k(-1)k(-8)		
E	1	7	13	19	3	10	18	12.6 min	00:14:09	k3k4k6k7k9k10k(-1)	k3k4k6k7k9k10k(-1)		
E	1	7	13	19	3	12	16	12.6 min	00:14:09	k4k6k7k10k(-1)k(-2)k(-8)	k4k6k7k10k(-1)k(-2)k(-8)		
E	1	7	13	19	3	12	18	12.6 min	00:14:09	k4k6k7k9k10k(-1)k(-2)	k4k6k7k9k10k(-1)k(-2)		

Appendix A

Table A.2(b): (Cont.) Rate constant products from the proposed and simplified mechanisms

Complex	One	Two	Three	Four	Five	Six	Seven	Time passed	Current Time	Valid pattern for all 20 reactions	Simplify Level 1 k(-3) = k(-7) = k(-10) = 0	Simplify Level 2 All reverse = 0, except k(-4)	Simplify Level 3 All reverse = 0
E	1	7	13	19	6	10	16	12.6 min	00:14:09	k3k4k7k10k(-1)k(-5)k(-8)	k3k4k7k10k(-1)k(-5)k(-8)		
E	1	7	13	19	6	10	18	12.6 min	00:14:09	k3k4k7k9k10k(-1)k(-5)	k3k4k7k9k10k(-1)k(-5)		
E	1	7	13	19	6	12	16	12.6 min	00:14:09	k4k7k10k(-1)k(-2)k(-5)k(-8)	k4k7k10k(-1)k(-2)k(-5)k(-8)		
E	1	7	13	19	6	12	18	12.6 min	00:14:09	k4k7k9k10k(-1)k(-2)k(-5)	k4k7k9k10k(-1)k(-2)k(-5)		
EA	12	1	3	8	9	16	17	26.1 min	00:27:40	k6k7k(-2)k(-3)k(-4)k(-8)k(-9)[C][Q]			
EA	12	1	3	8	9	16	19	26.1 min	00:27:40	k6k7k10k(-2)k(-3)k(-4)k(-8)[C][Q]			
EA	12	1	3	8	9	18	19	26.1 min	00:27:40	k6k7k9k10k(-2)k(-3)k(-4)[C][Q]			
EA	12	1	3	9	16	17	20	26.1 min	00:27:40	k6k7k(-2)k(-3)k(-8)k(-9)k(-10)[C][R]			
EA	12	1	6	8	9	16	17	26.1 min	00:27:40	k7k(-2)k(-3)k(-4)k(-5)k(-8)k(-9)[C][Q]			
EA	12	1	6	8	9	16	19	26.1 min	00:27:40	k7k10k(-2)k(-3)k(-4)k(-5)k(-8)[C][Q]			
EA	12	1	6	8	9	18	19	26.1 min	00:27:40	k7k9k10k(-2)k(-3)k(-4)k(-5)[C][Q]			
EA	12	1	6	9	16	17	20	26.1 min	00:27:40	k7k(-2)k(-3)k(-5)k(-8)k(-9)k(-10)[C][R]			
EA	12	2	4	6	9	16	17	26.1 min	00:27:40	k(-2)k(-3)k(-5)k(-6)k(-7)k(-8)k(-9)[C][P]			
EA	12	2	4	6	9	16	19	26.1 min	00:27:40	k10k(-2)k(-3)k(-5)k(-6)k(-7)k(-8)[C][P]			
EA	12	2	4	6	9	18	19	26.1 min	00:27:40	k9k10k(-2)k(-3)k(-5)k(-6)k(-7)[C][P]			
EA	12	4	6	8	9	16	17	26.1 min	00:27:40	k(-2)k(-3)k(-4)k(-5)k(-6)k(-8)k(-9)[C][Q]			
EA	12	4	6	8	9	16	19	26.1 min	00:27:40	k10k(-2)k(-3)k(-4)k(-5)k(-6)k(-8)[C][Q]			
EA	12	4	6	8	9	18	19	26.1 min	00:27:40	k9k10k(-2)k(-3)k(-4)k(-5)k(-6)[C][Q]			
EA	12	4	6	9	16	17	20	26.1 min	00:27:40	k(-2)k(-3)k(-4)k(-5)k(-6)k(-8)k(-9)k(-10)[C][R]			
EA	14	1	3	5	10	16	17	39.5 min	00:41:03	k1k3k5k6k7k(-8)k(-9)[A][B]	k1k3k5k6k7k(-8)k(-9)[A][B]		
EA	14	1	3	5	10	16	19	39.5 min	00:41:03	k1k3k5k6k7k10k(-8)[A][B]	k1k3k5k6k7k10k(-8)[A][B]		
EA	14	1	3	5	10	18	19	39.5 min	00:41:03	k1k3k5k6k7k9k10[A][B]	k1k3k5k6k7k9k10[A][B]	k1k3k5k6k7k9k10[A][B]	k1k3k5k6k7k9k10[A][B]
EA	14	1	3	7	10	16	17	39.5 min	00:41:03	k1k3k4k6k7k(-8)k(-9)[A]	k1k3k4k6k7k(-8)k(-9)[A]		
EA	14	1	3	7	10	16	19	39.5 min	00:41:03	k1k3k4k6k7k10k(-8)[A]	k1k3k4k6k7k10k(-8)[A]		
EA	14	1	3	7	10	18	19	39.5 min	00:41:03	k1k3k4k6k7k9k10[A]	k1k3k4k6k7k9k10[A]	k1k3k4k6k7k9k10[A]	k1k3k4k6k7k9k10[A]
EA	14	1	3	10	15	18	19	39.5 min	00:41:03	k1k3k7k8k9k10k(-5)[A][Q]	k1k3k6k7k8k9k10[A][Q]	k1k3k6k7k8k9k10[A][Q]	k1k3k6k7k8k9k10[A][Q]
EA	14	1	6	7	10	16	17	39.5 min	00:41:03	k1k3k4k7k(-5)k(-8)k(-9)[A]	k1k3k4k7k(-5)k(-8)k(-9)[A]		
EA	14	1	6	7	10	16	19	39.5 min	00:41:03	k1k3k4k7k10k(-5)k(-8)[A]	k1k3k4k7k10k(-5)k(-8)[A]		
EA	14	1	6	7	10	18	19	39.5 min	00:41:03	k1k3k4k9k10k(-5)k(-6)[A]	k1k3k4k9k10k(-5)k(-6)[A]		
EA	14	1	6	10	15	18	19	39.5 min	00:41:03	k1k3k8k9k10k(-5)k(-6)[A][Q]	k1k3k8k9k10k(-5)k(-6)[A][Q]		
EA	14	4	3	5	16	18	19	46.9 min	00:48:26	k1k5k6k7k(-2)k(-8)k(-9)[A][B]	k1k5k6k7k(-2)k(-8)k(-9)[A][B]		
EA	14	4	3	5	16	18	19	46.9 min	00:48:26	k1k5k6k7k10k(-2)k(-8)[A][B]	k1k5k6k7k10k(-2)k(-8)[A][B]		
EA	14	4	3	5	18	18	19	46.9 min	00:48:26	k1k5k6k7k9k10k(-2)[A][B]	k1k5k6k7k9k10k(-2)[A][B]		
EA	12	14	1	3	7	16	19	46.9 min	00:48:26	k1k4k6k7k(-2)k(-8)k(-9)[A]	k1k4k6k7k(-2)k(-8)k(-9)[A]		
EA	12	14	1	3	7	16	19	46.9 min	00:48:26	k1k4k6k7k10k(-2)k(-8)[A]	k1k4k6k7k10k(-2)k(-8)[A]		
EA	12	14	1	3	7	18	19	46.9 min	00:48:27	k1k4k6k7k9k10k(-2)[A]	k1k4k6k7k9k10k(-2)[A]		
EA	12	14	1	3	9	16	17	46.9 min	00:48:27	k1k6k7k(-2)k(-3)k(-5)k(-8)k(-9)[A][C]			
EA	12	14	1	3	9	16	19	46.9 min	00:48:27	k1k6k7k10k(-2)k(-3)k(-5)k(-8)[A][C]			
EA	12	14	1	3	9	18	19	46.9 min	00:48:27	k1k6k7k9k10k(-2)k(-3)k(-5)[A][C]			
EA	12	14	1	3	15	18	19	46.9 min	00:48:27	k1k6k7k8k9k10k(-2)[A][Q]	k1k6k7k8k9k10k(-2)[A][Q]		
EA	12	14	1	6	7	16	17	46.9 min	00:48:27	k1k4k7k(-2)k(-5)k(-8)k(-9)[A]	k1k4k7k(-2)k(-5)k(-8)k(-9)[A]		
EA	12	14	1	6	7	16	19	46.9 min	00:48:27	k1k4k7k10k(-2)k(-5)k(-8)[A]	k1k4k7k10k(-2)k(-5)k(-8)[A]		
EA	12	14	1	6	7	18	19	46.9 min	00:48:27	k1k4k7k9k10k(-2)k(-5)[A]	k1k4k7k9k10k(-2)k(-5)[A]		
EA	12	14	1	6	9	16	17	46.9 min	00:48:27	k1k7k(-2)k(-3)k(-5)k(-8)k(-9)[A][C]			
EA	12	14	1	6	9	16	19	46.9 min	00:48:27	k1k7k10k(-2)k(-3)k(-5)k(-8)[A][C]			
EA	12	14	1	6	9	18	19	46.9 min	00:48:27	k1k7k9k10k(-2)k(-3)k(-5)[A][C]			

Appendix A

Table A.2(c): (Cont.) Rate constant products from the proposed and simplified mechanisms

Complex	One	Two	Three	Four	Five	Six	Seven	Time passed	Current Time	Valid pattern for all 20 reactions	Simplify Level 1 k(-3) = k(-7) = k(-10) = 0	Simplify Level 2 All reverse = 0, except k(-4)	Simplify Level 3 All reverse = 0
EA	12	14	1	6	15	18	19	46.9 min	00:48:27	k1k7k8k9k10k(-2)k(-5)[A][Q]	k1k7k8k9k10k(-2)k(-5)[A][Q]		
EA	12	14	4	6	7	16	17	46.9 min	00:48:27	k1k4k(-2)k(-5)k(-6)k(-8)k(-9)[A]	k1k4k(-2)k(-5)k(-6)k(-8)k(-9)[A]		
EA	12	14	4	6	7	18	19	46.9 min	00:48:27	k1k4k10k(-2)k(-5)k(-6)k(-8)[A]	k1k4k10k(-2)k(-5)k(-6)k(-8)[A]		
EA	12	14	4	6	9	16	17	46.9 min	00:48:27	k1k4k9k10k(-2)k(-5)k(-6)[A]	k1k4k9k10k(-2)k(-5)k(-6)[A]		
EA	12	14	4	6	9	16	19	46.9 min	00:48:27	k1k(-2)k(3)k(-5)k(-6)k(-8)k(-9)[A][C]			
EA	12	14	4	6	9	18	19	46.9 min	00:48:27	k1k10k(-2)k(3)k(-5)k(-6)k(-8)[A][C]			
EA	12	14	4	6	15	18	19	46.9 min	00:48:27	k1k9k10k(-2)k(3)k(-5)k(-6)[A][C]			
EA	12	14	4	6	15	18	19	46.9 min	00:48:27	k1k8k9k10k(-2)k(-5)k(-6)[A][Q]	k1k8k9k10k(-2)k(-5)k(-6)[A][Q]		
EP	2	6	7	10	11	16	17	1.01 h	01:01:51	k2k3k4k(-5)k(7)k(-8)[P]			
EP	2	6	7	10	11	18	19	1.01 h	01:01:51	k2k3k4k10k(-5)k(-7)k(-8)[P]			
EP	2	6	7	10	11	18	19	1.01 h	01:01:51	k2k3k4k9k10k(-5)k(-7)[P]			
EP	2	6	7	10	13	16	17	1.01 h	01:01:51	k3k4k(-1)k(-5)k(7)k(-8)k(-9)[P]			
EP	2	6	7	10	13	16	19	1.01 h	01:01:51	k3k4k10k(-1)k(-5)k(-7)k(-8)[P]			
EP	2	6	7	10	13	18	19	1.01 h	01:01:51	k3k4k9k10k(-1)k(-5)k(-7)[P]			
EP	2	6	7	12	13	16	17	1.01 h	01:01:51	k4k(-1)k(-2)k(-5)k(7)k(-8)k(-9)[P]			
EP	2	6	7	12	13	16	19	1.01 h	01:01:52	k4k10k(-1)k(-2)k(-5)k(-7)k(-8)[P]			
EP	2	6	7	12	13	18	19	1.01 h	01:01:52	k4k9k10k(-1)k(-2)k(-5)k(-7)[P]			
EP	2	6	9	12	13	16	17	1.01 h	01:01:52	k(-1)k(-2)k(-3)k(-5)k(7)k(-8)k(-9)[C][P]			
EP	2	6	9	12	13	16	19	1.01 h	01:01:52	k10k(-1)k(-2)k(-3)k(-5)k(-7)k(-8)[C][P]			
EP	2	6	9	12	13	18	19	1.01 h	01:01:52	k9k10k(-1)k(-2)k(-3)k(-5)k(-7)[C][P]			
EP	2	6	10	11	15	18	19	1.01 h	01:01:52	k2k3k8k9k10k(-1)k(-5)k(7)[P][Q]			
EP	2	6	10	13	15	18	19	1.01 h	01:01:52	k3k8k9k10k(-1)k(-5)k(7)[P][Q]			
EP	2	6	12	13	15	18	19	1.01 h	01:01:52	k8k9k10k(-1)k(-2)k(-5)k(7)[P][Q]			
EP	3	5	8	10	11	16	17	1.23 h	01:15:23	k2k3k5k6k(-4)k(-8)k(-9)[B][Q]	k2k3k5k6k(-4)k(-8)k(-9)[B][Q]		
EP	3	5	8	10	11	18	19	1.23 h	01:15:23	k2k3k5k6k10k(-4)k(-8)[B][Q]	k2k3k5k6k10k(-4)k(-8)[B][Q]		
EP	3	5	8	10	13	18	19	1.23 h	01:15:23	k2k3k5k6k9k10k(-4)[B][Q]	k2k3k5k6k9k10k(-4)[B][Q]	k2k3k5k6k9k10k(-4)[B][Q]	
EP	3	5	8	10	13	16	17	1.23 h	01:15:23	k3k5k6k(-1)k(-4)k(-8)k(-9)[B][Q]	k3k5k6k(-1)k(-4)k(-8)k(-9)[B][Q]		
EP	3	5	8	10	13	16	19	1.23 h	01:15:23	k3k5k6k10k(-1)k(-4)k(-8)[B][Q]	k3k5k6k10k(-1)k(-4)k(-8)[B][Q]		
EP	3	5	8	10	13	18	19	1.23 h	01:15:23	k3k5k6k9k10k(-1)k(-4)[B][Q]	k3k5k6k9k10k(-1)k(-4)[B][Q]		
EP	3	5	8	12	13	16	17	1.23 h	01:15:23	k5k6k(-1)k(-2)k(-4)k(-8)k(-9)[B][Q]	k5k6k(-1)k(-2)k(-4)k(-8)k(-9)[B][Q]		
EP	3	5	8	12	13	16	19	1.23 h	01:15:23	k5k6k10k(-1)k(-2)k(-4)k(-8)[B][Q]	k5k6k10k(-1)k(-2)k(-4)k(-8)[B][Q]		
EP	3	5	8	12	13	18	19	1.23 h	01:15:23	k5k6k9k10k(-1)k(-2)k(-4)[B][Q]	k5k6k9k10k(-1)k(-2)k(-4)[B][Q]		
EP	3	5	10	11	14	16	17	1.23 h	01:15:23	k1k2k3k5k6k(-8)k(-9)[A][B]	k1k2k3k5k6k(-8)k(-9)[A][B]		
EP	3	5	10	11	14	18	19	1.23 h	01:15:23	k1k2k3k5k6k10k(-8)[A][B]	k1k2k3k5k6k10k(-8)[A][B]		
EP	3	5	10	11	14	18	19	1.23 h	01:15:24	k1k2k3k5k6k9k10[A][B]	k1k2k3k5k6k9k10[A][B]	k1k2k3k5k6k9k10k(-4)[A][B]	k1k2k3k5k6k9k10[A][B]
EP	3	5	10	13	16	17	20	1.23 h	01:15:24	k2k3k5k6k(-8)k(-9)k(-10)[B][R]			
EP	3	5	10	13	16	17	20	1.23 h	01:15:24	k3k5k6k(-1)k(-8)k(-9)k(-10)[B][R]			
EP	3	5	12	13	16	17	20	1.23 h	01:15:24	k5k6k(-1)k(-2)k(-8)k(-9)k(-10)[B][R]			
EP	2	3	5	10	11	16	17	1.35 h	01:22:44	k2k3k5k6k(-7)k(-8)k(-9)[B][P]			
EP	2	3	5	10	11	16	19	1.35 h	01:22:45	k2k3k5k6k9k10k(-7)[B][P]			
EP	2	3	5	10	11	18	19	1.35 h	01:22:45	k2k3k5k6k9k10k(-7)[B][P]			
EP	2	3	5	10	13	16	17	1.35 h	01:22:45	k3k5k6k(-1)k(-7)k(-8)k(-9)[B][P]			
EP	2	3	5	10	13	18	19	1.35 h	01:22:45	k3k5k6k10k(-1)k(-7)k(-8)[B][P]			
EP	2	3	5	10	13	18	19	1.35 h	01:22:45	k3k5k6k9k10k(-1)k(-7)[B][P]			
EP	2	3	5	12	13	16	17	1.35 h	01:22:45	k5k6k(-1)k(-2)k(7)k(-8)k(-9)[B][P]			
EP	2	3	5	12	13	16	19	1.35 h	01:22:45	k5k6k10k(-1)k(-2)k(7)k(-8)[B][P]			
EP	2	3	5	12	13	18	19	1.35 h	01:22:45	k5k6k9k10k(-1)k(-2)k(7)[B][P]			
EP	2	3	7	10	11	16	17	1.35 h	01:22:45	k2k3k4k6k(-7)k(-8)[P]			
EP	2	3	7	10	11	16	19	1.35 h	01:22:45	k2k3k4k6k10k(-7)k(-8)[P]			
EP	2	3	7	10	11	18	19	1.35 h	01:22:45	k2k3k4k6k9k10k(-7)[P]			

Appendix A

Table A.2(d): (Cont.) Rate constant products from the proposed and simplified mechanisms

Complex	Possible reaction patterns							Time passed	Current Time	Valid pattern for all 20 reactions	Simplify Level 1 k(-3) = k(-7) = k(-10) = 0	Simplify Level 2 All reverse = 0, except k(-4)	Simplify Level 3 All reverse = 0
	One	Two	Three	Four	Five	Six	Seven						
EP	2	3	7	10	13	16	17	1.35 h	01:22:45	k3k4k6k(-1)k(-7)k(-8)k(-9)[P]			
EP	2	3	7	10	13	16	19	1.35 h	01:22:45	k3k4k6k10k(-1)k(-7)k(-8)[P]			
EP	2	3	7	10	13	18	19	1.35 h	01:22:45	k3k4k69k10k(-1)k(-7)[P]			
EP	2	3	7	12	13	16	17	1.35 h	01:22:45	k4k6k(-1)k(-2)k(-7)k(-8)k(-9)[P]			
EP	2	3	7	12	13	16	19	1.35 h	01:22:45	k4k6k10k(-1)k(-2)k(-7)k(-8)[P]			
EP	2	3	7	12	13	18	19	1.35 h	01:22:45	k4k6k9k10k(-1)k(-2)k(-7)[P]			
EP	2	3	9	12	13	16	17	1.35 h	01:22:46	k6k(-1)k(-2)k(-3)k(-7)k(-8)k(-9)[C][P]			
EP	2	3	9	12	13	16	19	1.35 h	01:22:46	k6k10k(-1)k(-2)k(-3)k(-7)k(-8)[C][P]			
EP	2	3	9	12	15	18	19	1.35 h	01:22:46	k6k9k10k(-1)k(-2)k(-3)k(-7)[C][P]			
EP	2	3	10	11	15	18	19	1.35 h	01:22:46	k2k3k6k8k9k10k(-7)[P][Q]			
EP	2	3	10	13	15	18	19	1.35 h	01:22:46	k3k6k8k9k10k(-1)k(-7)[P][Q]			
EP	2	3	12	13	15	18	19	1.35 h	01:22:46	k6k8k9k10k(-1)k(-2)k(-7)[P][Q]			
EQ	6	2	4	12	14	18	19	1.38 h	01:24:23	k9k10k(-1)k(-2)k(-5)k(-6)k(-7)[P]	k6k7k9k10k(-1)k(-2)k(-4)[Q]		
EQ	8	1	3	11	14	18	19	1.41 h	01:25:59	k6k7k9k10k(-1)k(-2)k(-4)[Q]	k1k2k3k6k7k9k10[A]		
EQ	10	1	3	12	13	17	20	1.43 h	01:27:36	k1k2k3k6k7k9k10[A]		k1k2k3k6k7k9k10[A]	k1k2k3k6k7k9k10[A]
EQ	16	1	3	12	13	17	20	1.46 h	01:29:12	k6k7k(-1)k(-2)k(-8)k(-9)k(-10)[R]			
EQ	6	8	1	12	13	18	19	1.48 h	01:30:36	k7k9k10k(-1)k(-2)k(-4)k(-5)[Q]	k7k9k10k(-1)k(-2)k(-4)k(-5)[Q]		
EQ	6	8	4	12	13	18	19	1.48 h	01:30:36	k9k10k(-1)k(-2)k(-4)k(-5)k(-6)[Q]	k9k10k(-1)k(-2)k(-4)k(-5)k(-6)[Q]		
EQ	6	10	1	11	14	18	19	1.51 h	01:32:00	k1k2k3k7k9k10k(-5)[A]	k1k2k3k7k9k10k(-5)[A]		
EQ	6	10	2	4	11	18	19	1.51 h	01:32:00	k2k3k9k10k(-5)k(-6)k(-7)[P]			
EQ	6	10	2	4	13	18	19	1.51 h	01:32:00	k3k9k10k(-1)k(-5)k(-6)k(-7)[P]			
EQ	6	10	4	11	14	18	19	1.51 h	01:32:00	k1k2k3k9k10k(-5)k(-6)[A]	k1k2k3k9k10k(-5)k(-6)[A]		
EQ	6	16	2	12	13	17	20	1.53 h	01:33:24	k7(-1)k(-2)k(-5)k(-8)k(-9)k(-10)[R]			
EQ	6	16	2	4	12	13	17	1.53 h	01:33:24	k(-1)k(-2)k(-5)k(-6)k(-7)k(-8)k(-9)[P]			
EQ	6	16	2	4	12	13	19	1.53 h	01:33:24	k10k(-1)k(-2)k(-5)k(-6)k(-7)k(-8)[P]			
EQ	6	16	4	12	13	17	20	1.53 h	01:33:24	k(-1)k(-2)k(-5)k(-6)k(-8)k(-9)k(-10)[R]			
EQ	8	10	1	3	11	18	19	1.55 h	01:34:47	k2k3k6k7k9k10k(-4)[Q]	k2k3k6k7k9k10k(-4)[Q]	k2k3k6k7k9k10k(-4)[Q]	
EQ	8	10	1	3	11	18	19	1.55 h	01:34:47	k3k6k7k9k10k(-1)k(-4)[Q]	k3k6k7k9k10k(-1)k(-4)[Q]		
EQ	8	16	1	3	12	13	17	1.58 h	01:36:11	k6k7k(-1)k(-2)k(-4)k(-8)k(-9)[Q]	k6k7k(-1)k(-2)k(-4)k(-8)k(-9)[Q]		
EQ	8	16	1	3	12	13	19	1.58 h	01:36:11	k6k7k10k(-1)k(-2)k(-4)k(-8)[Q]	k6k7k10k(-1)k(-2)k(-4)k(-8)[Q]		
EQ	10	16	1	3	11	14	17	1.60 h	01:37:35	k1k2k3k6k7k(-8)k(-9)[A]	k1k2k3k6k7k(-8)k(-9)[A]		
EQ	10	16	1	3	11	14	19	1.60 h	01:37:35	k1k2k3k6k7k10k(-8)[A]			
EQ	10	16	1	3	13	17	20	1.60 h	01:37:35	k3k6k7k(-1)k(-8)k(-9)k(-10)[R]			
EQ	6	8	10	1	11	18	19	1.62 h	01:38:29	k2k3k7k9k10k(-4)k(-5)[Q]	k2k3k7k9k10k(-4)k(-5)[Q]		
EQ	6	8	10	1	13	18	20	1.62 h	01:38:29	k3k7k9k10k(-1)k(-4)k(-5)[Q]	k3k7k9k10k(-1)k(-4)k(-5)[Q]		
EQ	6	8	10	4	11	18	19	1.62 h	01:38:29	k2k3k9k10k(-4)k(-5)k(-6)[Q]	k2k3k9k10k(-4)k(-5)k(-6)[Q]		
EQ	6	8	10	4	13	18	19	1.62 h	01:38:29	k3k9k10k(-1)k(-4)k(-5)k(-6)[Q]	k3k9k10k(-1)k(-4)k(-5)k(-6)[Q]		
EQ	6	8	16	1	12	13	17	1.63 h	01:39:24	k7k(-1)k(-2)k(-4)k(-5)k(-8)k(-9)[Q]	k7k(-1)k(-2)k(-4)k(-5)k(-8)k(-9)[Q]		
EQ	6	8	16	1	12	13	19	1.63 h	01:39:24	k7k10k(-1)k(-2)k(-4)k(-5)k(-8)[Q]	k7k10k(-1)k(-2)k(-4)k(-5)k(-8)[Q]		
EQ	6	8	16	4	12	13	17	1.63 h	01:39:24	k(-1)k(-2)k(-4)k(-5)k(-6)k(-8)k(-9)[Q]	k(-1)k(-2)k(-4)k(-5)k(-6)k(-8)k(-9)[Q]		
EQ	6	8	16	4	12	13	19	1.63 h	01:39:24	k10k(-1)k(-2)k(-4)k(-5)k(-6)k(-8)[Q]	k10k(-1)k(-2)k(-4)k(-5)k(-6)k(-8)[Q]		
EQ	6	10	16	1	11	14	17	1.65 h	01:40:18	k1k2k3k7k(-5)k(-8)k(-9)[A]	k1k2k3k7k(-5)k(-8)k(-9)[A]		
EQ	6	10	16	1	11	14	19	1.65 h	01:40:18	k1k2k3k7k10k(-5)k(-8)[A]	k1k2k3k7k10k(-5)k(-8)[A]		
EQ	6	10	16	1	13	17	20	1.65 h	01:40:18	k2k3k7k(-5)k(-8)k(-9)k(-10)[R]			
EQ	6	10	16	1	13	17	20	1.65 h	01:40:19	k3k7k(-1)k(-5)k(-8)k(-9)k(-10)[R]			
EQ	6	10	16	2	4	11	17	1.65 h	01:40:19	k2k3k(-5)k(-6)k(-7)k(-8)k(-9)[P]			
EQ	6	10	16	2	4	11	19	1.65 h	01:40:19	k2k3k10k(-5)k(-6)k(-7)k(-8)[P]			
EQ	6	10	16	2	4	13	17	1.65 h	01:40:19	k3k(-1)k(-5)k(-6)k(-7)k(-8)k(-9)[P]			
EQ	6	10	16	2	4	13	19	1.65 h	01:40:19	k3k10k(-1)k(-5)k(-6)k(-7)k(-8)[P]			

Appendix A

Table A.2(e): (Cont.) Rate constant products from the proposed and simplified mechanisms

Complex	One	Two	Three	Four	Five	Six	Seven	Time passed	Current Time	Valid pattern for all 20 reactions	Simplify Level 1 k(-3) = k(-7) = k(-10) = 0	Simplify Level 2 All reverse = 0, except k(-4)	Simplify Level 3 All reverse = 0
EQ	6	10	16	4	11	14	17	1.65 h	01:40:19	k1k2k3k(-5)k(-6)k(-8)k(-9)[A]	k1k2k3k(-5)k(-6)k(-8)k(-9)[A]		
EQ	6	10	16	4	11	14	19	1.65 h	01:40:19	k1k2k3k10k(-5)k(-6)k(-8)[A]	k1k2k3k10k(-5)k(-6)k(-8)[A]		
EQ	6	10	16	4	11	17	20	1.65 h	01:40:19	k2k3k(-5)k(-6)k(-8)k(-9)k(-10)[R]			
EQ	6	10	16	4	13	17	20	1.65 h	01:40:19	k3k(-1)k(-5)k(-6)k(-8)k(-9)k(-10)[R]			
EQ	8	10	16	1	3	11	17	1.66 h	01:41:13	k2k3k6k7k(-4)k(-8)k(-9)[Q]	k2k3k6k7k(-4)k(-8)k(-9)[Q]		
EQ	8	10	16	1	3	11	19	1.66 h	01:41:13	k2k3k6k7k10k(-4)k(-8)[Q]	k2k3k6k7k10k(-4)k(-8)[Q]		
EQ	8	10	16	1	3	13	17	1.66 h	01:41:14	k3k6k7k(-1)k(-4)k(-8)k(-9)[Q]	k3k6k7k(-1)k(-4)k(-8)k(-9)[Q]		
EQ	8	10	16	1	3	13	19	1.66 h	01:41:14	k3k6k7k10k(-1)k(-4)k(-8)[Q]	k3k6k7k10k(-1)k(-4)k(-8)[Q]		
EQ	6	8	10	16	1	11	17	1.67 h	01:41:41	k2k3k7k(-4)k(-5)k(-8)k(-9)[Q]	k2k3k7k(-4)k(-5)k(-8)k(-9)[Q]		
EQ	6	8	10	16	1	13	19	1.67 h	01:41:41	k3k7k10k(-1)k(-4)k(-5)k(-8)[Q]	k3k7k10k(-1)k(-4)k(-5)k(-8)[Q]		
EQ	6	8	10	16	4	11	17	1.67 h	01:41:41	k2k3k(-4)k(-5)k(-6)k(-8)k(-9)[Q]	k2k3k(-4)k(-5)k(-6)k(-8)k(-9)[Q]		
EQ	6	8	10	16	4	11	19	1.67 h	01:41:41	k2k3k10k(-4)k(-5)k(-6)k(-8)[Q]	k2k3k10k(-4)k(-5)k(-6)k(-8)[Q]		
EQ	6	8	10	16	4	13	17	1.67 h	01:41:41	k3k(-1)k(-4)k(-5)k(-6)k(-8)k(-9)[Q]	k3k(-1)k(-4)k(-5)k(-6)k(-8)k(-9)[Q]		
EQ	6	8	10	16	4	13	19	1.67 h	01:41:41	k3k10k(-1)k(-4)k(-5)k(-6)k(-8)[Q]	k3k10k(-1)k(-4)k(-5)k(-6)k(-8)[Q]		
EQ	18	1	3	8	10	11	15	1.89 h	01:55:10	k2k3k6k7k8k9k(-4)[Q][Q]	k2k3k6k7k8k9k(-4)[Q][Q]	k2k3k6k7k8k9k(-4)[Q][Q]	
ER	18	1	3	8	10	13	15	1.89 h	01:55:10	k3k6k7k8k9k(-1)k(-4)[Q][Q]	k3k6k7k8k9k(-1)k(-4)[Q][Q]		
ER	18	1	3	8	11	14	15	1.89 h	01:55:10	k6k7k8k9k(-1)k(-2)k(-4)[Q][Q]	k6k7k8k9k(-1)k(-2)k(-4)[Q][Q]		
ER	18	1	3	10	11	14	15	1.89 h	01:55:10	k1k2k3k6k7k8k9[A][Q]	k1k2k3k6k7k8k9[A][Q]	k1k2k3k6k7k8k9[A][Q]	k1k2k3k6k7k8k9[A][Q]
ER	18	2	4	6	10	13	15	1.89 h	01:55:10	k2k3k7k8k9k(-4)k(-5)[Q][Q]	k2k3k7k8k9k(-4)k(-5)[Q][Q]		
ER	18	2	4	6	10	13	15	1.89 h	01:55:11	k3k7k8k9k(-1)k(-4)k(-5)[Q][Q]	k3k7k8k9k(-1)k(-4)k(-5)[Q][Q]		
ER	18	2	4	6	11	14	15	1.89 h	01:55:11	k7k8k9k(-1)k(-2)k(-4)k(-5)[Q][Q]	k7k8k9k(-1)k(-2)k(-4)k(-5)[Q][Q]		
ER	18	2	4	10	11	14	15	1.89 h	01:55:11	k1k2k3k8k9k(-5)[A][Q]	k1k2k3k8k9k(-5)[A][Q]		
ER	18	2	4	6	10	13	15	1.89 h	01:55:11	k2k3k8k9k(-5)k(-6)k(-7)[P][Q]			
ER	18	2	4	6	10	13	15	1.89 h	01:55:11	k8k9k(-1)k(-2)k(-5)k(-6)k(-7)[P][Q]			
ER	18	4	6	8	10	13	15	1.89 h	01:55:11	k2k3k8k9k(-4)k(-5)k(-6)[Q][Q]	k2k3k8k9k(-4)k(-5)k(-6)[Q][Q]		
ER	18	4	6	8	12	13	15	1.89 h	01:55:11	k3k8k9k(-1)k(-4)k(-5)k(-6)[Q][Q]	k3k8k9k(-1)k(-4)k(-5)k(-6)[Q][Q]		
ER	18	4	6	8	10	11	15	1.89 h	01:55:11	k8k9k(-1)k(-2)k(-4)k(-5)k(-6)[Q][Q]	k8k9k(-1)k(-2)k(-4)k(-5)k(-6)[Q][Q]		
ER	18	4	6	10	11	14	15	1.89 h	01:55:11	k1k2k3k8k9k(-5)k(-6)[A][Q]	k1k2k3k8k9k(-5)k(-6)[A][Q]		
ER	20	1	3	5	10	13	16	2.12 h	02:08:36	k2k3k5k6k7k(-8)k(-10)[B][R]			
ER	20	1	3	5	10	13	16	2.12 h	02:08:36	k3k5k6k7k(-1)k(-8)k(-10)[B][R]			
ER	20	1	3	5	12	13	16	2.12 h	02:08:36	k5k6k7k(-1)k(-2)k(-8)k(-10)[B][R]			
ER	20	1	3	7	10	11	16	2.12 h	02:08:36	k2k3k4k6k7k(-8)k(-10)[R]			
ER	20	1	3	7	10	13	16	2.12 h	02:08:36	k4k6k7k(-1)k(-8)k(-10)[R]			
ER	20	1	3	9	12	13	16	2.12 h	02:08:36	k4k6k7k(-1)k(-2)k(-8)k(-10)[R]			
ER	20	1	6	7	10	13	16	2.12 h	02:08:37	k6k7k(-1)k(-2)k(-3)k(-8)k(-10)[C][R]			
ER	20	1	6	7	12	13	16	2.12 h	02:08:37	k2k3k4k7k(-5)k(-8)k(-10)[R]			
ER	20	1	6	7	10	11	16	2.12 h	02:08:37	k4k7k(-1)k(-5)k(-8)k(-10)[R]			
ER	20	1	6	7	12	13	16	2.12 h	02:08:37	k4k7k(-1)k(-2)k(-5)k(-8)k(-10)[R]			
ER	20	1	6	9	12	13	16	2.12 h	02:08:37	k7k(-1)k(-2)k(-3)k(-5)k(-8)k(-10)[C][R]			
ER	20	1	6	7	11	14	16	2.12 h	02:08:37	k2k3k4k(-5)k(-6)k(-8)k(-10)[R]			
ER	20	4	6	7	10	13	16	2.12 h	02:08:37	k3k4k(-1)k(-5)k(-6)k(-8)k(-10)[R]			
ER	20	4	6	7	12	13	16	2.12 h	02:08:37	k4k(-1)k(-2)k(-5)k(-6)k(-8)k(-10)[R]			
ER	20	4	6	7	10	13	16	2.12 h	02:08:37	k(-1)k(-2)k(-3)k(-5)k(-6)k(-8)k(-10)[C][R]			
ER	18	20	1	3	5	10	11	2.24 h	02:16:01	k2k3k5k6k7k9k(-10)[B][R]			
ER	18	20	1	3	5	10	13	2.24 h	02:16:01	k3k5k6k7k9k(-1)k(-10)[B][R]			
ER	18	20	1	3	5	12	13	2.24 h	02:16:01	k5k6k7k9k(-1)k(-2)k(-10)[B][R]			
ER	18	20	1	3	7	10	11	2.24 h	02:16:01	k2k3k4k6k7k9k(-10)[R]			

Appendix A

Table A.2(f): (Cont.) Rate constant products from the proposed and simplified mechanisms

Complex	Possible reaction patterns							Time passed	Current Time	Valid pattern for all 20 reactions	Simplify Level 1 k(-3) = k(-7) = k(-10) = 0	Simplify Level 2 All reverse = 0, except k(-4)	Simplify Level 3 All reverse = 0
	One	Two	Three	Four	Five	Six	Seven						
ER	18	20	1	3	7	10	13	2.24 h	02:16:01	k3k4k6k7k9k(-1)k(-10)[R]			
ER	18	20	1	3	7	12	13	2.24 h	02:16:01	k4k6k7k9k(-1)k(-2)k(-10)[R]			
ER	18	20	1	3	9	12	13	2.24 h	02:16:01	k6k7k9k(-1)k(-2)k(-3)k(-10)[C][R]			
ER	18	20	1	3	10	11	15	2.24 h	02:16:01	k2k3k6k7k8k9k(-10)[Q][R]			
ER	18	20	1	3	10	13	15	2.24 h	02:16:01	k3k6k7k8k9k(-1)k(-10)[Q][R]			
ER	18	20	1	3	12	13	15	2.24 h	02:16:02	k6k7k8k9k(-1)k(-2)k(-10)[Q][R]			
ER	18	20	1	6	7	10	11	2.24 h	02:16:02	k2k3k4k7k9k(-5)k(-10)[R]			
ER	18	20	1	6	7	10	13	2.24 h	02:16:02	k3k4k7k9k(-1)k(-5)k(-10)[R]			
ER	18	20	1	6	7	12	13	2.24 h	02:16:02	k4k7k9k(-1)k(-2)k(-5)k(-10)[R]			
ER	18	20	1	6	9	12	13	2.24 h	02:16:02	k7k9k(-1)k(-2)k(-3)k(-5)k(-10)[C][R]			
ER	18	20	1	6	10	11	15	2.24 h	02:16:02	k2k3k7k8k9k(-5)k(-10)[Q][R]			
ER	18	20	1	6	10	13	15	2.24 h	02:16:02	k3k7k8k9k(-1)k(-5)k(-10)[Q][R]			
ER	18	20	4	6	7	10	13	2.24 h	02:16:02	k7k8k9k(-1)k(-2)k(-5)k(-10)[Q][R]			
ER	18	20	4	6	7	12	13	2.24 h	02:16:02	k2k3k4k9k(-5)k(-6)k(-10)[R]			
ER	18	20	4	6	9	12	13	2.24 h	02:16:02	k3k4k9k(-1)k(-5)k(-6)k(-10)[R]			
ER	18	20	4	6	7	12	13	2.24 h	02:16:03	k4k9k(-1)k(-2)k(-5)k(-6)k(-10)[R]			
ER	18	20	4	6	9	12	13	2.24 h	02:16:03	k9(-1)k(2)k(3)k(-5)k(-6)k(-10)[C][R]			
ER	18	20	4	6	10	11	15	2.24 h	02:16:03	k2k3k8k9k(-5)k(-6)k(-10)[Q][R]			
ER	18	20	4	6	10	13	15	2.24 h	02:16:03	k3k8k9k(-1)k(-5)k(-6)k(-10)[Q][R]			
ER	18	20	4	6	12	13	15	2.24 h	02:16:03	k8k9k(-1)k(-2)k(-5)k(-6)k(-10)[Q][R]			
EQB	4	2	7	10	11	16	17	2.47 h	02:29:32	k2k3k4k(-6)k(-7)k(-8)k(-9)[P]			
EQB	4	2	7	10	11	16	19	2.47 h	02:29:32	k2k3k4k10k(-6)k(-7)k(-8)[P]			
EQB	4	2	7	10	11	18	19	2.47 h	02:29:32	k2k3k4k9k10k(-6)k(-7)[P]			
EQB	4	2	7	10	13	16	17	2.47 h	02:29:32	k3k4k(-1)k(-6)k(-7)k(-8)k(-9)[P]			
EQB	4	2	7	10	13	16	19	2.47 h	02:29:32	k3k4k10k(-1)k(-6)k(-7)k(-8)[P]			
EQB	4	2	7	10	13	18	19	2.47 h	02:29:32	k3k4k9k10k(-1)k(-6)k(-7)[P]			
EQB	4	2	7	12	13	16	17	2.47 h	02:29:33	k4k(-1)k(-2)k(-6)k(-7)k(-8)k(-9)[P]			
EQB	4	2	7	12	13	16	19	2.47 h	02:29:33	k4k10k(-1)k(-2)k(-6)k(-7)k(-8)[P]			
EQB	4	2	7	12	13	18	19	2.47 h	02:29:33	k4k9k10k(-1)k(-2)k(-6)k(-7)[P]			
EQB	4	2	9	12	13	16	17	2.47 h	02:29:33	k(-1)k(-2)k(3)k(-6)k(-7)k(-8)k(-9)[C][P]			
EQB	4	2	9	12	13	16	19	2.47 h	02:29:33	k10k(-1)k(-2)k(-3)k(-6)k(-7)k(-8)[C][P]			
EQB	4	2	9	12	13	18	19	2.47 h	02:29:33	k9k10k(-1)k(-2)k(-3)k(-6)k(-7)[C][P]			
EQB	4	2	10	11	15	18	19	2.47 h	02:29:33	k2k3k8k9k10k(-6)k(-7)[P][Q]			
EQB	4	2	10	13	15	18	19	2.47 h	02:29:33	k3k8k9k10k(-1)k(-6)k(-7)[P][Q]			
EQB	4	2	12	13	15	18	19	2.47 h	02:29:34	k8k9k10k(-1)k(-2)k(-6)k(-7)[P][Q]			
EQB	5	1	8	10	11	16	17	2.69 h	02:42:55	k2k3k5k7k(-4)k(-8)k(-9)[B][Q]	k2k3k5k7k(-4)k(-8)k(-9)[B][Q]		
EQB	5	1	8	10	11	16	19	2.69 h	02:42:55	k2k3k5k7k10k(-4)k(-8)[B][Q]	k2k3k5k7k10k(-4)k(-8)[B][Q]		
EQB	5	1	8	10	11	18	19	2.69 h	02:42:55	k2k3k5k7k9k10k(-4)[B][Q]	k2k3k5k7k9k10k(-4)[B][Q]	k2k3k5k7k9k10k(-4)[B][Q]	
EQB	5	1	8	10	13	16	17	2.69 h	02:42:55	k3k5k7k(-1)k(-4)k(-8)k(-9)[B][Q]	k3k5k7k(-1)k(-4)k(-8)k(-9)[B][Q]		
EQB	5	1	8	10	13	16	19	2.69 h	02:42:56	k3k5k7k10k(-1)k(-4)k(-8)[B][Q]	k3k5k7k10k(-1)k(-4)k(-8)[B][Q]		
EQB	5	1	8	10	13	18	19	2.69 h	02:42:56	k3k5k7k9k10k(-1)k(-4)[B][Q]	k3k5k7k9k10k(-1)k(-4)[B][Q]		
EQB	5	1	8	12	13	16	17	2.69 h	02:42:56	k5k7k(-1)k(-2)k(-4)k(-8)k(-9)[B][Q]	k5k7k(-1)k(-2)k(-4)k(-8)k(-9)[B][Q]		
EQB	5	1	8	12	13	16	19	2.69 h	02:42:56	k5k7k10k(-1)k(-2)k(-4)k(-8)[B][Q]	k5k7k10k(-1)k(-2)k(-4)k(-8)[B][Q]		
EQB	5	1	8	12	13	18	19	2.69 h	02:42:56	k5k7k9k10k(-1)k(-2)k(-4)[B][Q]	k5k7k9k10k(-1)k(-2)k(-4)[B][Q]		
EQB	5	1	10	11	14	16	17	2.69 h	02:42:56	k1k2k3k5k7k(-8)k(-9)[A][B]	k1k2k3k5k7k(-8)k(-9)[A][B]		
EQB	5	1	10	11	14	16	19	2.69 h	02:42:56	k1k2k3k5k7k10k(-8)[A][B]	k1k2k3k5k7k10k(-8)[A][B]		
EQB	5	1	10	11	14	18	19	2.69 h	02:42:56	k1k2k3k5k7k9k10[A][B]	k1k2k3k5k7k9k10[A][B]	k1k2k3k5k7k9k10[A][B]	k1k2k3k5k7k9k10[A][B]
EQB	5	1	10	13	16	17	20	2.69 h	02:42:57	k3k5k7k(-1)k(-8)k(-9)k(-10)[B][R]			
EQB	5	1	12	13	16	17	20	2.69 h	02:42:57	k5k7k(-1)k(-2)k(-8)k(-9)k(-10)[B][R]			

Appendix A

Table A.2(g): (Cont.) Rate constant products from the proposed and simplified mechanisms

Complex	One	Two	Three	Four	Five	Six	Seven	Time passed	Current Time	Valid pattern for all 20 reactions	Simplify Level 1 k(-3) = k(-7) = k(-10) = 0	Simplify Level 2 All reverse = 0, except k(-4)	Simplify Level 3 All reverse = 0
EQB	4	5	2	10	11	16	17	2.81 h	02:50:20	k2k3k5k(-6)k(-7)k(-8)k(-9)[B][P]			
EQB	4	5	2	10	11	16	19	2.81 h	02:50:20	k2k3k5k10k(-6)k(-7)k(-8)[B][P]			
EQB	4	5	2	10	11	18	19	2.81 h	02:50:20	k2k3k5k9k10k(-6)k(-7)[B][P]			
EQB	4	5	2	10	13	16	17	2.81 h	02:50:20	k3k5k(-1)k(-6)k(-7)k(-8)k(-9)[B][P]			
EQB	4	5	2	10	13	16	19	2.81 h	02:50:21	k3k5k10k(-1)k(-6)k(-7)k(-8)[B][P]			
EQB	4	5	2	10	13	18	19	2.81 h	02:50:21	k3k5k9k10k(-1)k(-6)k(-7)[B][P]			
EQB	4	5	2	12	13	16	17	2.81 h	02:50:21	k5k(-1)k(-2)k(-6)k(-7)k(-8)k(-9)[B][P]			
EQB	4	5	2	12	13	16	19	2.81 h	02:50:21	k5k10k(-1)k(-2)k(-6)k(-7)k(-8)[B][P]			
EQB	4	5	2	12	13	18	19	2.81 h	02:50:21	k5k9k10k(-1)k(-2)k(-6)k(-7)[B][P]			
EQB	4	5	8	10	11	16	17	2.81 h	02:50:21	k2k3k5k(-4)k(-6)k(-8)k(-9)[B][Q]	k2k3k5k(-4)k(-6)k(-8)k(-9)[B][Q]		
EQB	4	5	8	10	11	16	19	2.81 h	02:50:21	k2k3k5k10k(-4)k(-6)k(-8)[B][Q]	k2k3k5k10k(-4)k(-6)k(-8)[B][Q]		
EQB	4	5	8	10	11	18	19	2.81 h	02:50:21	k2k3k5k9k10k(-4)k(-6)[B][Q]	k2k3k5k9k10k(-4)k(-6)[B][Q]		
EQB	4	5	8	10	13	16	17	2.81 h	02:50:21	k3k5k(-1)k(-4)k(-6)k(-8)k(-9)[B][Q]	k3k5k(-1)k(-4)k(-6)k(-8)k(-9)[B][Q]		
EQB	4	5	8	10	13	16	19	2.81 h	02:50:22	k3k5k10k(-1)k(-4)k(-6)k(-8)[B][Q]	k3k5k10k(-1)k(-4)k(-6)k(-8)[B][Q]		
EQB	4	5	8	10	13	18	19	2.81 h	02:50:22	k3k5k9k10k(-1)k(-4)k(-6)[B][Q]	k3k5k9k10k(-1)k(-4)k(-6)[B][Q]		
EQB	4	5	8	12	13	16	17	2.81 h	02:50:22	k5k(-1)k(-2)k(-4)k(-6)k(-8)k(-9)[B][Q]	k5k(-1)k(-2)k(-4)k(-6)k(-8)k(-9)[B][Q]		
EQB	4	5	8	12	13	16	19	2.81 h	02:50:22	k5k10k(-1)k(-2)k(-4)k(-6)k(-8)[B][Q]	k5k10k(-1)k(-2)k(-4)k(-6)k(-8)[B][Q]		
EQB	4	5	8	12	13	18	19	2.81 h	02:50:22	k5k9k10k(-1)k(-2)k(-4)k(-6)[B][Q]	k5k9k10k(-1)k(-2)k(-4)k(-6)[B][Q]		
EQB	4	5	10	11	14	16	17	2.81 h	02:50:22	k1k2k3k5k(-6)k(-8)k(-9)[A][B]	k1k2k3k5k(-6)k(-8)k(-9)[A][B]		
EQB	4	5	10	11	14	16	19	2.81 h	02:50:22	k1k2k3k5k10k(-6)k(-8)[A][B]	k1k2k3k5k10k(-6)k(-8)[A][B]		
EQB	4	5	10	11	14	18	19	2.81 h	02:50:22	k1k2k3k5k9k10k(-6)[A][B]	k1k2k3k5k9k10k(-6)[A][B]		
EQB	4	5	10	11	16	17	20	2.81 h	02:50:22	k2k3k5k(-6)k(-8)k(-9)k(-10)[B][R]			
EQB	4	5	10	13	16	17	20	2.81 h	02:50:23	k3k5k(-1)k(-6)k(-8)k(-9)k(-10)[B][R]			
EQB	4	5	12	13	16	17	20	2.81 h	02:50:23	k5k(-1)k(-2)k(-6)k(-8)k(-9)k(-10)[B][R]			
EQC	9	1	3	8	13	16	17	3.04 h	03:03:45	k6k7k(-1)k(-3)k(-4)k(-8)k(-9)[C][Q]			
EQC	9	1	3	8	13	16	19	3.04 h	03:03:45	k6k7k10k(-1)k(-3)k(-4)k(-8)[C][Q]			
EQC	9	1	3	8	13	18	19	3.04 h	03:03:45	k6k7k9k10k(-1)k(-3)k(-4)[C][Q]			
EQC	9	1	3	13	16	17	20	3.04 h	03:03:45	k6k7k9k10k(-10)[C][R]			
EQC	9	2	4	6	13	16	17	3.04 h	03:03:46	k(-1)k(-3)k(-5)k(-6)k(-7)k(-8)k(-9)[C][P]			
EQC	9	2	4	6	13	16	19	3.04 h	03:03:46	k10k(-1)k(-3)k(-5)k(-6)k(-7)k(-8)[C][P]			
EQC	9	2	4	6	13	18	19	3.04 h	03:03:46	k9k10k(-1)k(-3)k(-5)k(-6)k(-7)[C][P]			
EQC	9	4	6	8	13	16	17	3.04 h	03:03:46	k(-1)k(-3)k(-4)k(-5)k(-6)k(-8)k(-9)[C][Q]			
EQC	9	4	6	8	13	16	19	3.04 h	03:03:46	k10k(-1)k(-3)k(-4)k(-5)k(-6)k(-8)[C][Q]			
EQC	9	4	6	8	13	18	19	3.04 h	03:03:46	k9k10k(-1)k(-3)k(-4)k(-5)k(-6)[C][Q]			
EQC	9	4	6	13	16	17	20	3.04 h	03:03:46	k(-1)k(-3)k(-4)k(-5)k(-6)k(-8)k(-9)k(-10)[C][R]			
EQC	11	1	3	5	14	16	17	3.26 h	03:17:17	k1k2k5k6k7k(-8)k(-9)[A][B]	k1k2k5k6k7k(-8)k(-9)[A][B]		
EQC	11	1	3	5	14	16	19	3.26 h	03:17:17	k1k2k5k6k7k10k(-8)[A][B]	k1k2k5k6k7k10k(-8)[A][B]		
EQC	11	1	3	5	14	18	19	3.26 h	03:17:17	k1k2k5k6k7k9k10[A][B]	k1k2k5k6k7k9k10[A][B]	k1k2k5k6k7k9k10[A][B]	k1k2k5k6k7k9k10[A][B]
EQC	11	1	3	7	14	16	17	3.26 h	03:17:18	k1k2k4k6k7k(-8)k(-9)[A]	k1k2k4k6k7k(-8)k(-9)[A]		
EQC	11	1	3	7	14	16	19	3.26 h	03:17:18	k1k2k4k6k7k10k(-8)[A]	k1k2k4k6k7k10k(-8)[A]		
EQC	11	1	3	7	14	18	19	3.26 h	03:17:18	k1k2k4k6k7k9k10[A]	k1k2k4k6k7k9k10[A]	k1k2k4k6k7k9k10[A]	k1k2k4k6k7k9k10[A]
EQC	11	1	3	14	15	18	19	3.26 h	03:17:18	k1k2k6k7k8k9k10[A][Q]	k1k2k6k7k8k9k10[A][Q]	k1k2k6k7k8k9k10[A][Q]	k1k2k6k7k8k9k10[A][Q]
EQC	11	1	6	7	14	16	17	3.26 h	03:17:18	k1k2k4k7k(-5)k(-8)k(-9)[A]	k1k2k4k7k(-5)k(-8)k(-9)[A]		
EQC	11	1	6	7	14	16	19	3.26 h	03:17:18	k1k2k4k7k10k(-5)k(-8)[A]	k1k2k4k7k10k(-5)k(-8)[A]		
EQC	11	1	6	7	14	18	19	3.26 h	03:17:18	k1k2k4k7k9k10k(-5)[A]	k1k2k4k7k9k10k(-5)[A]		
EQC	11	1	6	14	15	18	19	3.26 h	03:17:18	k1k2k7k8k9k10k(-5)[A][Q]	k1k2k7k8k9k10k(-5)[A][Q]		

Table A.2(h): (Cont.) Rate constant products from the proposed and simplified mechanisms

Complex	One	Two	Three	Four	Five	Six	Seven	Time passed	Current Time	Valid pattern for all 20 reactions	Simplify Level 1 k(-3) = k(-7) = k(-10) = 0	Simplify Level 2 All reverse = 0, except k(-4)	Simplify Level 3 All reverse = 0
EQC	11	4	6	7	14	16	17	3.26 h	03:17:19	k1k2k4k(-5)k(-6)k(-8)k(-9)[A]	k1k2k4k(-5)k(-6)k(-8)k(-9)[A]		
EQC	11	4	6	7	14	16	19	3.26 h	03:17:19	k1k2k4k10k(-5)k(-6)k(-8)[A]	k1k2k4k10k(-5)k(-6)k(-8)[A]		
EQC	11	4	6	7	14	18	19	3.26 h	03:17:19	k1k2k4k9k10k(-5)k(-6)[A]	k1k2k4k9k10k(-5)k(-6)[A]		
EQC	11	4	6	14	15	18	19	3.26 h	03:17:19	k1k2k8k9k10k(-5)k(-6)[A][Q]	k1k2k8k9k10k(-5)k(-6)[A][Q]		
EQC	9	11	1	3	8	16	17	3.39 h	03:24:39	k2k6k7k(-3)k(-4)k(-8)k(-9)[C][Q]			
EQC	9	11	1	3	8	16	19	3.39 h	03:24:39	k2k6k7k10k(-3)k(-4)k(-8)[C][Q]			
EQC	9	11	1	3	8	18	19	3.39 h	03:24:39	k2k6k7k9k10k(-3)k(-4)[C][Q]			
EQC	9	11	1	3	14	16	17	3.39 h	03:24:39	k1k2k6k7k(-3)k(-8)k(-9)[A][C]			
EQC	9	11	1	3	14	16	19	3.39 h	03:24:39	k1k2k6k7k10k(-3)k(-8)[A][C]			
EQC	9	11	1	3	14	18	19	3.39 h	03:24:39	k1k2k6k7k9k10k(-3)[A][C]			
EQC	9	11	1	3	16	17	20	3.39 h	03:24:40	k2k6k7k(-3)k(-8)k(-9)k(-10)[C][R]			
EQC	9	11	1	6	8	16	17	3.39 h	03:24:40	k2k7k(-3)k(-4)k(-5)k(-8)k(-9)[C][Q]			
EQC	9	11	1	6	8	16	19	3.39 h	03:24:40	k2k7k10k(-3)k(-4)k(-5)k(-8)[C][Q]			
EQC	9	11	1	6	8	18	19	3.39 h	03:24:40	k2k7k9k10k(-3)k(-4)k(-5)[C][Q]			
EQC	9	11	1	6	14	16	17	3.39 h	03:24:40	k1k2k7k(-3)k(-5)k(-8)k(-9)[A][C]			
EQC	9	11	1	6	14	16	19	3.39 h	03:24:40	k1k2k7k10k(-3)k(-5)k(-8)[A][C]			
EQC	9	11	1	6	14	18	19	3.39 h	03:24:40	k1k2k7k9k10k(-3)k(-5)[A][C]			
EQC	9	11	1	6	16	17	20	3.39 h	03:24:40	k2k7k(-3)k(-5)k(-8)k(-9)k(-10)[C][R]			
EQC	9	11	2	4	6	16	17	3.39 h	03:24:41	k2k(-3)k(-5)k(-6)k(-7)k(-8)k(-9)[C][P]			
EQC	9	11	2	4	6	16	19	3.39 h	03:24:41	k2k10k(-3)k(-5)k(-6)k(-7)k(-8)[C][P]			
EQC	9	11	2	4	6	18	19	3.39 h	03:24:41	k2k9k10k(-3)k(-5)k(-6)k(-7)[C][P]			
EQC	9	11	4	6	8	16	17	3.39 h	03:24:41	k2k(-3)k(-4)k(-5)k(-6)k(-8)k(-9)[C][Q]			
EQC	9	11	4	6	8	16	19	3.39 h	03:24:41	k2k10k(-3)k(-4)k(-5)k(-6)k(-8)[C][Q]			
EQC	9	11	4	6	8	18	19	3.39 h	03:24:41	k2k9k10k(-3)k(-4)k(-5)k(-6)[C][Q]			
EQC	9	11	4	6	14	16	17	3.39 h	03:24:41	k1k2k(-3)k(-5)k(-6)k(-8)k(-9)[A][C]			
EQC	9	11	4	6	14	16	19	3.39 h	03:24:41	k1k2k10k(-3)k(-5)k(-6)k(-8)[A][C]			
EQC	9	11	4	6	16	17	20	3.39 h	03:24:42	k2k(-3)k(-5)k(-6)k(-8)k(-9)k(-10)[C][R]			
EQQ	15	1	3	8	10	11	19	3.61 h	03:38:09	k2k3k6k7k8k10k(-4)[Q][Q]	k2k3k6k7k8k10k(-4)[Q][Q]	k2k3k6k7k8k10k(-4)[Q][Q]	
EQQ	15	1	3	8	10	13	19	3.61 h	03:38:09	k3k6k7k8k10k(-1)k(-4)[Q][Q]	k3k6k7k8k10k(-1)k(-4)[Q][Q]		
EQQ	15	1	8	8	12	13	19	3.61 h	03:38:09	k6k7k8k10k(-1)k(-2)k(-4)[Q][Q]	k6k7k8k10k(-1)k(-2)k(-4)[Q][Q]		
EQQ	15	1	3	10	11	14	19	3.61 h	03:38:09	k1k2k3k6k7k8k10[A][Q]	k1k2k3k6k7k8k10[A][Q]	k1k2k3k6k7k8k10[A][Q]	k1k2k3k6k7k8k10[A][Q]
EQQ	15	1	6	8	10	11	19	3.61 h	03:38:10	k2k3k7k8k10k(-4)k(-5)[Q][Q]	k2k3k7k8k10k(-4)k(-5)[Q][Q]		
EQQ	15	1	6	8	10	13	19	3.61 h	03:38:10	k3k7k8k10k(-1)k(-4)k(-5)[Q][Q]	k3k7k8k10k(-1)k(-4)k(-5)[Q][Q]		
EQQ	15	1	6	8	12	13	19	3.61 h	03:38:10	k7k8k10k(-1)k(-2)k(-4)k(-5)[Q][Q]	k7k8k10k(-1)k(-2)k(-4)k(-5)[Q][Q]		
EQQ	15	1	6	10	11	14	19	3.61 h	03:38:10	k1k2k3k7k8k10k(-5)[A][Q]	k1k2k3k7k8k10k(-5)[A][Q]		
EQQ	15	2	4	6	10	11	19	3.61 h	03:38:10	k2k3k8k10k(-5)k(-6)k(-7)[P][Q]			
EQQ	15	2	4	6	10	13	19	3.61 h	03:38:10	k3k8k10k(-1)k(-5)k(-6)k(-7)[P][Q]			
EQQ	15	4	6	8	10	11	19	3.61 h	03:38:10	k2k3k8k10k(-4)k(-5)k(-6)[Q][Q]	k2k3k8k10k(-4)k(-5)k(-6)[Q][Q]		
EQQ	15	4	6	8	10	13	19	3.61 h	03:38:11	k3k8k10k(-1)k(-4)k(-5)k(-6)[Q][Q]	k3k8k10k(-1)k(-4)k(-5)k(-6)[Q][Q]		
EQQ	15	4	6	8	12	13	19	3.61 h	03:38:11	k8k10k(-1)k(-2)k(-4)k(-5)k(-6)[Q][Q]	k8k10k(-1)k(-2)k(-4)k(-5)k(-6)[Q][Q]		
EQQ	15	4	6	10	11	14	19	3.61 h	03:38:11	k1k2k3k8k10k(-5)k(-6)[A][Q]	k1k2k3k8k10k(-5)k(-6)[A][Q]		
EQQ	17	1	3	5	10	11	20	3.84 h	03:51:40	k3k5k6k7k(-9)k(-10)[B][R]			
EQQ	17	1	3	5	10	13	20	3.84 h	03:51:40	k3k5k6k7k(-1)k(-9)k(-10)[B][R]			
EQQ	17	1	3	5	12	13	20	3.84 h	03:51:40	k5k6k7k(-1)k(-2)k(-9)k(-10)[B][R]			
EQQ	17	1	3	7	10	11	20	3.84 h	03:51:40	k2k3k4k6k7k(-9)k(-10)[R]			
EQQ	17	1	3	7	10	13	20	3.84 h	03:51:40	k3k4k6k7k(-1)k(-9)k(-10)[R]			
EQQ	17	1	3	7	12	13	20	3.84 h	03:51:41	k4k6k7k(-1)k(-2)k(-9)k(-10)[R]			
EQQ	17	1	3	9	10	13	20	3.84 h	03:51:41	k6k7k(-1)k(-2)k(-3)k(-9)k(-10)[C][R]			

Appendix A

Table A.2(i): (Cont.) Rate constant products from the proposed and simplified mechanisms

Complex	Possible reaction patterns							Time passed	Current Time	Valid pattern for all 20 reactions	Simplify Level 1 k(-3) = k(-7) = k(-10) = 0	Simplify Level 2 All reverse = 0, except k(-4)	Simplify Level 3 All reverse = 0
	One	Two	Three	Four	Five	Six	Seven						
EQQ	17	1	6	7	10	11	20	3.84 h	03:51:41	k2k3k4k7k(-5)k(-9)k(-10)[R]			
EQQ	17	1	6	7	10	13	20	3.84 h	03:51:41	k3k4k7k(-1)k(-5)k(-9)k(-10)[R]			
EQQ	17	1	6	7	12	13	20	3.84 h	03:51:41	k4k7k(-1)k(-2)k(-5)k(-9)k(-10)[R]			
EQQ	17	1	6	9	12	13	20	3.84 h	03:51:41	k7k(-1)k(-2)k(-3)k(-5)k(-9)k(-10)[C][R]			
EQQ	17	4	6	7	10	11	20	3.84 h	03:51:41	k2k3k4k(-5)k(-6)k(-9)k(-10)[R]			
EQQ	17	4	6	7	10	13	20	3.84 h	03:51:41	k3k4k(-1)k(-5)k(-6)k(-9)k(-10)[R]			
EQQ	17	4	6	7	12	13	20	3.84 h	03:51:42	k4k(-1)k(-2)k(-5)k(-6)k(-9)k(-10)[R]			
EQQ	17	4	6	9	12	13	20	3.84 h	03:51:42	k(-1)k(-2)k(-3)k(-5)k(-6)k(-9)k(-10)[C][R]			
EQQ	15	17	1	3	8	10	11	3.96 h	03:59:05	k2k3k6k7k8k(-4)k(-9)[Q][Q]	k2k3k6k7k8k(-4)k(-9)[Q][Q]		
EQQ	15	17	1	3	8	10	13	3.96 h	03:59:05	k3k6k7k8k(-1)k(-4)k(-9)[Q][Q]	k3k6k7k8k(-1)k(-4)k(-9)[Q][Q]		
EQQ	15	17	1	3	8	12	13	3.96 h	03:59:05	k6k7k8k(-1)k(-2)k(-4)k(-9)[Q][Q]	k6k7k8k(-1)k(-2)k(-4)k(-9)[Q][Q]		
EQQ	15	17	1	3	10	11	14	3.96 h	03:59:05	k1k2k3k6k7k8k(-9)[A][Q]	k1k2k3k6k7k8k(-9)[A][Q]		
EQQ	15	17	1	3	10	13	20	3.96 h	03:59:05	k2k3k6k7k8k(-9)k(-10)[Q][R]			
EQQ	15	17	1	3	10	13	20	3.96 h	03:59:05	k3k6k7k8k(-1)k(-9)k(-10)[Q][R]			
EQQ	15	17	1	3	12	13	20	3.96 h	03:59:05	k6k7k8k(-1)k(-2)k(-9)k(-10)[Q][R]			
EQQ	15	17	1	6	8	10	11	3.96 h	03:59:05	k2k3k7k8k(-4)k(-5)k(-9)[Q][Q]	k2k3k7k8k(-4)k(-5)k(-9)[Q][Q]		
EQQ	15	17	1	6	8	10	13	3.96 h	03:59:05	k3k7k8k(-1)k(-4)k(-5)k(-9)[Q][Q]	k3k7k8k(-1)k(-4)k(-5)k(-9)[Q][Q]		
EQQ	15	17	1	6	8	12	13	3.96 h	03:59:06	k7k8k(-1)k(-2)k(-4)k(-5)k(-9)[Q][Q]	k7k8k(-1)k(-2)k(-4)k(-5)k(-9)[Q][Q]		
EQQ	15	17	1	6	10	11	14	3.96 h	03:59:06	k1k2k3k7k8k(-5)k(-9)[A][Q]	k1k2k3k7k8k(-5)k(-9)[A][Q]		
EQQ	15	17	1	6	10	11	20	3.96 h	03:59:06	k2k3k7k8k(-5)k(-9)k(-10)[Q][R]			
EQQ	15	17	1	6	10	13	20	3.96 h	03:59:06	k3k7k8k(-1)k(-5)k(-9)k(-10)[Q][R]			
EQQ	15	17	1	6	12	13	20	3.96 h	03:59:06	k7k8k(-1)k(-2)k(-5)k(-9)k(-10)[Q][R]			
EQQ	15	17	2	4	6	10	11	3.96 h	03:59:06	k2k3k8k(-5)k(-6)k(-7)k(-9)[P][Q]			
EQQ	15	17	2	4	6	10	13	3.96 h	03:59:07	k3k8k(-1)k(-2)k(-5)k(-6)k(-7)k(-9)[P][Q]			
EQQ	15	17	2	4	6	12	13	3.96 h	03:59:07	k8k(-1)k(-2)k(-5)k(-6)k(-7)k(-9)[P][Q]			
EQQ	15	17	4	6	8	10	11	3.96 h	03:59:07	k2k3k8k(-4)k(-5)k(-6)k(-9)[Q][Q]	k2k3k8k(-4)k(-5)k(-6)k(-9)[Q][Q]		
EQQ	15	17	4	6	8	10	13	3.96 h	03:59:07	k3k8k(-1)k(-4)k(-5)k(-6)k(-9)[Q][Q]	k3k8k(-1)k(-4)k(-5)k(-6)k(-9)[Q][Q]		
EQQ	15	17	4	6	8	12	13	3.96 h	03:59:07	k8k(-1)k(-2)k(-4)k(-5)k(-6)k(-9)[Q][Q]	k8k(-1)k(-2)k(-4)k(-5)k(-6)k(-9)[Q][Q]		
EQQ	15	17	4	6	10	11	14	3.96 h	03:59:07	k1k2k3k8k(-5)k(-6)k(-9)[A][Q]	k1k2k3k8k(-5)k(-6)k(-9)[A][Q]		
EQQ	15	17	4	6	10	11	20	3.96 h	03:59:07	k2k3k8k(-5)k(-6)k(-9)k(-10)[Q][R]			
EQQ	15	17	4	6	10	13	20	3.96 h	03:59:08	k3k8k(-1)k(-5)k(-6)k(-9)k(-10)[Q][R]			
EQQ	15	17	4	6	12	13	20	3.96 h	03:59:08	k8k(-1)k(-2)k(-5)k(-6)k(-9)k(-10)[Q][R]			

Appendix B

Calculation Of Dilution Factor For Two-Phase Emulsion Process With Acid Addition

j = 0

V_o

j = 1

Acid added

Sample taken

V_o $V_o + \Delta_1$ $V_o + \Delta_1 - \varepsilon$

j = 2

Acid added

Sample taken

$V_o + \Delta_1 - \varepsilon$ $V_o + (\Delta_1 + \Delta_2) - \varepsilon$ $V_o + (\Delta_1 + \Delta_2) - 2\varepsilon$

j = 3

Acid added

Sample taken

$V_o + (\Delta_1 + \Delta_2) - 2\varepsilon$ $V_o + (\Delta_1 + \Delta_2 + \Delta_3) - 2\varepsilon$ $V_o + (\Delta_1 + \Delta_2 + \Delta_3) - 3\varepsilon$
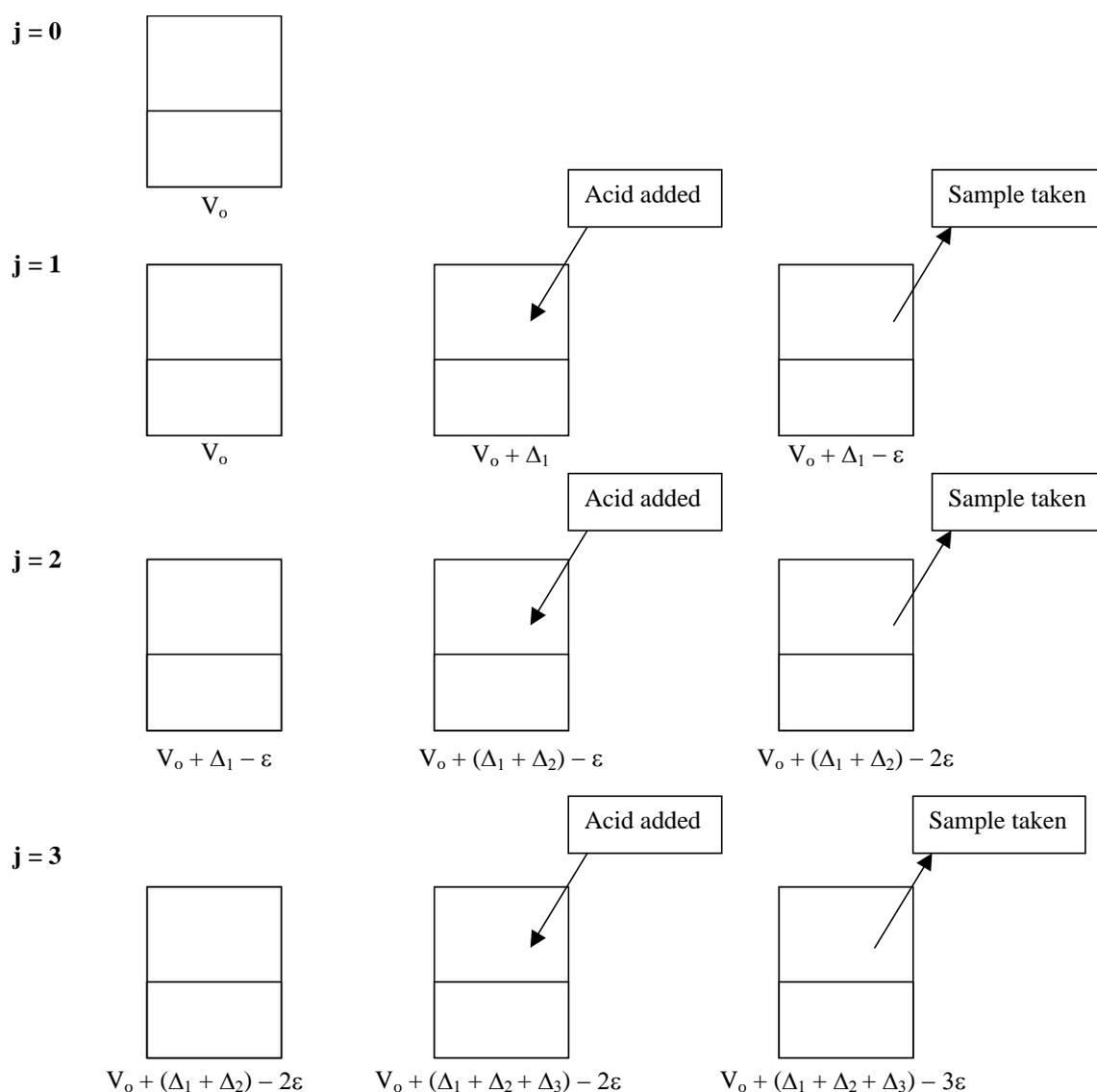
where: Δ = volume of acid added, ε = volume of sample withdrawn

Appendix B

At j = 0:   Increment dilution factor (IDF$_0$): $IDF_0 = 1.0$

At j = 1:   Increment dilution factor (IDF$_1$): $IDF_1 = \dfrac{V_o + \Delta_1}{V_0}$

At j = 2:   Increment dilution factor (IDF$_2$): $IDF_2 = \dfrac{V_o + (\Delta_1 + \Delta_2) - \varepsilon}{V_0 + \Delta_1 - \varepsilon}$

At j = 3:   Increment dilution factor (IDF$_3$): $IDF_3 = \dfrac{V_o + (\Delta_1 + \Delta_2 + \Delta_3) - 2\varepsilon}{V_0 + (\Delta_1 + \Delta_2) - 2\varepsilon}$

Dilution factor at j = 0 is 1.0

Dilution factor at j = 1 is IDF$_1$

Dilution factor at j = 2 is IDF$_1 \times$ IDF$_2$

Dilution factor at j = 3 is IDF$_1 \times$ IDF$_2 \times$ IDF$_3$

General dilution factor formula at j = N is thus:

$$IDF_N = \prod_{j=1}^{N} \left(\frac{V_o + \sum\limits_{i=1}^{j} \Delta_i - (j-1)\varepsilon}{V_o + \sum\limits_{i=1}^{j-1,\, j>1} \Delta_i - (j-1)\varepsilon} \right)$$

Example: Calculate dilution factor for each time point for the following two-phase emulsion system with initial reaction volume of 75 ml.

Table B.1: Acid addition data and sampling volume at each time point for the two-phase emulsion system.

Time (h)	Acid added (ml)	Sampling (ml)	Dilution factor
0.05	0.038	0.60	?
1	0.243	0.60	?
2	0.408	0.60	?
3	0.610	0.60	?
4	0.920	0.60	?
6	1.450	0.60	?
8	1.953	0.60	?
10	2.610	0.60	?
14	3.908	0.60	?
22.5	6.870	0.60	?
34	10.413	0.60	?
47.5	14.818	0.60	?
57	17.193	0.60	?
71	20.315	0.60	?
81	21.795	0.60	?
83.3	47.048	0.60	?
96	47.658	0.60	?
108	49.445	0.60	?

Appendix B

Solution:

Table B.2: Calculation of dilution factor from the data given in Table B.1.

j	Time (h)	V_o (ml)	Sum Delta j	Sum Delta j - 1	j - 1	Epsilon (ml)	IDF j	DF j
0	0	75	0.000	0	-1	0.6	1.00000	1.00000
1	0.05	75	0.038	0	0	0.6	1.00051	1.00051
2	1	75	0.243	0.038	1	0.6	1.00275	1.00326
3	2	75	0.408	0.243	2	0.6	1.00223	1.00550
4	3	75	0.610	0.408	3	0.6	1.00274	1.00826
5	4	75	0.920	0.610	4	0.6	1.00423	1.01253
6	6	75	1.450	0.920	5	0.6	1.00727	1.01989
7	8	75	1.953	1.450	6	0.6	1.00690	1.02693
8	10	75	2.610	1.953	7	0.6	1.00903	1.03620
9	14	75	3.908	2.610	8	0.6	1.01783	1.05467
10	22.5	75	6.870	3.908	9	0.6	1.04029	1.09717
11	34	75	10.413	6.870	10	0.6	1.04670	1.14841
12	47.5	75	14.818	10.413	11	0.6	1.05589	1.21259
13	57	75	17.193	14.818	12	0.6	1.02875	1.24745
14	71	75	20.315	17.193	13	0.6	1.03699	1.29360
15	81	75	21.795	20.315	14	0.6	1.01703	1.31563
16	83.3	75	47.048	21.795	15	0.6	1.28764	1.69405
17	96	75	47.658	47.048	16	0.6	1.00542	1.70324
18	108	75	49.445	47.658	17	0.6	1.01589	1.73031

Calculation with Microsoft EXCEL® spreadsheet:

(a)

	A	B	C	D	E
1	Time (h)	Acid added (ml)	Sampling (ml)	Dilution factor	
2	0.05	0.038	0.6	?	
3	1	0.243	0.6	?	
4	2	0.408	0.6	?	
5	3	0.61	0.6	?	
6	4	0.92	0.6	?	
7	6	1.45	0.6	?	
8	8	1.953	0.6	?	
9	10	2.61	0.6	?	
10	14	3.908	0.6	?	
11	22.5	6.87	0.6	?	
12	34	10.413	0.6	?	
13	47.5	14.818	0.6	?	
14	57	17.193	0.6	?	
15	71	20.315	0.6	?	
16	81	21.795	0.6	?	
17	83.3	47.048	0.6	?	
18	96	47.658	0.6	?	
19	108	49.445	0.6	?	
20					
21					

(b)

	F	G	H	I	J	K	L	M	N
1	j	Time (h)	Vo (ml)	Sum Delta j	Sum Delta j - 1	j - 1	Epsilon (ml)	IDF j	DF j
2	0	0	75	0	0	=F2-1	0.6	=IF(K2<0,1,(H2+I2-K2*L2)/(H2+J2-K2*L2))	1
3	1	0.05	75	=B2	0	=F3-1	0.6	=IF(K3<0,1,(H3+I3-K3*L3)/(H3+J3-K3*L3))	=M3*N2
4	2	1	75	=B3	=I3	=F4-1	0.6	=IF(K4<0,1,(H4+I4-K4*L4)/(H4+J4-K4*L4))	=M4*N3
5	3	2	75	=B4	=I4	=F5-1	0.6	=IF(K5<0,1,(H5+I5-K5*L5)/(H5+J5-K5*L5))	=M5*N4
6	4	3	75	=B5	=I5	=F6-1	0.6	=IF(K6<0,1,(H6+I6-K6*L6)/(H6+J6-K6*L6))	=M6*N5
7	5	4	75	=B6	=I6	=F7-1	0.6	=IF(K7<0,1,(H7+I7-K7*L7)/(H7+J7-K7*L7))	=M7*N6
8	6	6	75	=B7	=I7	=F8-1	0.6	=IF(K8<0,1,(H8+I8-K8*L8)/(H8+J8-K8*L8))	=M8*N7
9	7	8	75	=B8	=I8	=F9-1	0.6	=IF(K9<0,1,(H9+I9-K9*L9)/(H9+J9-K9*L9))	=M9*N8
10	8	10	75	=B9	=I9	=F10-1	0.6	=IF(K10<0,1,(H10+I10-K10*L10)/(H10+J10-K10*L10))	=M10*N9
11	9	14	75	=B10	=I10	=F11-1	0.6	=IF(K11<0,1,(H11+I11-K11*L11)/(H11+J11-K11*L11))	=M11*N10
12	10	22.5	75	=B11	=I11	=F12-1	0.6	=IF(K12<0,1,(H12+I12-K12*L12)/(H12+J12-K12*L12))	=M12*N11
13	11	34	75	=B12	=I12	=F13-1	0.6	=IF(K13<0,1,(H13+I13-K13*L13)/(H13+J13-K13*L13))	=M13*N12
14	12	47.5	75	=B13	=I13	=F14-1	0.6	=IF(K14<0,1,(H14+I14-K14*L14)/(H14+J14-K14*L14))	=M14*N13
15	13	57	75	=B14	=I14	=F15-1	0.6	=IF(K15<0,1,(H15+I15-K15*L15)/(H15+J15-K15*L15))	=M15*N14
16	14	71	75	=B15	=I15	=F16-1	0.6	=IF(K16<0,1,(H16+I16-K16*L16)/(H16+J16-K16*L16))	=M16*N15
17	15	81	75	=B16	=I16	=F17-1	0.6	=IF(K17<0,1,(H17+I17-K17*L17)/(H17+J17-K17*L17))	=M17*N16
18	16	83.3	75	=B17	=I17	=F18-1	0.6	=IF(K18<0,1,(H18+I18-K18*L18)/(H18+J18-K18*L18))	=M18*N17
19	17	96	75	=B18	=I18	=F19-1	0.6	=IF(K19<0,1,(H19+I19-K19*L19)/(H19+J19-K19*L19))	=M19*N18
20	18	108	75	=B19	=I19	=F20-1	0.6	=IF(K20<0,1,(H20+I20-K20*L20)/(H20+J20-K20*L20))	=M20*N19
21									

Figure B.1: Computation of dilution factor in Microsoft EXCEL® spreadsheet, (a) experimental data in Table B.1 is tabulated, (b) an example of formula set up in the spreadsheet to obtain the results shown in Table B.2.

Appendix C

Programming Codes Used In Parameters Searching Program

```
Sub LeksawasdiRSSMinimization()
     For i = 1 To ParaN
          UpperBound(i) = Cells(PR + i, PC + 2)
          LowerBound(i) = Cells(PR + i, PC + 3)
          Parameter(0, 0, i) = Cells(PR + i, PC)
          ParameterName(i) = Cells(PR + i, PC - 1)
     Next i

     For i = 1 To ParaN
          If Parameter(0, 0, i) > UpperBound(i) Or
               Parameter(0, 0, i) < LowerBound(i) Then

               MsgBox "You have made mistake in entering
                    parameter value and bound"

               If Parameter(0, 0, i) > UpperBound(i) Then

                    MsgBox "Initial value of parameter "
                         and ParameterName(i) and " is " _
                              and "greater than the upperbound"

               ElseIf Parameter(0, 0, i) < LowerBound(i) Then

                    MsgBox "Initial value of parameter " and
                         ParameterName(i) and " is lesser " _
                         and "than the lowerbound"
               End If
               Exit Sub
          End If
     Next i

     For i = 1 To SearchLevel
          For j = 1 To DivisionNumber
               USMF(i, j) = 1 + j * 10 ^ -i
               LSMF(i, j) = 1 / USMF(i, j)
          Next j
```

```
    Next i

RSS(0) = Cells(RowRSS, ColumnRSS)
LRSSifs(0) = Cells(RowRSS, ColumnRSS)

M = 0

Do
        Range(Cells(PR, PC + 4), Cells(PR + ParaN, PC + 4)).Clear
        Application.ScreenUpdating = True
        Application.ScreenUpdating = False

    For k = 1 To ParaN

NextParameter:

            If k = 1 Then Cells(PR, PC + 4) = "Loop : " and _
                    M + 1 and ", total of " _
                    and MxLoop and " loops available"
            Range(Cells(PR + k, PC), Cells(PR + k, PC)).Select
            Application.ScreenUpdating = True
            Application.ScreenUpdating = False

            L = 0

            If (Abs(Parameter(M, L, k) - UpperBound(k)) _
                    < CSC ^ 2) And Abs((Parameter(M, L, k) _
                    - LowerBound(k)) < CSC ^ 2) And _
                    Abs(UpperBound(k) - LowerBound(k)) < CSC Then

                    Cells(PR + k, PC + 4) = _
                            "This parameter is fixed, skip to " and _
                            _ "the next parameter"
                    Parameter(M + 1, L, k) = Parameter(M, L, k)
                    If k = ParaN Then
                            Exit For
                    Else
                            k = k + 1
                            Range(Cells(PR + k, PC), _
                                    Cells(PR + k, PC)).Select
                            Application.ScreenUpdating = True
                            Application.ScreenUpdating = False
                            GoTo NextParameter:
                    End If
            End If

            Do
                For i = 1 To SearchLevel
```

```
                                    For j = 1 To DivisionNumber
                                        USP(i, j) = USMF(i, j) * _
                                            and Parameter(M, L, k)
                                        If USP(i, j) > UpperBound(k) Then
                                            _ USP(i, j) = UpperBound(k)
                                        Cells(PR + k, PC) = USP(i, j)
                                        URI(i, j) = Cells(RowRSS, _
                                            ColumnRSS)

                                        LSP(i, j) = LSMF(i, j) * _
                                            Parameter(M, L, k)
                                        If LSP(i, j) < LowerBound(k) Then
                                            _ LSP(i, j) = LowerBound(k)
                                        Cells(PR + k, PC) = LSP(i, j)
                                        LRI(i, j) = Cells(RowRSS, _
                                            ColumnRSS)
                                    Next j
                            Next i

                            For i = 1 To SearchLevel
                                    For j = 1 To DivisionNumber
                                        ListRSS(9 * (i - 1) + j) = _
                                            URI(i, j)
                                        ListRSS(81 + 9 * (i - 1) + j) _
                                            = LRI(i, j)
                                        ListParameter(9 * (i - 1) + j) = _
                                            USP(i, j)
                                        ListParameter(81 + 9 * (i - 1) + _
                                            j) = LSP(i, j)
                                    Next j
                            Next i

                            For i = 1 To SearchLevel * DivisionNumber * 2
                                    Cells(i, ColumnForRSSList) = ListRSS(i)
                                    Cells(i, ColumnForParaList) = _
                                        ListParameter(i)
                            Next i

                    Range(Cells(1,ColumnForRSSList), _
                            Cells(SearchLevel * DivisionNumber * 2,
                            _ ColumnForParaList)).Select
                    Selection.Sort Key1:=Range(Cells(1, _
                            ColumnForRSSList), Cells(1, _
                            ColumnForRSSList)), Order1:=xlAscending,
                            _ Header:=xlNo, OrderCustom:=1, _
                            MatchCase:=False, _
```

```
                        Orientation:=xlTopToBottom


            If Cells(1, ColumnForRSSList) < RSS(M) Then
                    Parameter(M, L + 1, k) = Cells(1, _
                        ColumnForParaList)
                    Cells(PR + k, PC) = Cells(1, _
                        ColumnForParaList)
                    LRSSifs(L + 1) = Cells(RowRSS, _
                        ColumnRSS)


            Else
                    Parameter(M, L + 1, k) = Parameter(M, _
                        L, k)
                    Cells(PR + k, PC) = Parameter(M, L, k)
                    LRSSifs(L + 1) = Cells(RowRSS, _
                        ColumnRSS)
            End If

            Range(Cells(1, ColumnForRSSList), _
                    Cells(SearchLevel * DivisionNumber * 2,
                    _ ColumnForParaList)).ClearContents


            L = L + 1
            SearchConverge = False
            If L >= 2 Then
                    If (LRSSifs(L - 1) - LRSSifs(L) < CSC) _
                        And (LRSSifs(L - 2) - _
                        LRSSifs(L - 1) < CSC) Then _
                        SearchConverge = True
            End If
        Loop Until L >= MxLoop Or SearchConverge = True

        If L >= MxLoop Then MsgBox "Maximum number (" _
            and MxLoop and ") of search loop reached"

        Cells(PR + k, PC + 4) = "Search Completed :" and " "
        and   L and " loops searched, total of " _
            and MxLoop and " loops available"
        ActiveWorkbook.Save
        Application.ScreenUpdating = True
        Application.ScreenUpdating = False
    Next k

    M = M + 1
    RSS(M) = Cells(RowRSS, ColumnRSS)
```

```
        For i = 1 To ParaN
                Parameter(M, 0, i) = Cells(PR + i, PC)
        Next i
        SearchConverge = False
        If M >= 2 Then
                If (RSS(M - 1) - RSS(M) < CSC) And _
                    (RSS(M - 2) - RSS(M - 1) < CSC) Then _
                    SearchConverge = True
        End If

    Loop Until M >= MxLoop Or SearchConverge = True

    If M >= MxLoop Then MsgBox "Maximum number (" and MxLoop _
        and ") of iteration loop reached"

    ActiveWorkbook.Save
    ActiveWorkbook.Close

End Sub
```

Appendix D

Benzaldehyde Partitioning Studies

Type	Description of organic-aqueous two-phase system
1	[20 mM MOPS, 1 M (NH$_4$)$_2$SO$_4$] : [BZ, octanol]
2	[20 mM MOPS, 10% (w/v) tween-20] : [BZ, octanol]
3	[20 mM MOPS, 10% (w/v) tween-85] : [BZ, octanol]
4	[20 mM MOPS, 2 M benzyl alcohol] : [BZ, octanol]
5	[20 mM MOPS] : [BZ, pentanol]
6	[20 mM MOPS, 1 M KCl] : [BZ, octanol]
7	[20 mM MOPS] : [BZ, hexanol]
8	[20 mM MOPS, 10% (w/v) D-glucose] : [BZ, octanol]
9	[20 mM MOPS, 2 M butan-1-ol] : [BZ, octanol]
10	[20 mM MOPS, 10% (w/v) maltose] : [BZ, octanol]
11	[20 mM MOPS, 7% (w/v) D-mannitol] : [BZ, octanol]
12	[20 mM MOPS, 2 M isopropanol] : [BZ, octanol]
13	[20 mM MOPS] : [BZ, octanol]
14	[20 mM MOPS, 2 M acetonitrile] : [BZ, octanol]
15	[20 mM MOPS] : [BZ, heptanol]
16	[20 mM MOPS, 10% (w/v) fructose] : [BZ, octanol]
17	[20 mM MOPS] : [BZ, grapeseed oil]
18	[20 mM MOPS, 2 M ethanol] : [BZ, octanol]
19	[20 mM MOPS, 10% (w/v) sucrose] : [BZ, octanol]
20	[20 mM MOPS] : [BZ, corn oil]
21	[20 mM MOPS] : [10% (v/v) n-octane, BZ, octanol]
22	[20 mM MOPS, 2 M glycerol] : [BZ, octanol]
23	[20 mM MOPS] : [10% (v/v) n-hexane, BZ, octanol]
24	[20 mM MOPS] : [BZ, canola oil]
25	[20 mM MOPS] : [10% (v/v) paraffin, BZ, octanol]
26	[20 mM MOPS] : [10% (v/v) methylcyclohexane, BZ, octanol]
27	[20 mM MOPS] : [10% (v/v) n-heptane, BZ, octanol]

Type	Description of organic-aqueous two-phase system
28	[20 mM MOPS] : [50% (v/v) methylcyclohexane, BZ, octanol]
29	[20 mM MOPS] : [BZ, decyl alcohol]
30	[20 mM MOPS] : [50% (v/v) n-heptane, BZ, octanol]
31	[20 mM MOPS] : [50% (v/v) n-octane, BZ, octanol]
32	[20 mM MOPS] : [50% (v/v) n-hexane, BZ, octanol]
33	[20 mM MOPS] : [BZ, olive oil]
34	[20 mM MOPS, 2% (w/v) lactose] : [BZ, octanol]
35	[20 mM MOPS, 10% (w/v) PEG-6000] : [BZ, octanol]
36	[20 mM MOPS] : [50% (v/v) paraffin, BZ, octanol]
37	[20 mM MOPS, 22% (w/v) PEG-6000] : [BZ, octanol]
38	[20 mM MOPS, 10% (w/v) urea] : [BZ, octanol]
39	[20 mM MOPS, 18% (w/v) urea] : [BZ, octanol]
40	[20 mM MOPS, 2.0 M dipropylene glycol] : [BZ, octanol]
41	[20 mM MOPS, 26% (w/v) PEG-6000] : [BZ, octanol]
42	[20 mM MOPS, 30% (w/v) PEG-6000] : [BZ, octanol]
43	[20 mM MOPS, 2.5 M dipropylene glycol] : [BZ, octanol]
44	[2.5 M MOPS] : [BZ, octanol]
45	[20 mM MOPS, 35% (w/v) PEG-6000] : [BZ, octanol]
46	[20 mM MOPS, 40% (w/v) PEG-6000] : [BZ, octanol]
47	[20 mM MOPS, 3.0 M dipropylene glycol] : [BZ, octanol]
48	[20 mM MOPS, 30% (w/v) urea] : [BZ, octanol]
49	[20 mM MOPS, 26% (w/v) urea] : [BZ, octanol]
50	[20 mM MOPS, 3.5 M dipropylene glycol] : [BZ, octanol]
51	[20 mM MOPS, 40% (w/v) urea] : [BZ, octanol]
52	[20 mM MOPS, 4.0 M dipropylene glycol] : [BZ, octanol]
53	[20 mM MOPS, 4.5 M dipropylene glycol] : [BZ, octanol]

Figure D.1: Key to solvent type of Figure D.2 [concentration of MOPS buffer in aqueous phase, additive]:[additive, BZ (1.50 M benzaldehyde), organic phase].
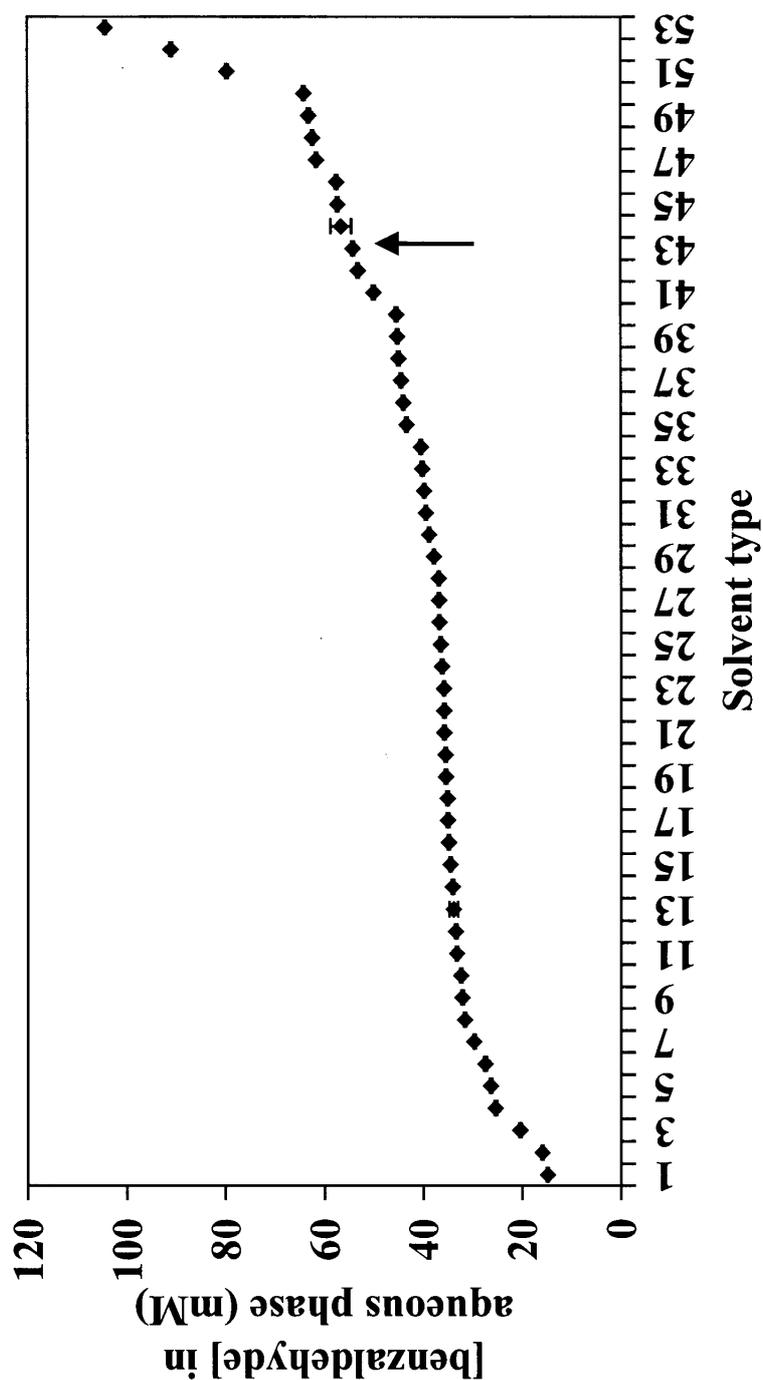
Figure D.2: The effect of various types of solvents and chemical additives on the partitioning of benzaldehyde in aqueous phase of organic-aqueous two-phase system at 6°C. Organic phase contained 1.50 M benzaldehyde in octanol. The aqueous phase contained 20 mM MOPS, 1 mM TPP, 1 mM MgSO$_4$ and chemical additives with initial pH of 7.0. The initial volume used in each phase was 0.75 ml. The key to each solvent type is given in Figure D.1. An arrow points to the selected additive (2.5 M DPG) used in the subsequent experiment.

Appendix E

Two-phase Calculations

Table E.1: Details of calculations of Table 7.1 for a system with 2.5 M MOPS (part 1) in the absence of pH-control.

Variables	Uncontrolled pH[*]
	2.5 M MOPS
T (h)	49
PAC$_{aq}$ (g l^{-1})	18.5
PAC$_{or}$ (g l^{-1})	141
V$_{aq}$:V$_{or}$ (l l^{-1})	1:1
PAC$_{tot}$ (g l^{-1})	79.8
E$_{ini}$ (Initial enzyme activity (U ml^{-1} aqueous phase))	8.50
PAC$_{tot}$ (total PAC produced (g l^{-1}))	=[18.5 g l^{-1}*(1 l) + 141 g l^{-1}*(1 l)]/(1+1 l)
Recheck with EXCEL	79.8
Total PAC produced (mg)	=[18.5 g l^{-1}*(1 l) + 141 g l^{-1}*(1 l)]* 1000 mg g^{-1}
Recheck with EXCEL	159500
Total enzyme used (U)	=8.50 U ml^{-1} * 1 l * 1000 ml l^{-1}
Recheck with EXCEL	8500
PAC$_{spec}$ (Specific PAC production (mg U^{-1}))	=159500 mg / 8500 U
Recheck with EXCEL	18.8
PAC$_{spec prod}$ (Specific PAC productivity (mg U^{-1} h^{-1}))	=18.8 mg U^{-1} / 49 h
Recheck with EXCEL	0.38
PAC$_{productivity}$ (Volumetric PAC productivity (g l^{-1} day^{-1}))	=79.8 g l^{-1} * 24 h day^{-1} / 49 h
Recheck with EXCEL	39.1

[*]   Rosche et al. (2002b), Sandford (2002)

Appendix E

Table E.2: Details of calculations of Table 7.1 for a system with 2.5 M MOPS (part 2) in the absence of pH-control.

Variables	Uncontrolled pH[*]
	2.5 M MOPS
$Y_{P/BZ}$ (mol PAC mol^{-1} benzaldehyde consumed)	0.90
$Y_{P/Pyr}$ (mol PAC mol^{-1} pyruvate consumed)	0.73
$Y_{Q/BZ}$ (mol acetaldehyde mol^{-1} pyruvate consumed)	3.1E-02
$Y_{R/BZ}$ (mol acetoin mol^{-1} pyruvate consumed)	6.2E-02
Pyr_{bal} (pyruvate accounted for (%))	$= 100*(0.73 + 0.031 + 2*0.062)$
Recheck with EXCEL	89
Bz_{bal} (benzaldehyde accounted for (%))	$= 100*(0.90)$
Recheck with EXCEL	90

Cost of MOPS = \$AUD 412.5 kg^{-1}
[Sigma, M-1254]
Cost of DPG = \$AUD 53 l^{-1} [Merck, 8.03265.1000]

Cost of buffer and chemical additives (\$AUD l^{-1} aqueous)	$=2.5$ mol l^{-1} * 0.2093 kg mol^{-1} * 1 l * \$412 kg^{-1}
Recheck with EXCEL	216
Cost (dollars spent for production of 1 g PAC) (\$AUD g^{-1})	$=$\$AUD216 / 79.8 g l^{-1} * (1/2)[#]
Recheck with EXCEL	1.35
	# volume ratio of aqueous to overall volume

[*]   Rosche et al. (2002b), Sandford (2002)

Similar computations were made for the pH-control two-phase systems with 2.5 M MOPS and 20 mM MOPS to obtain the results illustrated in Table 7.1.

Table E.3: Details of calculations of Table 7.1 for a system with 20 mM MOPS + 2.5 M DPG (part 1).

| Variables	Controlled pH at 7.0 with 3.6 M acetic acid
	20 mM MOPS + 2.5 M DPG
T (h)	47
PAC_{aq} (g l^{-1})	17.2
PAC_{or} (g l^{-1})	151
V_{aq}:V_{or} (l l^{-1})	0.88:1.12
PAC_{tot} (g l^{-1})	92.1
E_{ini} (Initial enzyme activity (U ml^{-1} aqueous phase))	10.0
PAC_{tot} (total PAC produced (g l^{-1}))	=[17.2 g l^{-1}*(0.88 l) + 151 g l^{-1}*(1.12 l)]/(0.88+1.12 l)
Recheck with EXCEL	92.1
Total PAC produced (mg)	=[17.2 g l^{-1}*(0.88 l) + 151 g l^{-1}*(1.12 l)]*1000 mg g^{-1}
Recheck with EXCEL	184256
Total enzyme used (U)	=10 U ml^{-1} * 0.88 l * 1000 ml l^{-1}
Recheck with EXCEL	8800
PAC_{spec} (Specific PAC production (mg U^{-1}))	=184256 mg / 8800 U
Recheck with EXCEL	20.9
$PAC_{spec\ prod}$ (Specific PAC productivity (mg U^{-1} h^{-1}))	=20.9 mg U^{-1} / 47 h
Recheck with EXCEL	0.45
$PAC_{productivity}$ (Volumetric PAC productivity (g l^{-1} day^{-1}))	=92.1 g l^{-1} * 24 h day^{-1} / 47 h
Recheck with EXCEL	47.0

Table E.4: Details of calculations of Table 7.1 for a system with 20 mM MOPS + 2.5 M DPG (part 2).

Variables	Controlled pH at 7.0 with 3.6 M acetic acid
	20 mM MOPS + 2.5 M DPG
$Y_{P/BZ}$ (mol PAC mol^{-1} benzaldehyde consumed)	0.99
$Y_{P/Pyr}$ (mol PAC mol^{-1} pyruvate consumed)	0.84
$Y_{Q/BZ}$ (mol acetaldehyde mol^{-1} pyruvate consumed)	6.8E-03
$Y_{R/BZ}$ (mol acetoin mol^{-1} pyruvate consumed)	2.4E-02
Pyr_{bal} (pyruvate accounted for (%))	= 100*(0.84 + 0.0068 + 2*0.024)
Recheck with EXCEL	90
Bz_{bal} (benzaldehyde accounted for (%))	= 100*(0.99)
Recheck with EXCEL	99

Cost of MOPS = $AUD 412.5 kg^{-1} [Sigma, M-1254]

Cost of DPG = $AUD 53 l^{-1} [Merck, 8.03265.1000]

Cost of buffer and chemical additives ($AUD l^{-1} aqueous)	= Cost of 20 mM MOPS ($1.72) + Cost of 2.5 M DPG (0.326 l * $53 l^{-1})
Recheck with EXCEL	19.0
Cost (dollars spent for production of 1 g PAC) ($AUD g^{-1})	=$AUD19 / 92.1 g l^{-1} * (0.88/2)$^{\#}$
Recheck with EXCEL	0.091
	# volume ratio of aqueous to overall volume

Appendix F

Effect of MOPS concentrations on partitioning of benzaldehyde in the aqueous phase of an organic-aqueous two-phase system
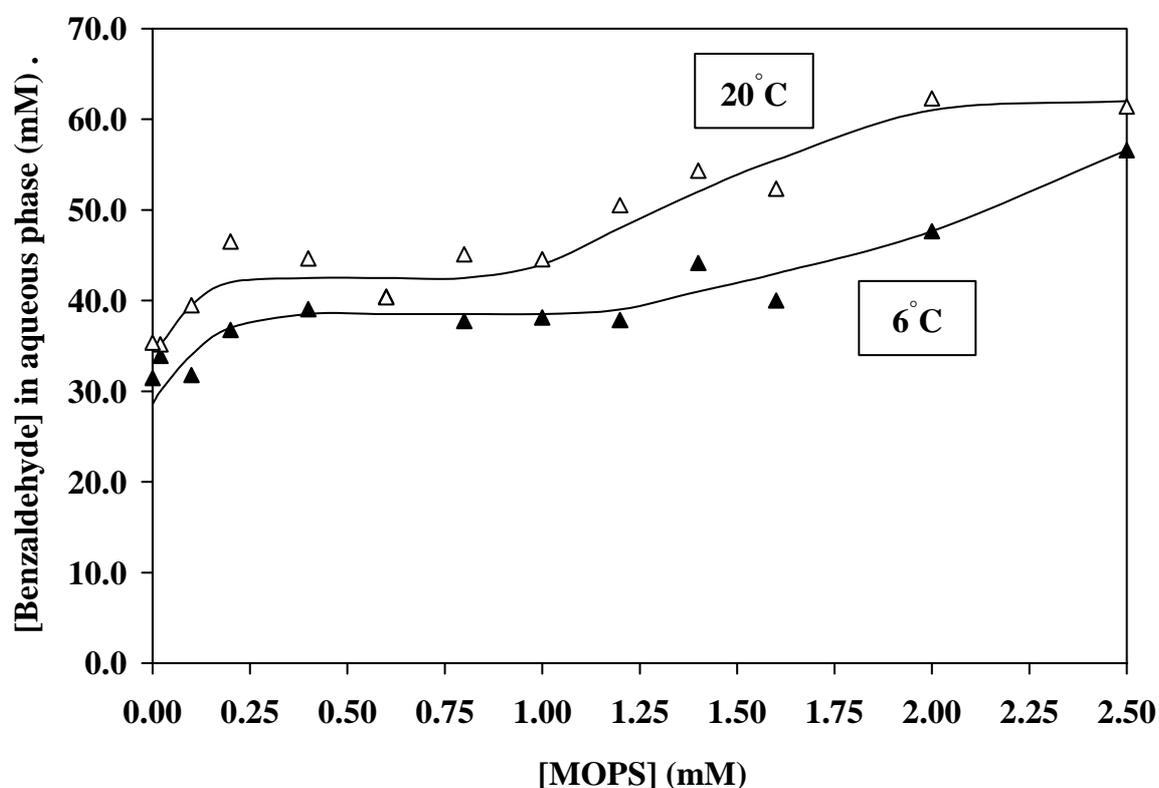
Figure F.1: The effect of MOPS concentrations and temperature (6 and 20°C) on the partitioning of benzaldehyde in aqueous phase of organic-aqueous two-phase system. Organic phase contained 1.50 M benzaldehyde in octanol. The aqueous phase contained MOPS of varied concentrations up to 2.5 M, 1 mM TPP, 1 mM MgSO$_4$ with initial pH of 7.0. The initial volume used in each phase was 0.75 ml.

Appendix G

Effect of benzaldehyde concentration in the organic phase on partitioning of benzaldehyde in the aqueous phase
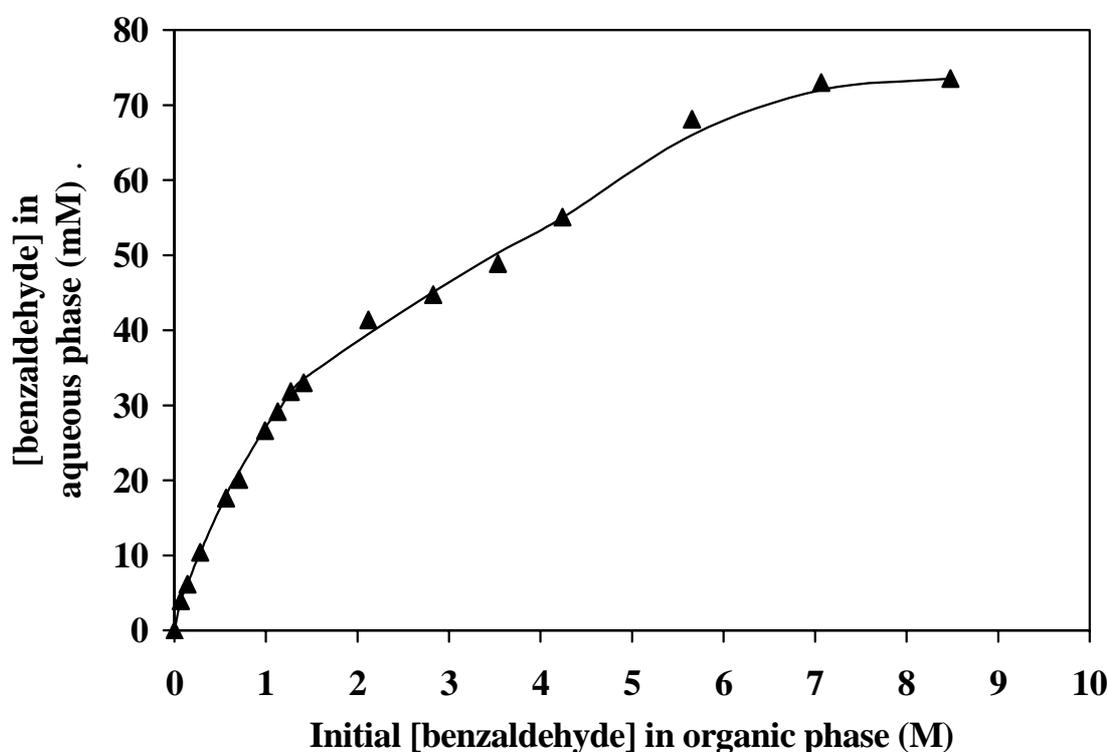
Figure G.1: The effect of varied benzaldehyde concentrations in organic phase (0.07-8.5 M) on the partitioning of benzaldehyde in aqueous phase of organic-aqueous two-phase system at 4°C. The aqueous phase contained 20 mM MOPS, 1 mM TPP, 1 mM MgSO$_4$ with initial pH 7.0. The initial volume used in each phase was 0.75 ml.

Appendix H

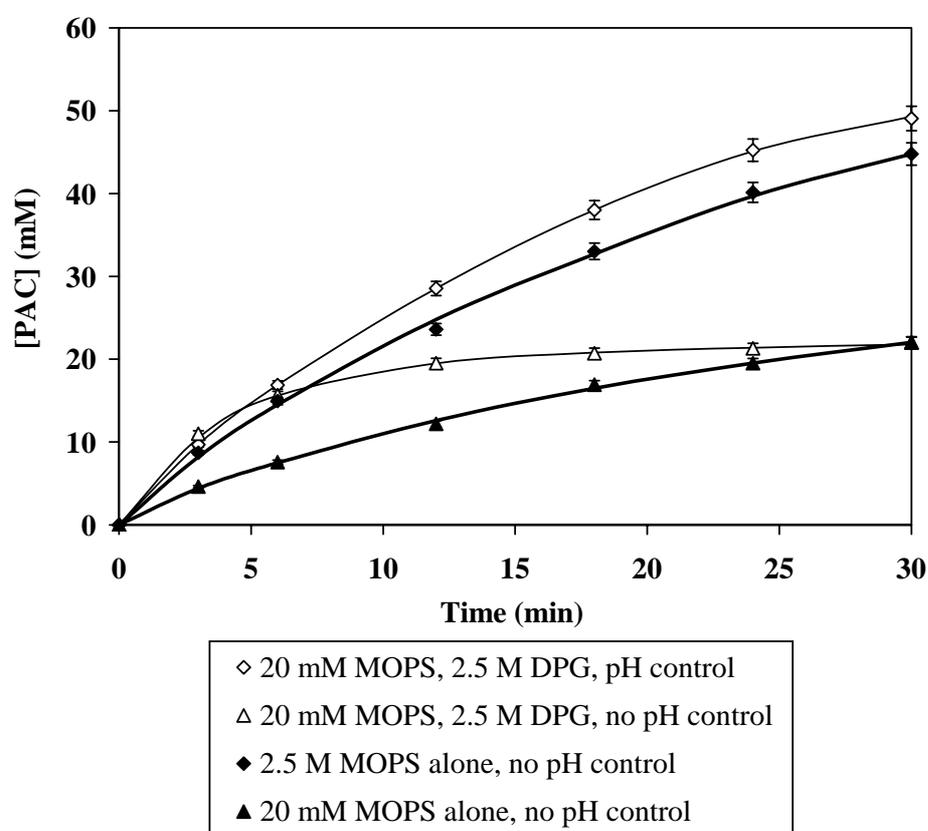# Production of PAC in the presence of 2.5 M DPG with pH control, investigation by initial rate studies (small scale)

Figure H.1: Time profiles of PAC formation with 20 mM MOPS alone, 2.5 M MOPS alone and 20 mM MOPS + 2.5 M DPG. Each initial rate buffer contained 120 mM sodium pyruvate, 100 mM benzaldehyde, 1 mM TPP, 1 mM $MgSO_4$, 3.5 U carboligase ml^{-1} with initial pH 7.0 at $6°C$. The investigations in the absence of pH control were done in a 1.5 ml scale. Manual pH control at 7.0 was carried out by adding 5 or 10 µl of 360 mM acetic acid to a system contained 20 mM MOPS + 2.5 M DPG with reaction volume of 10 ml.

Appendix I

Initial rate studies of PAC production in 30% (w/v) Urea and 30% (w/v) PEG-6000
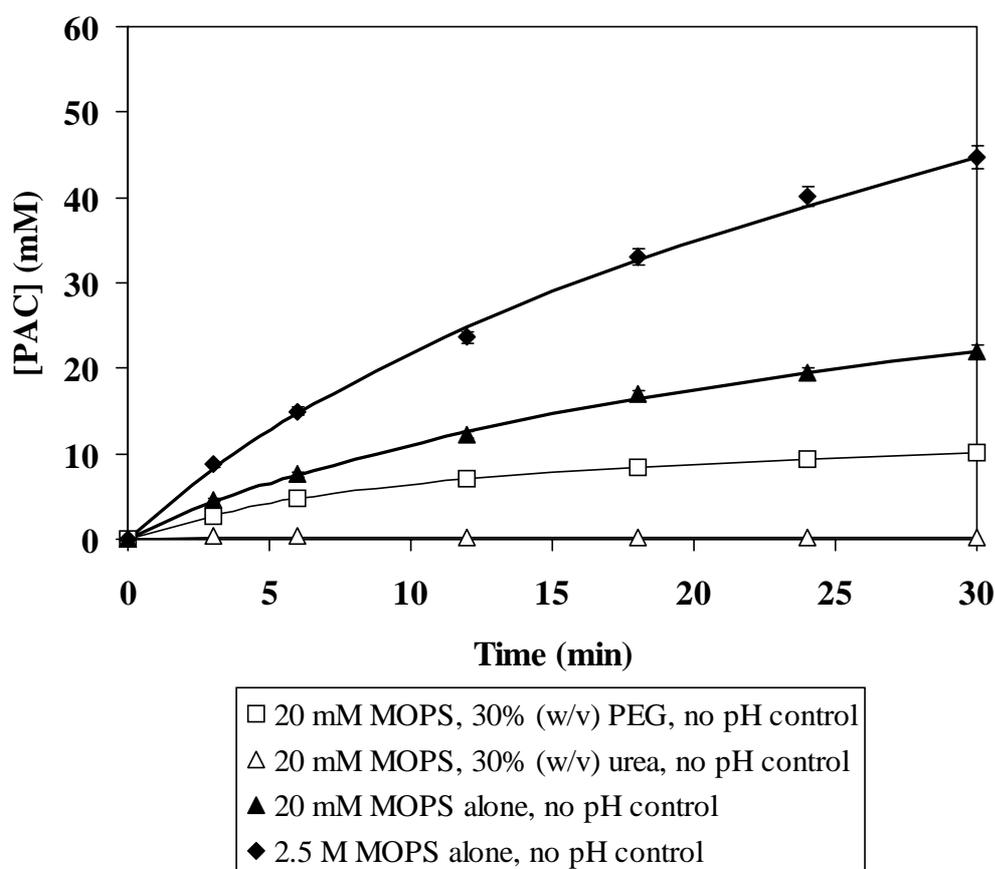
Figure I.1: Time profiles of PAC formation with 20 mM MOPS alone, 2.5 M MOPS alone, 20 mM MOPS + 30% (w/v) PEG-6000 and 20 mM MOPS + 30% (w/v) urea. Each initial rate buffer contained 120 mM sodium pyruvate, 100 mM benzaldehyde, 1 mM TPP, 1 mM MgSO$_4$, 3.5 U carboligase ml^{-1} with initial pH 7.0 at 6°C.

Appendix J

Abbreviations

%	percentage
Σ	sum of kappa products from all enzyme species for simplified model
$^\circ$C	degrees celcius
[ ]	concentration (mM)
A	pyruvate
ADH	alcohol dehydrogenase
ATCase	aspartate transcarbamylase
atm	atmospheric pressure
b	benzaldehyde concentration (mM)
B, BZ	benzaldehyde
BEHP	bis(2-ethylhexyl) phthalate
BSA	bovine serum albumin
C	carbon dioxide
C.I.	confidence interval
CER	carbon dioxide evolution rate (mmol l^{-1} h^{-1})
cm	centimeter
Da	dalton
dia.	diameter
DO	dissolved oxygen
E	PDC activity at time t (U ml^{-1})
E	free pyruvate decarboxylase (PDC) enzyme
E	relative enzyme activity at time t
E_0	initial PDC activity at time zero (U ml^{-1})
E_0	initial relative enzyme activity (100%)
EA	binary enzyme complex between PDC and pyruvate
EDTA	ethylenediaminetetraacetate

Appendix J

E_o	initial concentration of PDC enzyme (U carboligase ml^{-1})
EP	binary enzyme complex between PDC and PAC
EQ	binary enzyme complex between PDC and 'active acetaldehyde'
EQB	ternary enzyme complex between PDC, 'active acetaldehyde' and benzaldehyde
EQC	ternary enzyme complex between PDC, 'active acetaldehyde' and CO_2
EQQ	ternary enzyme complex between PDC, 'active acetaldehyde' and acetaldehyde
ER	binary enzyme complex between PDC and acetoin
Eth	ethanol concentration ($g\ l^{-1}$)
g	gram
g	relative centrifugal force (g-force)
GC	gas chromatography
Glu	glucose concentration ($g\ l^{-1}$)
h	hour, exponent with similar functionality to Hill coefficient for benzaldehyde (no units)
HPLC	high performance (or pressure) liquid chromatography
i	iteration loop identifier of each species to be used in numerical integration
k	benzaldehyde deactivation coefficient ($mM^{-1}\ h^{-0.5}$)
$k_{(-n)}$	rate constant for backward reactions; n ranges from 1 to 10
K_b	intrinsic or microscopic binding constant for benzaldehyde (mM^{1-h})
K_d	overall deactivation parameter (h^{-1} or h^{-n} in general form)
k_{d1}	first order reaction time deactivation constant (h^{-1})
k_{d2}	first order benzaldehyde deactivation coefficient ($mM^{-1}\ h^{-1}$)
kDa	kilodalton
K_m	affinity constant
K_{ma}	affinity constant for pyruvate (mM)
K_{mb}	affinity constant for benzaldehyde (mM)
k_n	rate constant for forward reactions; n ranges from 1 to 10
K_r	rate constant product for the simplified model; r ranges from 1 to 19
k_{rj}	*Rhizopus javanicus* PDC deactivation constant (h^{-1})

Appendix J

k_{sv}	spore viability decay constant (day^{-1})
l	litre
m	meter
M	molar
MES	2-[N-morpholino]ethanesulfonic acid
mg	milligram
min	minute
ml	millilitre
mm	millimeter
mM	millimolar
mmol	millimole
mol	mole
MOPS	3-[N-morpholino]propanesulfonic acid
MQ	milli Q
MS	mean sum of square
n	time exponent constant
N	number of replicates
N/a	not available
NAD$^+$	nicotinamide adenine dinucleotide (oxidised form)
NADH + H$^+$	nicotinamide adenine dinucleotide (reduced form)
nm	nanometer
NMR	nuclear magnetic resonance
ODxxx	optical density at a wavelength of xxx nm
OUR	oxygen uptake rate (mmol l^{-1} h^{-1})
P	*R*-phenylacetylcarbinol
PAC	*R*-phenylacetylcarbinol
PDC	pyruvate decarboxylase
PI	protease inhibitor
Q	acetaldehyde
q_p	instantaneous specific rate of ethanol production (g ethanol g^{-1}biomass h^{-1})
$q_{p,max}$	maximum specific rate of ethanol production (g ethanol g^{-1}biomass h^{-1})

Appendix J

q_s	instantaneous specific rate of glucose consumption (g glucose g^{-1} biomass h^{-1})
$q_{s,max}$	maximum specific rate of glucose consumption (g glucose g^{-1} biomass h^{-1})
R	acetoin
R^2	correlation coefficient
RCF	relative centrifugal force
RO	reverse osmosis
rpm	revolutions per minute
RQ	respiratory quotient
RQ_{avg}	average RQ during fermentative phase
RSS	residual sum of square
s	sample standard deviation
s_m	standard error of a mean
t	time
$t_{0.5}$	half-life of PDC (h)
$t_{0.8}$	eighty percent life of PDC (h)
TCA	trichloroacetic acid
ThDP	thiamine diphosphate
t_{lag}	lag time (h)
tpa	tonnes per annum
TPP	thiamine pyrophosphate
U	unit of enzyme activity (decarboxylase or carboligase)
UV	ultra violet
V	percentage of spore viability at time t
v/v	volume of solute per volume of solution
V_0	initial percentage of spore viability (100%)
V_p	overall rate constant for the formation of PAC (μmol h^{-1} U^{-1})
V_q	overall rate constant for the formation of acetaldehyde (ml h^{-1} U^{-1})
V_r	overall rate constant for the formation of acetoin (l^2 h^{-1} U^{-1} mol^{-1})
vvm	airflow rate (volume per min) per working volume of bioreactor
w/v	weight of solute per volume of solution

Appendix J

x	dry biomass weight concentration (g l^{-1})
Δt	step size constant of Euler-Cauchy numerical integration (0.01 h) for modelling and simulation of PAC biotransformation
Δt	the time periods during which the maximum specific glucose consumption and ethanol production were determined
μg	microgram
μl	microlitre